

UNIVERSITÀ
DEGLI STUDI
DI PADOVA

Sede Amministrativa: Università degli Studi di Padova

Dipartimento di Fisica e Astronomia “Galileo Galilei”

CORSO DI DOTTORATO DI RICERCA IN: FISICA
CICLO XXIX

Generalised Unitarity, Integrand Decomposition, and Hidden properties of QCD Scattering Amplitudes in Dimensional Regularisation

Tesi redatta con il contributo finanziario della Fondazione Cassa di Risparmio di Padova e Rovigo (CARIPARO)

Coordinatore: Ch.mo Prof. Gianguido Dall’Agata

Supervisore: Ch.mo Prof. Pierpaolo Mastrolia

Dottorando: William Javier Torres Bobadilla

Abstract

In this thesis, we present new developments for the analytic calculation of tree- and multi-loop level amplitudes. Similarly, we study and extend their analytic properties.

We propose a Four-dimensional formulation (FDF) equivalent to the four-dimensional helicity scheme (FDH). In our formulation, particles propagating inside the loop are represented by four-dimensional massive internal states regulating the divergences. We provide explicit four-dimensional representations of the polarisation and helicity states of the particles propagating in the loop. Within FDF, we use integrand reduction and four dimensional unitarity to perform analytic computations of one-loop scattering amplitudes. The calculation of tree level scattering amplitude, in this framework, allows for a simultaneous computation of cut-constructible and rational parts of one-loop scattering amplitudes. We present a set of non-trivial examples, showing that FDF scheme is suitable for computing important $2 \rightarrow 2, 3, 4$ partonic amplitudes at one-loop level. We start by considering two gluons production by quark anti-quark annihilation. Then, the (up to four) gluon production, $gg \rightarrow ng$ with $n = 2, 3, 4$. And finally, the Higgs and (up to three) gluons production via gluon fusion, $gg \rightarrow ngH$ with $n = 1, 2, 3$, in the heavy top mass limit.

We also investigate, by following a diagrammatic approach, the role of colour-kinematics (C/K) duality of off-shell diagrams in gauge theories coupled to matter. We study the behaviour of C/K-duality for theories in four- and in d -dimensions. The latter follows the prescriptions given by FDF. We show that the Jacobi relations for the kinematic numerators of off-shell diagrams, built with Feynman rules in axial gauge, reduce to a C/K-violating term due to the contributions of sub-graphs only. We discuss the role of the off-shell decomposition in the direct construction of higher-multiplicity numerators satisfying C/K-duality. We present the QCD process $gg \rightarrow q\bar{q}g$. An analogous study, within FDF, is carried out for d -dimensionally regulated amplitudes.

The computation of dual numerators generates, as byproduct, relations between tree-level amplitudes with different orderings. These relations turn to be the Bern-Carrasco-Johansson (BCJ) identities for four- and d -dimensionally regulated amplitudes. We combine BCJ identities and integrand reduction methods to establish relations between one-loop integral coefficients for dimensionally regulated QCD amplitudes.

We also elaborate on the radiative behaviour of tree-level scattering amplitudes in the soft regime. We show that the subleading soft term in single-gluon emission of quark-gluon amplitudes in QCD is controlled by differential operators, whose universal form can be derived from both Britto-Cachazo-Feng-Witten recursive relations and gauge invariance, as it was shown to hold for graviton and gluon scattering.

In the last part of the thesis, we describe the main features of the multi-loop calculations. We briefly describe the adaptive integrand decomposition (AID), a variant of the standard integrand reduction algorithm. AID exploits the decomposition of the space-time dimension in parallel and orthogonal subspaces. We focus, in particular, on the calculation of $2 \rightarrow 2, 3$ partonic amplitudes at two loop-level

Declaration

This document is the Ph.D. thesis of William Javier Torres Bobadilla.

No part of this thesis has previously been submitted for a degree at this or any other university.

The research of this thesis was carried out in collaboration with, Raffaele Fazio, Hui Luo, Pierpaolo Mastrolia, Edoardo Mirabella, Tiziano Peraro, Amedeo Primo and Ulrich Schubert. Aspect of chapters 2, 3, 5, 6, 7 and 8 are based on the following published works:

Articles

- [1] R. A. Fazio, P. Mastrolia, E. Mirabella and W. J. Torres Bobadilla, *On the Four-Dimensional Formulation of Dimensionally Regulated Amplitudes*, *Eur. Phys. J.* **C74** (2014) 3197, [[1404.4783](#)]
- [2] H. Luo, P. Mastrolia and W. J. Torres Bobadilla, *Subleading soft behavior of QCD amplitudes*, *Phys. Rev.* **D91** (2015) 065018, [[1411.1669](#)]
- [3] P. Mastrolia, A. Primo, U. Schubert and W. J. Torres Bobadilla, *Off-shell currents and color-kinematics duality*, *Phys. Lett.* **B753** (2016) 242–262, [[1507.07532](#)]
- [4] A. Primo and W. J. Torres Bobadilla, *BCJ Identities and d-Dimensional Generalized Unitarity*, *JHEP* **04** (2016) 125, [[1602.03161](#)]
- [5] P. Mastrolia, A. Primo and W. J. Torres Bobadilla, *Multi-gluon Scattering Amplitudes at One-Loop and Color-Kinematics Duality*, *In preparation* (2016)

Proceedings

- [6] W. J. Torres Bobadilla, A. R. Fazio, P. Mastrolia and E. Mirabella, *Generalised Unitarity for Dimensionally Regulated Amplitudes*, *Nucl. Part. Phys. Proc.* **267-269** (2015) 150–157, [[1505.05890](#)]
- [7] W. J. Torres Bobadilla, *Generalised unitarity for dimensionally regulated amplitudes within FDF*, in *Proceedings, 12th International Symposium on Radiative Corrections (Radcor 2015) and LoopFest XIV (Radiative Corrections for the LHC and Future Colliders): Los Angeles, CA, USA, June 15-19, 2015*, 2016. [1601.05742](#)
- [8] P. Mastrolia, T. Peraro, A. Primo and W. J. Torres Bobadilla, *Adaptive Integrand Decomposition*, *PoS* **LL2016** (2016) 007, [[1607.05156](#)]

Contents

Introduction	2
1 QCD Scattering Amplitudes	9
1.1 Colour-ordered amplitudes	10
1.2 Spinor-Helicity Formalism	13
1.2.1 Massless fermion wave functions	13
1.2.2 Massless vector boson wave functions	15
1.2.3 Parity and Charge Conjugation	15
1.2.4 Maximally Helicity Violating amplitudes	15
1.3 Britto-Cachazo-Feng-Witten Recursive relations	16
1.3.1 Derivation	16
1.4 Little group scaling	18
1.5 Momentum twistors	19
1.5.1 Definition	19
1.5.2 Momentum twistors variables	21
1.6 Discussion	23
2 On the Subleading-Soft Behaviour of QCD Amplitudes	25
2.1 Soft limit of gluon-amplitudes	25
2.2 Photon bremsstrahlung from quark-gluon amplitudes	27
2.2.1 Derivation from on-shell recursion	27
2.2.2 Derivation from gauge invariance	29
2.2.3 Connection between the two derivations	30
2.2.4 Examples	33
2.3 Soft-limit of quark-gluon amplitudes	35
2.3.1 Case 1: soft-gluon adjacent to the anti-quark and one gluon	35
2.3.2 Case 2: soft-gluon adjacent to two gluons	37
2.3.3 Examples	37
2.4 Discussion	40
3 Off-shell Currents and Colour-Kinematics Duality	41
3.1 Review of Colour-Kinematics duality	42
3.1.1 General considerations	42
3.1.2 Bern-Carrasco-Johansson relations	43
3.2 Off-shell Colour-Kinematics Duality	43
3.2.1 Scalars	44
3.2.2 Quarks	46
3.2.3 Gluons	47
3.3 Construction of dual numerators for higher-point amplitudes	49
3.3.1 Algorithm	49

3.3.2	Colour-kinematics duality for $gg \rightarrow gg$	52
3.3.3	Colour-kinematics duality for $gg \rightarrow q\bar{q}g$	53
3.4	Discussion	58
4	One-loop amplitudes	60
4.1	Tensor reduction	60
4.2	Unitarity based methods	62
4.2.1	Optical theorem	62
4.2.2	Generalised Unitarity	64
4.3	Ossola-Papadopoulos-Pittau decomposition	65
4.3.1	Fit on the cut at one loop	67
4.4	One-loop amplitudes via Laurent series expansion	69
4.4.1	Reduction algorithm	69
4.5	Discussion	72
5	Four-Dimensional-Formulation	73
5.1	Four-dimensional Feynman rules	73
5.2	Fermion and Boson wave functions within FDF	76
5.3	One-loop four-point amplitudes	78
5.3.1	The $gggg$ amplitude	79
5.3.2	The $ggq\bar{q}$ amplitude	82
5.3.3	The $gggH$ amplitude	85
5.4	UV renormalisation at one-loop	88
5.4.1	Renormalised QED Lagrangian	88
5.4.2	Renormalised QCD Lagrangian	90
5.5	Discussion	93
6	Multi-gluon and Higgs scattering amplitudes	94
6.1	Multi-gluon scattering amplitudes	95
6.1.1	Five-gluon amplitudes	95
6.1.2	Six-gluon amplitudes	97
6.2	Higgs plus gluon amplitudes	99
6.2.1	Higgs plus four gluon amplitudes	99
6.2.2	Higgs plus five gluon amplitudes	100
6.3	Discussion	101
7	Colour-Kinematics duality in d-dimensions	103
7.1	Tree-level identities in d -dimensions	103
7.2	Colour-kinematics duality for $g^\bullet g^\bullet (s^\bullet s^\bullet) \rightarrow q\bar{q}g$	107
7.3	Bern-Carrasco-Johansson relations in d -dimensions	109
7.4	Coefficient relations for one-loop amplitudes in d dimensions	110
7.4.1	Relations for pentagon coefficients	110
7.4.2	Relations for box coefficients	111
7.4.3	Relations for triangle coefficients	112
7.4.4	Relations for bubble coefficients	113
7.4.5	Examples	114
7.5	Discussion	120

8	Two-loop amplitudes	121
8.1	Basic notions	121
8.1.1	Integrand recurrence relation	122
8.1.2	All plus four-gluon amplitudes	122
8.2	Adaptive Integrand Decomposition	126
8.2.1	Definition	126
8.2.2	Algorithm	128
8.2.3	All plus five-gluon amplitudes	129
8.3	Discussion	132
	Conclusion	133
A	One-loop 2-point integrals	135
B	Further features of the Four-dimensional-formulation	137
B.1	One-loop equivalence	137
B.2	Proof of the completeness relations	138
B.3	Colour-ordered Feynman rules	138
C	Coefficient relations from 5-point BCJ identities	141
C.1	Relations for pentagon coefficients	141
C.2	Relations for box coefficients	142
C.3	Relations for triangle coefficients	143
C.4	Relations for bubble coefficients	143
	Acknowledgements	163

Introduction

After about a century of efforts to get unified theories for describing the fundamental forces in nature (strong nuclear, electromagnetic, weak nuclear and gravitational), the situation is perhaps reverse. Apart from the success of the unification of the weak interaction, still, there is the effort to try to unify gravitation and all the interactions. This investigation can start from mathematical schemes and then, look for the physical interpretation. Or, start with the physical principle and then, codify it into a mathematical form. Start from mathematical schemes always allows to create a delightful theory able to presume the physical behaviour of any physical system.

In order to describe the fundamental forces, we need to combine Special Relativity (SR) and Quantum Mechanics (QM) to formulate a Quantum Field Theory (QFT). QFT describes particles as quantum mechanical objects or quantum fields, in the sense that they obey the rules of QM. Furthermore, the definition and interactions of those fields are mathematically described by a symmetry group.

Currently, the Standard Model of Particle Physics (SM) is the best QFT model able to describe the interaction among elementary particles due to three of four forces existing in nature [9–13]. Gravitation, although being the most evident force is the weakest of the four forces and its proper quantum description is still an open issue. The SM consists of two basic ingredients: the electroweak theory, based on the symmetry group $SU(2)_L \times U(1)_Y$, which describes the electroweak interactions by combining the electromagnetic interaction of Quantum Electro-Dynamics (QED) and the weak interactions. And, Quantum Chromodynamics (QCD), whose symmetry group $SU(3)_c$, deals with strongly interacting particles. The latter is understood as an exact symmetry, while the former is predicted to be broken spontaneously via the Brout-Englert-Higgs mechanism. The Higgs particle is a scalar responsible of the spontaneous symmetry breaking and for all the masses of the other particles of the SM.

The huge success of the SM in predicting the experimental data confirmed its validation with the discovery of the Higgs boson by ATLAS and CMS experiments at the Large Hadron Collider (LHC), announced on the 4th of July of 2012 [14, 15]. This was, indeed, the missing piece to authenticate the validity of this theory. Nevertheless, the SM does not provide all the information of the subatomic world. The evidence of neutrino oscillations, which has been confirmed at the Super-Kamiokande experiment [16] and at the Sudbury Neutrino Observatory [17, 18], proved the existence of neutrino masses, that are not described by the SM. Additionally, the SM does not describe the existence of dark matter and dark energy, as well as, the asymmetric content of baryonic and antibaryonic matter in the universe.

Since the SM leaves too much physics without descriptions, the scientific community believes it must be part of a more complete and fundamental theory. Hence, new directions to describe physics beyond Standard Model (BSM) have been considered. So far there has been no evidence of new physics in the TeV region. Moreover, with the unexplored energy scales the LHC is currently running at, the evidence of new physics by either the production of new heavy particles or slight deviation of the measured SM parameter might manifest the physics BSM.

From these considerations, the LHC results point towards a refinement of our understanding of the SM physics. High precision predictions in such background processes are necessary in order

to possibly find and understand new physics at the TeV scale. Relevant observables are obtained from the computation of QCD scattering amplitudes. In particular, QCD is asymptotically free. Therefore, the strong coupling constant g becomes weak at large momentum transfers, justifying a perturbative expansion.

Scattering amplitudes have two main motivations. Firstly for their practical application in particle physics. Secondly, they have a mathematical elegance which attracts theoretical physicists. These motivations are very important and they complement each other. The first attempt to compute any scattering amplitude is based on a Lagrangian approach. Feynman rules are extracted and used to calculate a scattering amplitude, \mathcal{A} , as a sum of Feynman diagrams organised perturbatively in the loop expansion. From the scattering amplitudes we calculate the observables of interest for particle physics experiments, such as cross section, $\sigma \propto |\mathcal{A}|^2$. The scattering amplitudes are gauge invariant objects.

The Lagrangian approach is, in principle, suitable to compute any kind of process. Moreover, when increasing the multiplicity of the external particles or the order in the perturbation theory, we find that the calculation becomes cumbersome. The complexity of the calculation might arise from the intermediate states, due to the amount of indices contracted up and down in all the directions. And also, the number of Feynman diagrams to be considered starts increasing exponentially, not allowing to show any insight of the physics and any hint of simplicity.

Another issue is that each Feynman diagram, a gauge-dependent quantity, gets more complicated in its evaluation and in many cases impossible. It is true that the use of computer programs, that automatically generate matrix elements for multi-particle processes, can be really helpful. Nevertheless, the numerical evaluation sometimes does not take place, since spurious poles that might appear are canceled out between diagrams. Hence, compact expressions are desirable.

Despite of this, we can follow an alternative approach, where, instead of considering an unpolarised amplitude, whose squared will allow to write the cross section in terms of momentum invariants (Maldestam variables) and masses, we can split the calculation in several pieces. These pieces are the polarised or helicity amplitudes, which, can be seen as a complex number, whereby the cross section is obtained by simply squaring that number and sum over all possible configurations.

The helicity amplitudes are computed by picking a basis for the polarisation states of the external particles. In high energy physics, most of the particles are effectively massless. For massless fermions, their chirality and helicity coincide. Vector bosons are also described from their helicity. This fact allows us to write fermion and boson wave functions in terms of spinors, a procedure that is usually referred to as spinor-helicity formalism [19–22] and is used throughout this thesis. In this basis many tree-level amplitudes were found to vanish. In addition, compact and nice expressions were found, in particular the tree-level scattering amplitude with maximal helicity violation (MHV) found by Parke and Taylor [23]. This result was later proved recursively by Berends and Giele [24].

The use of the spinor-helicity formalism generated several outcomes in the computation of high-multiplicity tree-level processes. One of them, was that fact that by deforming real momenta in complex ones, keeping their on-shellness and asking them to satisfy momentum conservation, new properties for amplitudes arise. Indeed, Britto, Cachazo, Feng and Witten (BCFW) in Ref.s [25, 26] realised that with the use of complex kinematics and the analyticity of the S-matrix it is possible to work with on-shell quantities only. Consequently, this observation yields a recursive construction of the amplitude, in which, any colour-ordered helicity amplitude can be evaluated by breaking it down into amplitudes with a smaller number of legs. For instance, any n -point gluon amplitude can be straightforwardly computed by applying this recursion. The required ingredients are the basic building blocks, which are exactly, the MHV amplitudes. Besides massless theories, BCFW recursion formula has been successfully used in theories involving

the interplay of massless and massive particles [27–29].

In the context of one-loop calculations, the unitarity of the S-matrix has allowed to reconstruct an amplitude as the product of simpler ones. This framework defines the so-called unitarity based methods [30–41], nowadays, developed in a consistent way to perform one-loop calculations. Instead of the explicit set of loop Feynman integrals, the basic reference point is the linear expansion of the amplitude in terms of basis of Master Integrals (MIs), multiplied by coefficients that are rational functions of the kinematic variables, known as Passarino-Veltman decomposition [42]. The availability of the analytic expressions of MIs [43] has allowed us to focus on the development of efficient algorithms for extracting the coefficients multiplying each MI. Improved tensor decomposition [44], complex integration and contour deformation [45], on-shell and generalised unitarity methods, and integrand reduction techniques [41, 46–48] led to the explosion of new results in the computation of high multiplicity process at one-loop level. Several techniques have been automated [49–60], allowing to make phenomenological predictions in QFT.

The unitarity based methods, by putting on shell more than two propagators, allow to obtain the coefficients of the MIs by expanding the integrand of the tree level cut amplitudes into an expression that resembles the cut of the basis integrals. The dimensional regularisation is incorporated in this complex machinery. In fact, in dimensional regularisation, all one-loop amplitudes are cut-constructible, provided that the full dimensional dependence is kept in evaluating the branch cut. Each MI has a distinct branch cut, uniquely determined by its logarithmic and dilogarithmic arguments. Therefore, the decomposition in MIs can be used to solve for their coefficients separately using analytic properties. However, at integrand level a mathematical structure of the integrated amplitudes has been shown to be related to an universal decomposition valid for the integrand, called Ossola-Papadopoulos-Pittau (OPP) decomposition [46]. The coefficients of the MIs can be found by evaluating the integrand on multiple cuts.

More recently, a new approach to one-loop integrand reduction has been developed, namely the integrand reduction via Laurent expansion method [61], which elaborates on techniques first proposed in [39, 62] for analytic calculations. It turns out that within this approach, the computation of the coefficients of the MIs gets simpler when performing a Laurent expansion of the integrands with respect to the components of the loop momentum which are not constrained by the multiple-cut conditions.

Within integrand reduction methods, different approaches are available, according to the strategies adopted for the determination of cut-constructible and rational terms. In some algorithms, the computation of the two ingredients proceeds in two steps: the cut-constructible part is obtained by reducing the un-regularised integrand while the rational one is computed by introducing new counterterm-like diagrams which depend on the model under consideration [63, 64].

Other methods, instead, aim at the combined determination of the two ingredients by reducing the dimensionally regulated integrand. Therefore the numerator of the integrand has to be generated and manipulated in d dimensions and acquires a dependence on $(d - 4)$ and on the square of the $(d - 4)$ -dimensional components of the loop momentum [65–67]. The multi-particle residues are finally determined by performing generalised cuts by setting d -dimensional particles on shell.

If the integrand at a generic multiple cut is obtained as a product of tree-level amplitudes, the issues related to factorisation in presence of dimensional regularisation have to be addressed. An interesting approach [65] uses the linear dependence of the amplitude on the space-time dimensionality to compute the d -dimensional amplitude. In particular the latter is obtained by interpolating the values of the one-loop amplitude in correspondence to two different integer values of the space-time. When fermions are involved, the space-time dimensions have to admit an explicit representation of the Clifford algebra [66]. More recently, this idea has been combined

with the six-dimensional helicity formalism [68, 69] for the analytic reconstruction of one-loop scattering amplitudes in QCD via generalised unitarity.

In the context of multi-loop calculations, and in particular at two-loop, we can keep working with integrand reduction methods. However, it turns out that the basis of MIs is not known a priori as in the one-loop case. Therefore, the needed MIs are identified at the end of the reduction procedure. The most successful reduction method for higher loop amplitudes has been the so called integration by parts identities [70, 71], especially using the Laporta algorithm [72]. The computation of amplitudes beyond one-loop have been addressed using a wide range of techniques, such a difference [72, 73] and differential [74] equations, Mellin-Barnes integration [75], asymptotic expansions [76], sector decomposition [77], complex integration and contour deformation [78]. In the same manner, unitarity based methods at two-loop have been introduced for supersymmetric [79] and later applied to the case of QCD [80] amplitudes. More recently, a generalised unitarity approach has been proposed [81–88], which extracts the coefficients of the MIs by extending the one-loop OPP decomposition.

The use of the on-shell recursive relations within the spinor-helicity formalism allows to study, easily and directly, the behaviour of amplitudes in the soft regime. An amplitude displays an universal factorisation, into a soft and a hard contribution, when a particle becomes soft. Such factorisation is governed by the non-radiative process, perturbed by the action of operators that depend on the quantum numbers of the emitter, whose form can be derived by taking the soft limit when constructing the amplitude from recursive relations. At tree-level, for photon-, or similar gluon emission, as well as for graviton-emission, the leading terms in the momentum-expansion of a radiative amplitude are controlled by soft factors, whose shape was identified a long time ago [89, 90]. The recent study of Cachazo and Strominger, based on an on-shell recursive construction, about gravity [91], later extended to Yang-Mills [92, 93] and QCD amplitudes [94], pointed to the existence of differential operators that control the subleading behaviour. Likewise, these subleading-soft operators are found to depend on the total angular momentum (orbital and spin) of the radiator as explicit shown in Ref. [93] by following the proof of Low’s theorems [89, 95, 96]. The connection between the two derivations is carried out by comparing the results obtained from BCFW recursive relations and from gauge invariance.

The leading and subleading soft theorems have been generalised to arbitrary dimensions and other theories [97–110]. In [111–130], the theorem has been understood from various perspectives, especially those constraint by gauge and Poincarè symmetry. Double (or multiple) soft theorem limits [131–136], and generalisation to loop level [102, 137–142], have also been discussed.

Moreover, scattering amplitudes are found to admit the well known colour-kinematics (C/K) duality. The kinematic part of numerators of Feynman diagrams obey Jacobi identities and anti-symmetry relations similar to the ones holding for the corresponding structure constants of the Lie algebra. This property was discovered by Bern, Carrasco and Johansson [143, 144]. While first studies were interested in scattering amplitudes involving massless particles only, more recent ones drew their attention to the C/K-duality in gauge theory amplitudes containing (massless or massive) quarks or other particles in the fundamental representation of the gauge gauge [3, 145–152].

The C/K-duality led to linear relations between primitive tree amplitudes with different ordering in gauge theories, usually known as Bern-Carrasco-Johansson (BCJ) relations, whose coefficients depend on Lorentz-invariant combination of the momenta of the particles. These results together with $U(1)$ symmetry and Kleiss-Kuifj relations [153], can be used further to reduce the number of primitive amplitudes to be considered in tree-level calculations. C/K also yields a gauge-gravity dual representation of gravity amplitudes. The knowledge of the Yang-Mills amplitudes is recycled, in the sense that gauge-group structure constants are replaced by

a second copy of the C/K-dual numerator once the latter are organised to respect the duality. This is usually referred to as the double copy property [93, 154–182]. More details of these implications can be found in the recent review [183].

The BCJ relations were proved at tree-level by employing both string theory [156, 157, 161–164] and BCFW recursive relations [167–169]. Also, the generation of dual numerators starting from an effective Lagrangian was achieved in Ref. [184]. However, at loop level the duality is still a conjecture and has only been verified in examples. Up to two-loops in non-supersymmetric theories [93, 185, 186], and up to four loops in supersymmetric ones [144, 187–193]

Despite of the conjecture at multi-loop level, strong relations between one-loop integral coefficients have been studied for $\mathcal{N} = 4$ super Yang-Mills [157] and then, extended to the cut-constructible part of the QCD [194] one-loop amplitudes, by showing that the BCJ relations can significantly decrease the number of independent coefficients needed in one-loop calculations. When moving to d -dimensional generalised unitarity, extensions of tree-level identities to one-loop amplitudes are expected to hold also between rational contributions, as it was investigated in [195, 196].

By following a different approach, the BCJ relations have been used in [197] to reconstruct the non-planar two-loop integrand contributions to the all plus five-gluon amplitude from the planar ones.

In this thesis, we propose a four dimensional formulation (FDF) regularisation scheme, which at one-loop turns to be the extension of the four-dimensional helicity (FDH) scheme [32, 198, 199]. Within FDF, the d -dimensional regularisation of amplitudes can be carried out by using four dimensional ingredients only. In fact, the states in the loop are described as four dimensional massive particles. The four-dimensional degrees of freedom of the vector boson are carried by massive vectors bosons, while the $(d-4)$ -dimensional ones by real scalar particles obeying a simple set of four-dimensional Feynman rules. Instead, d -dimensional fermions are treated as tachyonic Dirac fields. The d -dimensional algebraic manipulations are replaced by four-dimensional ones complemented by a set of multiplicative selection rules.

Within integrand reduction methods, FDF allows for the simultaneous computation of both cut-constructible and rational part of one-loop amplitudes. By employing a four-dimensional representation, the formulation of generalised states running around the loop can be formulated. Therefore, a straightforward implementation of d -dimensional generalised unitarity within exactly four space-time dimensions can be realised, avoiding any higher-dimensional extension of either the Dirac [65, 66] or the spinor algebra [68].

The calculation of one-loop amplitudes, through generalised unitarity and integrand reduction methods from d -dimensional regulated amplitudes, is automated within the framework of FDF. This automation allows us to compute the one-loop QCD corrections of the processes: $gg \rightarrow q\bar{q}$, $gg \rightarrow ng$ with $n = 2, 3, 4$ [1, 6], and the Higgs and (up to three) gluons production via gluon fusion, $gg \rightarrow ngH$ with $n = 1, 2, 3$, in the heavy top mass limit [7].

Besides calculations of one-loop amplitudes within FDF, we also investigate the C/K-duality for dimensionally regulated amplitudes. We notice that the duality obeyed by the numerators of tree-level amplitudes within the FDF scheme are non-trivial relations involving the interplay of massless and massive particles. Furthermore, from the construction of dual numerators, we follow a diagrammatic approach and account for the knowledge of the gauge invariance of the amplitudes, finding BCJ relations for dimensionally regulated amplitudes, whose $(d-4)$ -dependence becomes explicit [3, 7].

Additionally, we combine the integrand reduction method via Laurent expansion and the set of BCJ identities to find relations between one-loop integral coefficients [4]. These relations can be established for the cut constructible contributions as well for the ones responsible for rational terms.

We also investigate on the low-energy behaviour of single-gluon radiation from QCD amplitudes with a quark pair and gluons. Upon colour decomposition [200], we can identify two situations according to the position of the soft gluon: *(i)* between an (anti)quark and a gluon, and *(ii)* between two gluons. Since the case *(ii)* is similar to the Yang-Mills case, discussed in Ref.s [92, 116] we focus on case *(i)*, where, the soft gluon can be radiated either from a gluon or from an (anti)quark. In order to derive the soft behaviour from fermionic emitters, we first analyse the QED case of photon bremsstrahlung from the quark line. For this case, we show the equivalence of the soft operators derived from gauge invariance and from the on-shell construction. This result is then, easily, extended to the quark-gluon amplitudes in QCD. We show that the leading and subleading soft terms in single-gluon emission of quark-gluon amplitudes in QCD is controlled by differential operators, whose universal form can be derived from both BCFW recursion and gauge invariance, as it was shown to hold for graviton- and gluon-scattering [2].

Finally, we review the development and applications of the integrand decomposition method for two-loop amplitudes. Since these methods rely on a new reformulation of the one-loop calculations. Firstly, we focus on the ones given by polynomial division module Gröbner basis. Within this framework, the calculation of the two-loop four-gluon amplitude [80] is carried out by following a diagrammatic approach. Similarly, we study basic and useful concepts of the new adaptive integrand decomposition (AID) method [201]. This method exploits the decomposition of space-time dimension in parallel and orthogonal subspaces, $d = d_{\parallel} + d_{\perp}$.

We apply AID to the two-loop five-gluon amplitude [8], finding agreement with known results [88]. These results correspond to a warming-up calculation and are oriented to develop algorithms and tools for the automated evaluation of two-loop scattering amplitudes, which, currently, is one of the main challenges the community is trying to solve.

This thesis is organised as follows: In Chapter 1, we recall all the concepts of QCD theory that are going to be useful throughout this thesis. From the Lagrangian and its symmetry group we show, as a first consequence of the theory, how the colour-dressed amplitudes can be decomposed in two terms. One depending on Lorentz variables only, usually called primitive amplitudes. The other one containing all the information regarding the colour-structure. The choice of the basis to compute helicity amplitudes are revisited, giving the proper study to fermion and boson wave functions. Within the spinor-helicity formalism we present the MHV amplitudes and the BCFW recursive relation, giving the main ingredients that are used in Chapter 2.

In Chapter 2, we study the behaviour of a radiative scattering amplitude in the soft regime. Since it is governed by the non-radiative process, perturbed by the action of operators that depend on the quantum numbers of the emitter, we approach it in two different and equivalent ways. The first one is based on recursive relations, whereas the second one takes into account the gauge invariance of the amplitude. While previous studies dealt with graviton and gluon amplitudes, we focus our description on QCD scattering amplitudes, in which the emitter can be either a fermion or a gluon. Each calculation is accompanied by explicit examples.

Chapter 3 is devoted to studying the relation between colour and kinematics of colour-dressed scattering amplitudes. As one of the main consequences of this duality, we review the fundamental BCJ relations and their properties. An alternative study of the colour-kinematics duality, based on a diagrammatic approach, is presented, which, with the knowledge of the gauge invariance of the amplitude, allows to end up with the set of BCJ relations. Explicit calculations for particles belonging to the adjoint (gluons and scalars) and fundamental (quarks) representations are considered. Furthermore, the derivation of the five-point BCJ relation is performed.

The description of one-loop amplitudes is presented in Chapter 4. We present a coherent description of the integrand reduction methods, starting from the tensor decomposition until the computation of one-loop amplitude via Laurent series expansion. Furthermore, we study the

formalism based on unitarity based methods, which turns out to be one of the main ingredients for the computations of multi-loop scattering amplitudes.

The four-dimensional-formulation (FDF) scheme is introduced in Chapter 5. All its features to compute one-loop amplitudes, by following either the traditional way of Feynman diagrams or the unitarity based approach, are discussed. For the latter, we provide explicit four-dimensional representations for the d -dimensional particles circulating into the the loop. Also, in order to satisfy the Clifford algebra in d -dimensions within FDF, we include a set of selection rules, which turn out to be just an internal symmetry and can be performed before doing any kind of reduction algorithm. Simple applications of the FDF, for the computation of d -dimensional regulated amplitudes, are given by presenting the one-loop analytic contribution of representatives four-point processes.

In Chapter 6, we show the analytic one-loop contributions, obtained by using the FDF scheme and the computation of one-loop via the Laurent series expansion, of multi-gluon- and Higgs plus gluon- amplitudes up to six external particles. We provide the full expression for the finite gluon amplitudes, $A_n^{1\text{-loop}}(1^+, \dots, n^+)$ and $A_n^{1\text{-loop}}(1^-, \dots, n^+)$, with $n = 5, 6$. While for the Higgs plus gluon amplitudes, we discuss the structure of $A_5^{1\text{-loop}}(H, 1^+, 2^+, 3^+, 4^+)$ and $A_6^{1\text{-loop}}(H, 1^+, 2^+, 3^+, 4^+, 5^+)$. Moreover, for the remaining helicity configurations of five-, six-gluon- and Higgs plus four-gluon-amplitudes we provide, for each one, a MATHEMATICA notebook file containing the list of coefficients for each MIs. The coefficients of the MIs are written in terms of momentum twistors variables.

The discussion of the C/K duality in d -dimensions is addressed in Chapter 7. Within FDF, we follow the very same diagrammatic approach of Chapter 3. The C/K-duality for the d -dimensional case, as for the four-dimensional case, is recovered by using momentum conservation and on-shellness of the particles. The d -dimensional regulated particles satisfy $p_i^2 = \mu^2$. Also, the BCJ relations are obtained for d -dimensional regulated amplitudes. On top of it, we show that the use of these BCJ relations together with the generalised unitarity and the integrand reduction yields the existence of relations between the integrand residues of partial amplitudes with different orderings of the external particles.

An introduction to two-loop techniques, based on integrand reduction methods is addressed in Chapter. 8. We first provide a description of the most used algorithm, which turns out to be the polynomial division module Gröbner basis. Then, we study the main feature of the adaptive integrand decomposition. The computation of the all plus two-loop four- and five-gluon amplitudes is presented.

Finally, in appendix B we collect additional features of the FDF, such as the one-loop equivalence between the regularisation schemes FDH and FDF. We also prove the completeness relation of generalised fermions and give the set of colour-order Feynman rules. In Appendix C we extend the results of Section 7.4 by providing the set of coefficient relations that can be derived from the BCJ identities between five-point amplitudes.

All algebraic manipulations and numerical evaluations have been carried out by using the MATHEMATICA packages FEYNARTS [202], FEYNCALC [203, 204], S@M [205] and T@M [206].

Chapter 1

QCD Scattering Amplitudes

Quantum Chromodynamics (QCD) is a non-abelian gauge theory based on the local symmetry group $SU(N_c)$ with $N_c = 3$. There exist n_f flavours of quarks (fermions of spin 1/2) and gluons (gauge bosons that mediate the interactions). This theory allows us to describe the dynamics of the strong nuclear force. The action for the path integral quantisation of the theory is

$$\mathcal{L} = -\frac{1}{4}F_{\mu\nu}^a F^{a\mu\nu} + \sum_{f=1}^{n_f} \bar{\psi}_f^i \left(i\gamma^\mu D_\mu^{i\bar{j}} - m_f \delta^{i\bar{j}} \right) \psi_f^j + \mathcal{L}_{GF} + \mathcal{L}_{FP}, \quad (1.1)$$

where the field tensor $F_{\mu\nu}^a$ can be written in terms of the gluon field, A_μ^a , as

$$F_{\mu\nu}^a = \partial_\mu A_\nu^a - \partial_\nu A_\mu^a + g_s f^{abc} A_\mu^b A_\nu^c, \quad (1.2)$$

which also defines the covariant derivative in the fundamental representation

$$(D_\mu)_{i\bar{j}} = \delta_{i\bar{j}} \partial_\mu - i g_s t_{i\bar{j}}^a A_\mu^a. \quad (1.3)$$

Furthermore, the ψ_f^i 's are the flavours f of quarks (anti-quarks) transforming into the fundamental (anti-fundamental) representation of $SU(N_c)$. Fundamental colour indices are denoted by $i_1, i_2, \dots \in \{1, 2, \dots, N_c\}$. Whereas, adjoint colour indices are denoted by $a, b, c, \dots a_i \in \{1, 2, \dots, N_c^2 - 1\}$. In these equations, g_s is the coupling constant of the interaction, whereas f^{abc} and t^a are the structure constants and the generators of the symmetry group $SU(N_c)$ respectively. The suffixes of the Lagrangian (1.1) stand for ‘‘gauge fixing’’ and ‘‘Faddeev-Popov’’,

$$\mathcal{L}_{GF} = -\frac{1}{2\xi} (\partial_\mu A^\mu)^2, \quad \mathcal{L}_{FP} = \partial^\mu \chi^a \mathcal{D}_\mu^{ab} \chi^b. \quad (1.4)$$

with

$$\mathcal{D}_\mu^{ab} = \delta^{ab} \partial_\mu - g_s f^{abc} A_\mu^c, \quad (1.5)$$

the covariant derivative in the adjoint representation. The choice of the parameter ξ determines the choice of the gauge. The typical choices of ξ are the Landau gauge, obtained by taking the limit $\xi \rightarrow 0$ and the Feynman-'t Hooft gauge, in which $\xi = 1$.

In the following, we review the efficient techniques to compute scattering amplitudes in QCD, which on the one hand, are based on the colour and helicity information and, on the other, on the analyticity and unitarity of the scattering-matrix. These techniques will allow us to work with gauge invariant objects only.

1.1 Colour-ordered amplitudes

The calculation of multi-gluon scattering amplitudes in perturbative QCD is very challenging, since the number of Feynman diagrams describing a given process grows very quickly. This proliferation of terms is due to the redundancy of the gauge-dependent pieces. Therefore, one way to simplify those calculations is dividing our amplitude (or set of diagrams) in terms of gauge-invariant pieces, meaning invariant under redefinition of the polarisation:

$$\varepsilon_i^\mu(p_i) \rightarrow \varepsilon_i^\mu(p_i) + \alpha_i(p_i) p_i^\mu, \quad (1.6)$$

with $\alpha_i(p_i)$'s being arbitrary functions.

In general, any scattering amplitude in a non-Abelian gauge theory can be decomposed in an orthogonal basis in the colour space. This decomposition brings to gauge invariant pieces. We identify the orthogonal linear independent colour structures by strings of $SU(N)$ generators.

We represent the generators of $SU(N_c)$ by the rescale Hermitian traceless matrices $T_{ij}^a = t_{ij}^a/\sqrt{2}$, so that T_{ij}^a 's are normalised to

$$\text{Tr}(T^a T^b) = \delta^{ab}. \quad (1.7)$$

The structure constants, defined by,

$$[T^a, T^b] = i\sqrt{2}f^{abc}T^c, \quad (1.8)$$

$$f^{abc} = -\frac{i}{\sqrt{2}}\text{Tr}\left([T^a, T^b]T^c\right), \quad (1.9)$$

satisfy the Jacobi identity,

$$f^{ade}f^{bce} + f^{bde}f^{cae} + f^{cde}f^{abd} = 0. \quad (1.10)$$

Writing all structure constants according to (1.9) produces linear combinations of strings of T^a 's. Therefore, in order to reduce the number of traces we perform a ‘Fierz rearrange’,

$$T_{i_1\bar{j}_1}^a T_{i_2\bar{j}_2}^a = \delta_{i_1\bar{j}_2}\delta_{i_2\bar{j}_1} - \frac{1}{N_c}\delta_{i_1\bar{j}_2}\delta_{i_2\bar{j}_1}. \quad (1.11)$$

Thus, an n -gluon tree amplitude can be reduced by a trace-based colour decomposition to a sum of colour-ordered amplitudes [207–211],

$$\mathcal{A}_n^{\text{tree}}(\{p_i, h_i, a_i\}) = g^{n-2} \sum_{\sigma \in S_n/Z_n} \text{Tr}(T^{a_{\sigma(1)}} \dots T^{a_{\sigma(n)}}) A_n^{\text{tree}}(\sigma(1^{h_1}), \dots, \sigma(n^{h_n})). \quad (1.12)$$

Moreover, we can stay with the colour structure or often called ‘ f ’-basis of Del Duca-Dixon-Maltoni [212–214]

$$\mathcal{A}_n^{\text{tree}}(\{p_i, h_i, a_i\}) = (ig)^{n-2} \sum_{\sigma \in S_{n-2}} f^{a_1 a_2 x_1} f^{x_1 a_3 x_2} \dots f^{x_{n-3} a_{n-1} a_n} A_n^{\text{tree}}(1^{h_1}, \sigma(2^{h_2}), \dots, n^h). \quad (1.13)$$

In Eq.s (1.12, 1.13), $\mathcal{A}_n^{\text{tree}}$ is the full amplitude, with dependence on the external gluon momentum $p_i, i = 1, 2, \dots, n$, helicities $h_i = \pm 1$, and adjoint indices a_i . Whereas, A_n^{tree} 's are the primitive amplitudes stripped by the colour factors but with all the kinematic informations. Primitive amplitudes accompanied by colour factors are called colour-ordered amplitudes.

These primitive amplitudes, denoted here generically by $A_n^{\text{tree}}(1, 2, \dots, n)$, are by construction colour independent and satisfy a number of important properties and relationships¹:

¹A detailed discussion about the topic can be found in Ref.s [215, 216]

- $A_n^{\text{tree}}(1, 2, \dots, n)$ is gauge invariant.
- Factorisation of $A_n^{\text{tree}}(1, 2, \dots, n)$ on multi-gluon poles.
- *Cyclic invariance:*

$$A_n^{\text{tree}}(1, 2, \dots, n) = A_n^{\text{tree}}(2, \dots, n, 1), \quad (1.14)$$

This statement follows from the trace structure of the colour-order amplitude. Cyclic invariance allows us to fix one external particle at a specified position, say position 1. This reduces the number of independent primitive amplitudes to $(n - 1)!$.

- *Reflection invariance:*

$$A_n^{\text{tree}}(n, n - 1, \dots, 2, 1) = (-1)^n A_n^{\text{tree}}(1, 2, \dots, n). \quad (1.15)$$

- *The photon decoupling identity:*

$$A_n^{\text{tree}}(1, 2, 3, \dots, n) + A_n^{\text{tree}}(2, 1, 3, \dots, n) + \dots + A_n^{\text{tree}}(2, 3, \dots, 1, n) = 0. \quad (1.16)$$

This relation follows from taking one of the generators T^a proportional to the identity matrix.

- *Kleiss-Kuijf relations:*

$$A_n^{\text{tree}}(1, \alpha_1, \dots, \alpha_j, n, \beta_1, \dots, \beta_{n-2-j}) = (-1)^{n-2-j} \sum_{\sigma \in \vec{\alpha} \sqcup \vec{\beta}^T} A_n^{\text{tree}}(1, \sigma_1, \dots, \sigma_{n-2-j}, n). \quad (1.17)$$

Here, $\vec{\alpha} = \{\alpha_1, \dots, \alpha_n\}$, $\vec{\beta}^T = \{\beta_{n-2-j}, \dots, \beta_2, \beta_1\}$, and $\vec{\alpha} \sqcup \vec{\beta}^T$ denotes the set of all shuffles of $\vec{\alpha}$ with $\vec{\beta}^T$, i.e. the set of all perturbations of the elements $\vec{\alpha}$ and $\vec{\beta}^T$, which preserve the relative order of the elements of $\vec{\alpha}$ and of the elements $\vec{\beta}^T$. The Kleiss-Kuijf relations allow us to fix two external particles, say 1 and n . This reduces the number of independent primitive amplitudes to $(n - 2)!$ [153].

- *Bern-Carrasco-Johansson relations:*

$$\sum_{i=3}^n \left(\sum_{j=3}^i s_{2j} \right) A_n^{\text{tree}}(1, 3, \dots, i, 2, i+1, \dots, n) = 0. \quad (1.18)$$

where $s_{2j} = (p_2 + p_j)^2$. The Bern-Carrasco-Johansson relations allow us to fix three external particles, say 1, 2 and n . Therefore, the number of independent primitive amplitudes is reduced to $(n - 3)!$ [143].

A deep study of the Bern-Carrasco-Johansson relations shall be given in Chap.s 3 and 7, for tree-level amplitudes in four- and in d -dimensions respectively.

Similarly, tree amplitudes with two external quarks and $(n - 2)$ gluons can be reduced to single strings of T^a matrices,

$$\begin{aligned} \mathcal{A}_n^{\text{tree}}(1_q, 2, \dots, n-1, n_{\bar{q}}) \\ = g^{n-2} \sum_{\sigma \in S_n/Z_n} (T^{a_{\sigma(2)}} \dots T^{a_{\sigma(n-1)}})_{i_1 \bar{j}_n} A_n^{\text{tree}}(1_q, \sigma(2), \dots, \sigma(n-1), n_{\bar{q}}). \end{aligned} \quad (1.19)$$

In Eq. (1.19), we have omitted the helicity labels, and numbers without subscripts in the argument of A_n^{tree} refer to gluons. There are $(n - 2)!$ terms corresponding to all possible gluon orderings between quarks.

With the prescriptions given in Eq.s. (1.12,1.19), we can write a set of colour-ordered Feynman rules for QCD in 't Hooft-Feynman gauge,

$$\begin{array}{c} \bullet \\ \alpha \end{array} \begin{array}{c} \text{-----} \\ \text{wavy} \\ \text{-----} \\ \beta \end{array} \begin{array}{c} k \\ \text{-----} \\ \bullet \end{array} = -i \frac{g^{\alpha\beta}}{k^2 + i0}, \quad (1.20a)$$

$$\begin{array}{c} \bullet \\ \text{-----} \\ \bullet \end{array} \begin{array}{c} k \\ \text{-----} \\ \bullet \end{array} = i \frac{\not{k} + m}{k^2 - m^2 + i0}, \quad (1.20b)$$

$$\begin{array}{c} \bullet \\ \text{-----} \\ a \end{array} \begin{array}{c} k \\ \text{-----} \\ \bullet \end{array} \begin{array}{c} \text{-----} \\ \text{dotted} \\ \text{-----} \\ b \end{array} = i \frac{1}{k^2 + i0}, \quad (1.20c)$$

$$\begin{array}{c} \text{-----} \\ \text{wavy} \\ \text{-----} \\ 1, \alpha \end{array} \begin{array}{c} 2, \beta \\ \text{-----} \\ \text{wavy} \\ \text{-----} \\ 3, \gamma \end{array} = \frac{i}{\sqrt{2}} [g_{\alpha\beta}(k_1 - k_2)_\gamma + g_{\beta\gamma}(k_2 - k_3)_\alpha + g_{\gamma\alpha}(k_3 - k_1)_\beta], \quad (1.20d)$$

$$\begin{array}{c} \text{-----} \\ \text{wavy} \\ \text{-----} \\ 1, \alpha \end{array} \begin{array}{c} 2, \beta \\ \text{-----} \\ \text{wavy} \\ \text{-----} \\ 3, \gamma \end{array} = ig_{\alpha\gamma}g_{\beta\delta} - \frac{i}{2}(g_{\alpha\beta}g_{\gamma\delta} + g_{\alpha\delta}g_{\beta\gamma}), \quad (1.20e)$$

$$\begin{array}{c} \text{-----} \\ \text{solid} \\ \text{-----} \\ 1 \end{array} \begin{array}{c} 2, \beta \\ \text{-----} \\ \text{wavy} \\ \text{-----} \\ 3 \end{array} = -\frac{i}{\sqrt{2}}\gamma^\beta, \quad \begin{array}{c} \text{-----} \\ \text{solid} \\ \text{-----} \\ 1 \end{array} \begin{array}{c} 2, \beta \\ \text{-----} \\ \text{wavy} \\ \text{-----} \\ 3 \end{array} = \frac{i}{\sqrt{2}}\gamma^\beta, \quad (1.20f)$$

$$\begin{array}{c} \text{-----} \\ \text{wavy} \\ \text{-----} \\ 1, \alpha, \alpha \end{array} \begin{array}{c} 2, b \\ \text{-----} \\ \text{dotted} \\ \text{-----} \\ 3, c \end{array} = \frac{i}{\sqrt{2}}k_2^\alpha. \quad (1.20g)$$

In order to understand how the colour decomposition works, we consider the simplest example of the four-gluon tree-level amplitude. Starting with the diagrams that contribute to this process, $0 \rightarrow 1(p_1) 2(p_2) 3(p_3) 4(p_4)$,

$$\begin{array}{c} 2 \\ \text{-----} \\ \text{wavy} \\ \text{-----} \\ 1 \end{array} \begin{array}{c} \text{-----} \\ \text{wavy} \\ \text{-----} \\ 3 \end{array} \begin{array}{c} \text{-----} \\ \text{wavy} \\ \text{-----} \\ 4 \end{array} + \begin{array}{c} 2 \\ \text{-----} \\ \text{wavy} \\ \text{-----} \\ 1 \end{array} \begin{array}{c} \text{-----} \\ \text{wavy} \\ \text{-----} \\ 3 \end{array} \begin{array}{c} \text{-----} \\ \text{wavy} \\ \text{-----} \\ 4 \end{array} + \begin{array}{c} 2 \\ \text{-----} \\ \text{wavy} \\ \text{-----} \\ 1 \end{array} \begin{array}{c} \text{-----} \\ \text{wavy} \\ \text{-----} \\ 3 \end{array} \begin{array}{c} \text{-----} \\ \text{wavy} \\ \text{-----} \\ 4 \end{array} + \begin{array}{c} 2 \\ \text{-----} \\ \text{wavy} \\ \text{-----} \\ 1 \end{array} \begin{array}{c} \text{-----} \\ \text{wavy} \\ \text{-----} \\ 3 \end{array} \begin{array}{c} \text{-----} \\ \text{wavy} \\ \text{-----} \\ 4 \end{array}, \quad (1.21)$$

The four diagram in (1.21) can be split into

$$c_4 n_4 = n_{4;s} f^{a_1 a_2 b} f^{a_3 a_4 b} + n_{4;t} f^{a_4 a_1 b} f^{a_2 a_3 b} + n_{4;u} f^{a_1 a_3 b} f^{a_2 a_4 b}, \quad (1.22)$$

adding the four contributions up, the amplitude becomes,

$$\begin{aligned} \mathcal{A}_4^{\text{tree}}(1, 2, 3, 4) &= \left(\frac{n_s}{s} + n_{4;s}\right) f^{a_1 a_2 b} f^{a_3 a_4 b} + \left(\frac{n_t}{t} + n_{4;t}\right) f^{a_4 a_1 b} f^{a_2 a_3 b} \\ &\quad + \left(\frac{n_u}{u} + n_{4;u}\right) f^{a_1 a_3 b} f^{a_2 a_4 b}. \end{aligned} \quad (1.23)$$

being s, t and u the Mandelstam invariants and, n 's the numerators of each diagram. Working out the product of the structure constants, we get,

$$-f^{a_1 a_2 b} f^{a_3 a_4 b} = \left\{ \frac{1}{2} [\text{tr}(T^{a_1} T^{a_2} T^{a_3} T^{a_4}) + \text{tr}(T^{a_4} T^{a_3} T^{a_2} T^{a_1})] \right\} - \{[1 \leftrightarrow 2]\}, \quad (1.24)$$

Hence, the colour-dressed four-gluon amplitude admits the following decomposition

$$\begin{aligned} \mathcal{A}_4^{\text{tree}}(1, 2, 3, 4) &= A_4^{\text{tree}}(1, 2, 3, 4) [\text{tr}(T^{a_1} T^{a_2} T^{a_3} T^{a_4}) + \text{tr}(T^{a_4} T^{a_3} T^{a_2} T^{a_1})] \\ &\quad + \text{non-cyclic perm's.} \end{aligned} \quad (1.25)$$

This confirms that only the primitive amplitude $A_4^{\text{tree}}(1, 2, 3, 4)$ is needed as stated in Eq (1.12).

A similar study can be done for one-loop scattering amplitudes, where, instead of single strings of T^a matrices we have the product of strings. For instance, in the pure gluon case, we have [211]

$$\begin{aligned} \mathcal{A}_n^{1\text{-loop}} &= g^n \sum_{c=1}^{[n/2]+1} \sum_{\sigma \in S_n/S_{n;c}} \text{Gr}_{n;c}(\sigma) A_{n;c}^{1\text{-loop}}(\sigma), \\ \text{Gr}_{n;1}(\sigma) &= N_c \text{Tr}(T^{a_{\sigma(1)}} \dots T^{a_{\sigma(n)}}), \\ \text{Gr}_{n;c}(\sigma) &= N_c \text{Tr}(T^{a_{\sigma(1)}} \dots T^{a_{\sigma(c-1)}}) \text{Tr}(T^{a_{\sigma(c)}} \dots T^{a_{\sigma(c-1)}}), \quad c > 1. \end{aligned} \quad (1.26)$$

As described before, $A_{n;c}^{1\text{-loop}}$'s are the primitive amplitudes computed through the set of colour-ordered Feynman rules (1.20), and $[m]$ is the greatest integer less than or equal to m .

1.2 Spinor-Helicity Formalism

The spinor helicity formalism [19–22] has shown delightful results due to the compact representation one achieves in the perturbative computation of scattering amplitudes at tree- and multi-loop level. Since this formalism relies on the fundamental spinor products, it clearly captures the analytic properties of amplitudes, like the factorisation behaviour on multi-particle channels. As well, the study of soft and collinear limits.

This section is devoted to reviewing the main features of this formalism. We start with the definition of spinor products and polarisation vectors. Further details on the topic can be found in Ref.s [217, 218].

1.2.1 Massless fermion wave functions

Consider a massless fermion of momentum p_i^μ . The spinor for this fermion satisfies the Dirac equation

$$\not{p}_i u(p_i) = 0. \quad (1.27)$$

This equation has two solutions, $u_-(p_i)$ and $u_+(p_i)$, for the left- and right-handed fermions respectively. These satisfy,

$$P_\pm u_\pm(p_i) = \frac{1}{2}(1 \pm \gamma^5)u_\pm(p_i) = u_\pm(p_i), \quad (1.28)$$

The spinors v for anti-particles, in the massless case, obey the same equation. Therefore, we can choose them to be equal to the ones for particles, namely $v_\pm(p_i) = u_\mp(p_i)$.

We define the square and angle brackets

$$\begin{aligned} |i\rangle &\equiv u_+(p_i) = v_-(p_i), & [i] &\equiv u_-(p_i) = v_+(p_i), \\ \langle i| &\equiv \bar{u}_-(p_i) = \bar{v}_+(p_i), & [i] &\equiv \bar{u}_+(p_i) = \bar{v}_-(p_i), \end{aligned} \quad (1.29)$$

The anti-symmetric spinor products

$$\langle ij\rangle \equiv \bar{u}_-(p_i) u_+(p_j), \quad [ij] \equiv \bar{u}_+(p_i) u_-(p_j).$$

Furthermore, because of the Gordon identity, we can connect the momentum p_i^μ to spinor products,

$$p_i^\mu = \frac{1}{2} \langle i | \gamma^\mu | i \rangle = \frac{1}{2} [i | \gamma^\mu | i], \quad (1.30)$$

or vice versa,

$$|i\rangle [i] = \frac{1}{2} (1 + \gamma^5) \not{p}_i, \quad |i] \langle i| = \frac{1}{2} (1 - \gamma^5) \not{p}_i. \quad (1.31)$$

These spinor products satisfy a series of useful identities,

$$\langle ij \rangle = -\langle ji \rangle, \quad [ij] = -[ji], \quad \langle ii \rangle = [ii] = 0, \quad \langle ij \rangle = [ij] = 0, \quad s_{ij} = \langle ij \rangle [ji]. \quad (1.32)$$

We can express $\text{tr}(\gamma_5 \not{p}_1 \not{p}_2 \not{p}_3 \not{p}_4)$ and $\text{tr}(\not{p}_1 \not{p}_2 \not{p}_3 \not{p}_4)$ as

$$\begin{aligned} \text{tr}(\gamma_5 \not{p}_1 \not{p}_2 \not{p}_3 \not{p}_4) &= \text{tr}_5(1234) = [1 | 234 | 1] - \langle 1 | 234 | 1 \rangle, \\ \text{tr}(\not{p}_1 \not{p}_2 \not{p}_3 \not{p}_4) &= \text{tr}(1234) = \langle 1 | 234 | 1 \rangle + [1 | 234 | 1]. \end{aligned} \quad (1.33)$$

The Fierz rearrangement,

$$\langle i | \gamma^\mu | j \rangle \langle k | \gamma_\mu | l \rangle = 2 \langle ik \rangle [lj], \quad (1.34)$$

charge conjugation,

$$\langle i | \gamma^\mu | j \rangle = [j | \gamma^\mu | i], \quad (1.35)$$

Schouten identity,

$$\begin{aligned} \langle ij \rangle \langle kl \rangle + \langle ik \rangle \langle lj \rangle + \langle il \rangle \langle jk \rangle &= 0, \\ [ij] [kl] + [ik] [lj] + [il] [jk] &= 0. \end{aligned} \quad (1.36)$$

We set the convention to convert spinors $|-k\rangle$ into $|k\rangle$,

$$|-k\rangle = i |k\rangle, \quad |-k] = i |k]. \quad (1.37)$$

So far we have not made use of the explicit representations for angle and square-spinors; this is because we can work abstractly with $|i\rangle$ and $|i]$ and, later relate the results to the momentum vectors. Nevertheless, in order to carry out numerical computations, we define those spinors in terms of momentum vector components. In more details, we define the components of angle and square spinors as follows,

$$|i\rangle = \begin{pmatrix} \xi_i \\ \eta_i \end{pmatrix}, \quad |i] = \begin{pmatrix} \bar{\xi}_i \\ \bar{\eta}_i \end{pmatrix}, \quad (1.38)$$

with the anti-symmetric spinor products,

$$\langle ij \rangle = -\xi_i \eta_j + \xi_j \eta_i, \quad [ij] = \bar{\xi}_i \bar{\eta}_j - \bar{\xi}_j \bar{\eta}_i, \quad (1.39)$$

being automatically satisfied all Schouten identities.

The calculable expressions of angle and square spinors in terms of momenta are

$$|i\rangle = \frac{1}{\sqrt{p_i^+}} \begin{pmatrix} p_i^+ \\ p_i^- e^{+i\varphi_k} \end{pmatrix}, \quad |i] = \frac{1}{\sqrt{p_i^+}} \begin{pmatrix} p_i^- e^{-i\varphi_k} \\ -p_i^+ \end{pmatrix}. \quad (1.40)$$

with

$$p_i^\pm = p_i^0 \pm p_i^3, \quad p_i^\perp = p_i^1 + i p_i^2 = |p^\perp| e^{i\varphi_k} = \sqrt{p_i^+ p_i^-} e^{i\varphi_k}, \quad e^{\pm i\varphi_k} = \frac{p_i^\pm}{\sqrt{p_i^+ p_i^-}}, \quad (1.41)$$

1.2.2 Massless vector boson wave functions

One can also define polarisation vectors for right- and left-handed massless gauge bosons as,

$$\begin{aligned}\varepsilon_+^\mu(p_i; q) &= -\frac{\langle i | \gamma^\mu | q \rangle}{\sqrt{2} [qi]}, & \varepsilon_-^\mu(p_i; q) &= \frac{[i | \gamma^\mu | q \rangle}{\sqrt{2} \langle qi \rangle}, \\ \varepsilon_+^{*\mu}(p_i; q) &= \frac{\langle q | \gamma^\mu | i \rangle}{\sqrt{2} \langle qi \rangle}, & \varepsilon_-^{*\mu}(p_i; q) &= -\frac{[q | \gamma^\mu | i \rangle}{\sqrt{2} [qi]},\end{aligned}\quad (1.42)$$

which are defined in terms of both, the momentum vector p_i and a reference vector q_i . The gauge invariance of the scattering amplitudes allows to choose any arbitrary reference momentum q_i satisfying $p_i \cdot q_i \neq 0$. This arbitrariness can be seen by examining the difference between two choices of q_i ,

$$\varepsilon_+^{*\mu}(p_i; r) - \varepsilon_+^{*\mu}(p_i; s) = \sqrt{2} \frac{\langle sr \rangle}{\langle ri \rangle \langle si \rangle} p_i^\mu, \quad (1.43)$$

showing that this ‘‘gauge-function’’ will not give any contribution to the amplitudes because of gauge invariance, (1.6).

These vectors have the usual properties

$$\begin{aligned}(\varepsilon^\pm)^* &= \varepsilon^\mp, & \varepsilon^\pm \cdot \varepsilon^\pm &= 0, & \varepsilon^\pm \cdot \varepsilon^\mp &= -1, \\ \varepsilon_+^\mu \varepsilon_+^{*\nu} + \varepsilon_-^\mu \varepsilon_-^{*\nu} &= -g^{\mu\nu} + \frac{p_i^\mu q^\nu + q^\mu p_i^\nu}{q \cdot p_i}.\end{aligned}\quad (1.44)$$

In addition, under an azimuthal rotation about p_i axis, polarisation vectors left- and right-handed transform as required for helicities +1 and -1,

$$\begin{aligned}\varepsilon_+^\mu(p_i, q) &\rightarrow \frac{\langle i' | \gamma^\mu | q \rangle}{\sqrt{2} [qi']} = e^{i\phi} \varepsilon_+^\mu(p_i, q), \\ \varepsilon_-^\mu(p_i, q) &\rightarrow \frac{[i' | \gamma^\mu | q \rangle}{\sqrt{2} [qi']} = e^{-i\phi} \varepsilon_-^\mu(p_i, q),\end{aligned}\quad (1.45)$$

due to the transformation of the angle and square bracket,

$$|i\rangle \rightarrow |i'\rangle = e^{i\phi/2} |i\rangle, \quad |i\rangle \rightarrow |i'\rangle = e^{-i\phi/2} |i\rangle. \quad (1.46)$$

1.2.3 Parity and Charge Conjugation

Within the spinor-helicity formalism, we get further simplifications by simply making use of the discrete symmetries of parity and charge conjugation. Parity simultaneously reverses all helicities in an amplitude; for example Eq.s (1.42) show that it is implemented by the exchange $\langle qk \rangle \leftrightarrow [kq]$. Charge conjugation is related to the anti-symmetry of the colour-ordered rules; for pure gluon primitive amplitudes it takes the form of a reflected identity

$$A_n^{\text{tree}}(1, 2, \dots, n) = (-1)^n A_n^{\text{tree}}(n, \dots, 2, 1), \quad (1.47)$$

whereas, for amplitudes with external quarks, it allows us to exchange a quark and an anti-quark.

1.2.4 Maximally Helicity Violating amplitudes

An important and compact result obtained within the spinor helicity formalism was observed by Parke and Taylor [23]. It classifies n -gluon amplitudes by the number of negative-helicity gluons occurring in them. Tree amplitudes with less than two negative helicity gluons vanish,

$$A_n^{\text{tree}}(1^\pm, \dots, i^+, \dots, j^+ \dots, n^+) = 0, \quad (1.48)$$

whereas, their formula for a maximally-helicity-violating (MHV) gluon amplitude, with two negative helicity gluons reads

$$A_n^{\text{tree}}(1^+, \dots, i^-, \dots, j^-, \dots, n^+) = i \frac{\langle ij \rangle^4}{\langle 12 \rangle \langle 23 \rangle \dots \langle (n-1) n \rangle \langle n1 \rangle}. \quad (1.49)$$

Similarly, the MHV amplitudes for processes with a pair of massless quark-antiquark,

$$A_n^{\text{tree}}(1_q^-, 2^+, \dots, i^-, \dots, (n-1)^+, n_q^+) = i \frac{\langle 1i \rangle^3 \langle ni \rangle}{\langle 12 \rangle \langle 23 \rangle \dots \langle (n-1) n \rangle \langle n1 \rangle}. \quad (1.50)$$

In order to build the MHV amplitudes for n gluons, we start considering the three-gluon amplitude

$$A_3^{\text{tree}}(1^-, 2^-, 3^+) = i \frac{\langle 12 \rangle^4}{\langle 12 \rangle \langle 23 \rangle \langle 31 \rangle}. \quad (1.51)$$

Moreover, there is an implication coming from momentum conservation, $p_1 + p_2 + p_3 = 0$, that says $s_{12} = s_{13} = s_{23} = 0$. Therefore, Eq. (1.51) has a meaning when the momenta is promoted to be complex. Making this distinction, we set

$$\langle 12 \rangle \neq \langle 23 \rangle \neq \langle 31 \rangle \neq 0, \quad [12] = [23] = [31] = 0, \quad (1.52)$$

where all three left-handed spinors haven been chosen to be proportional, $|1\rangle = c_1 |3\rangle$, $|3\rangle = c_2 |2\rangle$, while the right-handed spinors are not proportional, but obey the relation, $c_1 |1\rangle + c_2 |2\rangle + |3\rangle = 0$. For this kinematic choice, the tree-level primitive amplitude $A_3^{\text{tree}}(1^-, 2^-, 3^+)$ is non-zero, even though all momentum invariants vanish.

1.3 Britto-Cachazo-Feng-Witten Recursive relations

An important fact of the MHV amplitudes is their simplicity and what is extremely useful is that any n -point amplitude can be computed by considering their simplest block, Eq. (1.51). This, indeed, can be done working with off-shell quantities only. Moreover, thanks to Britto, Cachazo, Feng and Witten (BCFW) there was a transition between off- and on-shell quantities, which allowed to use main ideas of the analyticity of the S-matrix to reconstruct full scattering amplitudes [25, 26]. As shown in the previous section, the extension of real to complex momenta makes sense when reusing null amplitudes that vanish for the former. In addition, complex kinematics exploits analytic properties that are not visible for real ones.

BCFW recursive formula introduces an algorithm to calculate efficiently, and in a recursive way, all tree-level scattering amplitudes for various theories under certain conditions. These scattering amplitudes are generated as a sum over terms constructed from the product of two amplitudes with fewer particles times a propagator. Being these amplitudes with shifted momenta physical, in the sense that all particles are on-shell and momentum conservation is preserved. In the following, we illustrate the derivation of this method.

1.3.1 Derivation

We consider a primitive amplitude $A_n^{\text{tree}}(1, \dots, n)$, where the external particles can be either gluons or quarks. We pick two legs for special treatment; we define the shift $[j, l]$ shift to be

$$|j\rangle \rightarrow |\hat{j}\rangle = |j\rangle - z |l\rangle, \quad |l\rangle = |\hat{l}\rangle \rightarrow |l\rangle + z |j\rangle, \quad (1.53)$$

where z is a complex parameter. This shift leaves untouched the spinors $|j\rangle, |l\rangle$ and the spinors for all the other particles in the process. Under this shift, the correspondent momenta are

$$\begin{aligned} p_j^\mu &\rightarrow \hat{p}_j^\mu(z) = p_j^\mu - z\eta^\mu, \\ p_l^\mu &\rightarrow \hat{p}_l^\mu(z) = p_l^\mu + z\eta^\mu, \end{aligned} \quad (1.54)$$

with $\eta^\mu = \frac{1}{2}\langle j|\gamma^\mu|l\rangle$ a massless complex momentum orthogonal to p_j^μ and p_l^μ . These shifts are chosen in a particular form in order not to alter the momentum conservation, $\hat{p}_j^\mu + \hat{p}_l^\mu = p_j^\mu + p_l^\mu$, and on-shellness of the particles, $\hat{p}_j^2 = \hat{p}_l^2 = 0$.

This shift allows us to define the complex function

$$A_n^{\text{tree}}(z) := A_n^{\text{tree}}(1, 2, \dots, \hat{j}, \dots, \hat{l}, \dots, n), \quad (1.55)$$

the analytic continuation of A_n^{tree} , which is a rational function of z with simple poles in its variables. Also, by the polology theorem [219] the poles correspond to the exchanged of virtual particles and the corresponding residues to the coupling of such particles to all the spectrum of the theory. Hence, the physical amplitude is given by $A_n^{\text{tree}}(0)$.

Now, we consider the integral

$$\oint_C \frac{dz}{2\pi i} \frac{A_n^{\text{tree}}(z)}{z}, \quad (1.56)$$

the contour is taken around a large circle in the complex plane. If $A_n^{\text{tree}}(z) \rightarrow 0$ as $z \rightarrow \infty$, the integral vanishes and, because of the Cauchy's residue theorem, we obtain a relationship between the physical amplitude, at $z = 0$, and a sum over residues for the poles of $A_n^{\text{tree}}(z)$ located at z_α ,

$$\begin{aligned} \lim_{C \rightarrow \infty} \oint_C \frac{dz}{2\pi i} \frac{A_n^{\text{tree}}(z)}{z} &= \text{Res}_{z \rightarrow 0} \left[\frac{A_n^{\text{tree}}(z)}{z} \right] + \sum_{\text{poles } \alpha} \text{Res}_{z \rightarrow z_\alpha} \frac{A_n^{\text{tree}}(z)}{z} = 0, \\ A_n^{\text{tree}}(0) &= - \sum_{\text{poles } \alpha} \text{Res}_{z \rightarrow z_\alpha} \frac{A_n^{\text{tree}}(z)}{z}. \end{aligned} \quad (1.57)$$

Further poles in the amplitude come from the dependence on z of the propagators, which correspond to factorising the amplitude $A_n^{\text{tree}}(z)$ by separating the particles k_j and k_l . In consequence, any propagator of this form splits the external particles in two groups

- $(a, a + 1, \dots, \hat{j}, \dots, b)$ on its left,
- $(b + 1, \dots, \hat{l}, \dots, b - 1)$ on its right.

In this case, the propagator \hat{P}_{ab} becomes

$$\hat{P}_{ab}^\mu = P_{ab}^\mu - z\eta^\mu \quad (1.58)$$

being P_{ab}^μ the momentum flowing before the shift. Therefore, the residues in Eq. (1.57) take this parametric form,

$$\text{Res}_{z \rightarrow z_\alpha} \frac{A_n^{\text{tree}}(z)}{z} = - \sum_h A^{\text{tree}}(a, \dots, \hat{j}, \dots, b, \hat{P}_{ab}) \frac{i}{P_{ab}^2} A^{\text{tree}}(-\hat{P}_{ab}, b + 1, \dots, \hat{l}, \dots, b - 1), \quad (1.59)$$

where the sum is over all intermediate states. This expression is evaluated at $z = z_\alpha$, which is set when the internal propagator is put on-shell, $\hat{P}_{ab}^2 = 0$, giving

$$z_\alpha = \frac{P_{ab}^2}{2P_{ab} \cdot \eta}. \quad (1.60)$$

Doing the same for the other propagators, one finds,

$$\begin{aligned}
& A_n^{\text{tree}}(1, 2, \dots, n) \\
&= \sum_{\text{partitions } r} \sum_h A_L^{\text{tree}}(a_r, \dots, \hat{j}, \dots, b_r, \hat{P}_{a_r b_r}) \frac{i}{P_{ab}^2} A_R^{\text{tree}}(-\hat{P}_{a_r b_r}, b_r + 1, \dots, \hat{l}, \dots, b_r - 1). \quad (1.61)
\end{aligned}$$

The first sum goes over all the partitions r that separates the particles j and l . Also, each term of this sum has to be evaluated at the respective pole $z = z_\alpha$.

Recursive diagrams containing three-point amplitudes often vanish because of the “wrong” kinematics. In general, if a $[j, l]$ shift is used, meaning that the momenta k_j and k_l are shifted, and the recursive diagram contains a three-point amplitude with two positive helicities, one of which is j , the diagram vanishes. The reason is that the spinor $|j\rangle$ is unaffected by the shift, hence, its product with the spinor for the other external leg a in the three-point amplitude, $\langle ja \rangle$, remains non-vanishing. Therefore, $[ja]$ and all of the left-handed spinor products must vanish, and so the three-vertex with two helicities vanishes. Similarly, three-vertices with two negative helicities can also dropped, when one of the three legs is k_l .

1.4 Little group scaling

In Sec. 1.2 we introduced the spinors $|i\rangle$ and $|i]$, which, through the Gordon identity, allow to write the momentum as $p_i^\mu = \frac{1}{2}\langle i|\gamma^\mu|i]$. It is worth to see that this relation is invariant under the scaling

$$|i\rangle \rightarrow t|i\rangle, \quad |i] \rightarrow t^{-1}|i], \quad (1.62)$$

This is called little group scaling. The little group is a group of transformations that leaves the momentum of an on-shell particle invariant [219]. For real momenta, t has to be a complex phase such that $|i]^* = |i\rangle$ is preserved. For complex momenta, $|i\rangle$ and $|i]$ are considered as independent quantities and, we can exploit the holomorphicity and anti-holomorphicity of these spinors, where t can be any non-zero complex number [215, 216].

Since amplitudes that contain massless particles can always be written in terms of spinor products we need to scale the external line rules under (1.62); the internal ones are made of the invariant momenta,

- The scalar rules is a constant factor 1: it does not scale.
- Angle and square spinors for fermions: scale as t^{-2h} for $h = \pm\frac{1}{2}$.
- Polarisation vectors for spin-1 bosons: scale as t^{-2h} for $h = \pm 1$. They do not scale under scaling of the reference momentum.

Thus, for an amplitude of massless particles only, we have the following result

$$A_n(\{|1\rangle, |1], h_1\}, \dots, \{t_i|i\rangle, t_i^{-1}|i], h_i\}, \dots) = t_i^{-2h_i} A_n(\dots, \{|i\rangle, |i], h_i\}, \dots), \quad (1.63)$$

where h_i is the helicity of the the particle i .

As a consequence of the little group scaling, all three-point tree amplitudes are fixed.

Three-point amplitudes – As we saw in Sec. 1.2.4, three-point amplitudes can only depend on either angle or square brackets, therefore, we can write a general ansatz

$$A_3^{\text{tree}}(1^{h_1}, 2^{h_2}, 3^{h_3}) = c \langle 12 \rangle^{x_{12}} \langle 13 \rangle^{x_{13}} \langle 23 \rangle^{x_{23}}. \quad (1.64)$$

Little group scaling (1.62) fixes,

$$t_1^{x_{12}+x_{13}} t_2^{x_{12}+x_{23}} t_3^{x_{13}+x_{23}} = t_1^{-2h_1} t_2^{-2h_2} t_3^{-2h_3}, \quad (1.65)$$

solving the system for x_{ij}

$$A_3^{\text{tree}}(1^{h_1}, 2^{h_2}, 3^{h_3}) = c \langle 12 \rangle^{h_3-h_1-h_2} \langle 13 \rangle^{h_2-h_1-h_3} \langle 23 \rangle^{h_1-h_2-h_3}, \quad (1.66)$$

where the helicity structure has fixed the three-point amplitude up to an overall constant. The same behaviour is obtained for the three-point correlation function in a conformal field theory (see for instance Ref. [220]).

Working out a three-gluon amplitude with two negative and one positive helicity gluons,

$$A_3^{\text{tree}}(1^-, 2^-, 3^+) = g_{YM} \frac{\langle 12 \rangle^3}{\langle 13 \rangle \langle 23 \rangle}, \quad (1.67)$$

This matches our calculation (1.49). Moreover, if we change our general ansatz and assume that the amplitude depends on square brackets, we get

$$A_3^{\text{tree}}(1^-, 2^-, 3^+) = g' \frac{[13][23]}{[12]^3}. \quad (1.68)$$

In order to distinguish between (1.67) and (1.68), we use dimensional analysis. The momentum dependence in the former is $(\text{mass})^1$, which is compatible with the three-gluon interaction, (1.20d). While the latter has a mass dimension $(\text{mass})^{-1}$, which is discarded, since there is not such interaction in the local Lagrangian.

1.5 Momentum twistors

In this section, we show that starting from formal properties we can achieve efficient results in the computation of scattering amplitudes. We describe the momentum twistors, which allow us to write any n -point amplitude made of massless particles in term of $3n - 10$ variables. This approach is going to be used in the extraction of the coefficients of MIs for the analytic computations of gluon and Higgs one-loop amplitudes.

1.5.1 Definition

The momentum conservation can be seen geometrically. The fact that n momenta p_i^μ add to zero implies that the vectors close into a contour, see Fig. 1.1 for $n = 6$.

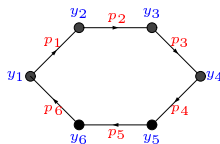


Figure 1.1: Relation between the ordered set of 6 four-vectors (y_1, \dots, y_6) and the ordered set of 6 four-vectors (p_1, \dots, p_n) constrained by $p_1 + \dots + p_n = 0$.

It means that the contour can be defined by the edges or by the cusps. The former is the usual representation. For the latter, we take the cusps to be located at point y_i^μ in a *dual space* [221]. They are defined by their relation to the momentum vectors

$$p_i^\alpha = (y_i - y_{i+1})^\alpha. \quad (1.69)$$

The *dual coordinates* y_i are not space-time coordinates and have mass-dimension 1. In dual space, n -point momentum conservation simply corresponds to the periodicity condition that $y_{n+1} = y_1$. Since the ordering of the external particles matters, we restrict our discussion to colour-ordered amplitudes, where, we can define

$$y_{ij}^\alpha \equiv (y_i - y_j)^\alpha = (p_i + p_{i+1} + \dots + p_{j-1})^\alpha. \quad (1.70)$$

Moreover, we can provide a definition of the dual coordinates in terms of spinors, by simply taking into account the Dirac equation,

$$\not{p}_i |i\rangle = (\not{y}_i - \not{y}_{i+1}) |i\rangle = 0, \quad (1.71)$$

This relation is usually called *incidence relation* and allows to define a new variable $|\mu_i]$,

$$|\mu_i] = \not{y}_i |i\rangle = \not{y}_{i+1} |i\rangle. \quad (1.72)$$

These prescriptions amount to

$$y_i^\alpha = \frac{1}{2} \frac{\langle i | \gamma^\alpha | \mu_{i-1}] - \langle i-1 | \gamma^\alpha | \mu_i]}{\langle i-1 i \rangle}. \quad (1.73)$$

We have translated the dual coordinates y_i to $Z_i \equiv (|i\rangle, |\mu_i])$. The new four-component spinor variables Z_i are called *momentum twistors* [222], which have been exhaustively studied in supersymmetric theories [223–226].

Under the little group scaling (1.62) the momentum twistors transform an uniform scaling

$$Z_i \rightarrow t_i Z_i(|i\rangle, |\mu_i]) = Z_i(t_i |i\rangle, t_i |\mu_i]). \quad (1.74)$$

Furthermore, the relation between y_i and $p_i^\alpha = \frac{1}{2} \langle i | \gamma^\alpha | i \rangle$ implies that $|i\rangle$ can be expressed in terms of $|i\rangle$ and $|\mu_i]$. Indeed, we find

$$|i\rangle = \frac{\langle i+1 i \rangle [\mu_{i-1}] + \langle i i-1 \rangle [\mu_{i+1}] + \langle i-1 i+1 \rangle [\mu_i]}{\langle i-1 i \rangle \langle i i+1 \rangle}. \quad (1.75)$$

Starting from n momentum twistors (Z_1, Z_2, \dots, Z_n) , we see that a momentum p_i satisfies, by definition the massless condition, $p_i^2 = 0$, and momentum conservation, $\sum_{i=1}^n p_i = 0$. This outcome suggests us that all momentum twistors can freely be chosen without any constraint. In addition, the momentum twistor has the following symmetries:

- Poincarè symmetry.
- $U(1)$ symmetry.

Therefore, any n -point amplitude that originally is written in terms of $4n$ twistor components, will be written, because of the symmetries, in terms of $4n - 10 - n = 3n - 10$ free components.

Working out the expressions for y_i , we notice that the arbitrariness of choosing the momentum twistor components can be seen from another point of view,

$$y_i^\alpha = -\frac{1}{\langle i-1, i \rangle} (\mathcal{Y}(i, \mu_{i-1}) \varepsilon_-^\alpha(p_i, q_{\mu_{i-1}}) - \mathcal{Y}(i-1, \mu_i) \varepsilon_-^\alpha(p_{i-1}, q_{\mu_i})), \quad (1.76)$$

with

$$\mathcal{Y}(i, \mu_{i-1}) = \frac{\langle i i-1 \rangle [\mu_{i-1} \mu_{i+1}] + \langle i-1 i+1 \rangle [\mu_{i-1} \mu_i]}{\sqrt{2} \langle i-1 i \rangle \langle i i+1 \rangle}. \quad (1.77)$$

From the definition of p_i in (1.69) we find

$$p_i^\alpha = -\frac{1}{\sqrt{2} \langle i-1 i \rangle^2 \langle i i+1 \rangle^2} \left\{ \begin{aligned} &\langle i-1 i \rangle \langle i i+1 \rangle [\mu_{i-1} \mu_{i+1}] (\varepsilon_-^\alpha(p_i, q_{\mu_{i-1}}) - \varepsilon_-^\alpha(p_i, q_{\mu_{i+1}})) \\ &+ \langle i i+1 \rangle \langle i+1 i-1 \rangle [\mu_i \mu_{i-1}] (\varepsilon_-^\alpha(p_i, q_{\mu_i}) - \varepsilon_-^\alpha(p_i, q_{\mu_{i-1}})) \\ &+ \langle i+1 i-1 \rangle \langle i-1 i \rangle [\mu_{i+1} \mu_i] (\varepsilon_-^\alpha(p_i, q_{\mu_{i+1}}) - \varepsilon_-^\alpha(p_i, q_{\mu_i})) \end{aligned} \right\}, \quad (1.78)$$

which, allows us to write any momentum p_i as a combination of three polarisation vectors with the same momentum but different reference momenta. The explicit value of p_i in the r.h.s of (1.78) is recovered by simply taking into account Eq. (1.43).

Since the aim of our discussion is to review the link between momentum twistors and spinors to compute efficiently scattering amplitudes we refer, for more details, to Ref.s. [215, 216].

1.5.2 Momentum twistors variables

In this subsection we review the representation of momentum twistors [88, 224, 227–229].

Four-point momentum twistors

The momentum twistor parametrisation at four-point needs two variables, say z_1 and z_2 . A possible choice of the Z matrix is

$$Z = \begin{pmatrix} |1\rangle & |2\rangle & |3\rangle & |4\rangle \\ |\mu_1\rangle & |\mu_2\rangle & |\mu_3\rangle & |\mu_4\rangle \end{pmatrix} = \begin{pmatrix} 1 & 0 & \frac{1}{z_1} & \frac{1}{z_1} + \frac{1}{z_2} \\ 0 & 1 & 1 & 1 \\ 0 & 0 & -1 & -1 \\ 0 & 0 & 0 & 1 \end{pmatrix}. \quad (1.79)$$

The components of the angle and square brackets were defined in Eq. (1.39). This matrix allows us to write the spinor products as follows,

$$\left\{ \begin{aligned} &\langle 12 \rangle \rightarrow -1, [21] \rightarrow -z_1, \langle 13 \rangle \rightarrow -1, [31] \rightarrow z_1(z_2 + 1), \langle 14 \rangle \rightarrow -1, [41] \rightarrow -z_1 z_2, \\ &\langle 23 \rangle \rightarrow \frac{1}{z_1}, [32] \rightarrow z_1^2 z_2, \langle 24 \rangle \rightarrow \frac{z_2 + 1}{z_1 z_2}, [42] \rightarrow -z_1^2 z_2, \langle 34 \rangle \rightarrow \frac{1}{z_1 z_2}, [43] \rightarrow z_1^2 z_2 \end{aligned} \right\}. \quad (1.80)$$

Therefore, we can see that z_1 and z_2 are related to the Maldestam variables, $s = s_{12}$ and $t = s_{14}$,

$$z_1 = s_{12}, \quad z_2 = \frac{s_{14}}{s_{12}}. \quad (1.81)$$

Let us write the four-gluon MHV amplitude in terms of momentum twistor variables

$$A_4^{\text{tree}}(1^-, 2^-, 3^+, 4^+) = i \frac{\langle 12 \rangle^4}{\langle 12 \rangle \langle 23 \rangle \langle 34 \rangle \langle 41 \rangle} \stackrel{\text{mt}}{=} i z_1^2 z_2 = i s_{12} s_{14}. \quad (1.82)$$

Since we are working with free-phase variables, in the sense that there is no physical information of the helicity, the r.h.s of (1.82) is what we call *phase-free* amplitude. Hence, the physical amplitude is recovered by Lorentz symmetry (see. Sec. 1.4),

$$A_4^{\text{tree}}(1^-, 2^-, 3^+, 4^+) = \Phi_4^{-++} \tilde{A}_4^{\text{tree}}(1^-, 2^-, 3^+, 4^+). \quad (1.83)$$

We set, under momentum twistors,

$$\Phi_4^{-++} \stackrel{\text{mt}}{=} 1, \quad (1.84)$$

where, because of the structure of Z , we have [230]

$$\langle i1 \rangle \stackrel{\text{mt}}{=} 1 \quad \text{For } i = 2, \dots, 4, \quad \frac{\langle 31 \rangle}{[1|2|3]} \stackrel{\text{mt}}{=} 1, \quad (1.85)$$

and Φ_4^{-++} takes the form

$$\Phi_4^{-++} = \frac{\langle 12 \rangle^2}{\langle 3|2|1 \rangle^2 \langle 14 \rangle^2}. \quad (1.86)$$

Five-point momentum twistors

A possible choice of the Z_i for the five-point parametrisation matrix is

$$Z = \begin{pmatrix} |1\rangle & |2\rangle & |3\rangle & |4\rangle & |5\rangle \\ |\mu_1\rangle & |\mu_2\rangle & |\mu_3\rangle & |\mu_4\rangle & |\mu_5\rangle \end{pmatrix} = \begin{pmatrix} 1 & 0 & \frac{1}{z_1} & \frac{1}{z_1} + \frac{1}{z_1 z_2} & \frac{1}{z_1} + \frac{1}{z_1 z_2} + \frac{1}{z_1 z_2 z_3} \\ 0 & 1 & 1 & 1 & 1 \\ 0 & 0 & -1 & -1 & \frac{z_5}{z_4} - 1 \\ 0 & 0 & 0 & \frac{z_4}{z_2} & 1 \end{pmatrix}. \quad (1.87)$$

This parametrisation allows to write the Lorentz invariants as

$$\begin{aligned} s_{12} &= z_1, & s_{23} &= z_1 z_4, & s_{34} &= \frac{z_1((z_5 - 1)z_2 z_3 + (z_3 + 1)z_4)}{z_2}, \\ s_{45} &= z_1 z_5, & s_{51} &= z_1 z_3(z_2 - z_4 + z_5), \end{aligned} \quad (1.88)$$

and for $\text{tr}_5(1234)$,

$$\text{tr}_5(1234) = -\frac{z_1^2((z_5 - 1)z_3 z_2^2 + (2z_3 + 1)z_4 z_2 - (z_3 + 1)z_4(z_4 - z_5))}{z_2}. \quad (1.89)$$

The system can be inverted to give

$$\begin{aligned} z_1 &= s_{12}, & z_2 &= \frac{\langle 14 \rangle \langle 23 \rangle}{\langle 12 \rangle \langle 34 \rangle}, & z_3 &= \frac{\langle 15 \rangle \langle 34 \rangle}{\langle 13 \rangle \langle 45 \rangle}, \\ z_4 &= \frac{s_{23}}{s_{12}}, & z_5 &= \frac{s_{123}}{s_{12}}. \end{aligned} \quad (1.90)$$

Momentum twistors at higher multiplicity

For $n \geq 5$, a choice of Z is given by [231],

$$Z = \begin{pmatrix} 1 & 0 & f_1 & f_2 & f_3 & \cdots & f_{n-3} & f_{n-2} \\ 0 & 1 & 1 & 1 & 1 & \cdots & 1 & 1 \\ 0 & 0 & 0 & \frac{z_{n-1}}{z_2} & z_n & \cdots & z_{2n-6} & 1 \\ 0 & 0 & 1 & 1 & z_{2n-5} & \cdots & z_{3n-11} & 1 - \frac{z_{3n-10}}{z_{n-1}} \end{pmatrix}, \quad (1.91)$$

with

$$f_i = \sum_{k=1}^i \frac{1}{\prod_{l=1}^k z_l}, \quad (1.92)$$

and

$$z_i = \begin{cases} s_{12} & i = 1, \\ -\frac{\langle i i+1 \rangle \langle i+2 1 \rangle}{\langle 1 i \rangle \langle i+1 i+2 \rangle} & i = 2, \dots, n-2, \\ s_{23} & i = n-1, \\ \sum_{j=2}^{i-n_1+4} \frac{s_{12} \langle i-n+5 | j | 2 \rangle}{[12] \langle 1 i-n+5 \rangle} & i = n, \dots, 2n-6 \\ \sum_{j=2}^{i-2n+9} \frac{\langle 1 | (2+3) j | i-2n+10 \rangle}{s_{23} \langle 1, i-2n+10 \rangle} & i = 2n-5, \dots, 3n-11 \\ \frac{s_{123}}{s_{12}} & i = 3n-10 \end{cases}. \quad (1.93)$$

As we saw for the four-point case, any physical quantity W can be, in general, decomposed as

$$W_n = \Phi_n \widetilde{W}_n \quad (1.94)$$

being \widetilde{W}_n phase-free and Φ_n a function that contains all the helicity information of W . We set under momentum twistors

$$\Phi_n^{h_1 \dots h_n} \stackrel{\text{mt}}{=} 1. \quad (1.95)$$

From the choice of Z , $\Phi_n^{h_1 \dots h_n}$ can be generalised to

$$\Phi_n^{h_1 \dots h_n} = \left(\frac{\langle 31 \rangle}{[1|2|3]} \right)^{-h_1} \prod_{i=2}^n \left(\frac{\langle 1i \rangle^2 [1|2|3]}{\langle 31 \rangle} \right)^{-h_i}. \quad (1.96)$$

We have written a MATHEMATICA package, T@M [206] based on S@M [205], that implements the technology of the spinor-helicity formalism through momentum twistor variables. The main outcome of this implementation is that we do not have to care about the re-organisation of the amplitude, since it is written in the minimal basis, namely the $3n - 10$ variables.

1.6 Discussion

In this chapter we have introduced the spinor helicity formalism, which allows to write compact expressions for amplitudes. The definition of spinor products accounts for Lorentz invariants. A remarkable result, within the spinor helicity formalism, is the structure of the Maximally Helicity Violating (MHV) amplitudes.

In the same line, we have shown the relation between spinor and momentum twistors. Due to the nice properties the momentum twistors have, we were able to express all spinors products in terms $3n - 10$ independent variables, with n the number of massless momenta.

Although the momentum twistors provide non-redundant analytical expressions in terms of a minimal set of variables it becomes cumbersome when increasing the number of external legs ($n \geq 6$). Nevertheless, their numerical evaluation is faster than spinor products. In the same manner, numerical codes are more stable when using a kinematics provide by momentum twistors.

We have reviewed traditional and modern techniques to compute tree-level amplitudes. While the diagrammatic approach of Feynman diagrams produces enormous expressions as the number of legs increases, the modern techniques take advantage of the analyticity of the S -matrix. The latter allows us to work with gauge invariant objects only, dropping spurious poles that appear when considering individually Feynman diagrams. This construction allowed the formulation of the Britto-Cachazo-Feng-Witten (BCFW) recursive relation, in which the calculation of any

n -point amplitude is under control. In particular, for $\mathcal{N} = 4$ SYM there is the automatic BCFW Recursion in MATHEMATICA [224].

In the next chapters, we will use these tools to build our fundamental pieces or inputs. These inputs correspond to the gauge invariant object or tree-level amplitudes needed to recover any multi-loop amplitude.

Chapter 2

On the Subleading-Soft Behaviour of QCD Amplitudes

In this chapter, we study the behaviour of tree-level scattering amplitudes in the soft regime. We make use of the techniques presented in Chap. 1. Apart from the leading contribution, we also consider the subleading one. It turns out that the latter is gauge invariant by itself.

Scattering amplitudes display an universal factorisation when a massless particle is radiated from an external leg. Such factorisation is governed by the non-radiative process, perturbed by operators. These operators depend on the quantum numbers of the emitter. In order to derive the leading and subleading soft operators we make use of the gauge invariance and on-shell recursive construction of the amplitude. From the former, it can be shown that the soft operators depend on the total angular momentum (orbital and spin) of the radiator, as explicitly shown for gluon and graviton amplitudes by Bern et al [116]. The latter, based on the spinor helicity formalism, writes these operators as differential operators, as pointed out by Cachazo and Strominger [91] and Casali [92] for graviton and gluon amplitudes respectively.

Since previous studies dealt with Yang-Mills and gravity amplitudes, we elaborate on the low energy behaviour of single gluon radiation for QCD amplitudes with a quark-pair and gluons. Upon colour decomposition [200], we can identify two situations according to the position of the soft gluon: (i) between a (anti-)quark and a gluon, and (ii) between two gluons. Case (ii) is similar to the pure Yang-Mills (YM) case, where the emitter is necessarily a gluon, and it can be considered well studied [91, 92, 116]. In case (i), instead, the soft gluon can be radiated either from a gluon or from a (anti-)quark. In order to derive the soft behaviour from fermionic emitters, we analyse the case of photon bremsstrahlung from the quark-line in QED [219]. For this case, we show the equivalence of the soft operators derived from gauge invariance and from the on-shell construction. This result is, then, easily extended to the quark-gluon amplitudes in QCD [2].

Furthermore, we explicitly apply the soft operators to describe the low-energy behaviour of quark-gluon amplitudes, emitting either a photon or a gluon, for non-trivial helicity configurations of six-parton scattering.

2.1 Soft limit of gluon-amplitudes

According to little group transformation (1.63), we recall the scaling behaviour of tree-level scattering amplitudes involving massless particles,

$$\mathcal{A}_n^{\text{tree}}(\{1\}, |1\rangle, h_1, \dots, \{t_i|i\rangle, t_i^{-1}|i\rangle, h_i, \dots) = t_i^{-2h_i} \mathcal{A}_n^{\text{tree}}(\dots, \{|i\rangle, |i\rangle, h_i\}, \dots), \quad (2.1)$$

Without loss of generality, we consider an n -gluon amplitude, $\mathcal{A}_n^{\text{tree}}$, with the gluon s as soft, helicity $h_s = +1$ and momentum $k_s^\mu = \frac{1}{2}\epsilon \langle s | \gamma^\mu | s \rangle$. ϵ parametrises the energy loss. As represented

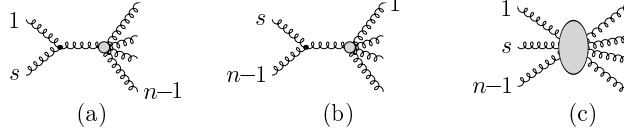


Figure 2.1: Soft-gluon behaviour of pure-gluon amplitudes

in Eq. (2.1), the corresponding amplitude transforms as

$$\mathcal{A}_n^{\text{tree}}(\dots, \{\sqrt{\epsilon}|s\rangle, \sqrt{\epsilon}|s\rangle, +1\}, \dots) = \epsilon \mathcal{A}_n^{\text{tree}}(\dots, \{\epsilon|s\rangle, |s\rangle, +1\}, \dots), \quad (2.2)$$

which means the soft limit can be taken through the holomorphic limit $\epsilon|s\rangle \rightarrow 0$, while keeping the anti-holomorphic variable, $|s\rangle$, as finite [91, 92].

The low-energy behaviour derived from the BCFW construction [25, 26], for primitive amplitudes, shows that in the soft-limit reads [92],

$$\begin{aligned} A_n^{\text{tree}}(\{\epsilon|s\rangle, |s\rangle\}, \{|1\rangle, |1\rangle\}, \dots, \{|n-1\rangle, |n-1\rangle\}) \\ = \left(\frac{1}{\epsilon^2} S_G^{(0)\lambda} + \frac{1}{\epsilon} S_G^{(1)\lambda} \right) A_{n-1}^{\text{tree}}(1, \dots, n-1) + \mathcal{O}(\epsilon^0) \end{aligned} \quad (2.3)$$

where the leading and the subleading terms are,

$$S_G^{(0)\lambda} = \frac{\langle n-1 \ 1 \rangle}{\langle s \ 1 \rangle \langle n-1 \ s \rangle}, \quad (2.4a)$$

$$S_G^{(1)\lambda} = \frac{1}{\langle s \ 1 \rangle} [s \partial_1] + \frac{1}{\langle n-1 \ s \rangle} [s \partial_{n-1}]. \quad (2.4b)$$

Operators $[s \partial_i]$ act on spinor products, according to

$$[s \partial_i][\bullet i] = [\bullet s], \quad [s \partial_i] \frac{1}{[\bullet i]} = -\frac{[\bullet s]}{[\bullet i]^2}. \quad (2.5)$$

As shown in [116], gauge invariance can also be used to determine the next-to-leading soft behaviour of the non-Abelian gauge theory. The primitive amplitude gets contribution from the three types of diagrams shown in Fig. 2.1. Diagrams (a) and (b) contribute to the leading pole term in the soft regime, while the third one, with the soft-gluon emitted from an internal propagator, is regular in this limit. By using gauge invariance, we obtain the soft behaviour,

$$A_n^{\text{tree}}(k_s; k_1, \dots, k_{n-1}) = \left[S_G^{(0)} + S_G^{(1)} \right] A_{n-1}^{\text{tree}}(k_1, \dots, k_{n-1}) + \mathcal{O}(k_s) \quad (2.6)$$

with

$$S_G^{(0)} \equiv \frac{k_1 \cdot \varepsilon(k_s; r_s)}{\sqrt{2}(k_1 \cdot k_s)} - \frac{k_{n-1} \cdot \varepsilon(k_s; r_s)}{\sqrt{2}(k_{n-1} \cdot k_s)}, \quad (2.7)$$

$$S_G^{(1)} \equiv -\frac{i\varepsilon_\mu(k_s; r_s)k_{s\sigma}}{\sqrt{2}} \left(\frac{J_{G1}^{\mu\sigma}}{(k_1 \cdot k_s)} - \frac{J_{Gn-1}^{\mu\sigma}}{(k_{n-1} \cdot k_s)} \right). \quad (2.8)$$

Here, J is the total angular momentum of the emitter, written in terms of the orbital momentum L and spin Σ ,

$$\begin{aligned} J_{Gi}^{\mu\sigma} &\equiv L_{Gi}^{\mu\sigma} + \Sigma_{Gi}^{\mu\sigma}, \\ L_{Gi}^{\mu\sigma} &\equiv i \left(k_i^\mu \frac{\partial}{\partial k_{i\sigma}} - k_i^\sigma \frac{\partial}{\partial k_{i\mu}} \right), \end{aligned}$$

$$\Sigma_{Gi}^{\mu\sigma} \equiv i \left(\varepsilon_i^\mu \frac{\partial}{\partial \varepsilon_{i\sigma}} - \varepsilon_i^\sigma \frac{\partial}{\partial \varepsilon_{i\mu}} \right). \quad (2.9)$$

In the derivation of this result [116], $L_{Gi}^{\mu\sigma}$ does not act on explicit polarisation vectors, i.e. $L_{Gi}^{\mu\sigma} \varepsilon_i^\nu = 0$.

As discussed in [116], the equivalence between the operators $S_G^{(1)}$, derived from gauge invariance, and $S_G^{(1)\lambda}$, derived from on-shell recurrence, can be seen through their explicit action on polarisation vectors. In fact, the next-to-soft operators $S_G^{(1)}$ and $S_G^{(1)\lambda}$ acting on $\varepsilon^{\pm\rho}(k_1; r_1)$ amount to,

$$S_G^{(1)} \varepsilon^{+\rho}(k_1; r_1) = -\frac{\langle r_1 s \rangle}{\langle r_1 1 \rangle \langle 1 s \rangle} \varepsilon^{+\rho}(k_s; r_1), \quad (2.10)$$

$$S_G^{(1)} \varepsilon^{-\rho}(k_1; r_1) = +\frac{[r_1 s]}{[r_1 1] [1 s]} \varepsilon^{+\rho}(k_s; r_1), \quad (2.11)$$

and

$$S_G^{(1)\lambda} \varepsilon^{+\rho}(k_1; r_1) = -\frac{\langle r_1 s \rangle}{\langle r_1 1 \rangle \langle 1 s \rangle} \varepsilon^{+\rho}(k_s; r_1), \quad (2.12)$$

$$S_G^{(1)\lambda} \varepsilon^{-\rho}(k_1; r_1) = +\frac{[r_1 s]}{[r_1 1] [1 s]} \left[\varepsilon^{+\rho}(k_s; r_1) - \frac{\sqrt{2} [r_1 s]}{[r_1 1] \langle 1 s \rangle} k_1^\rho \right]. \quad (2.13)$$

The second term in the last equation is proportional to k_1^ρ , and vanishes after contracting it with the polarisation stripped A_{n-1}^{tree} amplitude, due to Ward identity. Therefore, the next-to-leading soft (differential) operators obtained in these two frameworks are completely equivalent.

2.2 Photon bremsstrahlung from quark-gluon amplitudes

Since previous studies considered the radiation of gluons from gluon amplitudes [92, 116], one needs the radiation from fermion lines only. Hence, in order to isolate this contribution, we consider the radiation of a photon from a quark-pair of a quark-gluon amplitude. The radiation of a gluon from quark-gluon amplitudes will be studied in the next section.

The derivations of the leading and next-to-leading soft terms are done by following both, on-shell recurrence and gauge invariance approaches. Furthermore, we prove the equivalence of the respective results.

2.2.1 Derivation from on-shell recursion

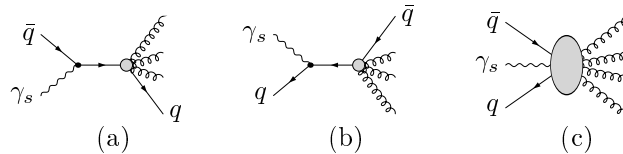


Figure 2.2: Soft-photon behaviour of quark-gluon amplitudes

We consider a colour-ordered amplitude $A_{n+3}^{\text{tree}}(\Lambda_{\bar{q}}, \gamma_s^+, \Lambda_q, g_1, \dots, g_n)$, where Λ_q and $\Lambda_{\bar{q}}$ denote a quark and an antiquark, and γ_s^+ stands for a soft photon of helicity $h_s = +1$, emitted from the fermionic current. Under the BCFW deformation involving γ_s and g_n we define the shift $[n, s]$,

$$|\hat{s}\rangle = |s\rangle + z |n\rangle, \quad (2.14)$$

$$|\hat{n}\rangle = |n\rangle - z |s\rangle, \quad (2.15)$$

the amplitude factorises as,

$$\begin{aligned} A_{n+3}^{\text{tree}}(\Lambda_{\bar{q}}, \gamma_s^+, \Lambda_q, g_1, \dots, g_n) &= \sum_{h=\pm\frac{1}{2}} A_L^{\text{tree}}(\widehat{\gamma}_s^+, \Lambda_q, \widehat{P}^h) \frac{1}{P_{s,q}^2} A_R^{\text{tree}}(-\widehat{P}^{-h}, g_1, \dots, \widehat{g}_n, \Lambda_{\bar{q}}) \\ &+ \sum_{h=\pm\frac{1}{2}} A_L^{\text{tree}}(\Lambda_{\bar{q}}, \widehat{\gamma}_s^+, \widehat{P}^h) \frac{1}{P_{\bar{q},s}^2} A_R^{\text{tree}}(-\widehat{P}^{-h}, \Lambda_q, g_1, \dots, \widehat{g}_n) \\ &+ \sum_{h=\pm 1} A_L^{\text{tree}}(\Lambda_{\bar{q}}, \widehat{\gamma}_s^+, \Lambda_q, g_1, \dots, g_j, \widehat{P}^h) \frac{1}{P_{\bar{q},s,q,1,\dots,j}^2} A_R^{\text{tree}}(-\widehat{P}^{-h}, g_{j+1}, \dots, \widehat{g}_n), \end{aligned} \quad (2.16)$$

as depicted in fig. 2.2.

In the first term, the on-shellness requires $z = -\frac{\langle qs \rangle}{\langle \bar{q} n \rangle}$, and \widehat{P} stands for a fermion with an opposite helicity with respect to Λ_q . By taking the soft limit, $|s\rangle \rightarrow \epsilon|s\rangle$, this term reads

$$\begin{aligned} &\frac{1}{\epsilon^2} \frac{\langle nq \rangle}{\langle ns \rangle \langle sq \rangle} A_{n+2}^{\text{tree}}(\{|q\rangle, |\hat{q}\rangle\}, \dots, \{|n\rangle, |\hat{n}\rangle\}, \{|q\rangle, |\bar{q}\rangle\}) \\ &= \left[\frac{1}{\epsilon^2} \frac{\langle nq \rangle}{\langle ns \rangle \langle sq \rangle} + \frac{1}{\epsilon} \left(\frac{1}{\langle sq \rangle} [s \partial_q] + \frac{1}{\langle ns \rangle} [s \partial_n] \right) \right] A_{n+2}^{\text{tree}}(\{|q\rangle, |q\rangle\}, \dots, \{|n\rangle, |n\rangle\}, \{|q\rangle, |\bar{q}\rangle\}) \end{aligned} \quad (2.17)$$

with $|\hat{q}\rangle = |q\rangle + \epsilon \frac{\langle ns \rangle}{\langle nq \rangle} |s\rangle$ and $|\hat{n}\rangle = |n\rangle + \epsilon \frac{\langle sq \rangle}{\langle nq \rangle} |s\rangle$.

In the second term of eq. (2.16), the on-shell condition implies $z = -\frac{\langle \bar{q} s \rangle}{\langle \bar{q} n \rangle}$, and \widehat{P} stands for a fermion with an opposite helicity with respect to $\Lambda_{\bar{q}}$. Under the soft limit, $|s\rangle \rightarrow \epsilon|s\rangle$, this term becomes

$$\begin{aligned} &-\frac{1}{\epsilon^2} \frac{\langle n\bar{q} \rangle}{\langle ns \rangle \langle s\bar{q} \rangle} A_{n+2}^{\text{tree}}(\{|q\rangle, |\hat{q}\rangle\}, \{|q\rangle, |q\rangle\}, \dots, \{|n\rangle, |\hat{n}\rangle\}) \\ &= -\left[\frac{1}{\epsilon^2} \frac{\langle n\bar{q} \rangle}{\langle ns \rangle \langle s\bar{q} \rangle} + \frac{1}{\epsilon} \left(\frac{1}{\langle s\bar{q} \rangle} [s \partial_{\bar{q}}] + \frac{1}{\langle ns \rangle} [s \partial_n] \right) \right] A_{n+2}^{\text{tree}}(\{|q\rangle, |\bar{q}\rangle\}, \{|q\rangle, |q\rangle\}, \dots, \{|n\rangle, |n\rangle\}) \end{aligned} \quad (2.18)$$

with $|\hat{q}\rangle = |\bar{q}\rangle + \epsilon \frac{\langle ns \rangle}{\langle n\bar{q} \rangle} |s\rangle$ and $|\hat{n}\rangle = |n\rangle + \epsilon \frac{\langle sq \rangle}{\langle nq \rangle} |s\rangle$.

The third term of eq. (2.16) is finite under the soft limit, hence does not contribute to any soft operators [91, 92].

Adding the first and second term up, the amplitude in the soft regime reads,

$$A_{n+3}^{\text{tree}}(\Lambda_{\bar{q}}, \gamma_s^+, \Lambda_q, g_1, \dots, g_n) = \left(\frac{1}{\epsilon^2} S^{(0)\lambda} + \frac{1}{\epsilon} S^{(1)\lambda} \right) A_{n+2}^{\text{tree}}(\Lambda_{\bar{q}}, \Lambda_q, g_1, \dots, g_n) + \mathcal{O}(1), \quad (2.19)$$

with

$$S^{(0)\lambda} = \frac{\langle nq \rangle}{\langle ns \rangle \langle sq \rangle} - \frac{\langle n\bar{q} \rangle}{\langle ns \rangle \langle s\bar{q} \rangle} = \frac{\langle \bar{q} q \rangle}{\langle \bar{q} s \rangle \langle sq \rangle}, \quad (2.20)$$

$$S^{(1)\lambda} = \frac{1}{\langle sq \rangle} [s \partial_q] - \frac{1}{\langle s\bar{q} \rangle} [s \partial_{\bar{q}}], \quad (2.21)$$

where A_{n+2}^{tree} is the non-radiative quark-gluon amplitude.

2.2.2 Derivation from gauge invariance

Within a diagrammatic approach, the amplitude $A_{n+3}^{\text{tree}}(\Lambda_{\bar{q}}, \gamma_s^+, \Lambda_q, g_1, \dots, g_n)$ gets contributions from the three diagrams in Fig. 2.2, and can be obtained by contracting the soft-photon polarisation $\varepsilon_\mu(k_s; r_s)$ and the current A_{n+3}^μ ,

$$A_{n+3}^{\text{tree}} = \varepsilon_\mu(k_s; r_s) A_{n+3}^\mu, \quad (2.22)$$

with

$$\begin{aligned} A_{n+3}^\mu(k_s; k_{\bar{q}}, k_q, k_1, \dots, k_n) &= -\frac{i}{\sqrt{2}} \bar{u}(k_q) \tilde{A}(k_{\bar{q}} + k_s, k_q, k_1, \dots, k_n) \frac{i(k_{\bar{q}}^\mu + k_s^\mu)}{(k_{\bar{q}} + k_s)^2} \gamma^\mu v(k_{\bar{q}}) \\ &+ \frac{i}{\sqrt{2}} \bar{u}(k_q) \gamma^\mu \frac{i(k_q^\mu + k_s^\mu)}{(k_q + k_s)^2} \tilde{A}(k_{\bar{q}}, k_q + k_s, k_1, \dots, k_n) v(k_{\bar{q}}) + N_{n+3}^\mu(k_s; k_{\bar{q}}, k_q, k_1, \dots, k_n). \end{aligned} \quad (2.23)$$

The first term, corresponding to fig. 2.2 (a), represents the case of soft-photon emission from an outgoing antiquark; the second term, corresponding to fig. 2.2 (b), represents the case of soft-photon emission from an outgoing quark; while the third term N_{n+3}^μ represents the case of soft-photon emission from internal fermion lines, as shown in fig. 2.2 (c). \tilde{A} is the internal part sandwiched by two free-particle states of fermions. By using the massless Dirac equation, $\bar{u}(p) \not{p} = \not{p} v(p) = 0$, the transversality conditions, $k_s \cdot \varepsilon^\pm(k_s; r_s) = 0$, and the relation $\gamma^\mu \not{p} = p_\nu (\eta^{\mu\nu} + [\gamma^\mu, \gamma^\nu]/2)$ from the anti-commutation of γ -matrix (for an arbitrary momentum p), the current A_{n+3}^μ can be cast as,

$$\begin{aligned} A_{n+3}^\mu(k_s; k_{\bar{q}}, k_q, k_1, \dots, k_n) &= \frac{k_{\bar{q}}^\mu}{\sqrt{2} k_{\bar{q}} \cdot k_s} \bar{u}(k_q) \tilde{A}(k_{\bar{q}} + k_s, k_q, k_1, \dots, k_n) v(k_{\bar{q}}) \\ &+ \frac{i k_{s\nu}}{\sqrt{2} k_{\bar{q}} \cdot k_s} \bar{u}(k_q) \tilde{A}(k_{\bar{q}} + k_s, k_q, k_1, \dots, k_n) \Sigma_F^{\mu\nu} v(k_{\bar{q}}) - \frac{k_q^\mu}{\sqrt{2} k_q \cdot k_s} \bar{u}(k_q) \tilde{A}(k_{\bar{q}}, k_q + k_s, k_1, \dots, k_n) v(k_{\bar{q}}) \\ &+ \frac{i k_{s\nu}}{\sqrt{2} k_q \cdot k_s} \bar{u}(k_q) \Sigma_F^{\mu\nu} \tilde{A}(k_{\bar{q}}, k_q + k_s, k_1, \dots, k_n) v(k_{\bar{q}}) + N_{n+3}^\mu(k_s; k_{\bar{q}}, k_q, k_1, \dots, k_n), \end{aligned} \quad (2.24)$$

where

$$\Sigma_F^{\mu\nu} \equiv \frac{i}{4} [\gamma^\mu, \gamma^\nu] \quad (2.25)$$

is the spin operator in a 4-dimensional representation of the Lorentz algebra corresponding to spin 1/2. Following [89, 116], we can determine N^μ by imposing gauge invariance. In fact, the condition

$$k_{s\mu} A_{n+3}^\mu(k_s; k_{\bar{q}}, k_q, k_1, \dots, k_n) = 0, \quad (2.26)$$

together with the on-shell massless condition $k_s^2 = 0$, implies

$$\begin{aligned} k_{s\mu} N_{n+3}^\mu(0; k_q, k_{\bar{q}}, k_1, \dots, k_n) \\ = -\frac{k_s^\mu}{\sqrt{2}} \bar{u}(k_q) \left[\frac{\partial}{\partial k_{\bar{q}\mu}} \tilde{A}(k_{\bar{q}}, k_q, k_1, \dots, k_n) - \frac{\partial}{\partial k_{q\mu}} \tilde{A}(k_{\bar{q}}, k_q, k_1, \dots, k_n) \right] v(k_{\bar{q}}). \end{aligned} \quad (2.27)$$

Consequently, we can write A_{n+3}^μ as,

$$A_{n+3}^\mu(k_s; k_{\bar{q}}, k_q, k_1, \dots, k_n) = \left(\frac{k_{\bar{q}}^\mu}{\sqrt{2} k_{\bar{q}} \cdot k_s} - \frac{k_q^\mu}{\sqrt{2} k_q \cdot k_s} \right) \bar{u}(k_q) \tilde{A}(k_{\bar{q}}, k_q, k_1, \dots, k_n) v(k_{\bar{q}})$$

$$\begin{aligned}
& + \frac{i k_{s\nu}}{\sqrt{2} k_{\bar{q}} \cdot k_s} \bar{u}(k_q) \tilde{A}(k_{\bar{q}}, k_q, k_1, \dots, k_n) \Sigma_F^{\mu\nu} v(k_{\bar{q}}) \\
& + \frac{i k_{s\nu}}{\sqrt{2} k_q \cdot k_s} \bar{u}(k_q) \Sigma_F^{\mu\nu} \tilde{A}(k_{\bar{q}}, k_q, k_1, \dots, k_n) v(k_{\bar{q}}) \\
& - \frac{i k_{s\nu}}{\sqrt{2} k_{\bar{q}} \cdot k_s} \bar{u}(k_q) \left[i \left(k_{\bar{q}}^\mu \frac{\partial}{\partial k_{\bar{q}\nu}} - k_{\bar{q}}^\nu \frac{\partial}{\partial k_{\bar{q}\mu}} \right) \tilde{A}(k_{\bar{q}}, k_q, k_1, \dots, k_n) \right] v(k_{\bar{q}}) \\
& + \frac{i k_{s\nu}}{\sqrt{2} k_q \cdot k_s} \bar{u}(k_q) \left[i \left(k_q^\mu \frac{\partial}{\partial k_{q\nu}} - k_q^\nu \frac{\partial}{\partial k_{q\mu}} \right) \tilde{A}(k_{\bar{q}}, k_q, k_1, \dots, k_n) \right] v(k_{\bar{q}}) + \mathcal{O}(k_s) . \quad (2.28)
\end{aligned}$$

Then, we contract back the polarisation vector of the soft-photon $\varepsilon_\mu^+(k_s; r_s)$, obtaining the following expression of the amplitude,

$$\begin{aligned}
A_{n+3}^{\text{tree}}(k_s; k_{\bar{q}}, k_q, k_1, \dots, k_n) & = \left(\frac{\varepsilon^+(k_s; r_s) \cdot k_{\bar{q}}}{\sqrt{2} k_{\bar{q}} \cdot k_s} - \frac{\varepsilon^+(k_s; r_s) \cdot k_q}{\sqrt{2} k_q \cdot k_s} \right) A_{n+2}(k_{\bar{q}}, k_q, k_1, \dots, k_n) \\
& + \frac{i \varepsilon_\mu^+(k_s; r_s) k_{s\nu}}{\sqrt{2}} \left\{ \bar{u}(k_q) \left(\frac{L_q^{\mu\nu}}{k_q \cdot k_s} - \frac{L_{\bar{q}}^{\mu\nu}}{k_{\bar{q}} \cdot k_s} \right) v(k_{\bar{q}}) \right. \\
& \left. + \frac{1}{k_{\bar{q}} \cdot k_s} \bar{u}(k_q) \tilde{A}(k_{\bar{q}}, k_q, k_1, \dots, k_n) \Sigma_F^{\mu\nu} v(k_{\bar{q}}) + \frac{1}{k_q \cdot k_s} \bar{u}(k_q) \Sigma_F^{\mu\nu} \tilde{A}(k_{\bar{q}}, k_q, k_1, \dots, k_n) v(k_{\bar{q}}) \right\} \\
& + \mathcal{O}(k_s) , \quad (2.29)
\end{aligned}$$

with

$$A_{n+2}^{\text{tree}}(k_{\bar{q}}, k_q, k_1, \dots, k_n) = \bar{u}(k_q) \tilde{A}(k_{\bar{q}}, k_q, k_1, \dots, k_n) v(k_{\bar{q}}) \quad (2.30)$$

being the lower-point, non-radiative amplitude. In the above expression,

$$L_{fi}^{\mu\nu} = i \left(k_i^\mu \frac{\partial}{\partial k_{i\nu}} - k_i^\nu \frac{\partial}{\partial k_{i\mu}} \right) , \quad (2.31)$$

is the orbital angular momentum of fermion i , which does not act on Dirac fields of incoming/outgoing spin 1/2 particles, namely

$$L_{f_i}^{\mu\nu} u_\pm(k_i) = L_{f_i}^{\mu\nu} v_\pm(k_i) = 0 , \quad (2.32a)$$

$$\bar{u}_\pm(k_i) L_{f_i}^{\mu\nu} = \bar{v}_\pm(k_i) L_{f_i}^{\mu\nu} = 0 . \quad (2.32b)$$

On the other hand, the Lorentz generators $\Sigma_F^{\mu\nu}$ of spin 1/2 act only on the Dirac fields $u_\pm(k_i)$ or $v_\pm(k_i)$ ($\bar{u}_\pm(k_i)$ or $\bar{v}_\pm(k_i)$).

2.2.3 Connection between the two derivations

In this section, we prove the equivalence of the limiting behaviour of quark-gluon amplitudes in the soft-photon emission regime obtained in (2.19) from BCFW recurrence, and in (2.29) from gauge invariance.

Leading soft singularity

The leading singularity factor of order $1/k_s$ in (2.29) can be denoted as

$$S^{(0)} = \frac{\varepsilon^+(k_s; r_s) \cdot k_{\bar{q}}}{\sqrt{2} k_{\bar{q}} \cdot k_s} - \frac{\varepsilon^+(k_s; r_s) \cdot k_q}{\sqrt{2} k_q \cdot k_s} . \quad (2.33)$$

In spinorial notations, we indeed find,

$$S^{(0)} = \frac{\varepsilon^+(k_s; r_s) \cdot k_{\bar{q}}}{\sqrt{2}k_{\bar{q}} \cdot k_s} - \frac{\varepsilon^+(k_s; r_s) \cdot k_q}{\sqrt{2}k_q \cdot k_s} = \frac{\langle q \bar{q} \rangle}{\langle \bar{q} s \rangle \langle s q \rangle} = -S^{(0)\lambda}, \quad (2.34)$$

where $S^{(0)\lambda}$ was defined in (2.20). This proves the equivalence of the leading soft term in the two approaches (up to an overall sign)

Next-to-leading soft singularity

The action of the differential operator $S^{(1)\lambda}$, defined in (2.21), on the lower-point amplitude $A_{n+2}^{\text{tree}}(\bar{q}, q, g_1, \dots, g_n)$ can be written as,

$$\begin{aligned} S^{(1)\lambda} A_{n+2}^{\text{tree}}(\bar{q}, q, g_1, \dots, g_n) &= S^{(1)\lambda} \left[\bar{u}(k_q) \tilde{A}(k_{\bar{q}}, k_q, k_1, \dots, k_n) v(k_{\bar{q}}) \right] \\ &= \bar{u}(k_q) \tilde{A}(k_{\bar{q}}, k_q, k_1, \dots, k_n) \left[S^{(1)\lambda} v(k_{\bar{q}}) \right] + \left[S^{(1)\lambda} \bar{u}(k_q) \right] \tilde{A}(k_{\bar{q}}, k_q, k_1, \dots, k_n) v(k_{\bar{q}}) \\ &\quad + \bar{u}(k_q) \left[S^{(1)\lambda} \tilde{A}(k_{\bar{q}}, k_q, k_1, \dots, k_n) \right] v(k_{\bar{q}}). \end{aligned} \quad (2.35)$$

On the other hand, the next-to-leading soft singularity as derived in Sec. 2.2.2, is

$$\begin{aligned} A_{n+3}^{\text{tree}}(k_s; k_{\bar{q}}, k_q, k_1, \dots, k_n) \Big|_{S^{(1)}} &= \frac{i \varepsilon_{\mu}^+(k_s; r_s) k_{s\nu}}{\sqrt{2}} \left\{ \bar{u}(k_q) \left(\frac{L_q^{\mu\nu}}{k_q \cdot k_s} - \frac{L_{\bar{q}}^{\mu\nu}}{k_{\bar{q}} \cdot k_s} \right) v(k_{\bar{q}}) \right. \\ &\quad \left. + \frac{1}{k_{\bar{q}} \cdot k_s} \bar{u}(k_q) \tilde{A}(k_{\bar{q}}, k_q, k_1, \dots, k_n) \Sigma_F^{\mu\nu} v(k_{\bar{q}}) + \frac{1}{k_q \cdot k_s} \bar{u}(k_q) \Sigma_F^{\mu\nu} \tilde{A}(k_{\bar{q}}, k_q, k_1, \dots, k_n) v(k_{\bar{q}}) \right\}. \end{aligned} \quad (2.36)$$

We proceed by identifying (2.35) and (2.36) term by term.

Proposition 1:

$$S^{(1)\lambda} v(k_{\bar{q}}) = - \left[\frac{i \varepsilon_{\mu}^+(k_s; r_s) k_{s\nu}}{\sqrt{2}k_{\bar{q}} \cdot k_s} \Sigma^{\mu\nu} v(k_{\bar{q}}) \right]. \quad (2.37)$$

Proof.

Outgoing antiquark with different helicities in terms of spinor notations are

$$h_{\bar{q}} = +\frac{1}{2}, \quad v_+(k_{\bar{q}}) = |\bar{q}], \quad (2.38)$$

$$h_{\bar{q}} = -\frac{1}{2}, \quad v_-(k_{\bar{q}}) = |\bar{q}]. \quad (2.39)$$

For $h_{\bar{q}} = +\frac{1}{2}$ case, the action of the next-to-soft operator on field $v_+(k_{\bar{q}})$, corresponding to the first term in (2.35), is

$$S^{(1)\lambda} v_+(k_{\bar{q}}) = \left(\frac{1}{\langle s q \rangle} [s \partial_q] - \frac{1}{\langle s \bar{q} \rangle} [s \partial_{\bar{q}}] \right) \tilde{\chi}_{\bar{q}}^b = -\frac{1}{\langle s \bar{q} \rangle} |s], \quad (2.40)$$

and the counter-part from (2.36), in spinor notation, is

$$\frac{i \varepsilon_{\mu}^+(k_s; r_s) k_{s\nu}}{\sqrt{2}k_{\bar{q}} \cdot k_s} \Sigma_F^{\mu\nu} v_+(k_{\bar{q}}) = +\frac{1}{\langle s \bar{q} \rangle} |s]. \quad (2.41)$$

The results of (2.40) and (2.41) differ only for a minus sign, which is an overall phase factor at the amplitude level and irrelevant for the physical content of cross-sections.

On the other side, for $h_{\bar{q}} = -\frac{1}{2}$ case, one has

$$S^{(1)\lambda} v_-(k_{\bar{q}}) = \frac{i \varepsilon_{\mu}^+(k_s; r_s) k_{s\nu}}{\sqrt{2} k_{\bar{q}} \cdot k_s} \Sigma^{\mu\nu} v_-(k_{\bar{q}}) = 0. \quad (2.42)$$

Proposition 2:

$$S^{(1)\lambda} \bar{u}(k_q) = - \left[\bar{u}(k_q) \frac{i \varepsilon_{\mu}^+(k_s; r_s) k_{s\nu}}{\sqrt{2} k_q \cdot k_s} \Sigma_F^{\mu\nu} \right]. \quad (2.43)$$

Proof.

Outgoing quark with different helicities in terms of spinor notations are

$$h = +\frac{1}{2}, \quad \bar{u}_+(k_q) = [\bar{q}], \quad (2.44)$$

$$h = -\frac{1}{2}, \quad \bar{u}_-(k_q) = \langle q|. \quad (2.45)$$

With a similar procedure dealing with outgoing antiquark, we have

$$- \left(\bar{u}_+(k_q) \frac{i \varepsilon_{\mu}^+(k_s; r_s) k_{s\nu}}{\sqrt{2} k_q \cdot k_s} \Sigma_F^{\mu\nu} \right) = + \frac{1}{\langle s q \rangle} [s], \quad (2.46)$$

and

$$S^{(1)\lambda} \bar{u}_-(k_q) = \bar{u}_-(k_q) \frac{i \varepsilon_{\mu}^+(k_s; r_s) k_{s\nu}}{\sqrt{2} k_q \cdot k_s} \Sigma_F^{\mu\nu} = 0. \quad (2.47)$$

Also in this case, the two results differ by an overall sign.

Proposition 3:

$$S^{(1)\lambda} \tilde{A}(k_{\bar{q}}, k_q, k_1, \dots, k_n) = -i \frac{\varepsilon_{\mu}^+(k_s; r_s) k_{s\nu}}{\sqrt{2}} \left(\frac{L_q^{\mu\nu}}{k_q \cdot k_s} - \frac{L_{\bar{q}}^{\mu\nu}}{k_{\bar{q}} \cdot k_s} \right) \tilde{A}(k_{\bar{q}}, k_q, k_1, \dots, k_n). \quad (2.48)$$

Proof.

Since \tilde{A} is a function that depends on gluon polarisations and momenta, it can, therefore, be expressed in terms of spinor chains.

Because tree-level amplitudes are rational functions of spinor products, we can focus on the action of the operators $S^{(1)\lambda}$ and $(-ig/\sqrt{2}) \varepsilon_{\mu}^+(k_s; r_s) k_{s\nu} \left(\frac{L_q^{\mu\nu}}{k_q \cdot k_s} - \frac{L_{\bar{q}}^{\mu\nu}}{k_{\bar{q}} \cdot k_s} \right)$ onto each ingredient separately.

The next-to-leading soft operator gives non-trivial result when acting on spinor products involving \bar{q} , as

$$S^{(1)\lambda} [\bullet \bar{q}] = - \frac{1}{\langle s \bar{q} \rangle} [\bullet s], \quad (2.49a)$$

$$S^{(1)\lambda} \frac{1}{[p \bar{q}]} = + \frac{1}{[p \bar{q}]} \frac{[p s]}{\langle s \bar{q} \rangle [p \bar{q}]}. \quad (2.49b)$$

On the other hand, the operator from gauge invariance acts on terms depending on the antiquark momentum, like

$$\frac{i \varepsilon_{\mu}^+(k_s; r_s) k_{s\nu}}{\sqrt{2}} \left(\frac{L_q^{\mu\nu}}{k_q \cdot k_s} - \frac{L_{\bar{q}}^{\mu\nu}}{k_{\bar{q}} \cdot k_s} \right) k_{\bar{q}}^{\rho} = + \frac{1}{\langle s \bar{q} \rangle} \frac{\langle \bar{q} | \gamma^{\rho} | s \rangle}{2}, \quad (2.50)$$

$$\frac{i \varepsilon_{\mu}^{+}(k_s; r_s) k_{s\nu}}{\sqrt{2}} \left(\frac{L_q^{\mu\nu}}{k_q \cdot k_s} - \frac{L_{\bar{q}}^{\mu\nu}}{k_{\bar{q}} \cdot k_s} \right) \frac{1}{p \cdot k_{\bar{q}}} = - \frac{1}{p \cdot k_{\bar{q}}} \frac{[p s]}{\langle s \bar{q} \rangle [p \bar{q}]}. \quad (2.51)$$

The coefficients are identical up to a physically irrelevant overall minus sign.

The same conclusion can be drawn from comparing the action of the subleading soft operators on the variables associated to quarks,

$$S^{(1)\lambda} [\bullet q] = + \frac{1}{\langle s q \rangle} [\bullet s], \quad S^{(1)\lambda} \frac{1}{[p q]} = - \frac{1}{[p q]} \frac{[p s]}{\langle s q \rangle [p q]}, \quad (2.52)$$

and

$$\frac{i \varepsilon_{\mu}^{+}(k_s; r_s) k_{s\nu}}{\sqrt{2}} \left(\frac{L_q^{\mu\nu}}{k_q \cdot k_s} - \frac{L_{\bar{q}}^{\mu\nu}}{k_{\bar{q}} \cdot k_s} \right) k_q^{\rho} = - \frac{1}{\langle s q \rangle} \frac{\langle q | \gamma^{\rho} | s \rangle}{2}, \quad (2.53)$$

$$\frac{i \varepsilon_{\mu}^{+}(k_s; r_s) k_{s\nu}}{\sqrt{2}} \left(\frac{L_q^{\mu\nu}}{k_q \cdot k_s} - \frac{L_{\bar{q}}^{\mu\nu}}{k_{\bar{q}} \cdot k_s} \right) \frac{1}{p \cdot k_q} = + \frac{1}{p \cdot k_q} \frac{[p s]}{\langle s q \rangle [p q]}. \quad (2.54)$$

This complete the proof that the (leading and subleading) soft operators derived from BCFW recurrence and gauge invariance are indeed equivalent (up to a physically irrelevant overall minus sign).

2.2.4 Examples

We consider amplitudes with one quark-antiquark pair and gluons, and a plus-helicity photon emitted from the fermion line.

MHV and $\overline{\text{MHV}}$ amplitudes

- The MHV amplitude is

$$A_{n+3}^{\text{tree}}(\Lambda_{\bar{q}}^{+}, \gamma_s^{+}, \Lambda_q^{-}, g_1^{+}, \dots, g_I^{-}, \dots, g_n^{+}) = \frac{i \langle q I \rangle^3 \langle \bar{q} I \rangle}{\langle \bar{q} s \rangle \langle s q \rangle \dots \langle n \bar{q} \rangle}. \quad (2.55)$$

By taking the holomorphic soft limit $|s\rangle \rightarrow \epsilon|s\rangle$, one gets,

$$A_{n+3}^{\text{tree}}(\Lambda_{\bar{q}}^{+}, \gamma_s^{+}, \Lambda_q^{-}, g_1^{+}, \dots, g_I^{-}, \dots, g_n^{+}) \Big|_{|s\rangle \rightarrow \epsilon|s\rangle} = \frac{1}{\epsilon^2} \frac{\langle \bar{q} q \rangle}{\langle \bar{q} s \rangle \langle s q \rangle} \times \frac{i \langle q I \rangle^3 \langle \bar{q} I \rangle}{\langle \bar{q} q \rangle \langle 1 2 \rangle \dots \langle n \bar{q} \rangle}. \quad (2.56)$$

On the other hand, the action of the operators $S^{(0)\lambda}$ and $S^{(1)\lambda}$ on the lower-point, non-radiative amplitude, $A_{n+3}^{\text{tree}}(\Lambda_{\bar{q}}^{+}, \Lambda_q^{-}, g_1^{+}, \dots, g_I^{-}, \dots, g_n^{+})$ reads,

$$\begin{aligned} \left(\frac{1}{\epsilon^2} S^{(0)\lambda} + \frac{1}{\epsilon} S^{(1)\lambda} \right) A_{n+2}^{\text{tree}}(\Lambda_{\bar{q}}^{+}, \Lambda_q^{-}, g_1^{+}, \dots, g_I^{-}, \dots, g_n^{+}) \\ = \frac{1}{\epsilon^2} \frac{\langle \bar{q} q \rangle}{\langle \bar{q} s \rangle \langle s q \rangle} \times \frac{i \langle q I \rangle^3 \langle \bar{q} I \rangle}{\langle \bar{q} q \rangle \langle 1 2 \rangle \dots \langle n \bar{q} \rangle}. \end{aligned} \quad (2.57)$$

The two results are identical, and in particular, for the MHV amplitude, no next-to-soft contribution arises, because $S^{(1)\lambda} A_{n+2}^{\text{tree}}(\Lambda_{\bar{q}}^{+}, \Lambda_q^{-}, g_1^{+}, \dots, g_I^{-}, \dots, g_n^{+}) = 0$.

- The case of the $\overline{\text{MHV}}$ amplitude is trivial. Since the amplitude has an anti-holomorphic expression,

$$A_{n+3}^{\text{tree}}(\Lambda_{\bar{q}}^{+}, \gamma_s^{+}, \Lambda_q^{-}, g_1^{-}, \dots, g_n^{-}) = \frac{i [\bar{q} s]^3 [q s]}{[\bar{q} s] [s q] [q 1] [1 2] \dots [n \bar{q}]}, \quad (2.58)$$

the holomorphic soft limit, $|s\rangle \rightarrow \epsilon|s\rangle$, has no effect. On the other hand, the soft operators $S^{(0)\lambda}$ and $S^{(1)\lambda}$ act on a vanishing amplitude, $A_{n+2}^{\text{tree}}(\Lambda_{\bar{q}}^{+}, \Lambda_q^{-}, g_1^{-}, \dots, g_n^{-})$.

NMHV 6-point amplitudes

The first non-trivial soft-behaviour can be found when considering next-to-MHV (NMHV) helicity configurations of six-point amplitudes.

Let us consider the amplitude $A_6^{\text{tree}}(\gamma_s^+, 1_q^-, 2_g^-, 3_g^-, 4_g^+, 5_{\bar{q}}^+) \equiv A_6^{\text{tree}}(s^+, 1_q^-, 2^-, 3^-, 4^+, 5_{\bar{q}}^+)$,

$$A_6^{\text{tree}}(s^+, 1_q^-, 2^-, 3^-, 4^+, 5_{\bar{q}}^+) = \frac{i \langle 35 \rangle \langle 3 | 4 + 5 | s \rangle^2}{P_{s12}^2 \langle 34 \rangle \langle 45 \rangle \langle 5 | s + 1 | 2 \rangle [12]} + \frac{i \langle 1 | s + 5 | 4 \rangle^2 \langle 5 | s + 1 | 4 \rangle}{P_{s15}^2 \langle s1 \rangle \langle s5 \rangle \langle 5 | s + 1 | 2 \rangle [32] [43]}, \quad (2.59)$$

with $P_{ij} = k_i + k_j$ and $P_{ijl} = k_i + k_j + k_l$. We construct the soft limit, first by rescaling $|s\rangle \rightarrow \epsilon |s\rangle$,

$$A_6^{\text{tree}}(s^+, 1_q^-, 2^-, 3^-, 4^+, 5_{\bar{q}}^+) \stackrel{|s\rangle \rightarrow \epsilon |s\rangle}{=} - \frac{i}{\epsilon \langle 5 | s | 2 \rangle + \langle 5 | 1 | 2 \rangle} \times \left(\frac{(\epsilon \langle 5 | s | 4 \rangle + \langle 5 | 1 | 4 \rangle)(\epsilon \langle 1 | s | 4 \rangle + \langle 1 | 5 | 4 \rangle)^2}{\epsilon^2 [32] [43] \langle s1 \rangle \langle s5 \rangle (\epsilon(P_{1s}^2 + P_{5s}^2) + P_{15}^2)} + \frac{\langle 35 \rangle \langle 3 | 4 + 5 | s \rangle^2}{[21] \langle 34 \rangle \langle 45 \rangle (\epsilon(P_{1s}^2 + P_{2s}^2) + P_{12}^2)} \right), \quad (2.60)$$

and then, by expanding around $\epsilon \rightarrow 0$,

$$A_6^{\text{tree}}(s^+, 1_q^-, 2^-, 3^-, 4^+, 5_{\bar{q}}^+) \stackrel{\epsilon \rightarrow 0}{=} \frac{a_{-2}}{\epsilon^2} + \frac{a_{-1}}{\epsilon} + \mathcal{O}(1), \quad (2.61)$$

with

$$a_{-2} = - \frac{i[41][54]^2 \langle 15 \rangle}{[21][32][43][51] \langle s1 \rangle \langle s5 \rangle}, \quad (2.62)$$

$$a_{-1} = \frac{1}{\langle s1 \rangle} \left(- \frac{i[54]^2 [4s]}{[21][32][43][51]} + \frac{i[41][54]^2 [2s]}{[21]^2 [32][43][51]} + \frac{i[41][54]^2 [5s]}{[21][32][43][51]^2} \right) + \frac{1}{\langle s5 \rangle} \left(- \frac{i[54][41]^2 [5s]}{[21][32][43][51]^2} - \frac{i[54][41][4s]}{[21][32][43][51]} \right). \quad (2.63)$$

Alternatively, the soft expansion can be obtained through the action of the differential soft operators on the non-radiative five-point amplitude, according to,

$$a_{-2} = S^{(0)\lambda} A_5^{\text{tree}}(1_q^-, 2^-, 3^-, 4^+, 5_{\bar{q}}^+), \quad (2.64)$$

$$a_{-1} = S^{(1)\lambda} A_5^{\text{tree}}(1_q^-, 2^-, 3^-, 4^+, 5_{\bar{q}}^+), \quad (2.65)$$

where, the operators $S^{(0)\lambda}$ and $S^{(1)\lambda}$, respectively defined in (2.20) and (2.21), read

$$S^{(0)\lambda} = \frac{\langle 15 \rangle}{\langle s1 \rangle \langle s5 \rangle}, \quad (2.66)$$

$$S^{(1)\lambda} = \frac{1}{\langle s1 \rangle} [s \partial_1] - \frac{1}{\langle s5 \rangle} [s \partial_5], \quad (2.67)$$

while the five-point quark-gluon amplitude is,

$$A_5^{\text{tree}}(1_q^-, 2^-, 3^-, 4^+, 5_{\bar{q}}^+) = \frac{i[14][54]^3}{[12][23][34][45][51]}. \quad (2.68)$$

In this case, the leading soft singularity is,

$$a_{-2} = \frac{\langle 15 \rangle}{\langle s1 \rangle \langle s5 \rangle} A_5^{\text{tree}}(1_q^-, 2^-, 3^-, 4^+, 5_{\bar{q}}^+) = - \frac{i[41][54]^2 \langle 15 \rangle}{[21][32][43][51] \langle s1 \rangle \langle s5 \rangle} \quad (2.69)$$

in full agreement with the result of (2.62).

To compute the next-to-leading soft term, we combine the derivatives,

$$\begin{aligned} \frac{1}{\langle s1 \rangle} [s \partial_1] A_5^{\text{tree}} (1_q^-, 2^-, 3^-, 4^+, 5_{\bar{q}}^+) &= -\frac{1}{\langle s1 \rangle} \left(\frac{[42][1s]}{[21][41]} + \frac{[5s]}{[51]} \right) A_5^{\text{tree}} (1_q^-, 2^-, 3^-, 4^+, 5_{\bar{q}}^+) \\ &= \frac{1}{\langle s1 \rangle} \left(\frac{i[42][54]^2[1s]}{[21]^2[32][43][51]} + \frac{i[41][54]^2[5s]}{[21][32][43][51]^2} \right), \end{aligned} \quad (2.70)$$

and

$$\begin{aligned} -\frac{1}{\langle s5 \rangle} [s \partial_5] A_5^{\text{tree}} (1_q^-, 2^-, 3^-, 4^+, 5_{\bar{q}}^+) &= \frac{1}{\langle s5 \rangle} \left(\frac{[4s]}{[54]} + \frac{[41][5s]}{[51][54]} \right) A_5^{\text{tree}} (1_q^-, 2^-, 3^-, 4^+, 5_{\bar{q}}^+) \\ &= \frac{1}{\langle s5 \rangle} \left(-\frac{i[54][41]^2[5s]}{[21][32][43][51]^2} - \frac{i[54][41][4s]}{[21][32][43][51]} \right), \end{aligned} \quad (2.71)$$

yielding,

$$a_{-1} = \frac{1}{\langle s1 \rangle} \left(\frac{i[42][54]^2[1s]}{[21]^2[32][43][51]} + \frac{i[41][54]^2[5s]}{[21][32][43][51]^2} \right) \quad (2.72)$$

$$- \frac{1}{\langle s5 \rangle} \left(\frac{i[54][41]^2[5s]}{[21][32][43][51]^2} + \frac{i[54][41][4s]}{[21][32][43][51]} \right). \quad (2.73)$$

After applying the Schouten identity, the result in (2.63) becomes identical to (2.73).

The agreement between the direct soft-limit expansion and the application of the soft operators can be analogously verified for the other NMHV helicity configurations, $A_6^{\text{tree}} (s^+, 1_q^-, 2^+, 3^-, 4^-, 5_{\bar{q}}^+)$ and $A_6^{\text{tree}} (s^+, 1_q^-, 2^-, 3^+, 4^-, 5_{\bar{q}}^+)$.

2.3 Soft-limit of quark-gluon amplitudes

In this section, we discuss the low-energy behaviour of soft-gluon radiation from quark-gluon tree-level amplitudes. Depending on the position of the soft-gluon, g_s , in the colour-ordered amplitude, we may have three situations [200],

$$A_{n+3}^{\text{tree}} (\Lambda_q; g_1, \dots, g_n, g_s; \Lambda_{\bar{q}}) , \quad (2.74)$$

$$A_{n+3}^{\text{tree}} (\Lambda_q; g_s, g_1, \dots, g_n; \Lambda_{\bar{q}}) , \quad (2.75)$$

$$A_{n+3}^{\text{tree}} (\Lambda_q; g_1, \dots, g_m, g_s, g_{m+1}, \dots, g_n; \Lambda_{\bar{q}}) . \quad (2.76)$$

The second case is analogous to the first one, since they both describe the soft-gluon adjacent to one fermion and one gluon, while the third case represents the soft-gluon adjacent to two gluons. Therefore, we will consider as independent only the first and the third configurations, which are discussed in the following. For both cases, by making use of the results in sections 2.1 and 2.2, we will establish the equivalence of the soft operators derived *via* gauge invariance and on-shell recurrence, representing the main result of this work.

2.3.1 Case 1: soft-gluon adjacent to the anti-quark and one gluon

The colour-ordered amplitude $A_{n+3}^{\text{tree}} (\Lambda_q; g_1, \dots, g_n, g_s; \Lambda_{\bar{q}})$ describes the radiation of a soft-gluon emitted from either the external anti-quark \bar{q} , the external gluon g_n or, internal gluon lines between g_n and \bar{q} . This amplitude receives contributions from three types of diagrams, as shown in fig. 2.3.

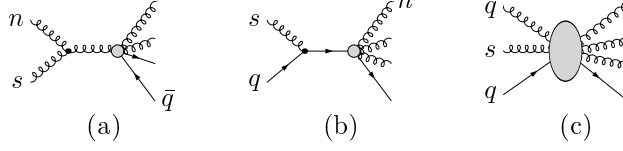


Figure 2.3: Soft-gluon behaviour of quark-gluon amplitudes: case 1

Following the procedure presented in sec. 2.2, from on-shell recursion relation, we can derive the soft behaviour,

$$A_{n+3}^{\text{tree}}(\Lambda_q; g_1, \dots, g_n, g_s; \Lambda_{\bar{q}}) = \left(\frac{1}{\epsilon^2} S_{QCD}^{(0)\lambda} + \frac{1}{\epsilon} S_{QCD}^{(1)\lambda} \right) A_{n+2}^{\text{tree}}(\Lambda_q; g_1, \dots, g_n; \Lambda_{\bar{q}}) + \mathcal{O}(1), \quad (2.77)$$

with

$$S_{QCD}^{(0)\lambda} = \frac{\langle n \bar{q} \rangle}{\langle \bar{q} s \rangle \langle s n \rangle}, \quad (2.78)$$

$$S_{QCD}^{(1)\lambda} = \frac{1}{\langle s \bar{q} \rangle} [s \partial_{\bar{q}}] - \frac{1}{\langle s n \rangle} [s \partial_n], \quad (2.79)$$

and A_{n+2}^{tree} the non-radiative quark-gluon amplitude.

Gauge invariance, on the other side, requires the amplitude to have the following expression,

$$\begin{aligned} A_{n+3}^{\text{tree}}(k_q; k_1, \dots, k_n, k_s; k_{\bar{q}}) &= \left(\frac{\varepsilon^+(k_s; r_s) \cdot k_{\bar{q}}}{\sqrt{2} k_{\bar{q}} \cdot k_s} - \frac{\varepsilon^+(k_s; r_s) \cdot k_n}{\sqrt{2} k_n \cdot k_s} \right) A_{n+2}^{\text{tree}}(k_q; k_1, \dots, k_n; k_{\bar{q}}) \\ &+ \frac{i \varepsilon_{\mu}^+(k_s; r_s) k_{s\nu}}{\sqrt{2}} \left\{ \frac{1}{k_q \cdot k_s} J_{Gn}^{\mu\nu} [\bar{u}(k_q) \tilde{A}(k_q; k_1, \dots, k_n; k_{\bar{q}}) v(k_{\bar{q}})] \right. \\ &+ \frac{1}{k_{\bar{q}} \cdot k_s} \bar{u}(k_q) \tilde{A}(k_q; k_1, \dots, k_n; k_{\bar{q}}) \Sigma_F^{\mu\nu} v(k_{\bar{q}}) \\ &\left. - \bar{u}(k_q) \left[\frac{L_{\bar{q}}^{\mu\nu}}{k_{\bar{q}} \cdot k_s} \tilde{A}(k_q; k_1, \dots, k_n; k_{\bar{q}}) \right] v(k_{\bar{q}}) \right\} + \mathcal{O}(k_s), \quad (2.80) \end{aligned}$$

with the non-radiative amplitude being

$$A_{n+2}^{\text{tree}}(k_{\bar{q}}, k_q, k_1, \dots, k_n) = \bar{u}(k_q) \tilde{A}(k_{\bar{q}}, k_q, k_1, \dots, k_n) v(k_{\bar{q}}). \quad (2.81)$$

In the above expression, $J_{Gn}^{\mu\nu}$ is the total angular momentum for gluon g_n , defined in (2.9), while $L_{\bar{q}}^{\mu\nu}$ and $\Sigma_F^{\mu\nu}$ are respectively the orbital and spin angular momenta of anti-quark \bar{q} , given in (2.29).

The equivalence of the two derivations can be established as follows.

Leading soft singularity

The leading soft term coming from $S_{QCD}^{(0)\lambda}$ in (2.78) and $\left(\frac{\varepsilon^+(k_s; r_s) \cdot k_{\bar{q}}}{\sqrt{2} k_{\bar{q}} \cdot k_s} - \frac{\varepsilon^+(k_s; r_s) \cdot k_n}{\sqrt{2} k_n \cdot k_s} \right)$ in (2.80) agree with each other, once they are expressed in spinor variables, exactly as in (2.34).

Next-to-leading soft singularity

The expression (2.80), obtained from gauge invariance, contains two contributions:

1. the operator $\frac{i\varepsilon_\mu^+(k_s;r_s)k_{s\nu}}{\sqrt{2k_q\cdot k_s}}J_{Gn}^{\mu\nu}$, related to the gluon g_n comes from fig. 2.3 (a) and (c). This term is equivalent to $-\frac{1}{(sn)}[s\partial_n]$ of $S_{QCD}^{(1)\lambda}$ defined in (2.79). The proof comes from the equivalence in the pure-gluon cases [116], whose result we recall in sec. 2.1, eqs. (2.10)-(2.13).
2. the operators $-\frac{i\varepsilon_\mu^+(k_s;r_s)k_{s\nu}}{\sqrt{2k_q\cdot k_s}}L_{\bar{q}}^{\mu\nu}$ and $\frac{i\varepsilon_\mu^+(k_s;r_s)k_{s\nu}}{\sqrt{2k_q\cdot k_s}}\Sigma_F^{\mu\nu}$ related to the anti-quark \bar{q} arise from fig. 2.3 (b) and (c). According to discussions in sec 2.2.3, eqs.(2.40)-(2.42) and (2.49)-(2.51), the combination of these two terms is equivalent to $\frac{1}{(s\bar{q})}[s\partial_{\bar{q}}]$ in $S_{QCD}^{(1)\lambda}$ of (2.79).

Therefore we can consider the soft behaviour of (2.79) equivalent to (2.80).

2.3.2 Case 2: soft-gluon adjacent to two gluons

In the colour-ordered amplitude $A_{n+3}^{\text{tree}}(\Lambda_q; g_1, \dots, g_m, g_s, g_{m+1}, \dots, g_n; \Lambda_{\bar{q}})$, the soft-gluon, g_s , can be emitted from either external gluons, internal gluon or fermion lines, as shown in fig. 2.4.

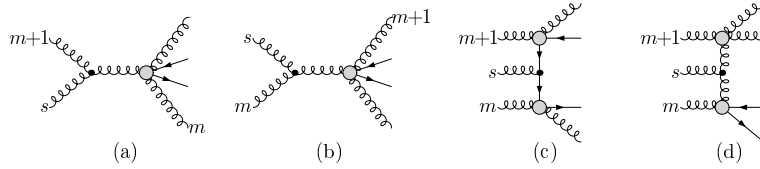


Figure 2.4: Soft-gluon behaviour of quark-gluon amplitudes: case 2

The proof of the equivalence between the derivation from the on-shell formalism and gauge-invariance is identical to the pure-gluon case [116]. The only difference is the term fixed by gauge invariance, called N in [116] and coming from fig. 2.1 (c), it receives now contributions from two pieces, corresponding to fig. 2.4 (c) and (d).

2.3.3 Examples

$$A_6^{\text{tree}}(1_q^-, 2_g^-, 3_g^-, 4_g^+, s_g^+, 5_{\bar{q}}^+)$$

We derive the soft behaviour for a colour-ordered six-point NMHV amplitude corresponding to the case in Sec. 2.3.1.

Let us consider $A_6^{\text{tree}}(1_q^-, 2_g^-, 3_g^-, 4_g^+, s_g^+, 5_{\bar{q}}^+) \equiv A_6^{\text{tree}}(1_q^-, 2^-, 3^-, 4^+, s^+, 5_{\bar{q}}^+)$, where the amplitude is written in [232],

$$A_6^{\text{tree}}(1_q^-, 2^-, 3^-, 4^+, s^+, 5_{\bar{q}}^+) = -\frac{i\langle 5|2+3|4\rangle\langle 1|2+3|4\rangle^2}{P_{234}^2[32][43]\langle 15\rangle\langle s|3+4|2\rangle\langle s5\rangle} - \frac{i\langle 3|s+4|1\rangle\langle 3|s+4|5\rangle^2}{P_{s34}^2[21][51]\langle 34\rangle\langle s|3+4|2\rangle\langle s4\rangle}. \quad (2.82)$$

We first construct the soft limit by rescaling $|s\rangle \rightarrow \epsilon|s\rangle$

$$A_6^{\text{tree}}(1_q^-, 2^-, 3^-, 4^+, s^+, 5_{\bar{q}}^+) \stackrel{|s\rangle \rightarrow \epsilon|s\rangle}{=} \frac{i}{\epsilon^2\langle s|3+4|2\rangle} \left(\frac{(\epsilon\langle 1|s|4\rangle + \langle 1|5|4\rangle)^2(\epsilon\langle 5|s|4\rangle + \langle 5|1|4\rangle)}{[32][43]\langle 15\rangle\langle s5\rangle(\epsilon\langle s|1+5|s\rangle + P_{15}^2)} - \frac{(\epsilon\langle 3|s|1\rangle + \langle 3|4|1\rangle)(\epsilon\langle 3|s|5\rangle + \langle 3|4|5\rangle)^2}{[21][51]\langle 34\rangle\langle s4\rangle(\epsilon\langle s|3+4|s\rangle + P_{34}^2)} \right), \quad (2.83)$$

and then by expanding around $\epsilon \rightarrow 0$

$$A_6^{\text{tree}}(1_q^-, 2^-, 3^-, 4^+, s^+, 5_{\bar{q}}^+) = \frac{a_{-2}}{\epsilon^2} + \frac{a_{-1}}{\epsilon} + \mathcal{O}(1), \quad (2.84)$$

with

$$a_{-2} = -\frac{i[54]^2\langle 3|4|1\rangle}{[21][51]\langle s|3+4|2\rangle\langle s|4|3\rangle} - \frac{i[4|5|1][14][54]}{[32][43]\langle s|3+4|2\rangle\langle s|5|1\rangle}, \quad (2.85)$$

$$a_{-1} = \frac{i[54]}{[21][51]\langle s|3+4|2\rangle} \left(\frac{[41][54][4s]}{[43]^2} - \frac{[54]\langle 3|s|1\rangle}{\langle s|4|3\rangle} + \frac{[41][54]\langle s|3|s\rangle}{[43]\langle s|4|3\rangle} + \frac{2[41]\langle 3|s|5\rangle}{\langle s|4|3\rangle} \right) \\ + \frac{i[54]}{[32][43]\langle s|3+4|2\rangle} \left(\frac{[54][4s]}{[51]} - \frac{[41][54]\langle s|1|s\rangle}{[51]\langle s|5|1\rangle} - \frac{[41][54][5s]}{[51]^2} + \frac{2[4|1|s][s4]}{\langle s|5|1\rangle} \right). \quad (2.86)$$

On the other hand, we obtain the soft expansion by acting the differential operators on the non-radiative five-point amplitude,

$$a_{-2} = S^{(0)\lambda} A_5(1_q^-, 2^-, 3^-, 4^+, 5_{\bar{q}}^+), \quad (2.87)$$

$$a_{-1} = S^{(1)\lambda} A_5(1_q^-, 2^-, 3^-, 4^+, 5_{\bar{q}}^+), \quad (2.88)$$

where operators $S^{(0)\lambda}$ and $S^{(1)\lambda}$ read

$$S^{(0)\lambda} = \frac{\langle 45 \rangle}{\langle s4 \rangle \langle s5 \rangle}, \quad (2.89)$$

$$S^{(1)\lambda} = \frac{1}{\langle s5 \rangle} [s \partial_5] - \frac{1}{\langle s4 \rangle} [s \partial_4]. \quad (2.90)$$

The leading soft singularity is

$$a_{-2} = \frac{\langle 45 \rangle}{\langle s4 \rangle \langle s5 \rangle} A_5(1_q^-, 2^-, 3^-, 4^+, 5_{\bar{q}}^+) = \frac{i[41][54]^2 \langle 45 \rangle}{[21][32][43][51] \langle s4 \rangle \langle s5 \rangle}, \quad (2.91)$$

and for the next-to-leading order soft terms,

$$\frac{1}{\langle s5 \rangle} [s \partial_5] A_5(1_q^-, 2^-, 3^-, 4^+, 5_{\bar{q}}^+) = \frac{1}{\langle s5 \rangle} \left(\frac{[41][5s]}{[51][54]} - \frac{[4s]}{[54]} \right) A_5(1_q^-, 2^-, 3^-, 4^+, 5_{\bar{q}}^+) \\ = \frac{1}{\langle s5 \rangle} \left(\frac{i[41][54][4s]}{[21][32][43][51]} - \frac{i[41]^2[54][5s]}{[21][32][43][51]^2} \right), \quad (2.92)$$

and

$$-\frac{1}{\langle s4 \rangle} [s \partial_4] A_5(1_q^-, 2^-, 3^-, 4^+, 5_{\bar{q}}^+) = -\frac{1}{\langle s4 \rangle} \left(\frac{[1s]}{[14]} - \frac{[3s]}{[34]} + \frac{2[5s]}{[54]} \right) A_5(1_q^-, 2^-, 3^-, 4^+, 5_{\bar{q}}^+) \\ = \frac{1}{\langle s4 \rangle} \left(-\frac{i[54]^2[1s]}{[21][32][43][51]} + \frac{i[41][54]^2[3s]}{[21][32][43]^2[51]} + \frac{2i[41][54][5s]}{[21][32][43][51]} \right) \quad (2.93)$$

yielding

$$a_{-1} = \frac{1}{\langle s5 \rangle} \left(\frac{i[41][54][4s]}{[21][32][43][51]} - \frac{i[41]^2[54][5s]}{[21][32][43][51]^2} \right) \\ + \frac{1}{\langle s4 \rangle} \left(-\frac{i[54]^2[1s]}{[21][32][43][51]} + \frac{i[41][54]^2[3s]}{[21][32][43]^2[51]} + \frac{2i[41][54][5s]}{[21][32][43][51]} \right). \quad (2.94)$$

Eqs. (2.85) and (2.86) agree numerically with (2.91) and (2.94) respectively.

$$A_6^{\text{tree}}(1_q^-, 2_g^-, 3_g^-, s_g^+, 4_g^+, 5_{\bar{q}}^+)$$

We derive the soft behaviour for a colour-ordered six-point NMHV amplitude corresponding to the case in Sec. 2.3.2.

Let us consider $A_6^{\text{tree}}(1_q^-, 2_g^-, 3_g^-, s_g^+, 4_g^+, 5_{\bar{q}}^+) \equiv A_6^{\text{tree}}(1_q^-, 2^-, 3^-, s^+, 4^+, 5_{\bar{q}}^+)$,

$$\begin{aligned} & A_6^{\text{tree}}(1_q^-, 2^-, 3^-, s^+, 4^+, 5_{\bar{q}}^+) \\ &= \frac{i\langle 1|2+3|s\rangle^2\langle 5|2+3|s\rangle}{P_{s23}^2[32]\langle 15\rangle\langle 45\rangle[3s]\langle 4|s+3|2\rangle} - \frac{i\langle 3|s+4|1\rangle\langle 3|s+4|5\rangle^2}{P_{s34}^2[21][51]\langle 4|s+3|2\rangle\langle s3\rangle\langle s4\rangle}. \end{aligned} \quad (2.95)$$

Taking the soft limit, $|s\rangle \rightarrow \epsilon|s\rangle$,

$$\begin{aligned} A_6^{\text{tree}}(1_q^-, 2^-, 3^-, s^+, 4^+, 5_{\bar{q}}^+) \stackrel{|s\rangle \rightarrow \epsilon|s\rangle}{=} & \frac{i}{\epsilon\langle 4|s|2\rangle + \langle 4|3|2\rangle} \left(\frac{\langle 1|2+3|s\rangle^2\langle 5|2+3|s\rangle}{[32]\langle 15\rangle\langle 45\rangle[3s](\epsilon\langle s|2+3|s\rangle + P_{23}^2)} \right. \\ & \left. - \frac{(\epsilon\langle 3|s|1\rangle + \langle 3|4|1\rangle)(\epsilon\langle 3|s|5\rangle + \langle 3|4|5\rangle)^2}{\epsilon^2[21][51]\langle s3\rangle\langle s4\rangle(\epsilon\langle s|3+4|s\rangle + P_{34}^2)} \right), \end{aligned} \quad (2.96)$$

then, expanding around $\epsilon \rightarrow 0$

$$A_6^{\text{tree}}(1_q^-, 2^-, 3^-, s^+, 4^+, 5_{\bar{q}}^+) = \frac{a_{-2}}{\epsilon^2} + \frac{a_{-1}}{\epsilon} + \mathcal{O}(1) \quad (2.97)$$

with

$$\begin{aligned} a_{-2} &= \frac{i[41][54]^2\langle 34\rangle}{[21][32][43][51]\langle s3\rangle\langle s4\rangle}, \quad (2.98) \\ a_{-1} &= \frac{1}{\langle s3\rangle} \left(\frac{i[41][54]^2[2s]}{[21][32]^2[43][51]} - \frac{i[41][54]^2[4s]}{[21][32][43]^2[51]} \right) \\ &+ \frac{1}{\langle s4\rangle} \left(\frac{i[54]^2[1s]}{[21][32][43][51]} - \frac{i[41][54]^2[3s]}{[21][32][43]^2[51]} - \frac{2i[41][54][5s]}{[21][32][43][51]} \right). \end{aligned} \quad (2.99)$$

The soft expansion is obtained by the action of differential soft operators on the non-radiative five-point amplitude as

$$a_{-2} = S^{(0)\lambda} A_5^{\text{tree}}(1_q^-, 2^-, 3^-, 4^+, 5_{\bar{q}}^+), \quad (2.100)$$

$$a_{-1} = S^{(1)\lambda} A_5^{\text{tree}}(1_q^-, 2^-, 3^-, 4^+, 5_{\bar{q}}^+), \quad (2.101)$$

where the operators $S^{(0)\lambda}$ and $S^{(1)\lambda}$ read

$$S^{(0)\lambda} = \frac{\langle 43\rangle}{\langle s4\rangle\langle s3\rangle}, \quad (2.102)$$

$$S^{(1)\lambda} = \frac{1}{\langle s4\rangle}[s\partial_4] - \frac{1}{\langle s3\rangle}[s\partial_3]. \quad (2.103)$$

The leading soft singularity is

$$a_{-2} = \frac{\langle 34\rangle}{\langle s4\rangle\langle s3\rangle} A_5^{\text{tree}}(1_q^-, 2^-, 3^-, 4^+, 5_{\bar{q}}^+) = \frac{i[41][54]^2\langle 45\rangle}{[21][32][43][51]\langle s4\rangle\langle s5\rangle}, \quad (2.104)$$

which agrees with the result of (2.98).

As well, for the next-to-leading order soft terms

$$\frac{1}{\langle s4\rangle}[s\partial_4]A_5^{\text{tree}}(1_q^-, 2^-, 3^-, 4^+, 5_{\bar{q}}^+) = \frac{1}{\langle s4\rangle} \left(\frac{[1s]}{[14]} - \frac{[3s]}{[34]} + \frac{2[5s]}{[54]} \right) A_5^{\text{tree}}(1_q^-, 2^-, 3^-, 4^+, 5_{\bar{q}}^+)$$

$$= \frac{1}{\langle s4 \rangle} \left(\frac{i[54]^2[1s]}{[21][32][43][51]} - \frac{i[41][54]^2[3s]}{[21][32][43]^2[51]} - \frac{2i[41][54][5s]}{[21][32][43][51]} \right) \quad (2.105)$$

$$\begin{aligned} -\frac{1}{\langle s3 \rangle} [s \partial_3] A_5^{\text{tree}}(1_q^-, 2^-, 3^-, 4^+, 5_q^+) &= -\frac{1}{\langle s3 \rangle} \left(-\frac{[2s]}{[23]} - \frac{[4s]}{[43]} \right) A_5^{\text{tree}}(1_q^-, 2^-, 3^-, 4^+, 5_q^+) \\ &= \frac{1}{\langle s3 \rangle} \left(\frac{i[41][54]^2[2s]}{[21][32]^2[43][51]} - \frac{i[41][54]^2[4s]}{[21][32][43]^2[51]} \right) \end{aligned} \quad (2.106)$$

yielding

$$\begin{aligned} a_{-1} &= \frac{1}{\langle s3 \rangle} \left(\frac{i[41][54]^2[2s]}{[21][32]^2[43][51]} - \frac{i[41][54]^2[4s]}{[21][32][43]^2[51]} \right) \\ &\quad + \frac{1}{\langle s4 \rangle} \left(\frac{i[54]^2[1s]}{[21][32][43][51]} - \frac{i[41][54]^2[3s]}{[21][32][43]^2[51]} - \frac{2i[41][54][5s]}{[21][32][43][51]} \right) \end{aligned} \quad (2.107)$$

in full agreement with (2.99).

2.4 Discussion

The study of the low-energy behaviour of radiative tree-level amplitudes in QCD has allowed to see a factorisation between the non-radiative process and the quantum data of the emitter. Our result, based on recursive relations and gauge invariance, points that the non-radiative process is perturbed by the action of universal operators.

The low-energy expansion is captured by universal operators, whose form is dictated by gauge invariance. While the leading soft term is expressed as an eikonal factor, the subleading soft term is found to be proportional to the total angular momentum (orbital and spin). The latter is gauge invariance by itself and requires conservation of angular momentum only.

Nevertheless, leading terms are often linked to infrared singularities, while subleading ones can also arise from contributions not linked to infrared singularities.

We have shown that, within the spinor formalism, the subleading soft operator of single-gluon emission from quark-gluon amplitudes appears as a differential operator. Its form does not depend on the spin of the emitter. Our result, derived from gauge invariance and on-shell recursive construction, is, therefore, in line with the results recently derived for pure gluon- and graviton-scattering.

Besides the results presented in this chapter, there has been an enormous development on this area. At tree-level, the behaviour of soft theorems in arbitrary dimensions and other theories has been generalised in Ref.s [97–110]. In the same manner, a very formal approach, based on gauge and Poincarè symmetry, has been considered in Ref.s [111–130]. The extension to double and multiple soft theorem limits has been achieved in Ref.s [131–136]. Finally, a generalisation to loop level [102, 137–142], has also been discussed.

Although the study of the new soft theorems is rather complete, this is not the end of the story. More work on the extension to one-loop and multiple-soft-theorem is desired. Similarly, studies of gravity from gauge theories are still in progress. We refer, for instance, to Ref.s [123, 233–235].

Chapter 3

Off-shell Currents and Colour-Kinematics Duality

In Sec. 1.1, we described the properties of the primitive amplitudes. In particular, we mentioned that by making use of cyclic, the Kless-Kuijf and the Bern-Carrasco-Johansson relations the number of independent primitive n -point amplitudes reduces to $(n - 3)!$.

In this chapter, we show that the kinematic terms of Feynman diagrams in QCD obey special relations that look like the Jacobi identities for the colour factors [236]. Bern, Carrasco and Johansson have exploited these relations to establish a novel set of identities for the colour stripped (primitive) amplitudes, establishing a duality between the colour and kinematics [143].

Indeed, tree-level amplitudes in gauge theories are found to admit a colour-kinematics (C/K) dual representation in terms of diagrams involving only cubic vertices. The kinematic part of the numerators obeys Jacobi identities and anti-symmetry relations similar to the ones holding for the corresponding structure constants of the Lie algebra [143, 144], as depicted in Fig. 3.1.

$$\begin{array}{c} 1 \\ \diagdown \\ \textcircled{\mathbf{J}} \\ \diagup \\ 4 \end{array} \begin{array}{c} 2 \\ \diagup \\ \textcircled{\mathbf{J}} \\ \diagdown \\ 3 \end{array} = - \begin{array}{c} 1 \\ \text{---} \\ \text{---} \\ \text{---} \\ 4 \end{array} \begin{array}{c} 2 \\ \text{---} \\ \text{---} \\ \text{---} \\ 3 \end{array} + \begin{array}{c} 1 \\ \diagdown \\ \text{---} \\ \diagup \\ 4 \end{array} \begin{array}{c} 2 \\ \diagup \\ \text{---} \\ \diagdown \\ 3 \end{array} + \begin{array}{c} 1 \\ \diagup \\ \text{---} \\ \diagdown \\ 4 \end{array} \begin{array}{c} 2 \\ \diagdown \\ \text{---} \\ \diagup \\ 3 \end{array}$$

Figure 3.1: The Jacobi combination: it can be applied both to Lie group structure constants and to the kinematic part of numerators.

This chapter studies the role of colour-kinematics duality within off-shell currents. Off-shell currents allow for constructing both higher-multiplicity tree and multi-loop level amplitudes. We investigate, in a purely diagrammatic approach, the origin of possible deviations from the C/K-dual behaviour, providing concrete evidence of their relation to contact interactions, which was already pointed out in [143, 237].

First, we consider the tree-level diagrams for $gg \rightarrow X$, for massless final state particles, with $X = ss, q\bar{q}, gg$. We work in axial gauge, describing scalars, s , in the adjoint representation. We deal with the Jacobi relation of the kinematic numerators keeping the partons off-shell. Due to the off-shellness of the external particles, the C/K-duality is broken, and an anomalous term emerges. This anomaly vanishes in the on-shell massless limit, as it should, recovering the exact C/K-duality.

Figure 3.2: Embedding of the Jacobi combination into either higher-point or multi-loop diagrams.

Later, we show that when the Jacobi combination of numerators is immersed into a richer topology, as depicted in Fig. 3.2, the anomaly corresponds to the contribution of subdiagrams, obtained by pinching the external lines of the Jacobi combination.

We discuss how our result, which provides a precise identification of the anomalies, can be used, together with generalised gauge transformations [143, 144, 155, 237], in order to re-shuffle contact terms between diagrams and build on-shell C/K-dual representations for higher-point tree-level amplitudes. We present the explicit calculation for the tree-level contribution to $gg \rightarrow q\bar{q}g$.

As byproduct of this procedure, we obtain linear relations between primitive tree-level amplitudes with different ordering. These relations usually known as Bern-Carrasco-Johansson relations, have coefficients that depend on Lorentz-invariant combination of the momenta of the particles.

3.1 Review of Colour-Kinematics duality

3.1.1 General considerations

Consider an m -point tree-level amplitude, which, we write in terms of cubic vertices

$$\mathcal{A}_m^{\text{tree}}(1, 2, \dots, m) = \sum_{i=1}^N \frac{c_i n_i}{D_i}, \quad D_i = \prod_{\alpha_i} s_{\alpha_i}, \quad (3.1)$$

where the sum runs over all diagrams i with only three-point vertices, the c_i are the colour factors, the n_i are the kinematic numerators, and D_i collect the denominators of all internal propagators. As we shall see in Sec.s 3.2.1 and 3.2.3, contact terms are absorbed once they are replaced with numerator factors cancelling propagators, i.e., s_α/s_α and assigning the contribution to the proper diagram according to the colour factor as done in Eq. (1.23).

The main property of the colour factors is that they satisfy the Jacobi identities, recalling Eq.s (1.8,1.10),

$$-\tilde{f}^{a_1 a_2 b} \tilde{f}^{b a_3 a_4} + \tilde{f}^{a_4 a_1 b} \tilde{f}^{b a_2 a_3} + \tilde{f}^{a_4 a_2 b} \tilde{f}^{b a_3 a_1} = 0, \quad (3.2)$$

$$-T_{3j}^{a_4} T_{j2}^{a_1} + T_{3j}^{a_1} T_{j2}^{a_4} + \tilde{f}^{a_4 a_1 b} T_{32}^b = 0, \quad (3.3)$$

where $\tilde{f}^{abc} = i\sqrt{2}f^{abc}$. The structure constant of Eq. (1.9) has been rescaled in order to avoid prefactors in the next calculations.

Furthermore, for any m -point amplitude, we can always find three colours factors built from Eq.s (3.2,3.3), say

$$c_i = \dots \tilde{f}^{a_1 a_2 b} \tilde{f}^{b a_3 a_4} \dots, \quad c_j = \dots \tilde{f}^{a_4 a_1 b} \tilde{f}^{b a_2 a_3} \dots, \quad c_k = \dots \tilde{f}^{a_4 a_2 b} \tilde{f}^{b a_3 a_1} \dots,$$

where the ‘...’ state for common terms in the three colour factors. Therefore, the Jacobi identity takes the form

$$-c_i + c_j + c_k = 0, \quad (3.4)$$

The Colour-Kinematics (C/K) duality states that the numerators n_i can always be found in such a way they satisfy Jacobi identities in the kinematical sector,

$$-c_i + c_j + c_k = 0 \quad \Rightarrow \quad -n_i + n_j + n_k = 0. \quad (3.5)$$

C/K-duality also requires that the n_i have to satisfy the same anti-symmetry relations as the c_i , i.e. if a colour factor is anti-symmetric under the change of two legs, the corresponding numerator has to transform in the way,

$$c_i \rightarrow -c_i \quad \Rightarrow \quad n_i \rightarrow -n_i.$$

3.1.2 Bern-Carrasco-Johansson relations

According to Eq. (3.1), a four-point amplitude can be written as

$$\mathcal{A}_4^{\text{tree}}(1, 2, 3, 4) = \frac{c_1 n_1}{s_{14}} + \frac{c_2 n_2}{s_{12}} + \frac{c_3 n_3}{s_{13}}, \quad (3.6)$$

the three colour factors are related by the Jacobi identity

$$-c_1 + c_2 + c_3 = 0. \quad (3.7)$$

Firstly, we demand that the corresponding numerators n_i fulfil the same identity

$$-n_1 + n_2 + n_3 = 0, \quad (3.8)$$

Secondly, we write the colour-ordered amplitudes

$$A_4^{\text{tree}}(1, 2, 3, 4) = \frac{n_1}{s_{14}} + \frac{n_2}{s_{12}}, \quad (3.9a)$$

$$A_4^{\text{tree}}(1, 2, 4, 3) = -\frac{n_1}{s_{14}} - \frac{n_3}{s_{13}}, \quad (3.9b)$$

$$A_4^{\text{tree}}(1, 4, 2, 3) = -\frac{n_2}{s_{12}} + \frac{n_3}{s_{13}}. \quad (3.9c)$$

We shall show in Sec. 3.3.2, by following an alternative procedure of the one describe in Ref. [143], that Eq.s. (3.7-3.9) allow us to end up with relations between colour-ordered amplitudes

$$s_{24} A_4^{\text{tree}}(1, 2, 4, 3) = s_{23} A_4^{\text{tree}}(1, 2, 3, 4), \quad (3.10)$$

These relations are usually called Bern-Carrasco-Johansson (BCJ) relations for four-point amplitudes. In the same manner, BCJ relations for five- and six-point turn out to be

$$s_{24} A_5^{\text{tree}}(1, 2, 4, 3, 5) = (s_{14} + s_{45}) A_5^{\text{tree}}(1, 2, 3, 4, 5) + s_{14} A_5^{\text{tree}}(1, 2, 3, 5, 4), \quad (3.11)$$

$$s_{24} A_5^{\text{tree}}(1, 2, 4, 3, 5, 6) = (s_{14} + s_{46} + s_{45}) A_6^{\text{tree}}(1, 2, 3, 4, 5, 6) + (s_{14} + s_{46}) A_6^{\text{tree}}(1, 2, 3, 5, 4, 6) + s_{14} A_6^{\text{tree}}(1, 2, 3, 5, 6, 4). \quad (3.12)$$

Thus, the BCJ relations among n -point colour-ordered amplitudes, usually called fundamental BCJ relations, can be written as [143]

$$\sum_{i=3}^n \left(\sum_{j=3}^i s_{2j} \right) A_n^{\text{tree}}(1, 3, \dots, i, 2, i+1, \dots, n) = 0. \quad (3.13)$$

3.2 Off-shell Colour-Kinematics Duality

In this section we study the C/K duality for off-shell diagrams in gauge theories coupled to matter. By investigating the scattering process $gg \rightarrow ss, q\bar{q}, gg$, we show that the Jacobi relations for the kinematic numerators of off-shell diagrams, built with Feynman rules in axial gauge, reduce to an anomalous term. Such anomaly vanishes when the four particles connected by the Jacobi relation are on their mass shell with vanishing squared momenta, being either external or cut particles, where the validity of the colour-kinematics duality is recovered.

3.2.1 Scalars

The process $gg \rightarrow ss$ gets contributions from four tree-level diagrams, three of which contain cubic interactions, due to either ggg or gss couplings, while one is given by the quartic vertex $ggss$. Their colour factors satisfy the Jacobi identity (3.2), where a similar relation can be established for the kinematic part of the numerators of suitably defined graphs involving only cubic vertices.

Figure 3.3: Jacobi combination for $gg \rightarrow ss$.

The four-point vertex can be distributed to the numerators of the diagrams with cubic vertices only, as done in Eq. (1.23), hence, yielding the identification of three colour-kinematics dual diagrams [143]. The corresponding numerators, say n_1 , n_2 and n_3 , can be combined in Jacobi-like fashion,

$$N_s = -n_1 + n_2 + n_3, \quad (3.14)$$

as shown in Fig. 3.3.

In axial gauge - that we will consider throughout our calculations - the numerator of the gluon propagator takes the form

$$\Pi^{\mu\nu}(p, q) = \Pi_{\text{Fey}}^{\mu\nu} + \Pi_{\text{Ax}}^{\mu\nu}(p, q), \quad (3.15)$$

where $\Pi_{\text{Fey}}^{\mu\nu}$ corresponds to the numerator of the propagator in Feynman gauge and $\Pi_{\text{Ax}}^{\mu\nu}(p, q)$ labels the term depending on an arbitrary light-like reference momentum q^μ ,

$$\Pi_{\text{Fey}}^{\mu\nu} = -i g^{\mu\nu}, \quad \Pi_{\text{Ax}}^{\mu\nu}(p, q) = i \frac{p^\mu q^\nu + q^\mu p^\nu}{q \cdot p}. \quad (3.16)$$

The explicit form of (3.14) is given by the contraction of an off-shell current with gluon polarizations as

$$N_s = (J_{\text{s-Fey}}^{\mu_1\mu_4} + J_{\text{s-Ax}}^{\mu_1\mu_4}) \varepsilon_{\mu_1}(p_1) \varepsilon_{\mu_4}(p_4) = N_{\text{s-Fey}} + N_{\text{s-Ax}}, \quad (3.17)$$

where $J_{\text{s-Fey}}^{\mu_1\mu_4}$ is the sum of the Feynman gauge-like terms of the three numerators,

$$-i J_{\text{s-Fey}}^{\mu_1\mu_4}(p_1, p_2, p_3, p_4) = p_1^{\mu_1} (p_1^{\mu_4} + 2p_3^{\mu_4}) - (2p_3^{\mu_1} + p_4^{\mu_1}) p_4^{\mu_4} \quad (3.18)$$

and

$$\begin{aligned} -i J_{\text{s-Ax}}^{\mu_1\mu_4}(p_1, p_2, p_3, p_4) = & \frac{1}{q \cdot (p_1 + p_4)} \left\{ - (p_1^{\mu_1} p_1^{\mu_4} - p_4^{\mu_1} p_4^{\mu_4} - (p_1^2 - p_4^2) g^{\mu_1\mu_4}) q \cdot (p_2 - p_3) \right. \\ & \left. + (p_2^2 - p_3^2) [(p_4 + 2p_1)^{\mu_4} q^{\mu_1} + q \cdot (p_4 - p_1) g^{\mu_1\mu_4} - (p_1 + 2p_4)^{\mu_1} q^{\mu_4}] \right\} \end{aligned} \quad (3.19)$$

is the contribution, depending on the reference momentum, which only originates from n_2 .

From this Jacobi-like tensor we see that the colour-kinematics duality on the kinematics side holds, *i.e.* $N_s = 0$, once the four external particles are put on-shell, $p_i^2 = 0$, and, imposed transversality condition for gluons, $p_i \cdot \varepsilon(p_i) = 0$. We want to remark that $N_{\text{s-Fey}}$ and $N_{\text{s-Ax}}$

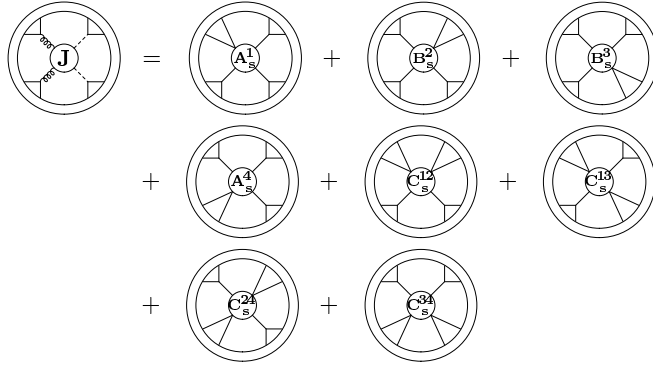


Figure 3.4: Off-shell colour-kinematics duality for gluons and scalars. The Jacobi combination of tree-level numerators (l.h.s) is expressed in terms of subdiagrams only (r.h.s.).

vanish separately, so that the C/K duality is satisfied at tree-level also in ordinary Feynman gauge.

A similar calculation was performed in [236], where tree-level numerators for $gg \rightarrow X$ were studied as well. This result differs in the choice of axial gauge, which, as we are going to show, plays an important role in the identification of the C/K-duality violating terms in the numerator of higher-multiplicity graphs.

The expressions of the currents in Eqs. (3.18,3.19) are valid for off-shell kinematics. Therefore, they can be exploited for providing a better understanding of C/K-duality within more complex numerators obtained by embedding the Jacobi-like combination of tree-level numerators into a generic diagram, as depicted in Fig. 3.2, where the double circle shall represent an arbitrary number of loops and external legs.

In the most general case, the legs p_1, p_2, p_3 and p_4 become internal lines and polarisations associated to the particles are replaced by the numerator of their propagators, which, for the scalar case, simply corresponds to a factor i . Accordingly, Eq. (3.14) generalises to the following contraction,

$$N_s = (N_s)_{\alpha_1 \alpha_4} X^{\alpha_1 \alpha_4}. \quad (3.20)$$

between the tensor $(N_s)_{\alpha_1 \alpha_4}$, defined as,

$$(N_s)_{\alpha_1 \alpha_4} = - (J_{s\text{-Fey}}^{\mu_1 \mu_4} + J_{s\text{-AX}}^{\mu_1 \mu_4}) \Pi_{\mu_1 \alpha_1}(p_1, q_1) \Pi_{\mu_4 \alpha_4}(p_4, q_4). \quad (3.21)$$

and the arbitrary tensor $X^{\alpha_1 \alpha_4}$, standing for the residual kinematic dependence of the diagrams, associated to either higher-point tree-level or to multi-loop topologies.

Using momentum conservation, we find that the r.h.s. of (3.21) can be cast in the following form,

$$(N_s)_{\alpha_1 \alpha_4} = p_1^2 (A_s^1)_{\alpha_1 \alpha_4} + p_4^2 (A_s^4)_{\alpha_1 \alpha_4} + p_2^2 (B_s^2)_{\alpha_1 \alpha_4} + p_3^2 (B_s^3)_{\alpha_1 \alpha_4} \\ + p_1^2 p_2^2 (C_s^{12})_{\alpha_1 \alpha_4} + p_1^2 p_3^2 (C_s^{13})_{\alpha_1 \alpha_4} + p_4^2 p_2^2 (C_s^{24})_{\alpha_1 \alpha_4} + p_4^2 p_3^2 (C_s^{34})_{\alpha_1 \alpha_4}, \quad (3.22)$$

where A_s^i, B_s^i and C_s^{ij} are tensors depending both on the momenta p_i of gluons and scalars, eventually depending on the loop variables, and on the reference momenta q_i of each gluon propagators.

Remarkably, Eq.(3.22) shows the full decomposition of a generic numerator built from the Jacobi relation in terms of squared momenta of the particles entering the Jacobi combination

defined in Fig. 3.3. In particular, this result implies that the C/K duality is certainly satisfied when imposing the on-shell cut-conditions $p_i^2 = 0$.

A diagrammatic representation of the consequences of the decomposition (3.22) in (3.20) is given in Fig. 3.4, where the eight terms appearing in r.h.s. of (3.22) generate subdiagrams, obtained by pinching one or two denominators. In these subdiagrams A_s^i , B_s^i and C_s^{ij} play the role of effective vertices contracted with the tensor $X^{\alpha_1\alpha_4}$.

The existence of contact terms responsible for the violation of the C/K-duality was conceptually pointed out already in [143]. Here, we identified, by following a purely diagrammatic approach, the source of such *anomaly*, exposed in the (single and double) momentum-square dependance of formula (3.22).

The choice of axial gauge turned out to be crucial within our derivation, since the p^2 -terms appear, besides from the trivial contraction $p^\mu p_\mu$, also from the contraction of $\Pi^{\mu\nu}(p, q)$ with the corresponding gluon momentum (Ward identity),

$$p_\mu \Pi^{\mu\nu}(p, q) = i p_\mu \left(-g^{\mu\nu} + \frac{p^\mu q^\nu + q^\mu p^\nu}{q \cdot p} \right) = i p^2 \frac{q^\nu}{q \cdot p}. \quad (3.23)$$

By inspection of (3.18) and (3.19), we observe that $J_{s\text{-Fey}}$ only gives contribution to A_s^1 and A_s^4 , while $J_{s\text{-Ax}}$ produces terms proportional to the momenta of all the four particles as well as to all the possible pairs of gluon-scalar denominators, *i.e.* contributes to all the eight effective vertices.

In addition, because of the explicit symmetries of $J_{s\text{-Fey}}$ and $J_{s\text{-Ax}}$ under $1 \leftrightarrow 4$ and $2 \leftrightarrow 3$, the two effective vertices associated to the pinch of one scalar propagator, namely A_s^1 and A_s^4 , are related to each other by particle relabelling. The same happens for B_s^2 and B_s^3 , which correspond to the pinch of one gluon propagator. For the same reason, there is only one independent C_s function, corresponding to the pinch of two denominators, say $p_i^2 p_j^2$, which are originated from terms proportional to $p_i^\mu p_j^\mu$ in Eq.(3.19).

3.2.2 Quarks

For the tree-level scattering $gg \rightarrow q\bar{q}$ there are three Feynman graphs contributing to it, each one contains only cubic interactions due to ggg and $gg\bar{q}$ couplings. The corresponding colour factors obey the Jacobi identity (3.3), which allows to build the combination of colour-kinematics numerators for the tree-level graph (3.14), as shown in Fig. 3.5.

$$\text{Diagram 1} = - \text{Diagram 2} + \text{Diagram 3} + \text{Diagram 4}$$

Figure 3.5: Jacobi combination for $gg \rightarrow q\bar{q}$.

Following the same derivation as for gluons and scalars, the Jacobi relation for gluons and fermions can be built from the contraction of fermion currents and polarisations,

$$N_q = \bar{u}(p_3)(J_{q\text{-Fey}}^{\mu_1\mu_4} + J_{q\text{-Ax}}^{\mu_1\mu_4})v(p_2)\varepsilon_{\mu_4}(p_4)\varepsilon_{\mu_1}(p_1) = N_{q\text{-Fey}} + N_{q\text{-Ax}}. \quad (3.24)$$

Using Dirac algebra and momentum conservation, $J_{q\text{-Fey}}^{\mu_1\mu_4}$ and $J_{q\text{-Ax}}^{\mu_1\mu_4}$ can be organised into compact forms as,

$$-i J_{q\text{-Fey}}^{\mu_1\mu_4}(p_1, p_2, p_3, p_4) = -\not{p}_3 \gamma^{\mu_4} \gamma^{\mu_1} - \gamma^{\mu_1} \gamma^{\mu_4} \not{p}_2 + (\not{p}_3 + \not{p}_2) g^{\mu_1\mu_4} p_4^{\mu_4} \gamma^{\mu_1} - p_1^{\mu_1} \gamma^{\mu_4} \quad (3.25)$$

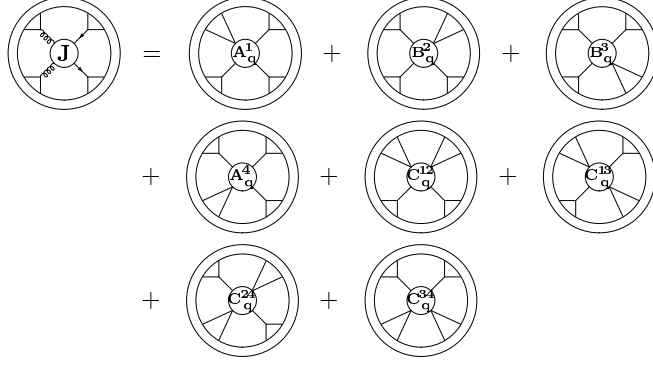


Figure 3.6: Off-shell colour-kinematics duality for gluons and quarks.

and

$$\begin{aligned}
-i J_{\text{q-Ax}}^{\mu_1\mu_4}(p_1, p_2, p_3, p_4) &= \frac{1}{q \cdot (p_4 + p_1)} \left\{ (\not{p}_3 + \not{p}_2) [g^{\mu_1\mu_4} q \cdot (p_4 - p_1) \right. \\
&\quad \left. - q^{\mu_4} (p_1 + 2p_4)^{\mu_1} + q^{\mu_1} (p_4 + 2p_1)^{\mu_4}] + \not{q} [p_1^{\mu_4} p_1^{\mu_1} - p_4^{\mu_4} p_4^{\mu_1} + g^{\mu_1\mu_4} (p_4^2 - p_1^2)] \right\}. \quad (3.26)
\end{aligned}$$

We observe that (3.24) vanishes when the four external particles are on-shell, due to transversality conditions and Dirac equation, $\bar{u}(p_3)\not{p}_3 = \not{p}_2 v(p_2) = 0$.

The C/K duality is satisfied at tree-level also in Feynman gauge, since on-shellness enforces $N_{\text{q-Fey}}$ and $N_{\text{q-Ax}}$ to vanish independently.

In order to study the Jacobi combination within higher-point numerators or multi-loop integrands, we repeat the procedure adopted in Section 3.2.1. Accordingly, we promote the external states of gluons and quarks to propagating particles, and define the off-shell tensor,

$$(N_{\text{q}})_{\alpha_1\alpha_4} = i\not{p}_3 (J_{\text{q-Fey}}^{\mu_1\mu_4} + J_{\text{q-Ax}}^{\mu_1\mu_4}) i\not{p}_2 \Pi_{\mu_4\alpha_4}(p_4, q_4) \Pi_{\mu_1\alpha_1}(p_1, q_1), \quad (3.27)$$

by replacing the polarisation vectors with the numerators of the gluon propagators, and the spinors $\bar{u}(p_3)$ and $v(p_2)$ with the numerators of fermionic propagators. As before, the full numerator is obtained contracting (3.27) with a generic tensor $X^{\alpha_1\alpha_4}$.

Manipulating the r.h.s. of (3.27), we obtain an expression analogous to the decomposition (3.22), where the denominators of the four particles are manifestly factored out,

$$\begin{aligned}
(N_{\text{q}})_{\alpha_1\alpha_4} &= p_1^2 (A_q^1)_{\alpha_1\alpha_4} + p_4^2 (A_q^4)_{\alpha_1\alpha_4} + p_2^2 (B_q^2)_{\alpha_1\alpha_4} + p_3^2 (B_q^3)_{\alpha_1\alpha_4} \\
&\quad + p_1^2 p_2^2 (C_q^{12})_{\alpha_1\alpha_4} + p_1^2 p_3^2 (C_q^{13})_{\alpha_1\alpha_4} + p_4^2 p_2^2 (C_q^{24})_{\alpha_1\alpha_4} + p_4^2 p_3^2 (C_q^{34})_{\alpha_1\alpha_4}. \quad (3.28)
\end{aligned}$$

In the above expression, A_q^i and B_q^i receive contribution both from $J_{\text{q-Fey}}$ and $J_{\text{q-Ax}}$ while C_q^{ij} 's are determined only by $J_{\text{q-Ax}}$. This can be understood by inspection of (3.25) and (3.26), observing that denominators may appear because of (3.23), as well as because of the identity $\not{p}\not{p} = p^2$. Also in this case, we only have three independent functions: two for the effective vertices corresponding to the pinch of one quark- or one gluon- propagator, namely A_q^i and B_q^i , and a single vertex C_q^{ij} for the pinch of a quark-gluon pair. We remark that these functions contain non-trivial Dirac structure. The interpretation of (3.28) is similar to the one of (3.22) and it is illustrated in Fig. 3.6.

3.2.3 Gluons

Finally, we consider the C/K duality for the pure gauge interaction process $gg \rightarrow gg$. As for $gg \rightarrow ss$, there are four diagrams to be considered, three involving the tri-gluon interaction, and

As in the previous Sections, we can build a generic off-shell tensor, to be embedded in a more complex topology, either with more loops or more legs, by replacing polarisation vectors with the numerator of the corresponding propagators,

$$(N_g)_{\alpha_1 \dots \alpha_4} = (J_{g\text{-Fey}}^{\mu_1 \dots \mu_4} + J_{g\text{-Ax}}^{\mu_1 \dots \mu_4}) \Pi_{\mu_1 \alpha_1}(p_1, q_1) \Pi_{\mu_2 \alpha_2}(p_2, q_2) \Pi_{\mu_3 \alpha_3}(p_3, q_3) \Pi_{\mu_4 \alpha_4}(p_4, q_4), \quad (3.32)$$

and by contracting this expression with an appropriate tensor $X^{\alpha_1 \dots \alpha_4}$.

Because of the Ward identity (3.23), $(N_g)_{\alpha_1 \dots \alpha_4}$ turns out to be decomposed as

$$(N_g)_{\alpha_1 \dots \alpha_4} = \sum_{i=1}^4 p_i^2 (A_g^i)_{\alpha_1 \dots \alpha_4} + \sum_{\substack{i,j=1 \\ i \neq j}}^4 p_i^2 p_j^2 (C_g^{ij})_{\alpha_1 \dots \alpha_4}. \quad (3.33)$$

We observe that, differently from the scalar and fermionic cases, $J_{g\text{-Ax}}$ produces all the possible combinations of two different denominators. This is a consequence of the permutation symmetry of the gauge-dependent part of the numerators, which is an exclusive feature of the Jacobi identity for pure gauge interactions. The same symmetry reduces from three to two the number of independent effective vertices, corresponding to the pinch of one or two gluon propagators.

The diagrammatic effect of (3.33) contracted with $X^{\alpha_1 \dots \alpha_4}$ is depicted in Fig. 3.8, which shows that, as it happened for the $gg \rightarrow ss$, and $gg \rightarrow q\bar{q}$, the Jacobi combination of the kinematic numerators for $gg \rightarrow gg$ with off-shell particles always reduces to subdiagrams.

Let us, finally, remark that the form factors A^i -, B^i - and C^{ij} -type appearing in the decompositions (3.22), (3.28), and (3.33) still depend on the momenta p_i and p_j . Therefore, within multiloop integrands, they can generate tensor integrals which can be subject to further integral reductions.

3.3 Construction of dual numerators for higher-point amplitudes

In the previous sections, we saw that the Jacobi-like identity for kinematic numerators is satisfied for all four-point tree amplitudes. Moreover, once the number of external legs start increasing those numerators do not satisfy it anymore, giving rise to anomalous terms. Nevertheless, in order to satisfy it we can always absorb that anomaly in the re-definition of the numerators. This re-definition can be done as a consequence of the gauge invariance of the amplitude. The non-uniqueness of the kinematic numerators is referred to as *generalised gauge-invariance* [143, 144, 155, 237].

In this Section we illustrate how the previous results can be used, together with generalised gauge invariance in order to explicitly determine dual representation of higher-point amplitudes starting from Feynman diagrams. In addition, we show that our construction allows a purely diagrammatic derivation of monodromy relations for amplitudes, [157].

3.3.1 Algorithm

From Eq. (3.1) we can see that any amplitude can be written in terms of N colour factors, which, satisfy a set of M , $M < N$, Jacobi identities, (3.4), whose solution allows us to express M colour factors in terms of $N - M$ independent ones $\{c_{\sigma(1)}, \dots, c_{\sigma(N-M)}\}$, so that (3.1) can be organised as

$$\mathcal{A}_m^{\text{tree}}(p_1, p_2, \dots, p_m) = \sum_{i=1}^{N-M} c_{\sigma(i)} K_{\sigma(i)}(\{n\}), \quad (3.34)$$

where

$$K_{\sigma(i)}(\{n\}) = \sum_{j=1}^N \frac{\alpha_{\sigma(i)j} n_j}{D_j}, \quad \alpha_{\sigma(i)j} \in \{0, \pm 1\}. \quad (3.35)$$

The set of identities (3.4) is not, in general, trivially satisfied by the corresponding kinematic numerators, whose Jacobi combinations produce non-vanishing anomalous terms,

$$-n_i + n_j + n_k = \phi_{[i,j,k]}. \quad (3.36)$$

We observe that the two sets of equations (3.35) and (3.36) can be conveniently organised into the matrix equation,

$$\mathbb{A} \mathbf{n} = \mathbf{K} + \boldsymbol{\phi}, \quad (3.37)$$

with

$$\begin{aligned} \mathbf{n} &= (n_1, n_2, \dots, n_N)^T, \\ \mathbf{K} &= (\{K_{\sigma(i)}\}, 0, 0, \dots, 0)^T, \\ \boldsymbol{\phi} &= (0, 0, \dots, 0, \{\phi_{[i,j,k]}\})^T \end{aligned} \quad (3.38)$$

and

$$\mathbb{A}_{ij} \in \{0, \pm 1, \pm D_j^{-1}\}. \quad (3.39)$$

As shown by the decompositions (3.22), (3.28) and (3.33), the anomalies are proportional to the off-shell momenta of the particle entering the Jacobi combination itself. Therefore, the rise of these anomalies seems to be related to the allocation of contact terms between cubic diagrams, which naturally provides numerators satisfying C/K-duality in the four-point case only. As a consequence, in order to obtain a dual representation of the amplitude, we need to re-shuffle contact terms, leaving (3.1) unchanged. This can be achieved through a generalised gauge transformation, which consists in a set of shifts of the kinematic numerators,

$$n_i \rightarrow n'_i = n_i - \Delta_i, \quad (3.40)$$

satisfying

$$\delta \mathcal{A}_m^{\text{tree}}(p_1, p_2, \dots, p_m) \equiv \sum_{i=1}^{N-M} c_{\sigma(i)} \sum_{j=1}^N \frac{\alpha_{\sigma(i)j} \Delta_j}{D_j} = 0, \quad (3.41)$$

in such a way that the amplitude can still be written as

$$\mathcal{A}_m^{\text{tree}}(p_1, p_2, \dots, p_m) = \sum_{i=1}^N \frac{c_i n'_i}{D_i} = \sum_{i=1}^{N-M} c_{\sigma(i)} K_{\sigma(i)}(\{n'\}). \quad (3.42)$$

By imposing the vanishing of the coefficient of each $c_{\sigma(i)}$ in (3.41), the gauge invariance requirement is translated into a set equations for the shifts, which leaves M of them undetermined. This means that, in principle, we have enough freedom to ask the shifts to be solution of M additional equations,

$$-\Delta_i + \Delta_j + \Delta_k = \phi_{[i,j,k]}, \quad (3.43)$$

which, inserted in (3.36), make the new set of numerators n'_i manifestly dual. Thus, the simultaneous imposition of (3.41) and (3.43) leads the determination of numerators satisfying the C/K-duality back to the solution of the $N \times N$ linear system

$$\mathbb{A} \Delta = \phi, \quad (3.44)$$

with

$$\Delta = (\Delta_1, \Delta_2, \dots, \Delta_N)^T, \quad (3.45)$$

whereas the vector ϕ and the matrix \mathbb{A} are the ones defined by (3.38) and (3.39).

By solving (3.44), we can determine the shifts to be performed on the numerators obtained from Feynman diagrams ensuring C/K-duality as a function of anomalies $\phi_{[i,j,k]}$ and denominators D_i . We note that the existence of a dual representation of the amplitude is bound to the consistency of the non-homogenous system (3.44), *i.e.* to the condition

$$\text{rank}(\mathbb{A}|\phi) = \text{rank}(\mathbb{A}), \quad (3.46)$$

where $\mathbb{A}|\phi$ is the augmented matrix associated to \mathbb{A} .

In particular, if the system had maximum rank N , the expression of the numerators would be completely fixed by C/K-duality. However, as we will show in an explicit example, the rank of the system turns out to be smaller than N , so that its solution will depend on a set of arbitrary shifts, which are left completely undetermined by the imposition of C/K-duality. The existence of a residual freedom in the choice of the dual representation was first observed in [143] and more recently, in [238], where the reduction of the tree-level C/K-duality to an underconstrained linear problem is addressed in terms of a *pseudo-inverse* operation, it has been interpreted as the hint of a possible analogous construction at loop-level.

Moreover, we observe that, because of (3.37) and (3.44), applying the matrix \mathbb{A} to the new set of numerators n'_i , we obtain

$$\mathbb{A} \mathbf{n}' = \mathbf{K}, \quad (3.47)$$

with \mathbf{K} given by (3.38).

Also, if $\text{rank}(\mathbb{A}) < N$, the consistency condition

$$\text{rank}(\mathbb{A}|\mathbf{K}) = \text{rank}(\mathbb{A}), \quad (3.48)$$

implies the existence of $N - \text{rank}(\mathbb{A})$ constraints between the kinematic factors $K_{\sigma(i)}$, which are in one-by-one correspondence with the relations between colour ordered amplitudes. Therefore, this construction shows that all these non-trivial relations can be derived from the expansion of the amplitudes in terms of Feynman graphs through purely algebraic manipulation on the matrix \mathbb{A} .

Summarising the diagrammatic approach to the construction of C/K-dual numerators for higher-point amplitudes:

- given the decomposition of an amplitude in terms of Feynman diagrams, it is organised into N cubic graphs, whose numerators satisfy the system of equations

$$\mathbb{A} \mathbf{n} = \mathbf{K} + \phi. \quad (3.49)$$

- A generalised gauge transformation

$$n_i \rightarrow n'_i + \Delta_i, \quad (3.50)$$

such that

$$\mathbb{A} \Delta = \phi, \quad (3.51)$$

$$\mathbb{A} \mathbf{n}' = \mathbf{K}, \quad (3.52)$$

is performed on the amplitude in order to obtain a new set of numerators satisfying the C/K-duality. The solution of (3.51) determines the shifts linking the starting set of numerators to the dual representation.

- The existence of solutions for the the systems (3.51) and (3.52) is related to the constraint

$$\text{rank}(\mathbb{A}|\phi) = \text{rank}(\mathbb{A}|\mathbf{K}) = \text{rank}(\mathbb{A}). \quad (3.53)$$

This consistency condition is able to detect all $N - \text{rank}(\mathbb{A})$ non-trivial constraints both between the C/K-violating terms $\phi_{[i,j,k]}$ and the kinematic factors $K_{\sigma(i)}$, the latter corresponding to the well-known relations between colour ordered amplitudes which were first observed, for gluon amplitudes, in [143]. Note the $N - \text{rank}(\mathbb{A})$ also determines the number of completely free parameters the set of C/K-dual numerators will depend on.

In the following Section we give an example of this method, determining the C/K-dual representation for $gg \rightarrow q\bar{q}g$ and showing that the knowledge of the matrix \mathbb{A} can be used to determine the constraints on kinematic factors $K_{\sigma(i)}$ as well on the anomalies $\phi_{[i,j,k]}$, which rise as direct consequence of the off-shell decompositions worked out in Sections 3.2.1-3.2.3.

3.3.2 Colour-kinematics duality for $gg \rightarrow gg$

Starting from Eq. (3.6), we see that the colour factor c_2 can be eliminated because of the Jacobi identity, Eq. (3.7). It allows us to rewrite the amplitude in terms of two colour factors only,

$$\mathcal{A}_4(p_1, p_2, p_3, p_4) = c_1 K_1 + c_3 K_3, \quad (3.54)$$

with

$$K_1 = \frac{n_1}{s_{23}} + \frac{n_2}{s_{12}}, \quad K_3 = \frac{n_3}{s_{24}} - \frac{n_2}{s_{12}}. \quad (3.55)$$

The kinematic numerators obey the same Jacobi identity as the colour factors, (3.8). The set of equations (3.8,3.55) can be conveniently organised into a linear system $\mathbb{A} \mathbf{n} = \mathbf{K}$,

$$\begin{pmatrix} \frac{1}{s_{23}} & \frac{1}{s_{12}} & 0 \\ 0 & -\frac{1}{s_{12}} & \frac{1}{s_{24}} \\ -1 & 1 & 1 \end{pmatrix} \begin{pmatrix} n_1 \\ n_2 \\ n_3 \end{pmatrix} = \begin{pmatrix} K_1 \\ K_3 \\ 0 \end{pmatrix}. \quad (3.56)$$

Due to momentum conservation, $s_{12} + s_{23} + s_{24} = 0$, we can verify that the matrix \mathbb{A} has

$$\text{rank}(\mathbb{A}) = 2 \quad (3.57)$$

or, equivalently, that a linear relation can be established between its rows,

$$s_{23} \mathbb{A}_1 - s_{24} \mathbb{A}_2 + \mathbb{A}_3 = 0. \quad (3.58)$$

Therefore, because of the consistency condition of the inhomogeneous system (3.56),

$$\text{rank}(\mathbb{A}) = \text{rank}(\mathbb{A}|\mathbf{K}) = 2, \quad (3.59)$$

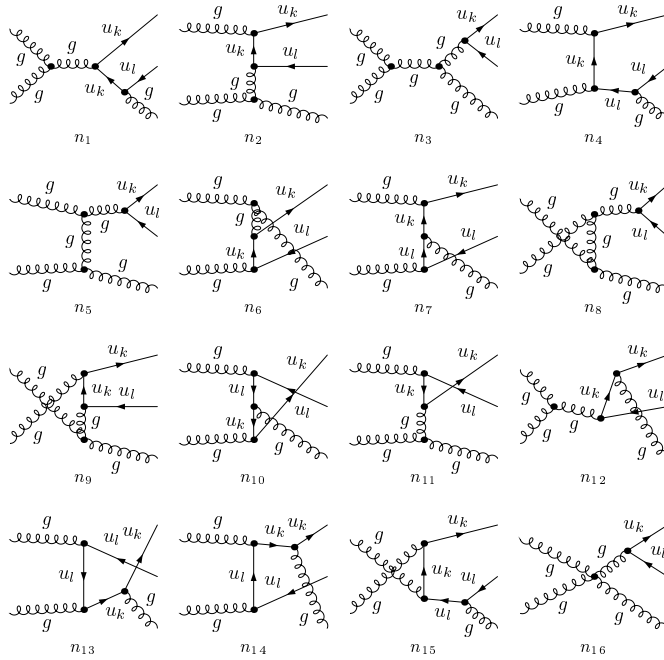


Figure 3.9: Feynman diagrams for $gg \rightarrow q\bar{q}g$

a constraint analogous to (3.58) must hold between the elements of the vector \mathbf{K} ,

$$s_{24} K_3 = s_{24} K_1. \quad (3.60)$$

Starting from the Feynman diagram expansions (3.55), it can be checked that the kinematic factors K_i exactly correspond to two different colour-orderings of the amplitude,

$$K_1 = A_4^{\text{tree}}(1, 2, 3, 4), \quad K_3 = A_4^{\text{tree}}(1, 2, 4, 3), \quad (3.61)$$

so that (3.60) can be rewritten as

$$s_{24} A_4^{\text{tree}}(1, 2, 4, 3) = s_{24} A_4^{\text{tree}}(1, 2, 3, 4). \quad (3.62)$$

With similar considerations we can verify that

$$s_{24} A_4^{\text{tree}}(1, 3, 2, 4) = s_{12} A_4^{\text{tree}}(1, 2, 3, 4), \quad s_{23} A_4^{\text{tree}}(1, 4, 2, 3) = s_{12} A_4^{\text{tree}}(1, 2, 4, 3). \quad (3.63)$$

3.3.3 Colour-kinematics duality for $gg \rightarrow q\bar{q}g$

In this subsection we provide a further example of C/K-duality in QCD, by determining dual numerators for $gg \rightarrow q\bar{q}g$. Analogous considerations of C/K duality in QCD amplitudes with fundamental matter have been discussed in [145, 148], where manifest duality has been verified for several processes. The process under consideration contains a single external quark-antiquark pair and, as a consequence, receives contribution from the four-gluon vertex. This allows us to show, in a concrete case, how contact interactions can be treated. We go step by step through the procedure outlined in Sec. 3.3, adopting notation and conventions similar to [143].

Fig. 3.9 shows the 16 Feynman diagrams for the process $gg \rightarrow q\bar{q}g$. The contribution of n_{16} , which, containing the four-gluon vertex, depends on three different colour structures,

$$c_{16} n_{16} = c_3 n_{3;16} + c_5 n_{5;16} + c_8 n_{8;16} \quad (3.64)$$

can be split between n_3 , n_5 and n_8 , so that the new cubic numerators read

$$\begin{aligned} n_3 + s_{12}n_{3;16} &\rightarrow n_3, \\ n_5 + s_{15}n_{5;16} &\rightarrow n_5, \\ n_8 + s_{25}n_{3;16} &\rightarrow n_8. \end{aligned} \quad (3.65)$$

Thus, the decomposition of the amplitude in terms of cubic graphs reads

$$\mathcal{A}_5^{\text{tree}}(g(1), g(2), q(3), \bar{q}(4), g(5)) = \frac{c_1 n_1}{s_{12} s_{45}} + \frac{c_2 n_2}{s_{32} s_{51}} + \frac{c_3 n_3}{s_{34} s_{12}} + \frac{c_4 n_4}{s_{45} s_{23}} + \frac{c_5 n_5}{s_{15} s_{34}} \quad (3.66)$$

$$+ \frac{c_6 n_6}{s_{14} s_{25}} + \frac{c_7 n_7}{s_{23} s_{14}} + \frac{c_8 n_8}{s_{25} s_{34}} + \frac{c_9 n_9}{s_{13} s_{25}} + \frac{c_{10} n_{10}}{s_{24} s_{13}} \quad (3.67)$$

$$+ \frac{c_{11} n_{11}}{s_{15} s_{24}} + \frac{c_{12} n_{12}}{s_{12} s_{35}} + \frac{c_{13} n_{13}}{s_{35} s_{24}} + \frac{c_{14} n_{14}}{s_{14} s_{35}} + \frac{c_{15} n_{15}}{s_{13} s_{45}}, \quad (3.68)$$

where only n_3 , n_5 and n_8 differ for an additional contact term from the expression given by Feynman rules.

The colour factors,

$$\begin{aligned} c_1 &= \tilde{f}^{a_1 a_2 b} T_{3\bar{k}}^b T_{k\bar{4}}^{a_5}, & c_2 &= T_{3\bar{k}}^{a_2} T_{k\bar{4}}^b \tilde{f}^{b a_5 a_1}, \\ c_3 &= -T_{3\bar{4}}^b \tilde{f}^{b a_5 c} \tilde{f}^{c a_1 a_2}, & c_4 &= -T_{3\bar{k}}^{a_2} T_{k\bar{l}}^{a_1} T_{l\bar{4}}^{a_5}, \\ c_5 &= -\tilde{f}^{a_5 a_1 b} \tilde{f}^{b a_2 c} T_{3\bar{4}}^c, & c_6 &= T_{3\bar{k}}^b T_{k\bar{4}}^{a_1} \tilde{f}^{b a_2 a_5}, \\ c_7 &= T_{3\bar{k}}^{a_2} T_{k\bar{l}}^{a_5} T_{l\bar{4}}^{a_1}, & c_8 &= -\tilde{f}^{a_2 a_5 b} \tilde{f}^{b a_1 c} T_{3\bar{4}}^c, \\ c_9 &= T_{3\bar{k}}^{a_1} T_{k\bar{4}}^b \tilde{f}^{b a_2 a_5}, & c_{10} &= -T_{3\bar{k}}^{a_1} T_{k\bar{l}}^{a_5} T_{l\bar{4}}^{a_2}, \\ c_{11} &= \tilde{f}^{a_5 a_1 b} T_{3\bar{k}}^b T_{k\bar{4}}^{a_2}, & c_{12} &= T_{3\bar{k}}^{a_5} T_{k\bar{4}}^b \tilde{f}^{b a_1 a_2}, \\ c_{13} &= T_{3\bar{k}}^{a_5} T_{k\bar{l}}^{a_1} T_{l\bar{4}}^{a_2}, & c_{14} &= -T_{3\bar{k}}^{a_5} T_{k\bar{l}}^{a_2} T_{l\bar{4}}^{a_1}, \\ c_{15} &= T_{3\bar{k}}^{a_1} T_{k\bar{l}}^{a_2} T_{l\bar{4}}^{a_5}. \end{aligned} \quad (3.69)$$

satisfy a set of 10 Jacobi identities,

$$\begin{aligned} -c_1 + c_3 + c_{12} &= 0, \\ -c_1 + c_4 + c_{15} &= 0, \\ -c_2 + c_4 + c_7 &= 0, \\ -c_2 + c_5 + c_{11} &= 0, \\ -c_6 + c_7 + c_{14} &= 0, \\ -c_6 + c_8 + c_9 &= 0, \\ -c_9 + c_{10} + c_{15} &= 0, \\ -c_{11} + c_{10} + c_{13} &= 0, \\ -c_{12} + c_{13} + c_{14} &= 0, \\ (-c_5 + c_3 + c_8) &= 0. \end{aligned} \quad (3.70)$$

The system is redundant, since any of the above equations, for instance the last one, can be expressed as a linear combination of the others 9. Therefore, it can be freely dropped.

We solve (3.70), choosing $\{c_1, c_2, c_3, c_4, c_5, c_6\}$ as independent colour factor, and we re-express the amplitude as

$$\mathcal{A}_5^{\text{tree}}(g(1), g(2), q(3), \bar{q}(4), g(5)) = \sum_{i=1}^6 c_i K_i \quad (3.71)$$

with

$$\begin{aligned}
K_1 &= \frac{n_1}{s_{12}s_{45}} + \frac{n_{12}}{s_{12}s_{35}} + \frac{n_{13}}{s_{24}s_{35}} - \frac{n_{10}}{s_{13}s_{42}} + \frac{n_{15}}{s_{13}s_{45}}, \\
K_2 &= \frac{n_2}{s_{23}s_{51}} + \frac{n_7}{s_{14}s_{32}} - \frac{n_{14}}{s_{14}s_{35}} + \frac{n_{13}}{s_{24}s_{35}} + \frac{n_{11}}{s_{42}s_{51}}, \\
K_3 &= \frac{n_3}{s_{12}s_{34}} + \frac{n_9}{s_{13}s_{25}} - \frac{n_{12}}{s_{12}s_{35}} - \frac{n_{13}}{s_{24}s_{35}} + \frac{n_{10}}{s_{13}s_{42}} - \frac{n_8}{s_{25}s_{43}}, \\
K_4 &= \frac{n_4}{s_{23}s_{45}} - \frac{n_7}{s_{14}s_{32}} + \frac{n_{14}}{s_{14}s_{35}} - \frac{n_{13}}{s_{24}s_{35}} + \frac{n_{10}}{s_{13}s_{42}} - \frac{n_{15}}{s_{13}s_{45}}, \\
K_5 &= \frac{n_5}{s_{34}s_{51}} - \frac{n_9}{s_{13}s_{25}} - \frac{n_{10}}{s_{13}s_{42}} + \frac{n_8}{s_{25}s_{43}} - \frac{n_{11}}{s_{42}s_{51}}, \\
K_6 &= \frac{n_6}{s_{14}s_{25}} + \frac{n_9}{s_{13}s_{25}} + \frac{n_{14}}{s_{14}s_{35}} - \frac{n_{13}}{s_{24}s_{35}} + \frac{n_{10}}{s_{13}s_{42}}.
\end{aligned} \tag{3.72}$$

We remark that this choice is by no means unique and other admissible sets of independent colour factors lead to different but equivalent decompositions.

Now we introduce the shifts (3.40) and, by imposing generalised gauge invariance on (3.71), $\delta\mathcal{A}_5^{\text{tree}} = 0$, we obtain a set of 6 homogenous equations. Furthermore, in order to establish C/K-duality for the new numerators n'_i , we require the shifts to absorb the anomalous terms, *i.e.* to be solution of an additional set of 9 non-homogeneous equations, that are obtained from (3.70) by replacing each colour factors c_i with the corresponding shift Δ_i and the r.h.s. with the proper anomaly. Thus, dual numerators are determined from the solution of the linear system (3.44), where \mathbb{A} is the 15×15 matrix

$$\mathbb{A} = \begin{pmatrix}
0 & 0 & 0 & 0 & \frac{1}{s_{34}s_{15}} & 0 & 0 & \frac{1}{s_{25}s_{34}} & -\frac{1}{s_{13}s_{25}} & -\frac{1}{s_{13}s_{24}} & -\frac{1}{s_{24}s_{15}} & 0 & 0 & 0 & 0 \\
0 & 0 & \frac{1}{s_{12}s_{34}} & 0 & 0 & 0 & 0 & 0 & 0 & 0 & 0 & -\frac{1}{s_{12}s_{35}} & -\frac{1}{s_{24}s_{35}} & 0 & 0 \\
0 & \frac{1}{s_{23}s_{15}} & 0 & 0 & 0 & 0 & \frac{1}{s_{14}s_{23}} & 0 & 0 & 0 & \frac{1}{s_{24}s_{15}} & 0 & \frac{1}{s_{24}s_{35}} & -\frac{1}{s_{14}s_{35}} & 0 \\
0 & 0 & 0 & 0 & 0 & \frac{1}{s_{14}s_{25}} & 0 & 0 & \frac{1}{s_{13}s_{25}} & \frac{1}{s_{13}s_{24}} & 0 & 0 & \frac{1}{s_{24}s_{35}} & \frac{1}{s_{14}s_{35}} & 0 \\
0 & 0 & 0 & \frac{1}{s_{23}s_{45}} & 0 & 0 & -\frac{1}{s_{14}s_{23}} & 0 & 0 & \frac{1}{s_{13}s_{24}} & 0 & 0 & -\frac{1}{s_{24}s_{35}} & \frac{1}{s_{14}s_{35}} & -\frac{1}{s_{13}s_{45}} \\
\frac{1}{s_{12}s_{45}} & 0 & 0 & 0 & 0 & 0 & 0 & 0 & 0 & -\frac{1}{s_{13}s_{24}} & 0 & \frac{1}{s_{12}s_{35}} & \frac{1}{s_{24}s_{35}} & 0 & \frac{1}{s_{13}s_{45}} \\
-1 & 0 & 1 & 0 & 0 & 0 & 0 & 0 & 0 & 0 & 0 & 1 & 0 & 0 & 0 \\
-1 & 0 & 0 & 1 & 0 & 0 & 0 & 0 & 0 & 0 & 0 & 0 & 0 & 0 & 1 \\
0 & -1 & 0 & 1 & 0 & 0 & 1 & 0 & 0 & 0 & 0 & 0 & 0 & 0 & 0 \\
0 & -1 & 0 & 0 & 1 & 0 & 0 & 0 & 0 & 0 & 1 & 0 & 0 & 0 & 0 \\
0 & 0 & 0 & 0 & 0 & 0 & -1 & 1 & 0 & 0 & 0 & 0 & 0 & 1 & 0 \\
0 & 0 & 0 & 0 & 0 & 0 & -1 & 0 & 1 & 1 & 0 & 0 & 0 & 0 & 0 \\
0 & 0 & 0 & 0 & 0 & 0 & 0 & 0 & 0 & -1 & 1 & 0 & 0 & 0 & 1 \\
0 & 0 & 0 & 0 & 0 & 0 & 0 & 0 & 0 & 0 & 1 & -1 & 0 & 1 & 0 \\
0 & 0 & 0 & 0 & 0 & 0 & 0 & 0 & 0 & 0 & 0 & -1 & 1 & 1 & 0
\end{pmatrix} \tag{3.73}$$

and the vector ϕ is given by

$$\phi = (0, 0, 0, 0, 0, 0, \phi_{[1,3,12]}, \phi_{[1,4,15]}, \phi_{[2,4,7]}, \phi_{[2,5,11]}, \phi_{[6,7,14]}, \phi_{[6,8,9]}, \phi_{[9,10,15]}, \phi_{[11,10,13]}, \phi_{[12,13,14]})^T. \tag{3.74}$$

The anomalies $\phi_{[i,j,k]}$ can be directly obtained from our off-shell decompositions. We observe that, since we decided to drop, without loss of generality, the last of equations (3.70), which involves a Jacobi identities for gluons, we can express all anomalies in terms of the fermionic current $J_q = J_{q\text{-Feyn}} + J_{q\text{-Ax}}$, whose explicit expression is given by equations (3.25) and (3.26). Likewise, the three anomalies involving the numerators n_3 , n_5 and n_8 receive an additional contribution from the four-gluon interaction, since no contact term was considered in the definition of J_q ,

$$\begin{aligned}
\phi_{[1,3,12]} &= \bar{u}_3[J_q(p_1 + p_2, p_4, p_3, p_5)_{\alpha\alpha_5}]v_4\Pi^{\alpha\beta}(p_1 + p_2, q)V_{\beta\alpha_1\alpha_2}(-p_1 - p_2, p_1, p_2)\varepsilon_1^{\alpha_1}\varepsilon_2^{\alpha_2}\varepsilon_5^{\alpha_5} \\
&+ n_{3;16} = s_{12}\varphi_{[1,3,12]},
\end{aligned}$$

$$\begin{aligned}
\phi_{[1,4,15]} &= \bar{u}_3[J_q(p_2, p_4 + p_5, p_3, p_1)_{\alpha_2\alpha_1}(\not{p}_4 + \not{p}_5)\not{p}_5]v_4 \varepsilon_1^{\alpha_1}\varepsilon_2^{\alpha_2} = s_{45}\varphi_{[1,4,15]}, \\
\phi_{[2,4,7]} &= \bar{u}_3[\not{p}_2(\not{p}_3 + \not{p}_2)J_q(p_1, p_4, p_3 + p_2, p_5)_{\alpha_1\alpha_5}]v_4 \varepsilon_1^{\alpha_1}\varepsilon_5^{\alpha_5} = s_{23}\varphi_{[2,4,7]}, \\
\phi_{[2,5,11]} &= \bar{u}_3[J_q(p_1 + p_5, p_4, p_3, p_2)_{\alpha_2\alpha_1}]v_4 \Pi^{\alpha\beta}(p_1 + p_5, q)V_{\beta\alpha_1\alpha_5}(-p_1 - p_5, p_1, p_5)\varepsilon_1^{\alpha_1}\varepsilon_2^{\alpha_2}\varepsilon_5^{\alpha_5} \\
&\quad + n_{5;16} = s_{15}\varphi_{[2,5,11]}, \\
\phi_{[6,7,14]} &= \bar{u}_3[J_q(p_5, p_4 + p_1, p_3, p_2)_{\alpha_5\alpha_2}(\not{p}_4 + \not{p}_1)\not{p}_1]v_4 \varepsilon_2^{\alpha_2}\varepsilon_5^{\alpha_5} = s_{14}\varphi_{[6,7,14]}, \\
\phi_{[6,8,9]} &= \bar{u}_3[J_q(p_2 + p_5, p_4, p_3, p_1)_{\alpha_1\alpha_5}]v_4 \Pi^{\alpha\beta}(p_2 + p_5, q)V_{\beta\alpha_2\alpha_5}(-p_2 - p_5, p_2, p_5)\varepsilon_1^{\alpha_1}\varepsilon_2^{\alpha_2}\varepsilon_5^{\alpha_5} \\
&\quad + n_{8;16} = s_{25}\varphi_{[6,8,9]}, \\
\phi_{[9,10,15]} &= \bar{u}_3[\not{p}_1(\not{p}_3 + \not{p}_1)J_q(p_5, p_4, p_3 + p_1, p_2)_{\alpha_5\alpha_2}]v_4 \varepsilon_2^{\alpha_2}\varepsilon_5^{\alpha_5} = s_{13}\varphi_{[9,10,15]}, \\
\phi_{[11,10,13]} &= \bar{u}_3[J_q(p_1, p_4 + p_2, p_3, p_5)_{\alpha_1\alpha_5}(\not{p}_4 + \not{p}_2)\not{p}_2]v_4 \varepsilon_1^{\alpha_1}\varepsilon_5^{\alpha_5} = s_{24}\varphi_{[11,10,13]}, \\
\phi_{[12,13,14]} &= \bar{u}_3[\not{p}_5(\not{p}_3 + \not{p}_5)J_q(p_2, p_4, p_3 + p_5, p_1)_{\alpha_2\alpha_1}]v_4 \varepsilon_1^{\alpha_1}\varepsilon_2^{\alpha_2} = s_{35}\varphi_{[12,13,14]}, \tag{3.75}
\end{aligned}$$

where $V_{\mu_1\mu_2\mu_3}(p_1, p_2, p_3)$ stands for the kinematic part of three-gluon vertex.

We remark that in (3.75) the factorisation of Mandelstam invariants s_{ij} follows from the decomposition (3.28) and that, for the anomalies with an internal gluon propagator, namely $\phi_{[1,3,12]}$, $\phi_{[2,5,11]}$ and $\phi_{[6,8,9]}$, it can be achieved in a straightforward way thanks to the choice of axial gauge.

As we have already anticipated, the system of equations is redundant. In fact, by using momentum conservation to express all the invariants s_{ij} in terms of 5 independent ones, for instance $\{s_{12}, s_{23}, s_{34}, s_{45}, s_{51}\}$, we obtain

$$\text{rank}(\mathbb{A}) = 11. \tag{3.76}$$

Therefore, if a solution exists, there must be constraints between the non-zero elements of ϕ able to lower the rank of the adjoint matrix. In particular, we expect these relations to correspond to four independent vanishing linear combinations of rows of the matrix \mathbb{A} . This observation provides a constructive criterion to find out the constraints between anomalous terms.

First, we build the most general linear combination of rows of the matrix \mathbb{A} and we fix the coefficients by requiring

$$\sum_{i=1}^{15} \beta_i \mathbb{A}_i = 0. \tag{3.77}$$

According to (3.76), one can find at most four linear independent solutions $\{\beta_i^{(j)}\}$ to (3.77).

Secondly, after selecting an arbitrary complete set of solutions $\{\beta_i^{(j)}\}$, $j = 1, 2, 3, 4$, we can verify that

$$\sum_{i=1}^{15} \beta_i^{(j)} \phi_i = 0, \quad \forall j = 1, 2, 3, 4, \tag{3.78}$$

that gives the desired constraints between the C/K-violating terms.

For this specific case we find,

$$\begin{aligned}
\frac{\phi_{[6,7,14]}}{s_{14}} + \frac{\phi_{[9,10,15]}}{s_{13}} - \frac{\phi_{[12,13,14]}}{s_{35}} - \frac{\phi_{[1,4,15]}}{s_{45}} &= 0, \\
\frac{\phi_{[6,8,9]}}{s_{25}} + \frac{\phi_{[9,10,15]}}{s_{13}} - \frac{\phi_{[12,13,14]}}{s_{35}} - \frac{\phi_{[1,3,12]}}{s_{12}} &= 0, \\
\frac{\phi_{[6,7,14]}}{s_{14}} + \frac{\phi_{[9,10,15]}}{s_{13}} - \frac{\phi_{[11,10,13]}}{s_{24}} - \frac{\phi_{[2,4,7]}}{s_{23}} &= 0,
\end{aligned}$$

$$\frac{\phi_{[6,8,9]}}{s_{25}} + \frac{\phi_{[11,10,13]}}{s_{24}} + \frac{\phi_{[2,5,11]}}{s_{15}} - \frac{\phi_{[6,7,14]}}{s_{14}} = 0, \quad (3.79)$$

which, thanks to (3.75), can be written as

$$\varphi_{[6,7,14]} + \varphi_{[9,10,15]} - \varphi_{[12,13,14]} - \varphi_{[1,4,15]} = 0, \quad (3.80)$$

$$\varphi_{[6,8,9]} + \varphi_{[9,10,15]} - \varphi_{[12,13,14]} - \varphi_{[1,3,12]} = 0, \quad (3.81)$$

$$\varphi_{[6,7,14]} + \varphi_{[9,10,15]} - \varphi_{[11,10,13]} - \varphi_{[2,4,7]} = 0, \quad (3.82)$$

$$\varphi_{[6,8,9]} + \varphi_{[11,10,13]} + \varphi_{[2,5,11]} - \varphi_{[6,7,14]} = 0. \quad (3.83)$$

These relations follow as a direct consequence of the off-shell decomposition (3.28). For instance, if we specify it for the anomalies appearing in (3.80) by using the explicit form of J_q , we obtain

$$\begin{aligned} \varphi_{[1,4,15]} &= \bar{u}_3 \left[\gamma^{\alpha_2} \gamma^{\alpha_1} \gamma^{\alpha_5} - g^{\alpha_1 \alpha_2} \gamma^{\alpha_5} - \frac{g^{\alpha_1 \alpha_2} q \cdot (p_1 - p_2) - 2(q^{\alpha_1} p_1^{\alpha_2} - q^{\alpha_2} p_2^{\alpha_1})}{q \cdot (p_1 + p_2)} \gamma^{\alpha_5} \right] v_4 \varepsilon_{\alpha_1} \varepsilon_{\alpha_2} \varepsilon_{\alpha_5}, \\ \varphi_{[6,7,14]} &= \bar{u}_3 \left[\gamma^{\alpha_5} \gamma^{\alpha_2} \gamma^{\alpha_1} - g^{\alpha_2 \alpha_5} \gamma^{\alpha_1} - \frac{g^{\alpha_2 \alpha_5} q \cdot (p_2 - p_5) - 2(q^{\alpha_2} p_2^{\alpha_5} - q^{\alpha_5} p_5^{\alpha_2})}{q \cdot (p_2 + p_5)} \gamma^{\alpha_1} \right] v_4 \varepsilon_{\alpha_1} \varepsilon_{\alpha_2} \varepsilon_{\alpha_5}, \\ \varphi_{[12,13,14]} &= \bar{u}_3 \left[-\gamma^{\alpha_5} \gamma^{\alpha_1} \gamma^{\alpha_2} + g^{\alpha_1 \alpha_2} \gamma^{\alpha_5} + \frac{g^{\alpha_1 \alpha_2} q \cdot (p_1 - p_2) - 2(q^{\alpha_1} p_1^{\alpha_2} - q^{\alpha_2} p_2^{\alpha_1})}{q \cdot (p_1 + p_2)} \gamma^{\alpha_5} \right] v_4 \varepsilon_{\alpha_1} \varepsilon_{\alpha_2} \varepsilon_{\alpha_5}, \\ \varphi_{[9,10,15]} &= \bar{u}_3 \left[-\gamma^{\alpha_1} \gamma^{\alpha_2} \gamma^{\alpha_5} + g^{\alpha_2 \alpha_5} \gamma^{\alpha_1} + \frac{g^{\alpha_2 \alpha_5} q \cdot (p_2 - p_5) - 2(q^{\alpha_2} p_2^{\alpha_5} - q^{\alpha_5} p_5^{\alpha_2})}{q \cdot (p_2 + p_5)} \gamma^{\alpha_1} \right] v_4 \varepsilon_{\alpha_1} \varepsilon_{\alpha_2} \varepsilon_{\alpha_5}. \end{aligned} \quad (3.84)$$

By using Clifford algebra we can verify that

$$\varphi_{[1,4,15]} + \varphi_{[12,13,14]} - \varphi_{[6,7,14]} - \varphi_{[9,10,15]} = 2\varepsilon_{\alpha_1} \varepsilon_{\alpha_2} \varepsilon_{\alpha_5} \bar{u}_3 [g^{\alpha_1 \alpha_2} \gamma^{\alpha_5} - g^{\alpha_1 \alpha_2} \gamma^{\alpha_5}] v_4 = 0. \quad (3.85)$$

Similar cancellation are encountered in all other cases.

The constraints (3.79) make the consistency relation satisfied,

$$\text{rank}(\mathbb{A}|\phi) = \text{rank}(\mathbb{A}) = 11. \quad (3.86)$$

As a consequence, the system admits a solution which leaves four shifts completely undetermined and the amplitude has a C/K-dual representation, consistent with generalised gauge invariance, whose numerators depend of four free parameters. This number agrees with the $(n-2)! - (n-3)!$ degrees of freedom found in [143] for the pure Yang-Mills case.

In order to find an explicit expressions for the shifts, we build a maximum-rank system by selecting a subset of 11 independent equations and proceed by Gaussian elimination. We observe that, as for the solution of the Jacobi identities for colour factors, also in this case there is a remarkably large freedom in the choice of the independent equations to be solved and, furthermore, in the set of four arbitrary shifts to appear in the solution.

In our case, by selecting equations corresponding to rows 1-2 and 9-15 of (3.73), we express Δ_i , $i = 5, 6, \dots, 15$ as linear combination of the anomalies $\phi_{[i,j,k]}$ and of the four arbitrary shifts $\{\Delta_1, \Delta_2, \Delta_3, \Delta_4\}$,

$$\Delta_i = \sum_{j=1}^4 \mathcal{R}_{ij}(s_{kl}) \Delta_j + \sum_{[m,n,p]} \mathcal{R}_{i[m,n,p]}(s_{kl}) \phi_{[m,n,p]}, \quad \text{for } i = 5, \dots, 15, \quad (3.87)$$

where \mathcal{R}_{ij} and $\mathcal{R}_{i[mnp]}$ are dimensionless rational functions of the invariants s_{kl} .

The analytic expression of (3.87), which is not provided here for sake of simplicity, has been obtained for arbitrary polarisations and has been numerically checked for all helicity configurations. In particular, the complete independence on the actual values of the four independent shifts has been verified for the full colour-dressed amplitude as well as for each ordering appearing in (3.71). We observe that the choice $\Delta_i = 0$, $i = 1, \dots, 4$ leads to a dual representation where four numerators correspond exactly to the starting ones and three anomalous terms are attributed to single diagrams

$$\Delta_7 = \phi_{[2,4,7]}, \quad \Delta_{12} = \phi_{[1,3,12]}, \quad \Delta_{15} = \phi_{[1,4,15]}. \quad (3.88)$$

In addition, for any choice of the free parameters, the set of new numerators n'_i , satisfies the system of equations (3.47), where

$$\mathbf{K} = (K_1, K_2, \dots, K_6, 0, 0, \dots, 0)^T. \quad (3.89)$$

Therefore, the consistency requirement

$$\text{rank}(\mathbb{A}|\mathbf{K}) = \text{rank}(\mathbb{A}) = 11 \quad (3.90)$$

allow us to use the exactly the same solutions $\{\beta_i^{(j)}\}$ of (3.77), to establish relations between the kinematic factors,

$$\sum_{i=1}^{15} \beta_i^{(j)} \mathbf{K}_i = 0, \quad \forall j = 1, 2, \dots, 4, \quad (3.91)$$

which, in this case, read

$$\begin{aligned} s_{45}K_1 - s_{34}K_3 - s_{14}K_6 &= 0, \\ s_{12}K_1 - s_{23}K_4 - s_{25}K_6 &= 0, \\ s_{15}K_2 - s_{45}K_4 - s_{25}K_6 &= 0, \\ s_{23}K_2 - s_{34}K_5 + (s_{23} + s_{35})K_6 &= 0. \end{aligned} \quad (3.92)$$

This set of constraints reduces from 6 to 2 the number of independent kinematic factors.

Therefore, as we have already pointed out, (3.92) can be considered as equivalent to the well-known monodromy relations which have been shown, for the pure-gluon case, to reduce to $(n-3)!$ the number of independent colour ordered amplitudes.

Nevertheless, we want to remark that, in the approach we have presented, the origin of (3.92), as well as the one of (3.79), is shown to be purely diagrammatic. In particular, whereas in [157] monodromy relations analogous to (3.92) are derived from the field-limit of string theory and a set of relations equivalent to (3.79) is presented as a parametrisation of their solution, here both are derived as a necessary consequence of the redundancy of kinematic matrix \mathbb{A} and they have been shown to naturally emerge from the off-shell decomposition of the Jacobi-combination of kinematic numerators in axial gauge.

3.4 Discussion

In this chapter we have studied the colour-kinematics (C/K) duality by following a diagrammatic approach. We reviewed the main features, known in the literature, of this duality. Firstly, the relation between kinematic terms of Feynman diagrams and their colour factors. Secondly, the fundamental Bern-Carrasco-Johansson (BCJ) relations, which turned to be a consequence of an elaborated study of the C/K-duality.

The diagrammatic approach has allowed to investigate the off-shell C/K duality for amplitudes in gauge theories. This duality, first observed at tree-level for on-shell four-point amplitudes, is non-trivially satisfied within higher-multiplicity tree-level or multi-loop graphs, due to presence of contact terms which violate the Jacobi identity for numerators. We studied the source of such anomalous terms in $gg \rightarrow ss, q\bar{q}, gg$ scattering processes. Working in axial gauge, we have explicitly shown that, whenever the Lie structure constants obey a Jacobi identity, the analogous combination of their kinematic numerators can always be reduced to a sum of numerators of sub-diagrams, with one or two denominators less.

Furthermore, we want to remark that, whereas in the usual top-down approach [143, 144, 155, 237], the numerators appearing in the r.h.s. of (3.1) are interpreted as abstract re-organisation of Feynman rules-numerators on which, by assumptions, the C/K-duality is imposed. Instead, our approach provides a systematic way to identify the link between dual numerators and Feynman diagrams. Starting from the set of explicitly C/K-violating but well-defined Feynman rule-numerators we determine, by mean of generalised gauge transformations, the actual redistribution of contact terms which has to be performed in order to establish the duality.

We have focused on the C/K-duality for tree-level amplitudes, nevertheless, the construction of dual numerators for multi-loop amplitude follows the very same algorithm presented in Sec. 3.3. Moreover, for non-supersymmetric theories, say QCD, we need to provide dimensionally regulated amplitudes. This extension is presented in chapter 7. In the same manner, the structure of the BCJ identities in d -dimensions.

Chapter 4

One-loop amplitudes

Tree-level or Leading-Order (LO) computations provide a qualitative information, affected by large uncertainties due to the poor convergence of the coupling constant. Therefore, to establish a proper comparison between theory and data, Next-to-Leading-Order (NLO) is needed. As a main ingredient of the NLO contributions we consider one-loop corrections, in which, any amplitude can be decomposed in an explicit set of Master Integrals (MIs), where the coefficients appearing in this combination are rational functions of the kinematic variables, known as Passarino Veltman tensor reduction [42]. It is possible to recover the structure of scattering amplitudes at integral level by constructing the integrands through the multi-particle pole expansion rising from the analyticity and unitarity properties of the S-matrix [239]. In fact, scattering amplitudes analytically continued to complex momenta, reveal their singularity structures in terms of poles and branch cuts. The unitarity based methods [240–247] allow to determine the coefficients of the MIs by expanding the integrand of tree level cut amplitudes into an expression that resembles the cut of the basis integrals.

Integrand-reduction methods [46, 248], instead, allow one to decompose the integrands of scattering amplitudes into multi-particle poles, and the multi-particle residues are expressed in terms of irreducible scalar products (ISPs) formed by the loop momenta and either external momenta or polarisation vectors constructed out of them. The polynomial structure of the multi-particle residues is a qualitative information that turns into a quantitative algorithm for decomposing arbitrary amplitudes in terms of Master Integrals (MIs) by polynomial fitting at the integrand level. In this context, the on-shell conditions have been used as a computational tool reducing the complexity of the algorithm. A more intimate connection among the idea of reduction under the integral sign and analyticity and unitarity has been pointed out recently. Using basic principles of algebraic geometry, Ref.s [85, 86, 249–251] have shown that the structure of the multi-particle poles is determined by the zeros of the denominators involved in the corresponding multiple cut. This new approach to integrand reduction methods allows for their systematisation and for their all-loop extension.

This chapter is organised as follows: Sec. 4.1 is devoted to the description of the tensor decomposition. Sec. 4.2 reviews the main features of the unitarity based methods, while Sec.s 4.3 and 4.4 describe the Ossola-Papadopoulos-Pittau method and the Laurent series expansion respectively.

4.1 Tensor reduction

The Passarino-Veltman [42] tensor reduction (PV) has become an important tool in the computation of one-loop integrals. This algorithm has the advantage of expressing any tensor integral as the sum of scalar integrals only, each one multiplied by some coefficients depending on the external kinematics.

In order to compute any process at one-loop level, one has to deal with integrals of the form

$$I_{i_1 \dots i_k} [\mathcal{N}(\bar{l})] = h(\mu_R^2, d) \int d^d \bar{l} \frac{\mathcal{N}_{i_1 \dots i_k}(\bar{l})}{D_{i_1} \dots D_{i_k}}, \quad (4.1)$$

where $i_1 \dots i_n$ are indices labeling loop propagators. The numerator \mathcal{N} and denominators D_i 's are polynomials of the loop momentum \bar{l} . The function h is a conventional normalisation factor given by [252]

$$h(\mu_R^2, d) = h(\mu_R^2, 4 - 2\epsilon) = \frac{\mu_R^{-2\epsilon}}{i\pi^{2-\epsilon}} \frac{\Gamma(1 - 2\epsilon)}{\Gamma^2(1 - \epsilon) \Gamma(1 + \epsilon)}, \quad (4.2)$$

as a function of the renormalisation scale μ_R^2 and the dimension $d = 4 - 2\epsilon$.

In general, the loop denominators are quadratic polynomials, $D_i = (\bar{l}_i + q_i)^2 - m_i^2$, where q_i is a linear combination of external momenta, $q_i = p_2 + p_2 + \dots + p_i$, and m_i 's are the masses of the particles running in the loop.

The scalar master integrals are obtained by setting $\mathcal{N} = 1$,

$$I_{i_1 \dots i_k} [1] = I_{i_1 \dots i_k}. \quad (4.3)$$

Integral reduction [42, 253] has allowed to express any one-loop Feynman integral as a linear combination of scalar pentagons, boxes, triangles, bubbles and, tadpoles

$$\begin{aligned} I_{i_1 \dots i_k} [\mathcal{N}(\bar{l})] = & \sum_{\{i_1, i_2, i_3, i_4, i_5\}} c_0^{(i_1 i_2 i_3 i_4 i_5)} I_{i_1 i_2 i_3 i_4 i_5} + \sum_{\{i_1, i_2, i_3, i_4\}} c_0^{(i_1 i_2 i_3 i_4)} I_{i_1 i_2 i_3 i_4} + \sum_{\{i_1, i_2, i_3\}} c_0^{(i_1 i_2 i_3)} I_{i_1 i_2 i_3} \\ & + \sum_{\{i_1, i_2\}} c_0^{(i_1 i_2)} I_{i_1 i_2} + \sum_{i_1} c_0^{(i_1)} I_{i_1}, \end{aligned} \quad (4.4)$$

where the coefficients are rational functions that depend on the dimensional regulator, $d - 4$. Additionally, tadpole contributions arise with internal masses. Pentagon scalar integrals appear if we keep higher order contributions in the dimensional regulator.

In order to see how the tensor decomposition works, we consider $\mathcal{N} = \bar{l}^\mu$, one power of loop momentum in the numerator

$$I_{i_1 \dots i_k} [\bar{l}^\mu] = h(\mu_R^2, d) \int d^d \bar{l} \frac{\bar{l}^\mu}{D_{i_1} \dots D_{i_k}}, \quad (4.5)$$

the value of this integral must be a function of external momenta p_1, p_2, \dots, p_{n-1} ,

$$I_{i_1 \dots i_k} [\bar{l}^\mu] = \sum_{k=1}^{n-1} C_k p_k^\mu, \quad (4.6)$$

contracting both sides with p_j^μ ,

$$I_{i_1 \dots i_k} [\bar{l} \cdot p_j] = \sum_{k=1}^{n-1} C_k \Delta_{jk}, \quad (4.7)$$

here $\Delta_{jk} = p_j \cdot p_k$ is the ‘‘Gram’’ matrix. Since $p_j = q_j - q_{j-1}$ (with $q_0 = 0$) we can write the numerator of the integral as

$$\bar{l} \cdot p_j = \frac{1}{2} (D_j - D_{j-1} + m_j^2 - m_{j-1}^2 - q_j^2 + q_{j-1}^2), \quad (4.8)$$

this is the PV reduction formula, which allows us to write a system of $n - 1$ linear equations for the coefficients C ,

$$\sum_{k=1}^{n-1} C_k \Delta_{jk} = \frac{1}{2} \left(I_{i_1 \dots i_k}^{(j)} - I_{i_1 \dots i_k}^{(j-1)} + (m_j^2 - m_{j-1}^2 - q_j^2 + q_{j-1}^2) I_{i_1 \dots i_k} \right), \quad (4.9)$$

where $I_{i_1 \dots i_k}^{(j)}$ stands for MIs where the propagator D_j has been canceled. Therefore, the set of coefficients is given by

$$C_j = \frac{1}{2} \sum_{k=1}^{n-1} \Delta_{jk}^{-1} \left(I_{i_1 \dots i_k}^{(j)} - I_{i_1 \dots i_k}^{(j-1)} + (m_j^2 - m_{j-1}^2 - q_j^2 + q_{j-1}^2) I_{i_1 \dots i_k} \right). \quad (4.10)$$

As a second example, we consider $\mathcal{N} = \bar{l}^\mu \bar{l}^\nu$. Since the integral is a rank two tensor it can be formed out of the outer products of external momenta $p_j^\mu p_k^\nu$ and the metric tensor $\bar{g}^{\mu\nu}$,

$$I_{i_1 \dots i_n}[\bar{l}^\mu \bar{l}^\nu] = C_{00} \bar{g}^{\mu\nu} + \sum_{j,k=1} C_{jk} p_j^\mu p_k^\nu, \quad (4.11)$$

The first set of equation can be derived by contracting both sides with $\bar{g}^{\mu\nu}$,

$$I_{i_1 \dots i_n}[\bar{l}^2] = C_{00} d + \sum_{j,k=1} C_{jk} \Delta_{jk}, \quad (4.12)$$

the other set of equations is obtained by contracting both sides with $p_j^\mu p_k^\nu$ and using (4.8).

4.2 Unitarity based methods

As saw in Sec. 1.3, the S-matrix has a lot of properties that can be exploited to compute efficiently scattering amplitudes in perturbation theory. Besides its analyticity, it is also unitarity, $SS^\dagger = 1$. This fact has allowed to compute the imaginary (absorptive) part of one-loop amplitudes by taking products of (or sewing) on-shell tree amplitudes, where the full loop amplitude can be reconstructed using dispersion relations. Moreover, it has been show that the unitarity method, allows to compute the full amplitude, not only the imaginary parts, by simply considering the discontinuities across the branch cuts in different channels.

4.2.1 Optical theorem

The optical theorem is a consequence of the unitarity of the S -matrix, given by $SS^\dagger = 1$. Inserting $S = 1 + iT$, where T is the interaction matrix, it translates into a condition for the T -matrix

$$-i(T - T^\dagger) = T^\dagger T. \quad (4.13)$$

We now consider the matrix element of this equation between two particle states $|a\rangle$ and $|b\rangle$. In order to evaluate the r.h.s of this equation we insert a complete set of final states $\left(1 = \sum_f |f\rangle\langle f|\right)$ between T and T^\dagger to obtain

$$\langle b|TT^\dagger|a\rangle = \sum_f \langle b|T|f\rangle\langle f|T^\dagger|a\rangle = \sum_f \int d\Pi_f A^*(a \rightarrow f) A(b \rightarrow f) (2\pi)^4 \delta^4(a - b), \quad (4.14)$$

where $d\Pi_f = \prod_{i=1}^n \frac{d^3 f_i}{(2\pi)^3} \frac{1}{2E_i}$ and the sum runs over all possible sets f of final-state particles. This term is related to the sum of all possible cuts where the final states f are on-shell and have

$$2 \operatorname{Im} \left(a \text{---} \text{---} \text{---} \text{---} \text{---} b \right) = \sum_f \int d\Pi_f \left(a \text{---} \text{---} \text{---} \text{---} f \right) \left(f \text{---} \text{---} \text{---} \text{---} b \right)$$

Figure 4.1: The optical theorem: the imaginary part of a forward scattering amplitudes arises from a sum of contributions from all possible intermediate state particles

positive energy.

While for the l.h.s.

$$-i(\langle b|T|a\rangle - \langle b|T|\dagger a\rangle) = -i[A(a \rightarrow b) - A^*(a \rightarrow b)], \quad (4.15)$$

is clearly related to the discontinuity or imaginary part of a diagram in a given channel:

$$-i[A(a \rightarrow b) - A^*(a \rightarrow b)] = \sum_f \int d\Pi_f A^*(a \rightarrow f) A(b \rightarrow f) (2\pi)^4 \delta^4(a - b). \quad (4.16)$$

Finally, for the important case of forward scattering, we set $a = b$ to obtain the optical theorem,

$$\begin{aligned} -i[A(a \rightarrow a) - A^*(a \rightarrow a)] &= \sum_f \int d\Pi_f A^*(a \rightarrow f) A(a \rightarrow f), \\ 2\operatorname{Im}A^{1\text{-loop}}(a \rightarrow a) &= \sum_f \int d\Pi_f A^{\text{tree}*}(a \rightarrow f) A^{\text{tree}}(a \rightarrow f), \end{aligned} \quad (4.17)$$

shows pictorial in fig. 4.2. Where the imaginary part of the amplitude is related to a product of two tree amplitudes. Effectively, two loop propagators are put on-shell. This imaginary part can be understood as a discontinuity across a branch cut singularity of the amplitude.

We can use perturbation theory to build an one-loop amplitude $A^{1\text{-loop}}(s)$ as analytic function of the complex variable $s = E_{\text{cm}}^2$. We consider s_0 to be threshold energy for production of the lightest multi-particle states. For real $s < s_0$ the intermediate states cannot go on-shell, so $A^{1\text{-loop}}(s)$ is real and we have the Schwartz reflection principle

$$A^{1\text{-loop}}(s) = A^{1\text{-loop}}(s^*)^*. \quad (4.18)$$

Being $A^{1\text{-loop}}(s)$ an analytic function it can be analytically continued to the entire complex s plane. In particular, near the real axis for $s < s_0$,

$$\operatorname{Re} A^{1\text{-loop}}(s + i\epsilon) = \operatorname{Re} A^{1\text{-loop}}(s - i\epsilon), \quad \operatorname{Im} A^{1\text{-loop}}(s + i\epsilon) = -\operatorname{Im} A^{1\text{-loop}}(s - i\epsilon), \quad (4.19)$$

there is a branch cut across the real axis, starting at the threshold energy s_0 ,

$$\operatorname{Disc} A^{1\text{-loop}}(s) = 2i \operatorname{Im} A^{1\text{-loop}}(s - i\epsilon),$$

which, allow to state that physical scattering amplitudes have to be evaluated above the cut, at $s + i\epsilon$.

In order to calculate the discontinuity in the s -channel, we need to consider the sum of all Feynman diagrams and then the optical theorem dictates the diagrams we have to cut in tree diagrams (see fig. 4.2). This procedure for computing the physical discontinuity is specified by a set of rules, usually, called ‘‘Cutkosky rules’’ and are based on the following algorithm [254]:

1. We cut the diagram so that the two propagators can simultaneously be put on-shell.

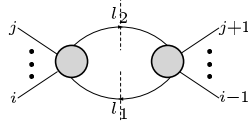


Figure 4.2: Unitarity: The two propagators are put on-shell. The disks represent the sum of all Feynman diagrams linking the fixed external lines and the two cut propagators.

2. For each propagator, we replace

$$\frac{i}{l^2 - m^2 + i\epsilon} \rightarrow -2\pi i \delta^{(+)}(l^2 - m^2), \quad (4.20)$$

here, the superscript “+” on the delta functions of the cut propagators denotes the choice of a positive-energy solution.

3. Perform the loop integrals
4. Sum the contributions over all cuts.

By using this set of rules the optical theorem can be proven at all orders in perturbation theory.

Moreover, we can apply the Cutkosky rules at the amplitude level, rather than at the diagram level [30, 32, 255]. This is advantageous because amplitudes are generally more compact than diagrams. Therefore, in order to compute the amplitude we study its discontinuity in various momentum channels,

$$\begin{aligned} \text{Disc } A_n^{1\text{-loop}}|_{i\text{-cut}} &= \int \frac{d^4 l_1}{(2\pi)^4} \frac{d^4 l_2}{(2\pi)^4} 2\pi i \delta^{(+)}(l_1^2 - m_1^2) 2\pi i \delta^{(+)}(l_2^2 - m_2^2) \\ &\quad \times A^{\text{tree}}(-l_1, 1, 2, \dots, k, l_2) A^{\text{tree}}(-l_2, k+1, \dots, n, l_1), \end{aligned} \quad (4.21)$$

where, because of the tensor reduction, we get information about the coefficient of the MIs, since, the branch cuts are located only in the MIs. Thus eq.(4.4) becomes

$$\text{Disc } A_n^{1\text{-loop}}|_{i\text{-cut}} = \sum_k c_n^{(j_1 \dots j_k)} \text{Disc } I_{j_1 \dots j_k}. \quad (4.22)$$

This result has two important features *i)* we see from eq.(4.21) that it is a relation involving tree-level quantities and *ii)* many of the terms of the r.h.s vanish, because only a subset of MIs have a cut involving the given *i*-cut.

4.2.2 Generalised Unitarity

As studied in Sec. 4.1 any tensor integral can be written as a linear combination of scalar MIs with coefficients that are rational functions. Each coefficient can be independently computed by “generalising” the unitarity cuts in the sense of putting a different number of propagators on-shell. This procedure distinguishes different kind of singularities of the amplitude and allows us to isolate the coefficient of each MI.

These generalised unitarity techniques for quadruple-[31, 62], triple-[38, 39, 62], double-[34, 36] and single-[256–258] cut allowed tremendous simplifications in one-loop calculations by simply recycling the knowledge of tree amplitudes.

In the following, we show how we can extract the box contribution to the amplitude by performing a quadruple-cut. While, in the next sections we will describe the contribution of lower topologies.

Quadruple-cut The direct application of generalised unitarity is to use a 4-cut to find any box coefficient. If we cut or put on-shell four propagators according to Eq. (4.20) the four dimensional integral becomes trivial

$$\text{Disc}_4 A_n^{1\text{-loop}} = \int d\Pi_4 (2\pi)^4 \delta^{(+)}(l_1^2 - m_1^2) \delta^{(+)}(l_2^2 - m_2^2) \delta^{(+)}(l_3^2 - m_3^2) \delta^{(+)}(l_4^2 - m_4^2) \\ \times A_1^{\text{tree}} A_2^{\text{tree}} A_3^{\text{tree}} A_4^{\text{tree}}, \quad (4.23)$$

with $d\Pi_4 = \prod_{i=1}^4 \frac{dl_i}{(2\pi)^4}$. This 4-cut selects the contribution from one box integral, namely with momenta (K_1, K_2, K_3, K_4) at the corners. Therefore, the cut expansion collapses to a single term

$$\text{Disc}_4 A_n^{1\text{-loop}} = c_0^{(i_1 i_2 i_3 i_4)} \text{Disc } I_{i_1 i_2 i_3 i_4}. \quad (4.24)$$

The value of the coefficient is simply

$$c_0^{(i_1 i_2 i_3 i_4)} = \frac{1}{2} \sum_{l \in \mathcal{S}} A_1^{\text{tree}}(l) A_2^{\text{tree}}(l) A_3^{\text{tree}}(l) A_4^{\text{tree}}(l), \quad (4.25)$$

where \mathcal{S} is the solution set for the four delta functions of the cut propagators,

$$\mathcal{S} = \{l^2 = m_1^2, \quad (l - K_1)^2 = m_2^2, \quad (l - K_1 - K_2)^2 = m_3^2, \quad (l + K_4)^2 = m_4^2\}. \quad (4.26)$$

There are exactly two solutions, provided that momenta are allowed to take complex values.

4.3 Ossola-Papadoupoulos-Pittau decomposition

An arbitrary one-loop amplitude in d -dimensions is a sum of contributions \mathcal{M} of the form

$$\mathcal{M} = h(\mu_R^2, d) \int d^d \bar{l} \mathcal{I}_{i_1 \dots i_n}, \quad \mathcal{I}_{i_1 \dots i_n} \equiv \frac{\mathcal{N}_{i_1 \dots i_n}}{D_{i_1} \dots D_{i_n}}, \quad (4.27)$$

where $i_1 \dots i_n$ are indices labeling loop propagators. The numerator \mathcal{N} and denominators D_i 's of the integrand $\mathcal{I}_{i_1 \dots i_n}$ are polynomials of the loop momentum \bar{l} .

Since now on, d -dimensional quantities are denoted by a bar, whereas objects living in -2ϵ -dimensions by a tilde. The d -dimensional loop momentum is split as follows,

$$\bar{l} = l + \tilde{l}, \quad \bar{l}^2 = l^2 - \mu^2, \quad (4.28)$$

being μ^2 the scalar product of the extra dimensional component, i.e. $\mu^2 \equiv -\tilde{l} \cdot \tilde{l}$. Therefore, the integrand will be a rational function of five loop coordinates, namely the components of the four dimensional vectors l_i and the extra-dimensional coordinate μ^2 .

Since we are working with five loop coordinates, every loop integrand in dimensional regularisation can be decomposed as a sum of integrands with five or less denominators

$$\mathcal{I} \equiv \frac{\mathcal{N}}{D_0 \dots D_{n-1}} = \sum_{k=1}^5 \sum_{\{i_1, \dots, i_k\}} \frac{\Delta_{i_1 \dots i_k}}{D_{i_1} \dots D_{i_k}}, \quad (4.29)$$

where the residues $\Delta_{i_1 \dots i_k}$'s are irreducible polynomials, which means they cannot be expressed in terms of the set of propagators. The second sum on the r.h.s. runs over all the denominator indices $\{0, \dots, n-1\}$ containing k elements.

In order to find their parametric structure according to the cut (D_i, D_j, \dots, D_k) under consideration, the loop momentum is parametrised with respect to a suitable basis of four-dimensional

massless momenta [39, 46, 47] $\mathcal{E}^{(i_1 \dots i_k)} = \{e_1, e_2, e_3, e_4\}$. The first two elements of this basis are the massless projections of two external momenta K_1 and K_2 of the subdiagrams represented by the loop denominators presented in the cut.

More explicitly, we define

$$e_1^\mu = \frac{1}{1 - r_1 r_2} (K_1^\mu - r_1 K_2^\mu), \quad e_2^\mu = \frac{1}{1 - r_1 r_2} (K_2^\mu - r_2 K_1^\mu) \quad (4.30)$$

with

$$r_1 = \frac{K_1^2}{\gamma}, \quad r_2 = \frac{K_2^2}{\gamma}, \quad \gamma = (K_1 \cdot K_2) \left(1 + \sqrt{1 + \frac{K_1^2 K_2^2}{(K_1 \cdot K_2)^2}} \right). \quad (4.31)$$

It turns out that when K_1 and K_2 are massive momenta spurious squared roots arise. In this context, spurious terms are referred to terms that drop when all contributions are added up. This cancellation is not evident and becomes problematic for analytic computations. Moreover, we can make use of the relation that γ obeys in order to cancel its dependence,

$$\gamma^2 - 2\gamma K_1 \cdot K_2 + K_1^2 K_2^2 = 0. \quad (4.32)$$

A detailed explanation of the cancelation of spurious terms is addressed in chapter 6.

For subdiagrams that have less than two independent external momenta, the remaining ones are replaced by arbitrary massless vectors in the definition of e_1 and e_2 . On the other hand, the momenta e_3 and e_4 are chosen to be orthogonal to $e_{1,2}$ and can be written, in terms of spinor products, as

$$e_3^\mu = \frac{1}{2} \langle e_1 | \gamma^\mu | e_2 \rangle, \quad e_4^\mu = \frac{1}{2} \langle e_2 | \gamma^\mu | e_1 \rangle, \quad (4.33)$$

satisfying the property $e_3 \cdot e_4 = -e_1 \cdot e_2$. For box diagrams we define the massive vectors v and v_\perp ,

$$v^\mu = (e_4 \cdot K_3) e_3^\mu + (e_3 \cdot K_3) e_4^\mu, \quad v_\perp^\mu = (e_4 \cdot K_3) e_3^\mu - (e_3 \cdot K_3) e_4^\mu, \quad (4.34)$$

being v_\perp^μ an orthogonal vector to all the external legs of the box diagram.

With a suitable choice of the basis $\mathcal{E}^{(i_1 \dots i_k)}$, the loop momentum l can be written as [57, 259]

$$l^\alpha = -p_i^\alpha + \frac{1}{e_1 \cdot e_2} (x_1 e_1^\alpha + x_2 e_2^\alpha - x_3 e_3^\alpha - x_4 e_4^\alpha), \quad (4.35)$$

being the coordinates x'_i s written as scalar products

$$x_1 = (L_1 \cdot e_2), \quad x_2 = (L_1 \cdot e_1), \quad x_3 = (L_1 \cdot e_4), \quad x_4 = (L_1 \cdot e_3), \quad (4.36)$$

with $L_1 = l + p_i$.

For diagrams of $k = 4$ loop denominators, the loop momentum takes the form,

$$l^\alpha = -p_i^\alpha + \frac{1}{e_1 \cdot e_2} (x_1 e_1^\alpha + x_2 e_2^\alpha) + \frac{1}{v^2} (x_{3,v} v^\alpha - x_{4,v} v_\perp^\alpha), \quad (4.37)$$

with

$$x_{3,v} = (L_1 \cdot v), \quad x_{4,v} = (L_1 \cdot v_\perp), \quad (4.38)$$

According to this parameterisation, the numerator \mathcal{N} becomes a polynomial in the coordinates x_i ,

$$\mathcal{N}(\bar{q}) = \mathcal{N}(q, \mu^2) = \mathcal{N}(x_1, x_2, x_3, x_4, \mu^2), \quad (4.39)$$

therefore, it admits the universal parametric form

$$\mathcal{N}_{i_1 \dots i_n} \equiv \sum_{j_1, j_2, j_3, j_4, j_5} n_{j_1 j_2 j_3 j_4 j_5} x_1^{j_1} x_2^{j_2} x_3^{j_3} x_4^{j_4} \mu^{2j_5}, \quad j_1 + j_2 + j_3 + j_4 + 2j_5 \leq r_{\max}, \quad (4.40)$$

here r_{\max} is the number of loop denominators presented in the diagram under consideration.

Given such decomposition of the loop momentum, (4.35) and (4.37), the parametric expression of $\Delta_{i_1 \dots i_k}$ is process independent and, for renormalisable theories, it turns out to be [41, 46, 249, 251]

$$\begin{aligned} \Delta_{i_1 i_2 i_3 i_4 i_5} &= c_0 \mu^2, \\ \Delta_{i_1 i_2 i_3 i_4} &= c_0 + c_1 x_{4,v} + \mu^2 (c_2 + c_3 x_{4,v} + \mu^2 c_4), \\ \Delta_{i_1 i_2 i_3} &= c_0 + c_1 x_4 + c_2 x_4^2 + c_3 x_4^3 + c_4 x_3 + c_5 x_3^2 + c_6 x_3^3 + \mu^2 (c_7 + c_8 x_4 + c_9 x_3), \\ \Delta_{i_1 i_2} &= c_0 + c_1 x_1 + c_2 x_1^2 + c_3 x_4 + c_4 x_4^2 + c_5 x_3 + c_6 x_3^2 + c_7 x_1 x_4 + c_8 x_1 x_3 + c_9 \mu^2, \\ \Delta_{i_1} &= c_0 + c_1 x_1 + c_2 x_2 + c_3 x_3 + c_4 x_4, \end{aligned} \quad (4.41)$$

where, for each coefficient, a superscript labelling the specific cut is understood, $c_m = c_m^{(i \dots k)}$.

Although the residue of the pentagon is just a constant, it is useful to use a different parametrisation in which the μ^2 -dependence is explicit [67]. The advantage of this choice is that this residue vanishes upon integration. In addition, this parametrisation recovers the four-dimensional part of the lower residues in the reduction, i.e. $\bar{q} = q, \mu^2 = 0$.

As a consequence of the (4.41), by neglecting all spurious terms which vanish upon integration, the contribution \mathcal{M} can be written in terms of MI's,

$$I_{i_1 \dots i_k}[\alpha] = h(\mu_R^2, d) \int d^d \bar{l} \frac{\alpha}{D_{i_1} \dots D_{i_k}}, \quad I_{i_1 \dots i_k}[1] = I_{i_1 \dots i_k} \quad (4.42)$$

and of the coefficients of the residues as

$$\begin{aligned} \mathcal{M} &= \sum_{\{i_1, i_2, i_3, i_4\}} \left\{ c_0^{(i_1 i_2 i_3 i_4)} I_{i_1 i_2 i_3 i_4} + c_4^{(i_1 i_2 i_3 i_4)} I_{i_1 i_2 i_3 i_4}[\mu^4] \right\} \\ &+ \sum_{\{i_1, i_2, i_3\}} \left\{ c_0^{(i_1 i_2 i_3)} I_{i_1 i_2 i_3} + c_7^{(i_1 i_2 i_3)} I_{i_1 i_2 i_3}[\mu^2] \right\} \\ &+ \sum_{\{i_1, i_2\}} \left\{ c_0^{(i_1 i_2)} I_{i_1 i_2} + c_1^{(i_1 i_2)} I_{i_1 i_2}[(l + p_i) \cdot e_2] + c_2^{(i_1 i_2)} I_{i_1 i_2}[(l + p_i) \cdot e_2]^2 + c_9^{(i_1 i_2)} I_{i_1 i_2}[\mu^2] \right\} \\ &+ \sum_{i_1} c_0^{(i_1)} I_{i_1}. \end{aligned} \quad (4.43)$$

The relations between two-point tensor and scalar integrals are presented in App. A.

4.3.1 Fit on the cut at one loop

The fitting of the coefficients of eq.(4.43) is obtained by evaluating the numerator of the integrand on multiple cuts, i.e. values of the loop momentum where the loop denominators of an specific subset (cut) vanish. In the same manner, residues are computed by sampling the numerator of the integrand, after all non-vanishing contributions to higher-point residues have been subtracted on a finite set of on-shell solution of the multiple cuts. This algorithm based on a top-down approach have been automated in several codes, some of which are public CutTools [260] and Samurai [47].

In the following we briefly review this method, as proposed in Ref.s [41, 46, 47], studying in details the computation of 5-, 4-, 3- 2- and 1-point residues.

5-point residues The maximal cut in $d = 4 - 2\epsilon$ of any one-loop amplitude is a 5-ple cut, which, corresponds to putting five propagators on-shell. This on-shellness allows us to write the cut solution, eq.(4.35), by solving the system of equations of $D_{i_1} = \dots = D_{i_5} = 0$, where all coordinates x_i and μ^2 are fixed. Hence, the coefficient c_0 of the pentagon is found as

$$c_0 = \frac{1}{\mu_s^2} \frac{\mathcal{N}(l_s, \mu_s^2)}{\prod_{h \neq i_1, \dots, i_5} D_h}, \quad (4.44)$$

where l_s and μ_s^2 are the 5-ple cut solution and value of μ^2 at the cut, respectively.

4-point residues The 4-ple cut solution is obtained by solving the on-shell conditions $D_{i_1} = \dots = D_{i_4} = 0$. This cut has two solutions l_+ and l_- which are used to fix the residue $\Delta_{i_1 \dots i_4}$,

$$\Delta_{i_1 i_2 i_3 i_4} = \frac{\mathcal{N}(l, \mu^2)}{\prod_{h \neq i_1, \dots, i_4} D_h} - \sum_{i_5} \frac{\Delta_{i_1 i_2 i_3 i_4 i_5}}{D_{i_5}}, \quad (4.45)$$

Coefficients c_0, c_2 and c_4 are fitted from the average of the integrand evaluated on the two solutions,

$$\frac{1}{2} \left(\frac{\mathcal{N}(l, \mu^2)}{\prod_{h \neq i_1, \dots, i_4} D_h} - \sum_{i_5} \frac{\Delta_{i_1 i_2 i_3 i_4 i_5}}{D_{i_5}} \Big|_{l=l_+} + \frac{\mathcal{N}(l, \mu^2)}{\prod_{h \neq i_1, \dots, i_4} D_h} - \sum_{i_5} \frac{\Delta_{i_1 i_2 i_3 i_4 i_5}}{D_{i_5}} \Big|_{l=l_-} \right), \quad (4.46)$$

while c_1 and c_3 from the difference.

3-point residues For the 3-ple cut solution there are three on-shell conditions $D_{i_1} = D_{i_2} = D_{i_3} = 0$. On the solutions, the integrand decomposition reads,

$$\Delta_{i_1 i_2 i_3} = \frac{\mathcal{N}(l, \mu^2)}{\prod_{h \neq i_1, i_2, i_3} D_h} - \sum_{i_4} \frac{\Delta_{i_1 i_2 i_3 i_4}}{D_{i_4}} - \sum_{i_4, i_5} \frac{\Delta_{i_1 i_2 i_3 i_4 i_5}}{D_{i_4} D_{i_5}}, \quad (4.47)$$

where the coefficients of the residue are computed by sampling the integrand at ten different values of l . These solutions, parametrised, according to Eq. (4.35) have two fulfil the on-shell conditions.

2-point residues In order to compute the 2-ple cut solution, l is parametrised by solving the on-shell conditions $D_{i_1} = D_{i_2} = 0$. For this cut there is only one solution and the integrand decomposition reads

$$\Delta_{i_1 i_2} = \frac{\mathcal{N}(l, \mu^2)}{\prod_{h \neq i_1, i_2} D_h} - \sum_{i_3} \frac{\Delta_{i_1 i_2 i_3}}{D_{i_3}} - \sum_{i_3, i_4} \frac{\Delta_{i_1 i_2 i_3 i_4}}{D_{i_3} D_{i_4}} - \sum_{i_3, i_4, i_5} \frac{\Delta_{i_1 i_2 i_3 i_4 i_5}}{D_{i_3} D_{i_4} D_{i_5}}, \quad (4.48)$$

As for the 2-point residues, the coefficients of the residue are fitted by sampling the integrand at ten different values of l .

1-point residues Finally, the single cut solution is obtained by solving the on-shell condition $D_{i_1} = 0$. The integrand decomposition becomes,

$$\Delta_{i_1} = \frac{\mathcal{N}(l, \mu^2)}{\prod_{h \neq i_1} D_h} - \sum_{i_2} \frac{\Delta_{i_1 i_2}}{D_{i_2}} - \sum_{i_2, i_3} \frac{\Delta_{i_1 i_2 i_3}}{D_{i_2} D_{i_3}} - \sum_{i_2, i_3, i_4} \frac{\Delta_{i_1 i_2 i_3 i_4}}{D_{i_2} D_{i_3} D_{i_4}} - \sum_{i_2, i_3, i_4, i_5} \frac{\Delta_{i_1 i_2 i_3 i_4 i_5}}{D_{i_2} D_{i_3} D_{i_4} D_{i_5}}, \quad (4.49)$$

the coefficients of the residue are fitted by sampling the integrand at five different values of l .

4.4 One-loop amplitudes via Laurent series expansion

In the previous section, we saw how any numerator can be decomposed in terms of irreducible polynomials, called residues, which admit a parametric form independent of the process. In addition, we can promote them to be the full integrand of an amplitude, which, depending on the cut under consideration, can be extracted from the product of tree amplitudes. In this section, we review the integrand reduction of one-loop scattering amplitudes through Laurent series expansion, proposed by Mastrolia, Mirabella and Peraro [61].

This approach elaborates on the techniques proposed to compute triangle and bubbles coefficients developed by Forde [39] for massless theories, then generalised to massive cases by Kilgore [256] and, later extended to the calculation of finite parts of the amplitude by Badger [62]. The series expansion is applied systematically to the integrand decomposition formula of OPP/EGKM.

The main features of this algorithm are the following

- The coefficients of the 5-point functions are never needed and do not have to be computed.
- The spurious coefficients of the 4-point functions do not enter into the reduction and are not computed. Hence, the computation of 3-, 2- and 1-point coefficients is independent of the 4-point ones.
- The subtraction at integrand level is replaced by the subtraction at the coefficient level.
- The correction terms of 2- and 1-point functions are parametrised by universal functions in terms of the higher point coefficients.
- The application of the Laurent expansion for the determination of 3-, 2- and 1-point coefficients is implemented via polynomial division. The Laurent series is obtained as the quotient of the division between the numerator and the product of the uncut denominators, neglecting the remainder.

In the following, we briefly review the extraction of coefficients by performing a suitable Laurent expansion of the cut integrand with respect to one of the components of the loop momenta which are left unconstrained by the on-shell conditions.

4.4.1 Reduction algorithm

In this subsection, we show how to get the coefficients c of each polynomial Δ of (4.41)

5-ple cut The coefficient c_0 of eq. (4.41) can be computed as explained in Sec. 4.3. Moreover, this cut is not needed in the reduction, therefore, its computation is omitted.

4-ple cut The cut solution can be expressed, according to (4.37), as

$$l^\alpha = -p_i^\alpha + x_1 e_1^\alpha + x_2 e_2^\alpha + x_{3,v} v^\alpha \pm \sqrt{\alpha_\perp + \frac{\mu^2}{v_\perp^2} v_\perp^\alpha}, \quad (4.50)$$

where the coefficients $x_1, x_2, x_{3,v}$ and α_\perp are frozen by the on-shell conditions, $D_{i_1} = \dots = D_{i_4} = 0$. The only two coefficients that are needed are obtained from [31, 61, 62]

$$\frac{1}{2} \left(\frac{\mathcal{N}(l, \mu^2)}{\prod_{h \neq i_1, \dots, i_4} D_h} \Big|_{\substack{l=l_+ \\ \mu^2 \rightarrow 0}} + \frac{\mathcal{N}(l, \mu^2)}{\prod_{h \neq i_1, \dots, i_4} D_h} \Big|_{\substack{l=l_- \\ \mu^2 \rightarrow 0}} \right) = c_0, \quad (4.51)$$

$$\frac{\mathcal{N}(l, \mu^2)}{\prod_{h \neq i_1, \dots, i_4} D_h} \Big|_{\mu^2 \rightarrow \infty} = c_4 \mu^4 + \mathcal{O}(\mu^3). \quad (4.52)$$

3-ple cut The solutions of the 3-cut can be parametrised, according to (4.35), as

$$l_+^\alpha = -p_i^\alpha + x_1 e_1^\alpha + x_2 e_2^\alpha + t e_3^\alpha + \frac{\alpha_0 + \mu^2}{2t(e_3 \cdot e_4)} e_4^\alpha, \quad (4.53a)$$

$$l_-^\alpha = -p_i^\alpha + x_1 e_1^\alpha + x_2 e_2^\alpha + t e_4^\alpha + \frac{\alpha_0 + \mu^2}{2t(e_3 \cdot e_4)} e_3^\alpha, \quad (4.53b)$$

where x_1, x_2 and α_0 are frozen by the three cut conditions, $D_{i_1} = D_{i_2} = D_{i_3} = 0$. The coefficients of the residue $\Delta_{i_1 i_2 i_3}$ can be obtained in the large- t limit according to

$$\frac{\mathcal{N}(l, \mu^2)}{\prod_{h \neq i_1, \dots, i_4} D_h} \Big|_{\substack{l=l_+ \\ t \rightarrow \infty}} = n_0^+ + n_7^+ \mu^2 + (n_4 + n_9 \mu^2)t + n_5 t^2 + n_6 t^3 + \mathcal{O}(1/t), \quad (4.54a)$$

$$\frac{\mathcal{N}(l, \mu^2)}{\prod_{h \neq i_1, \dots, i_4} D_h} \Big|_{\substack{l=l_- \\ t \rightarrow \infty}} = n_0^- + n_7^- \mu^2 + (n_1 + n_8 \mu^2)t + n_2 t^2 + n_3 t^3 + \mathcal{O}(1/t), \quad (4.54b)$$

where the relations between n'_i s and c_i 's of (4.41) for the $\Delta_{i_1 i_2 i_3}$ are given by,

$$c_{0,7} = \frac{1}{2}(n_{0,7}^+ + n_{0,7}^-), \quad c_{1,4,8,9} = \frac{n_{1,4,8,9}}{(e_3 \cdot e_4)}, \quad c_{2,5} = \frac{n_{2,5}}{(e_3 \cdot e_4)^2}, \quad c_{3,6} = \frac{n_{3,6}}{(e_3 \cdot e_4)^3}. \quad (4.55)$$

The Laurent expansion allows to determine the 3-point residues without any subtraction of higher-point terms. The average of the two solutions cancels the spurious coefficients coming from boxes. In addition, pentagon contributions behaves as $\mathcal{O}(1/t)$.

2-ple cut The solutions of the double cut $D_i = D_j = 0$ are parametrised as follows

$$l_+^\alpha = -p_i^\alpha + x_1 e_1^\alpha + (\alpha_0 + x_1 \alpha_1) e_2^\alpha + t e_3^\alpha + \frac{\beta_0 + \beta_1 x_1 + \beta_2 x_1^2 + \mu^2}{2t(e_3 \cdot e_4)} e_4^\alpha, \quad (4.56a)$$

$$l_-^\alpha = -p_i^\alpha + x_1 e_1^\alpha + (\alpha_0 + x_1 \alpha_1) e_2^\alpha + t e_4^\alpha + \frac{\beta_0 + \beta_1 x_1 + \beta_2 x_1^2 + \mu^2}{2t(e_3 \cdot e_4)} e_3^\alpha, \quad (4.56b)$$

in terms of three free parameters x, t and μ^2 , while the constants α_i and β_i are determined by on-shell conditions, $D_{i_1} = D_{i_2} = 0$. The coefficients of the residue $\Delta_{i_1 i_2 i_3}$ can be extracted from the large- t expansion,

$$\frac{\mathcal{N}(l, \mu^2)}{\prod_{h \neq i_1, i_2} D_h} - \sum_{i_3} \frac{\Delta_{i_1 i_2 i_3}}{D_{i_3}} \Big|_{\substack{l=l_+ \\ t \rightarrow \infty}} = n_0 + n_9 \mu^2 + n_1 x_1 + n_2 x_1^2 + n_5 t + n_6 t^2 + n_8 x_1 t + \mathcal{O}(1/t), \quad (4.57a)$$

$$\frac{\mathcal{N}(l, \mu^2)}{\prod_{h \neq i_1, i_2} D_h} - \sum_{i_3} \frac{\Delta_{i_1 i_2 i_3}}{D_{i_3}} \Big|_{\substack{l=l_- \\ t \rightarrow \infty}} = n_0 + n_9 \mu^2 + n_1 x_1 + n_2 x_1^2 + n_3 t + n_4 t^2 + n_7 x_1 t + \mathcal{O}(1/t). \quad (4.57b)$$

It turns out that the individual expansion of

$$\frac{\mathcal{N}(l, \mu^2)}{\prod_{h \neq i_1, i_2} D_h} \Big|_{\substack{l=l_+ \\ t \rightarrow \infty}} \quad \text{and} \quad \sum_{i_3} \frac{\Delta_{i_1 i_2 i_3}}{D_{i_3}} \Big|_{\substack{l=l_+ \\ t \rightarrow \infty}}$$

have the same polynomial structure of the r.h.s of eq. (4.57). For the “+” case we have

$$\frac{\mathcal{N}(l, \mu^2)}{\prod_{h \neq i_1, i_2} D_h} \Big|_{\substack{l=l_+ \\ t \rightarrow \infty}} = a_0 + a_9 \mu^2 + a_1 x_1 + a_2 x_1^2 + a_5 t + a_6 t^2 + a_8 x_1 t + \mathcal{O}(1/t), \quad (4.58a)$$

$$\frac{\Delta_{i_1 i_2 i_3}}{D_{i_3}} \Big|_{\substack{l=l_+ \\ t \rightarrow \infty}} = b_0^{(i_3)} + b_9^{(i_3)} \mu^2 + b_1^{(i_3)} x_1 + b_2^{(i_3)} x_1^2 + b_5^{(i_3)} t + b_6^{(i_3)} t^2 + b_8^{(i_3)} x_1 t + \mathcal{O}(1/t). \quad (4.58b)$$

The “−” case is obtained by replacing (5, 6, 8) → (3, 4, 7). Therefore, the coefficients a and b can be computed separately, obtaining the coefficients n by their difference,

$$n_k = a_k - \sum_j b_k^{(j)}. \quad (4.59)$$

As done for the 3-cut, the coefficients of the residue $\Delta_{i_1 i_2}$, after normalisation, are given by

$$c_{0,9} = n_{0,9}, \quad c_{1,3,5} = \frac{n_{1,3,5}}{(e_3 \cdot e_4)}, \quad c_{2,4,6,7,8} = \frac{n_{2,4,6,7,8}}{(e_3 \cdot e_4)^2}. \quad (4.60)$$

Single cut We consider the following solutions of the single cut $D_{i_1} = 0$,

$$l_+^\alpha = -p_i^\alpha + t e_3^\alpha + \frac{\mu^2}{2t(e_3 \cdot e_4)} e_4^\alpha, \quad l_-^\alpha = -p_i^\alpha + t e_4^\alpha + \frac{\mu^2}{2t(e_3 \cdot e_4)} e_3^\alpha, \quad (4.61)$$

The non-spurious term c_0 of eq. (4.41) is extracted from the large- t limit

$$\frac{\mathcal{N}(l, \mu^2)}{\prod_{h \neq i_1} D_h} - \sum_{i_2} \frac{\Delta_{i_1 i_2}}{D_{i_2}} - \sum_{i_2, i_3} \frac{\Delta_{i_1 i_2 i_3}}{D_{i_2} D_{i_3}} \Big|_{\substack{l=l_+ \\ t \rightarrow \infty}} = n_0 + n_4 t + \mathcal{O}(1/t),$$

where bubble and triangle subtraction terms are non-vanishing.

Similarly to the 2-cut, the expansion of

$$\frac{\mathcal{N}(l, \mu^2)}{\prod_{h \neq i_1} D_h} \Big|_{\substack{l=l_+ \\ t \rightarrow \infty}}, \quad \sum_{i_2} \frac{\Delta_{i_1 i_2}}{D_{i_2}} \Big|_{\substack{l=l_+ \\ t \rightarrow \infty}} \quad \text{and,} \quad \sum_{i_2, i_3} \frac{\Delta_{i_1 i_2 i_3}}{D_{i_2} D_{i_3}} \Big|_{\substack{l=l_+ \\ t \rightarrow \infty}} \quad (4.62)$$

have the same polynomial behaviour as the residue, i.e.

$$\frac{\mathcal{N}(l, \mu^2)}{\prod_{h \neq i_1} D_h} \Big|_{\substack{l=l_+ \\ t \rightarrow \infty}} = a_0 + a_4 t + \mathcal{O}(1/t), \quad (4.63)$$

$$\sum_{i_2} \frac{\Delta_{i_1 i_2}}{D_{i_2}} \Big|_{\substack{l=l_+ \\ t \rightarrow \infty}} = b_0^{(i_2)} + b_4^{(i_2)} t + \mathcal{O}(1/t), \quad (4.64)$$

$$\sum_{i_2, i_3} \frac{\Delta_{i_1 i_2 i_3}}{D_{i_2} D_{i_3}} \Big|_{\substack{l=l_+ \\ t \rightarrow \infty}} = b_0^{(i_2 i_3)} + b_4^{(i_2 i_3)} t + \mathcal{O}(1/t), \quad (4.65)$$

The coefficients $a, b^{(i_2)}$ and $b^{(i_2 i_3)}$ give the 1-point coefficient, according to

$$c_0 = n_0 = a_0 - \sum_j b_0^{(j)} - \sum_{j < k} b_0^{(jk)}. \quad (4.66)$$

4.5 Discussion

The methods studied in this chapter, used to compute one-loop amplitudes, are part of an arsenal of tools for physicists to make physical predictions to the phenomenology of high energy physics. Because of their analytical construction and the established algorithm, the automation of the calculation of one-loop amplitudes could be carried out. Several numerical and semi-numerical codes, capable of computing observables of the theory, were produced [49–60]. This dramatic development allowed the scientific community to understand, with more accuracy, the behaviour of the so-called interacting particles. In particular, processes given by QCD allow for reducing the background of collisions produced by hadrons, giving, eventually, raise to new physics. In the next chapters, we will make use of these modern methods to give phenomenological and mathematical approaches to the computation of scattering amplitudes.

In chapter 5, we provide a new regularisation scheme which allows us to compute any one-loop scattering amplitude. Within our regularisation scheme, this computation can be carried out by using traditional and modern methods such a computation of Feynman diagrams or unitarity based methods in d dimensions, respectively. For the latter, explicit representation of particles circulating in the loop are given. Simple applications of $2 \rightarrow 2$ processes are addressed. In the same manner, within our scheme, we provide renormalisation at one-loop of QED and QCD.

In chapter 6, we stress on the analytical computation of one-loop scattering amplitudes with high multiplicity (up six external legs). Its procedure takes advantage of fundamental pieces, tree-level amplitudes, as input. It also combines generalised unitarity in d -dimensions and Laurent series expansion. In particular, the processes $gg \rightarrow ngH$ ($n = 1, 2, 3$), in the heavy top mass limit, show how our regularisation scheme is suitable for effective theories. These analytical results, besides contributing to the NLO, are also part of the ingredients for the NNLO prediction.

On the other side, chapter 7 studies the relations that the colour-kinematics (C/K) duality can generate for the computation of d -dimensionally regulated amplitudes and integrands from generalised unitarity. In general, both relations require as input a regularisation scheme, which, in our case turns out to be the one proposed in chapter 5. It shall be shown that, because of the C/K-duality and the integrand reduction methods via Laurent series expansion, relations between integrands reduce the amount of needed coefficients to recover any one-loop amplitude.

Chapter 8 addresses the algorithms to compute multi-loop scattering amplitudes. Without loose of generality, we consider the computation of two-loop scattering amplitudes. Firstly, we present the integrand reduction methods via polynomial division module Gröbner basis. The all plus four-gluon amplitude is studied in details by following this method. Secondly, we briefly describe the adaptive integrand decomposition method, which relies on the decomposition of the space-time, $d = d_{\parallel} + d_{\perp}$, in parallel and perpendicular subspaces. The all plus five-gluon amplitude is studied by following this algorithm, numerical results are presented.

Chapter 5

Four-Dimensional-Formulation

In this chapter, we study the four dimensional formulation (FDF) regularisation scheme. This scheme, at one-loop, is equivalent to the four-dimensional helicity (FDH) scheme [32, 198, 199], and allows for a purely four-dimensional regularisation of the amplitudes. Within FDF, the states in the loop are described as four dimensional massive particles. The four-dimensional degrees of freedom of the gauge bosons are carried by *massive vector bosons* of mass μ and their $(d-4)$ -dimensional ones by *real scalar particles* obeying a simple set of four-dimensional Feynman rules. A d -dimensional fermion of mass m is instead traded for a *tachyonic Dirac field* with mass $m + i\mu\gamma^5$. The d dimensional algebraic manipulations are replaced by four-dimensional ones complemented by a set of multiplicative selection rules. The latter are treated as an algebra describing internal symmetries.

Within integrand reduction methods, FDF allows for the simultaneous computation of both the cut-constructible and the rational terms by employing a purely four-dimensional formulation of the integrands. As a consequence, an explicit four-dimensional representation of generalised states propagating around the loop can be formulated. Therefore, a straightforward implementation of d -dimensional generalised unitarity within exactly four space-time dimensions can be realised, avoiding any higher-dimensional extension of either the Dirac [65, 66] or the spinor algebra [68].

This chapter is organised as follows. Sec. 5.1 is devoted to the description of FDF, while Sec. 5.2 describes how generalised unitarity method can be applied in presence of a FDF of one-loop amplitudes. Sec. 5.3 shows the decomposition in terms of MIs of certain classes of $2 \rightarrow 2$ one-loop amplitudes. It is preliminary to Sec.s 5.3.1, 5.3.2 and 5.3.3, which collect the applications of generalised unitarity methods within the FDF. In particular they present results for representative helicity amplitudes of $gg \rightarrow gg$, $q\bar{q} \rightarrow gg$ with massless quarks, and $gg \rightarrow Hg$ in the heavy-top limit. In Sec. 5.4 we discuss the renormalisation at one-loop within FDF for QED and QCD using on-shell and minimal subtraction scheme, respectively.

5.1 Four-dimensional Feynman rules

The FDH scheme [32, 198, 199] defines a d -dimensional vector space embedded in a larger d_s -dimensional space, $d_s \equiv (4 - 2\epsilon) > d > 4$. The scheme is determined by the following rules

- The loop momenta are considered to be d -dimensional. All observed external states are considered as four-dimensional. All unobserved internal states, i.e. virtual states in loops and intermediate states in trees, are treated as d_s -dimensional.
- Since $d_s > d > 4$, the scalar product of any d - or d_s -dimensional vector with a four-dimensional vector is a four-dimensional scalar product. Moreover, any dot product between a d_s -dimensional tensor and a d -dimensional one is a d -dimensional dot product.

- The Lorentz and the Clifford algebra are performed in d_s dimensions, which has to be kept distinct from d . The matrix γ^5 is treated using the 't Hooft-Veltman prescription, *i.e.* γ^5 commutes with the Dirac matrices carrying -2ϵ indices.
- After the γ -matrix algebra has been performed, the limit $d_s \rightarrow 4$ has to be performed, keeping d fixed. The limit $d \rightarrow 4$ is taken at the very end.

Starting with the d_s -dimensional metric tensor, we split it as

$$\bar{g}^{\mu\nu} = g^{\mu\nu} + \tilde{g}^{\mu\nu}, \quad (5.1)$$

in terms of a four-dimensional tensor g and a -2ϵ -dimensional one, \tilde{g} , such that

$$\tilde{g}^{\mu\rho} g_{\rho\nu} = 0, \quad \tilde{g}^\mu{}_\mu = -2\epsilon \xrightarrow{d_s \rightarrow 4} 0, \quad g^\mu{}_\mu = 4, \quad (5.2)$$

The tensors g and \tilde{g} project a d_s -dimensional vector \bar{l} into the four-dimensional and the -2ϵ -dimensional subspaces respectively,

$$l^\mu \equiv g^\mu{}_\nu \bar{l}^\nu, \quad \tilde{l}^\mu \equiv \tilde{g}^\mu{}_\nu \bar{l}^\nu. \quad (5.3)$$

At one loop, the only d -dimensional object is the loop momentum \bar{l} . The square of its -2ϵ dimensional component is defined as:

$$\tilde{l}^2 = \tilde{g}^{\mu\nu} \bar{l}_\mu \bar{l}_\nu \equiv -\mu^2. \quad (5.4)$$

The properties of the matrices $\tilde{\gamma}^\mu = \tilde{g}^\mu{}_\nu \bar{\gamma}^\nu$ can be obtained from Eq. (5.2)

$$[\tilde{\gamma}^\alpha, \gamma^5] = 0, \quad \{\tilde{\gamma}^\alpha, \gamma^\mu\} = 0, \quad (5.5a)$$

$$\{\tilde{\gamma}^\alpha, \tilde{\gamma}^\beta\} = 2\tilde{g}^{\alpha\beta}. \quad (5.5b)$$

We remark that the -2ϵ tensors can not have a four-dimensional representation. Indeed, its square is traceless

$$\tilde{g}^{\mu\rho} \tilde{g}_{\rho\mu} = \tilde{g}^\mu{}_\mu \xrightarrow{d_s \rightarrow 4} 0. \quad (5.6)$$

Moreover, the component \tilde{l} of the loop momentum vanishes when contracted with the metric tensor g ,

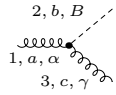
$$\tilde{l}^\mu g_{\mu\nu} = \bar{l}_\rho \tilde{g}^{\rho\mu} g_{\mu\nu} = 0, \quad (5.7)$$

and in four dimensions the only four vector fulfilling (5.7) is the null one. Finally, in four dimensions the only non-null matrices fulfilling the conditions (5.5a) are proportional to γ^5 , hence $\tilde{\gamma} \sim \gamma^5$. However, the matrices $\tilde{\gamma}$ fulfil the Clifford algebra (5.5b), thus

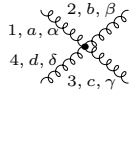
$$\tilde{\gamma}^\mu \tilde{\gamma}_\mu \xrightarrow{d_s \rightarrow 4} 0, \quad \text{while} \quad \gamma^5 \gamma^5 = \mathbb{I}. \quad (5.8)$$

These arguments exclude any four-dimensional representation of the -2ϵ subspace. It is possible, however, to find such a representation by introducing additional rules, called in the following -2ϵ selection rules, (-2ϵ) -SRs. Indeed, as shown in App. B.1, the Clifford algebra (5.5b) is equivalent to

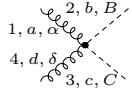
$$\dots \tilde{\gamma}^\alpha \dots \tilde{\gamma}_\alpha \dots = 0, \quad \tilde{l} \tilde{l} = -\mu^2. \quad (5.9)$$



$$= \mp g f^{abc} (i\mu) g^{\gamma\alpha} Q^B, \quad (\tilde{k}_1 = 0, \quad \tilde{k}_3 = \pm\tilde{l}), \quad (5.12h)$$



$$= -ig^2 \left[f^{xad} f^{xbc} \left(g^{\alpha\beta} g^{\delta\gamma} - g^{\alpha\gamma} g^{\beta\delta} \right) + f^{xac} f^{xbd} \left(g^{\alpha\beta} g^{\delta\gamma} - g^{\alpha\delta} g^{\beta\gamma} \right) \right. \\ \left. + f^{xab} f^{xdc} \left(g^{\alpha\delta} g^{\beta\gamma} - g^{\alpha\gamma} g^{\beta\delta} \right) \right], \quad (5.12i)$$



$$= 2ig^2 g^{\alpha\delta} \left(f^{xab} f^{xcd} + f^{xac} f^{xbd} \right) G^{BC}, \quad (5.12j)$$



$$= -ig \left(t^b \right)_{ji} \gamma^\beta, \quad (5.12k)$$



$$= -ig \left(t^b \right)_{ji} \gamma^5 \Gamma^B. \quad (5.12l)$$

In the Feynman rules (5.12) all the momenta are incoming and the scalar particle s_g can circulate in the loop only. The terms μ^2 appearing in the the propagators (5.12a)–(5.12d) enter only if the corresponding momentum k is d -dimensional, *i.e.* only if the corresponding particle circulates in the loop. In the vertex (5.12h) the momentum k_1 is four-dimensional while the other two are d -dimensional. The possible combinations of the -2ϵ components of the momenta involved are

$$\{\tilde{k}_1, \tilde{k}_2, \tilde{k}_3\} = \{0, \mp\tilde{l}, \pm\tilde{l}\}. \quad (5.13)$$

The overall sign of the Feynman rule (5.12h) depends on which of the combinations (5.13) is present in the vertex.

As already pointed out, the (-2ϵ) -SRs constitute a formal algebra, thus they cannot have a purely numerical matrix implementation. Therefore the manipulations related to the (-2ϵ) -SRs have to be performed algebraically by using algebraic manipulations programs such as MATHEMATICA [262] or FORM [263]. It is worth to mention that the manipulations are extremely simple and have to be performed once and for all. In particular they can be performed before any other manipulation or any recursive construction and would allow us to know in advance whether the diagram or the cut vanishes. The selection rules (5.11) are more trivial than the colour algebra, since no interference with tree-level is needed.

Our prescriptions, Eq. (5.10), can be related to a five-dimensional theory characterised by $g^{55} = -1$, $l^5 = \mu$ and a 4×4 representation of the Clifford algebra, $\{\gamma^0, \dots, \gamma^3, i\gamma^5\}$. Regularisation methods in five dimensions have been proposed as an alternative formulation of the Pauli-Villars regularisation [264] or as regulators of massless pure Yang Mills theories at one loop [265]. Our method distinguishes itself by the presence of the (-2ϵ) -SRs, a crucial ingredient for the correct reconstruction of dimensionally-regularised amplitudes.

5.2 Fermion and Boson wave functions within FDF

Generalised-unity methods in d dimensions require an explicit representation of the polarisation vectors and the spinors of d -dimensional particles. The latter ones are essential ingredients

for the construction of the tree-level amplitudes that are sewn along the generalised cuts. In this respect, the FDF scheme is suitable for the four-dimensional formulation of d -dimensional generalised unitarity. The main advantage of the FDF is that the four-dimensional expression of the propagators of the particles in the loop admits an explicit representation in terms of generalised spinors and polarisation expressions, whose expression is collected below.

In the following discussion the d -dimensional momentum, \bar{l} , will be put on-shell and decomposed according to Eq. (4.28). Its four-dimensional component, l , will be expressed as

$$l = l^b + \hat{q}_l, \quad \hat{q}_l \equiv \frac{m^2 + \mu^2}{2l \cdot q_l} q_l, \quad (5.14)$$

in terms of the two massless momenta l^b and q_l .

Spinors – The spinors of a d -dimensional fermion have to fulfil a completeness relation which reconstructs the numerator of the cut propagator,

$$\sum_{\lambda=1}^{2^{(d_s-2)/2}} u_{\lambda, (d)}(\bar{l}) \bar{u}_{\lambda, (d)}(\bar{l}) = \bar{l} + m, \quad \sum_{\lambda=1}^{2^{(d_s-2)/2}} v_{\lambda, (d)}(\bar{l}) \bar{v}_{\lambda, (d)}(\bar{l}) = \bar{l} - m. \quad (5.15)$$

The substitutions (5.10) allow one to express Eq. (5.15) as follows:

$$\sum_{\lambda=\pm} u_{\lambda}(l) \bar{u}_{\lambda}(l) = \not{l} + i\mu\gamma^5 + m, \quad \sum_{\lambda=\pm} v_{\lambda}(l) \bar{v}_{\lambda}(l) = \not{l} + i\mu\gamma^5 - m. \quad (5.16)$$

As shown in the App. B.2, the generalised massive spinors

$$\begin{aligned} u_+(l) &= |l^b\rangle + \frac{(m - i\mu)}{[l^b q_l]} |q_l\rangle, & u_-(l) &= |l^b] + \frac{(m + i\mu)}{\langle l^b q_l \rangle} |q_l\rangle, \\ v_-(l) &= |l^b\rangle - \frac{(m - i\mu)}{[l^b q_l]} |q_l\rangle, & v_+(l) &= |l^b] - \frac{(m + i\mu)}{\langle l^b q_l \rangle} |q_l\rangle, \end{aligned} \quad (5.17a)$$

$$\begin{aligned} \bar{u}_+(l) &= [l^b| + \frac{(m + i\mu)}{\langle q_l l^b \rangle} \langle q_l|, & \bar{u}_-(l) &= \langle l^b| + \frac{(m - i\mu)}{[q_l l^b]} [q_l|, \\ \bar{v}_-(l) &= [l^b| - \frac{(m + i\mu)}{\langle q_l l^b \rangle} \langle q_l|, & \bar{v}_+(l) &= \langle l^b| - \frac{(m - i\mu)}{[q_l l^b]} [q_l|, \end{aligned} \quad (5.17b)$$

fulfil the completeness relation (5.16). The spinors (5.17a) are solutions of the tachyonic Dirac equations [264, 266–268]

$$(\not{l} + i\mu\gamma^5 + m) u_{\lambda}(l) = 0, \quad (\not{l} + i\mu\gamma^5 - m) v_{\lambda}(l) = 0, \quad (5.18)$$

which leads to a Hermitian Hamiltonian. It is worth to notice that the spinors (5.17) fulfil the Gordon's identities

$$\frac{\bar{u}_{\lambda}(l) \gamma^{\nu} u_{\lambda}(l)}{2} = \frac{\bar{v}_{\lambda}(l) \gamma^{\nu} v_{\lambda}(l)}{2} = l^{\nu}. \quad (5.19)$$

Polarisation vectors – The d -dimensional polarisation vectors of a spin-1 particle fulfil the following relation

$$\sum_{i=1}^{d_s-2} \varepsilon_{i(d)}^{\mu}(\bar{l}, \bar{\eta}) \varepsilon_{i(d)}^{*\nu}(\bar{l}, \bar{\eta}) = -\bar{g}^{\mu\nu} + \frac{\bar{l}^{\mu} \bar{\eta}^{\nu} + \bar{l}^{\nu} \bar{\eta}^{\mu}}{\bar{l} \cdot \bar{\eta}}. \quad (5.20)$$

As saw in Sec. 4.1, a massless four-point one-loop amplitude can be decomposed in terms MIs, as follows

$$A_4 = \frac{1}{(4\pi)^{2-\epsilon}} \left[c_{1|2|3|4;0} I_{1|2|3|4} + (c_{12|3|4;0} I_{12|3|4} + c_{1|2|34;0} I_{1|2|34} + c_{1|23|4;0} I_{1|23|4} + c_{2|3|41;0} I_{2|3|41}) \right. \\ \left. + (c_{12|34;0} I_{12|34} + c_{23|41;0} I_{23|41}) \right] + \mathcal{R}, \quad (5.30a)$$

$$\mathcal{R} = \frac{1}{(4\pi)^{2-\epsilon}} \left[c_{1|2|3|4;4} I_{1|2|3|4} [\mu^4] + (c_{12|3|4;2} I_{12|3|4} [\mu^2] + c_{1|2|34;2} I_{1|2|34} [\mu^2] + c_{1|23|4;2} I_{1|23|4} [\mu^2] \right. \\ \left. + c_{2|3|41;2} I_{2|3|41} [\mu^2]) (c_{12|34;2} I_{12|34} [\mu^2] + c_{23|41;2} I_{23|41} [\mu^2]) \right]. \quad (5.30b)$$

Also, we consider the process involving three gluons, 1, 2, 3, and a Higgs boson, H ,

$$0 \rightarrow 1(p_1) 2(p_2) 3(p_3) H(p_H), \quad (5.31)$$

in the large top-mass limit [270, 271]. The one-loop amplitude for this process is decomposed as follows,

$$A_{4,H} = \frac{1}{(4\pi)^{2-\epsilon}} \left[(c_{1|2|3|H;0} I_{1|2|3|H} + c_{1|2|H|3;0} I_{1|2|H|3} + c_{1|H|2|3;0} I_{1|H|2|3}) + (c_{12|3|H;0} I_{12|3|H} \right. \\ \left. + c_{12|H|3;0} I_{12|H|3} + c_{1|23|H;0} I_{1|23|H} + c_{1|H|23;0} I_{1|H|23} + c_{2|H|31;0} I_{2|H|31} \right. \\ \left. + c_{H|2|31;0} I_{H|2|31} + c_{1|2|3H;0} I_{1|2|3H} + c_{1|2H|3;0} I_{1|2H|3} + c_{1H|2|3;0} I_{1H|2|3}) \right. \\ \left. + (c_{12|3H;0} I_{12|3H} + c_{23|H1;0} I_{23|H1} + c_{H2|31;0} I_{H2|31}) + c_{123|H;0} I_{123|H} \right] + \mathcal{R}_H, \quad (5.32a)$$

$$\mathcal{R}_H = \frac{1}{(4\pi)^{2-\epsilon}} \left[(c_{1|2|3|H;4} I_{1|2|3|H} [\mu^4] + c_{1|2|H|3;4} I_{1|2|H|3} [\mu^4] + c_{1|H|2|3;4} I_{1|H|2|3} [\mu^4]) \right. \\ \left. + (c_{12|3|H;2} I_{12|3|H} [\mu^2] + c_{12|H|3;2} I_{12|H|3} [\mu^2] + c_{1|23|H;2} I_{1|23|H} [\mu^2] + c_{1|H|23;2} I_{1|H|23} [\mu^2] \right. \\ \left. + c_{2|H|31;2} I_{2|H|31} [\mu^2] + c_{H|2|31;2} I_{H|2|31} [\mu^2] + c_{1|2|3H;2} I_{1|2|3H} [\mu^2] + c_{1|2H|3;2} I_{1|2H|3} [\mu^2] \right. \\ \left. + c_{1H|2|3;2} I_{1H|2|3} [\mu^2]) + (c_{12|3H;2} I_{12|3H} [\mu^2] + c_{23|H1;2} I_{23|H1} [\mu^2] \right. \\ \left. + c_{H2|31;2} I_{H2|31} [\mu^2] + c_{123|H;2} I_{123|H} [\mu^2]) \right], \quad (5.32b)$$

In Eq. (5.30) and (5.32), the contribution generating the rational terms have been collected in \mathcal{R} and \mathcal{R}_H , respectively, hence distinguished by the so-called cut-constructible terms. We remark that within the FDF this distinction is pointless and has been performed only to improve the readability of the formulas. Indeed, within the FDF the two contributions are computed simultaneously from the same cuts.

5.3.1 The $gggg$ amplitude

As a first example we consider the all plus four-gluon colour-ordered helicity amplitude $A_4(1_g^+, 2_g^+, 3_g^+, 4_g^+)$, which, at tree-level vanished, while at one-loop its contribution is finite, rational and can be obtained from the quadruple cut $C_{1|2|3|4}$ [32, 198, 272–274]. Therefore, the relevant tree-level three-point amplitudes are the ones involving either three gluons or two scalars and one gluon. The tree-level amplitudes with two gluons and one scalar should be included as well but they are not needed since their cut diagrams vanish because of the (-2ϵ) -SRs, see the discussion below. The tree-level are computed by using the colour-ordered Feynman rules collected in App. B.3.

The general expression of the three-point all-gluon amplitude is given by

$$\begin{array}{c} \mathbf{1}^{\lambda_1} \\ \text{-----} \\ 2^{\lambda_2} \\ \text{-----} \\ \mathbf{3}^{\lambda_3} \end{array} = \frac{ig}{\sqrt{2}} \left[g^{\mu\nu} (\mathbf{1}-2)^\sigma + g^{\nu\sigma} (2-\mathbf{3})^\mu + g^{\sigma\mu} (\mathbf{3}-\mathbf{1})^\nu \right] \varepsilon_\mu^{\lambda_1}(\mathbf{1}) \varepsilon_\nu^{\lambda_2}(2, r_2) \varepsilon_\sigma^{\lambda_3}(\mathbf{3}) .$$

(5.33)

Generalised massive momenta, carrying dependence on μ , are denoted by a bold font, and the polarisation of the particle will be the superscript of the corresponding momentum. The momenta are outgoing,

$$\mathbf{1} + 2 + \mathbf{3} = 0 , \quad (5.34)$$

and in general \hat{q}_1 and \hat{q}_3 can be chosen to be proportional,

$$\hat{q}_3 = \xi \hat{q}_1 . \quad (5.35)$$

Moreover, the spinors associated to the momenta \mathbf{j}^b and \hat{q}_j are such that

$$\langle \mathbf{j}^b | \hat{q}_j \rangle = [\hat{q}_j | \mathbf{j}^b] = \mu , \quad \mathbf{j} = \mathbf{1}, \mathbf{3} . \quad (5.36)$$

The explicit expressions of the polarised amplitudes in the FDF are:

$$\begin{array}{c} \mathbf{1}^+ \\ \text{-----} \\ 2^+ \\ \text{-----} \\ \mathbf{3}^+ \end{array} = 0 ,$$

$$\begin{array}{c} \mathbf{1}^+ \\ \text{-----} \\ 2^+ \\ \text{-----} \\ \mathbf{3}^- \end{array} = ig \left(\frac{[\mathbf{1}^b | 2][\hat{q}_1 | 2]}{\mu} + \frac{\langle r_2 | \mathbf{1} | 2 \rangle}{\langle r_2 | 2 \rangle} \right) ,$$

$$\begin{array}{c} \mathbf{1}^0 \\ \text{-----} \\ 2^+ \\ \text{-----} \\ \mathbf{3}^+ \end{array} = 0 ,$$

$$\begin{array}{c} \mathbf{1}^0 \\ \text{-----} \\ 2^+ \\ \text{-----} \\ \mathbf{3}^- \end{array} = \frac{\sqrt{2}ig [\hat{q}_1 | 2]^2}{\mu} ,$$

$$\begin{array}{c} \mathbf{1}^- \\ \text{-----} \\ 2^+ \\ \text{-----} \\ \mathbf{3}^- \end{array} = ig \frac{[\hat{q}_1 | 2][\hat{q}_3 | 2] \langle \mathbf{1}^b | \mathbf{3}^b \rangle}{\mu^2} ,$$

$$\begin{array}{c} \mathbf{1}^0 \\ \text{-----} \\ 2^+ \\ \text{-----} \\ \mathbf{3}^0 \end{array} = -ig \frac{\langle r_2 | \mathbf{1} | 2 \rangle}{\langle r_2 | 2 \rangle} \left[1 - \frac{(1+\xi)}{\xi \mu^2} ((1+\xi)\mu^2 + \xi \langle \hat{q}_1 | 2 | \hat{q}_1 \rangle) \right] . \quad (5.37)$$

The three-point amplitude involving a gluon and two scalars is

$$\begin{array}{c} \mathbf{1} \\ \text{-----} \\ 2^+ \\ \text{-----} \\ \mathbf{3} \end{array} = \frac{ig}{\sqrt{2}} (\mathbf{3}-\mathbf{1})^\mu \varepsilon_\mu^+(2, r_2) G^{AB} = -ig \frac{\langle r_2 | \mathbf{1} | 2 \rangle}{\langle r_2 | 2 \rangle} G^{AB} . \quad (5.38)$$

The tree-level amplitudes computed above can be used in the cut construction of the one-loop amplitude.

In the FDF, the quadruple-cut $C_{1|2|3|4}$ and the coefficients $c_{1|2|3|4; n}$ can be decomposed into a sum of five contributions,

$$C_{1|2|3|4} = \sum_{i=0}^4 C_{1|2|3|4}^{[i]}, \quad c_{1|2|3|4; n} = \sum_{i=0}^4 c_{1|2|3|4; n}^{[i]}, \quad (5.39)$$

where $C^{[i]}$ ($c^{[i]}$) is the contribution to the cut (coefficient) involving i internal scalars. In the picture below, internal lines are understood to be on-shell. The quadruple cuts read as follows

$$C_{1|2|3|4}^{[0]} = \begin{array}{c} 2^+ \quad + - \quad 3^+ \\ \diagdown \quad \diagup \\ 1^+ \quad - + \quad 4^+ \end{array} + \begin{array}{c} 2^+ \quad - + \quad 3^+ \\ \diagdown \quad \diagup \\ 1^+ \quad + - \quad 4^+ \end{array} + \begin{array}{c} 2^+ \quad 0 \ 0 \quad 3^+ \\ \diagdown \quad \diagup \\ 1^+ \quad 0 \ 0 \quad 4^+ \end{array}, \quad (5.40a)$$

$$C_{1|2|3|4}^{[1]} = \sum_{h_i = \pm, 0} \mathcal{T}_1 \begin{array}{c} 2^+ \quad -h_3 h_3 \quad 3^+ \\ \diagdown \quad \diagup \\ 1^+ \quad -h_2 \quad -h_1 h_1 \quad 4^+ \end{array} + \text{c.p.}, \quad (5.40b)$$

$$C_{1|2|3|4}^{[2]} = \sum_{h_i = \pm, 0} \mathcal{T}_1^2 \begin{array}{c} 2^+ \quad -h_2 h_2 \quad 3^+ \\ \diagdown \quad \diagup \\ 1^+ \quad -h_1 h_1 \quad 4^+ \end{array} + \mathcal{T}_2 \begin{array}{c} 2^+ \quad \quad \quad 3^+ \\ \diagdown \quad \diagup \\ 1^+ \quad -h_2 \quad -h_1 h_1 \quad 4^+ \end{array} + \text{c.p.}, \quad (5.40c)$$

$$C_{1|2|3|4}^{[3]} = \sum_{h_1 = \pm, 0} \mathcal{T}_3 \begin{array}{c} 2^+ \quad \quad \quad 3^+ \\ \diagdown \quad \diagup \\ 1^+ \quad \quad \quad -h_1 h_1 \quad 4^+ \end{array} + \text{c.p.}, \quad (5.40d)$$

$$C_{1|2|3|4}^{[4]} = \mathcal{T}_4 \begin{array}{c} 2^+ \quad \quad \quad 3^+ \\ \diagdown \quad \diagup \\ 1^+ \quad \quad \quad \quad \quad 4^+ \end{array}, \quad (5.40e)$$

where the abbreviation ‘‘c.p.‘‘ means ‘‘cyclic permutations of the external particles’’. In Eqs. (5.40), the (-2ϵ) -SR have been stripped off and collected in the prefactors \mathcal{T}_i ,

$$\begin{aligned} \mathcal{T}_1 &= Q^A \hat{G}^{AB} Q^B = 0, \\ \mathcal{T}_2 &= Q^A \hat{G}^{AB} G^{BC} \hat{G}^{CD} Q^D = 0, \\ \mathcal{T}_3 &= Q^A \hat{G}^{AB} G^{BC} \hat{G}^{CD} G^{DE} \hat{G}^{EF} Q^F = 0, \\ \mathcal{T}_4 &= \text{tr} \left(G \hat{G} G \hat{G} G \hat{G} G \hat{G} \right) = -1. \end{aligned} \quad (5.41)$$

The prefactors $\mathcal{T}_1, \dots, \mathcal{T}_3$ force the cuts (5.40b) - (5.40d) to vanish identically. The only cuts contributing, Eqs. (5.40a) and (5.40e), lead to the following coefficients

$$\begin{aligned} c_{1|2|3|4; 0}^{[0]} &= 0, & c_{1|2|3|4; 4}^{[0]} &= 3i \frac{[12] [34]}{\langle 12 \rangle \langle 34 \rangle}, \\ c_{1|2|3|4; 0}^{[4]} &= 0, & c_{1|2|3|4; 4}^{[4]} &= -i \frac{[12] [34]}{\langle 12 \rangle \langle 34 \rangle}. \end{aligned} \quad (5.42)$$

Therefore, the only non-vanishing coefficient, $c_{1|2|3|4; 4}$, is

$$c_{1|2|3|4; 4} = c_{1|2|3|4; 4}^{[0]} + c_{1|2|3|4; 4}^{[4]} = 2i \frac{[12] [34]}{\langle 12 \rangle \langle 34 \rangle}. \quad (5.43)$$

The colour-ordered one-loop amplitude can be obtained from Eq. (5.30), which in this simple case reduces to

$$A_4(1_g^+, 2_g^+, 3_g^+, 4_g^+) = c_{1|2|3|4; 4} I_{1|2|3|4}[\mu^4] = -\frac{i}{48\pi^2} \frac{[12][34]}{\langle 12 \rangle \langle 34 \rangle}, \quad (5.44)$$

and is in agreement with the literature [272]. This example clearly shows the difference between our computation and the one based on the supersymmetric decomposition [274]. In the latter one, the result is uniquely originated by the complex scalar contribution. Instead, in this procedure the result arises from both the massive gluons and the massive scalars s_g .

For clarity reasons, in this example we have computed the (-2ϵ) -SRs factors, \mathcal{T}_i , explicitly. It is worth to notice that in practice the (-2ϵ) -SRs can be easily automated and can be performed cut-by-cut once and for all, even before the tree-level amplitudes are computed. Therefore the cut topologies which vanish because of the (-2ϵ) -SRs can be discarded at the beginning of the computation without affecting its complexity.

5.3.2 The $ggq\bar{q}$ amplitude

In this section we apply generalised-unity methods within the FDF scheme to a more involved $2 \rightarrow 2$ process. In particular we show the calculation of the leading colour one-loop contribution to the helicity amplitude $A_4(1_g^-, 2_g^+, 3_{\bar{q}}^-, 4_q^+)$, which at tree-level reads,

$$A_4^{\text{tree}} = -i \frac{\langle 13 \rangle^3 \langle 14 \rangle}{\langle 12 \rangle \langle 23 \rangle \langle 34 \rangle \langle 41 \rangle}. \quad (5.45)$$

The leading-colour contribution to a one-loop amplitude with n particles and two external fermions can be decomposed in terms of primitive amplitudes [275]. Following the notation of Ref. [69], we have

$$A_4^{\text{1 loop}} = A_4^{\text{L}} - \frac{1}{N_c^2} A_4^{\text{R}} + \frac{N_f}{N_c} A_4^{\text{L},[1/2]} + \frac{N_s}{N_c} A_4^{\text{L},[0]}, \quad (5.46)$$

where N_c is the number of colours while N_f (N_s) the number of fermions (scalars). For the helicity configuration we consider both $A_4^{\text{L},[1/2]}$ and $A_4^{\text{L},[0]}$ vanish, thus we will only focus on the contributions of the left-turning amplitude A_4^{L} and on the right-turning one, A_4^{R} . The Feynman diagrams leading to the relevant tree-level amplitudes are computed by using the colour-ordered Feynman rules collected in App. B.3.

Left-turning amplitude – The quadruple cut is given by

$$C_{1|2|3|4}^{[\text{L}]} = \begin{array}{c} \begin{array}{c} \text{Diagram 1: } \text{Cut on } (1,2) \text{ and } (3,4) \text{ with } \pm \text{ signs} \\ \text{Diagram 2: } \text{Cut on } (1,2) \text{ and } (3,4) \text{ with } \pm \text{ signs} \\ \text{Diagram 3: } \text{Cut on } (1,2) \text{ and } (3,4) \text{ with } 00 \text{ signs} \\ \text{Diagram 4: } \text{Cut on } (1,2) \text{ and } (3,4) \text{ with } 00 \text{ signs} \end{array} \end{array},$$

$$c_{1|2|3|4; 0}^{[\text{L}]} = \frac{1}{2} A_4^{\text{tree}} \left(1 - \frac{s_{14}^3}{s_{13}^3} \right) s_{12} s_{14},$$

$$c_{1|2|3|4; 4}^{[\text{L}]} = 0. \quad (5.47)$$

The first two cut diagrams contribute to both the cut-constructible and to the rational part, while the last two cut diagrams cancel against each other.

The triple cuts are given by

$$\begin{aligned}
C_{12|3|4}^{[L]} &= \text{diagram 1} + \text{diagram 2} + \text{diagram 3} + \text{diagram 4} + \text{diagram 5} + \text{diagram 6}, \\
c_{12|3|4; 0}^{[L]} &= \frac{1}{2} A_4^{\text{tree}} \left(1 - \frac{s_{14}^3}{s_{13}^3} \right) s_{12}, \\
c_{12|3|4; 2}^{[L]} &= \frac{1}{2} A_4^{\text{tree}} \left(2 - \frac{s_{12}^2}{s_{13}^2} \right); \tag{5.48a}
\end{aligned}$$

$$\begin{aligned}
C_{1|2|3|4}^{[L]} &= \text{diagram 1} + \text{diagram 2} + \text{diagram 3} + \text{diagram 4}, \\
c_{1|2|3|4; 0}^{[L]} &= -\frac{1}{2} A_4^{\text{tree}} \left(1 + \frac{s_{14}^3}{s_{13}^3} \right) s_{12}, \\
c_{1|2|3|4; 2}^{[L]} &= -\frac{1}{2} A_4^{\text{tree}} \frac{s_{12}^2}{s_{13}^2}; \tag{5.48b}
\end{aligned}$$

$$\begin{aligned}
C_{1|2|3|4}^{[L]} &= \text{diagram 1} + \text{diagram 2} + \text{diagram 3}, \\
c_{1|2|3|4; 0}^{[L]} &= -\frac{1}{2} A_4^{\text{tree}} \left(1 + \frac{s_{14}^3}{s_{13}^3} \right) s_{14}, \\
c_{1|2|3|4; 2}^{[L]} &= -\frac{1}{2} A_4^{\text{tree}} \frac{s_{14} s_{12}}{s_{13}^2}; \tag{5.48c}
\end{aligned}$$

$$\begin{aligned}
C_{2|3|4|1}^{[L]} &= \text{diagram 1} + \text{diagram 2} + \text{diagram 3}, \\
c_{2|3|4|1; 0}^{[L]} &= -\frac{1}{2} A_4^{\text{tree}} \left(1 + \frac{s_{14}^3}{s_{13}^3} \right) s_{14}, \\
c_{2|3|4|1; 2}^{[L]} &= -\frac{1}{2} A_4^{\text{tree}} \frac{s_{14} s_{12}}{s_{13}^2}. \tag{5.48d}
\end{aligned}$$

In all the triple cuts the last two cut diagrams cancel against each other. In the cut $C_{12|3|4}^{[L]}$. The double cuts read as follows

$$\begin{aligned}
C_{12|3|4}^{[L]} &= \text{diagram 1} + \text{diagram 2} + \text{diagram 3} + \text{diagram 4} + \text{diagram 5}, \\
c_{12|3|4; 0}^{[L]} &= A_4^{\text{tree}} \frac{s_{14}}{s_{13}} \left(\frac{s_{14}}{s_{13}} - \frac{1}{2} \right), \\
c_{12|3|4; 2}^{[L]} &= 0; \tag{5.49a}
\end{aligned}$$

$$\begin{aligned}
C_{23|4|1}^{[L]} &= \text{diagram 1} + \text{diagram 2} + \text{diagram 3} + \text{diagram 4}, \\
c_{23|4|1; 0}^{[L]} &= A_4^{\text{tree}} \left(\frac{3}{2} - \frac{s_{14}^2}{s_{13}^2} + \frac{1}{2} \frac{s_{14}}{s_{13}} \right),
\end{aligned}$$

$$c_{23|41; 2}^{[L]} = 0. \quad (5.49b)$$

In both cases the last two diagrams cancel against each other.

Right-turning amplitude – The quadruple cut is given by

$$\begin{aligned}
C_{1|2|3|4}^{[R]} &= \text{diagram 1} + \text{diagram 2} + \text{diagram 3}, \\
c_{1|2|3|4; 0}^{[R]} &= -\frac{1}{2} A_4^{\text{tree}} \frac{s_{12}^3}{s_{13}^3} s_{12} s_{14}, \\
c_{1|2|3|4; 4}^{[R]} &= 0.
\end{aligned} \quad (5.50)$$

The first helicity configuration contributes only to the cut-constructible part while the second one cancels against the box with internal scalars.

The triple cuts are given by

$$\begin{aligned}
C_{12|3|4}^{[R]} &= \text{diagram 1} + \text{diagram 2} + \text{diagram 3} + \text{diagram 4}, \\
c_{12|3|4; 0}^{[R]} &= -\frac{1}{2} A_4^{\text{tree}} \left(2 + \frac{s_{12}^3}{s_{13}^3} \right) s_{12}, \\
c_{12|3|4; 2}^{[R]} &= -\frac{1}{2} A_4^{\text{tree}} \left(1 + \frac{s_{14}^2}{s_{13}^2} \right);
\end{aligned} \quad (5.51a)$$

$$\begin{aligned}
C_{1|2|34}^{[R]} &= \text{diagram 1} + \text{diagram 2}, \\
c_{1|2|34; 0}^{[R]} &= -\frac{1}{2} A_4^{\text{tree}} \frac{s_{12}^3}{s_{13}^3} s_{12}, \\
c_{1|2|34; 2}^{[R]} &= -\frac{1}{2} A_4^{\text{tree}} \frac{s_{12}}{s_{13}} \left(1 - \frac{s_{14}}{s_{13}} \right);
\end{aligned} \quad (5.51b)$$

$$\begin{aligned}
C_{1|23|4}^{[R]} &= \text{diagram 1} + \text{diagram 2} + \text{diagram 3}, \\
c_{1|23|4; 0}^{[R]} &= -\frac{1}{2} A_4^{\text{tree}} \frac{s_{12}^3}{s_{13}^3} s_{14}, \\
c_{1|23|4; 2}^{[R]} &= -\frac{1}{2} A_4^{\text{tree}} \frac{s_{12} s_{14}}{s_{13}^2};
\end{aligned} \quad (5.51c)$$

$$\begin{aligned}
C_{2|3|41}^{[R]} &= \text{diagram 1} + \text{diagram 2} + \text{diagram 3}, \\
c_{2|3|41; 0}^{[R]} &= -\frac{1}{2} A_4^{\text{tree}} \frac{s_{12}^3}{s_{13}^3} s_{14}, \\
c_{2|3|41; 2}^{[R]} &= -\frac{1}{2} A_4^{\text{tree}} \frac{s_{12} s_{14}}{s_{13}^2}.
\end{aligned} \quad (5.51d)$$

In the case of the cuts $C_{12|3|4}^{[R]}$ and $C_{1|2|34}^{[R]}$ the first diagram gives contributions to the both cut-constructible and the rational part, while the second one contributes to the rational part only. In the cuts $C_{12|3|4}^{[R]}$, $C_{1|23|4}^{[R]}$ and $C_{2|3|41}^{[R]}$ the last two diagrams cancel against each other, i.e. the scalar contribution exactly compensates the contribution of the longitudinal polarisation of the gluon. The double cuts are

$$\begin{aligned}
C_{12|3|4}^{[R]} &= \text{Diagram 1} , \\
c_{12|3|4; 0}^{[R]} &= A_4^{\text{tree}} \left[\frac{s_{12}}{s_{13}} \left(\frac{s_{14}}{s_{13}} + \frac{3}{2} \right) + \frac{3}{2} \right] , \\
c_{12|3|4; 2}^{[R]} &= 0 ;
\end{aligned} \tag{5.52a}$$

$$\begin{aligned}
C_{23|4|1}^{[R]} &= \text{Diagram 2} + \text{Diagram 3} + \text{Diagram 4} , \\
c_{23|4|1; 0}^{[R]} &= -A_4^{\text{tree}} \frac{s_{12}}{s_{13}} \left(\frac{s_{14}}{s_{13}} + \frac{3}{2} \right) , \\
c_{23|4|1; 2}^{[R]} &= 0 .
\end{aligned} \tag{5.52b}$$

Leading-colour amplitude – The leading colour amplitude can be obtained from the decomposition (5.30) by using the coefficients

$$c_{i_1 \dots i_k; n} = c_{i_1 \dots i_k; n}^{[L]} - \frac{1}{N_c^2} c_{i_1 \dots i_k; n}^{[R]} , \tag{5.53}$$

The result agrees with the one presented in Ref. [272].

5.3.3 The $gggH$ amplitude

In this section, we show the calculation of the leading colour one-loop contribution to the helicity amplitude $A_4(1_g^-, 2_g^+, 3_g^+, H)$ in the heavy top-mass limit. This example allows us to show how the FDF scheme can be applied in the context of an effective theory, where the Higgs boson couples directly to the gluon. The Feynman rules for the Higgs-gluon and Higgs-scalar couplings in the FDF are given in App. B.3. They are used to compute the tree-level amplitudes sewn along the cuts. In the following, we present directly the determination of the coefficients by means of generalised unitarity methods.

The leading-order contribution reads as follows

$$A_{4,H}^{\text{tree}} = i \frac{[23]^4}{[12][23][31]} . \tag{5.54}$$

The quadruple cuts are given by:

$$\begin{aligned}
C_{1|2|3|H} &= \text{Diagram 5} + \text{Diagram 6} , \\
c_{1|2|3|H; 0} &= -\frac{1}{2} A_{4,H}^{\text{tree}} s_{12} s_{23} ,
\end{aligned}$$

The cut $C_{123|H}$ does not give any contribution.

Finally, the one-loop amplitude can be obtained by using the coefficients collected in Eqs. (5.55-5.58) and the decomposition (5.32). The result agrees with the literature [276].

5.4 UV renormalisation at one-loop

In this section we study the renormalisation at one-loop. In order to do so, we firstly study the known results that the conventional dimensional reduction (CDR) deliver. For this regularisation scheme we set $d_s = d$ since the very begin of the calculation. The second one is FDF, we see how the renormalisation at one-loop turns to be equivalent to what is expected from FDH. We work out QED and QCD theories.

5.4.1 Renormalised QED Lagrangian

We start considering the renormalised QED Lagrangian

$$\mathcal{L}_{\text{QED}} = \mathcal{L}_r + \mathcal{L}_{CT}, \quad (5.59)$$

where

$$\mathcal{L}_r = -\frac{1}{4}F^{\mu\nu}F_{\mu\nu} + \bar{\psi}(i\cancel{\partial} - e\cancel{A} - m)\psi, \quad (5.60)$$

$$\begin{aligned} \mathcal{L}_{CT} = & -(Z_3 - 1)\frac{1}{4}F^{\mu\nu}F_{\mu\nu} + (Z_2 - 1)\bar{\psi}i\cancel{\partial}\psi - (Z_2Z_m - 1)m\bar{\psi}\psi \\ & + (Z_2Z_e\sqrt{Z_3} - 1)e\bar{\psi}\cancel{A}\psi. \end{aligned} \quad (5.61)$$

The bare fields ψ^i, A_μ^a and bare parameters e, m have been redefined in terms of renormalised quantities,

$$\begin{aligned} \psi_0^i &= \sqrt{Z_2}\psi^i, & A_\mu^{0a} &= \sqrt{Z_3}A_\mu^a, \\ e_0 &= Z_e e, & m_0 &= Z_m m, \end{aligned} \quad (5.62)$$

The counter-terms (CT), δ 's, are obtained by expanding the field strengths around 1,

$$Z_x = 1 + \delta_x, \quad x = 2, 3, e, m. \quad (5.63)$$

Counter-terms

The set of CTs is, in principle, obtained in the on-shell scheme. Moreover, the minimal subtraction (MS) or modified minimal subtraction ($\overline{\text{MS}}$) schemes are easily recovered by taking the divergent part plus an universal constant that arises along with the divergencies in Feynman diagram calculations.

For the listed results, we write, with the help of integration by parts identities [70, 71], the CTs in terms of one-point scalar integrals $A_0(m_e^2)$. This MI is chosen to be normalised as follows

$$A_0(m_e^2) = \frac{m_e^2}{16\pi^4} \left(\Delta + \log\left(\frac{\mu^2}{m_e^2}\right) + 1 \right), \quad \Delta = \frac{1}{\epsilon} - \gamma + \log 4\pi. \quad (5.64)$$

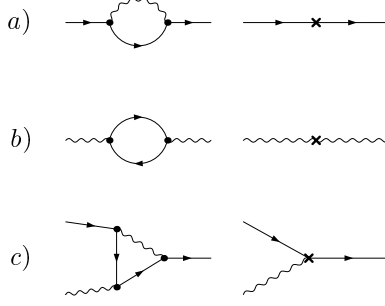


Figure 5.1: Diagrams contributing to a) electron self energy, b) photon self energy, and c) vertex correction at one-loop in CDR. The cross denotes the insertion of a coupling counter-term.

CDR – In CDR, the needed diagrams to compute the counter-terms are depicted in Fig. 5.1.

By setting $d_s = d$, the counter-terms of (5.63), in the on-shell scheme, take the form

$$\begin{aligned}
\delta_2 &= -\frac{2\pi^3\alpha(d-2)(d-1)}{(d-3)m_e^2}A_0(m_e^2) \stackrel{d \rightarrow 4}{=} -\frac{\alpha}{4\pi} \left(3\Delta + 3 \log \left(\frac{\mu^2}{m_e^2} \right) + 4 \right) \\
\delta_3 &= -\frac{8\pi^3\alpha(d-2)}{3m_e^2}A_0(m_e^2) \stackrel{d \rightarrow 4}{=} -\frac{\alpha}{3\pi} \left(\Delta + \log \left(\frac{\mu^2}{m_e^2} \right) \right) \\
\delta_e &= \frac{4\pi^3\alpha(d-2)}{3m_e^2}A_0(m_e^2) \stackrel{d \rightarrow 4}{=} \frac{\alpha}{6\pi} \left(\Delta + \log \left(\frac{\mu^2}{m_e^2} \right) \right) \\
\delta_m &= -\frac{2\pi^3\alpha(d-2)(d-1)}{(d-3)m_e^2}A_0(m_e^2) \stackrel{d \rightarrow 4}{=} -\frac{\alpha}{4\pi} \left(3\Delta + 3 \log \left(\frac{\mu^2}{m_e^2} \right) + 4 \right) \quad (5.65)
\end{aligned}$$

FDF – The needed diagrams to compute the counter-terms, within FDF, are collected in Fig. 5.2.

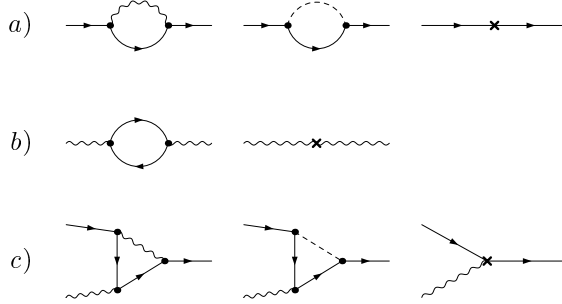


Figure 5.2: Diagrams contributing to a) electron self energy, b) photon self energy, and c) vertex correction at one-loop in FDF. The cross denotes the insertion of a coupling counter-term. Dash lines represents -2ϵ -scalars.

The diagrams with an internal -2ϵ -scalar vanish because of the (-2ϵ) -SRs.

In the on-shell scheme, the counter-terms of (5.63) take the form

$$\begin{aligned}
\delta_2 &= -\frac{4\pi^3\alpha(2d-5)}{(d-3)m_e^2}A_0(m_e^2) \stackrel{d \rightarrow 4}{=} -\frac{\alpha}{4\pi} \left(3\Delta + 3 \log \left(\frac{\mu^2}{m_e^2} \right) + 5 \right), \\
\delta_3 &= -\frac{4\pi^3\alpha(d-2)((d-2)d+10)}{9(d-1)m_e^2}A_0(m_e^2) \stackrel{d \rightarrow 4}{=} -\frac{\alpha}{3\pi} \left(\Delta + \log \left(\frac{\mu^2}{m_e^2} \right) \right), \\
\delta_e &= \frac{2\pi^3\alpha(d-2)((d-2)d+10)}{9(d-1)m_e^2}A_0(m_e^2) \stackrel{d \rightarrow 4}{=} \frac{\alpha}{6\pi} \left(\Delta + \log \left(\frac{\mu^2}{m_e^2} \right) \right),
\end{aligned}$$

$$\delta_m = -\frac{4\pi^3\alpha(2d-5)}{(d-3)m_e^2}A_0(m_e^2) \stackrel{d \rightarrow 4}{=} -\frac{\alpha}{4\pi} \left(3\Delta + 3 \log \left(\frac{\mu^2}{m_e^2} \right) + 5 \right). \quad (5.66)$$

5.4.2 Renormalised QCD Lagrangian

Consider the QCD Lagrangian

$$\mathcal{L}_{\text{QCD}} = \mathcal{L}_r + \mathcal{L}_{CT}, \quad (5.67)$$

with

$$\begin{aligned} \mathcal{L}_r &= \bar{\psi}^i (i\gamma^\mu D_\mu^{ij} - m\delta^{ij})\psi^j - \frac{1}{4}F_{\mu\nu}^a F^{a\mu\nu} + (\partial^\mu \chi^{a*}) \mathcal{D}_\mu^{ab} \chi^b \\ \mathcal{L}_{CT} &= (Z_2 - 1)\bar{\psi}^i i\gamma^\mu \partial_\mu \psi^i - (Z_2 Z_m - 1)m\bar{\psi}^i \psi^i \\ &\quad + (Z_3 - 1)\frac{1}{2}A^{a\mu} \delta_{ab} (g_{\mu\nu} \square - \partial_\mu \partial_\nu) A^{b\nu} + (\tilde{Z}_3 - 1)\chi^a \delta_{ab} (-\square)\chi^b \\ &\quad + (Z_{1F} - 1)g_s \bar{\psi}^i T_{ij}^a \gamma^\mu \psi^j A^{a\mu} - (Z_1 - 1)\frac{g_s}{2}f^{abc}(\partial_\mu A_\nu^a - \partial_\nu A_\mu^a)A^{b\mu}A^{c\nu} \\ &\quad - (Z_4 - 1)\frac{g_s^2}{4}f^{abe}f^{cde}A_\mu^a A_\nu^b A^{c\mu} A^{d\nu} - (\tilde{Z}_1 - 1)g_s f^{abc}(\partial^\mu \chi^a)^* \chi^b A_\mu^c \end{aligned} \quad (5.68)$$

where

$$\begin{aligned} D_\mu^{ij} &= \delta^{ij} \partial_\mu - ig_s (T^c)^{ij} A_\mu^c, & \mathcal{D}_\mu^{ab} &= \delta^{ab} \partial_\mu - g_s f^{abc} A_\mu^c, \\ Z_{1F} &= Z_g Z_2 \sqrt{Z_3}, & Z_1 &= Z_g \sqrt{Z_3^3}, \\ Z_4 &= Z_g^2 Z_3^2, & \tilde{Z}_1 &= Z_g \tilde{Z}_3 \sqrt{Z_3}. \end{aligned} \quad (5.70)$$

We redefine bare fields ψ^i, A_μ^a, χ^a and bare parameters g_s, m in terms of renormalised quantities as follows

$$\begin{aligned} \psi_0^i &= \sqrt{Z_2} \psi^i, & A_\mu^{0a} &= \sqrt{Z_3} A_\mu^a, & \chi^{0a} &= \sqrt{\tilde{Z}_3} \chi^a, \\ g_{s,0} &= Z_g g_s, & m_0 &= Z_m m, \end{aligned} \quad (5.71)$$

Counter-terms

For the QCD renormalisation we compute the counter-terms in the $\overline{\text{MS}}$ scheme. We find agreement between the CDR (Fig. 5.3) and FDF (Fig. 5.4) schemes.

We summarise the results for all the counter-terms in QCD at 1-loop in Feynman gauge:

$$\begin{aligned} \delta_1 &= \frac{\alpha_s(C_A - 2N_f)}{6\pi\epsilon_{\text{UV}}}, \\ \delta_{1F} &= -\frac{\alpha_s(C_A + C_F)}{4\pi\epsilon_{\text{UV}}}, \\ \tilde{\delta}_1 &= -\frac{\alpha_s C_A}{8\pi\epsilon_{\text{UV}}}, \\ \delta_2 &= -\frac{\alpha_s C_F}{4\pi\epsilon_{\text{UV}}}, \\ \delta_3 &= \frac{\alpha_s(5C_A - 4N_f)}{12\pi\epsilon_{\text{UV}}}, \\ \tilde{\delta}_3 &= \frac{\alpha_s C_A}{8\pi\epsilon_{\text{UV}}}, \end{aligned}$$

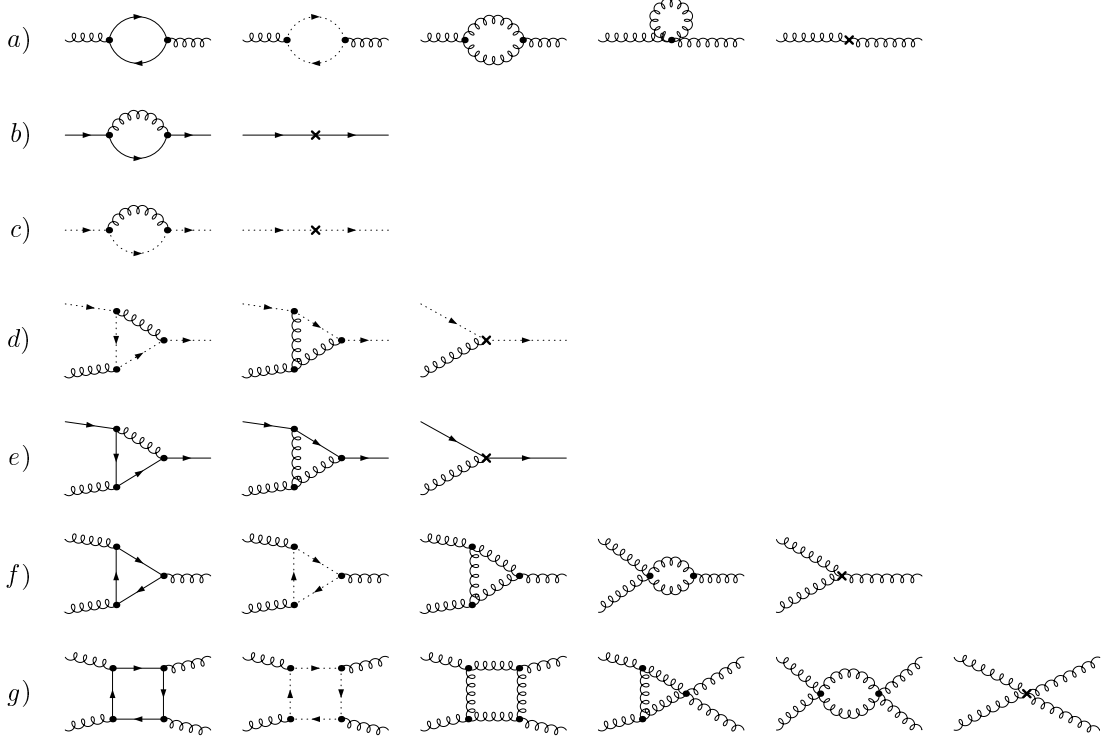


Figure 5.3: Diagrams contributing to a) gluon self energy, b) quark self energy, c) ghost self energy, d) ghost-gluon vertex, e) quark-gluon vertex, f) three-gluon vertex and g) four-gluon vertex at one-loop in CDR. The cross denotes the insertion of a coupling counter-term.

$$\delta_4 = -\frac{\alpha_s(C_A + 4N_f)}{12\pi\varepsilon_{UV}},$$

$$\delta_m = -\frac{3\alpha_s C_F}{4\pi\varepsilon_{UV}}. \quad (5.72)$$

We remark that our results are normalised according to Eq. (1.7). Moreover, a general result is easily recovered by shifting $N_f \rightarrow T_R N_f$, being $\text{Tr}(t^a t^b) = T_R \delta^{ab}$.

It is clear that the amount of terms to be computed within FDF increases with respect to traditional computations, e.g. CDR. Nevertheless, the fact of using four-dimensional ingredients allows to use existing codes. In particular, we use FEYNARTS together with FEYNCALC.

Additionally, according to the gauge we use, further simplifications can arise. In Feynman gauge, used in these calculations, there are no contributions coming from scalar loops. This is due to the (-2ϵ) -SRs,

$$G^{A_1 A_2} G^{A_2 A_3} \dots G^{A_k A_1} = G^{A_1 A_1} = 0. \quad (5.73)$$

Similarly, for diagrams with internal scalars and fermions we get the same cancellation,

$$\Gamma^{A_1} G^{A_1 A_2} \dots G^{A_{k-1} A_k} \Gamma^{A_k} = \Gamma^{A_1} \Gamma^{A_1} = 0. \quad (5.74)$$

With the use of axial gauge, we obtain the opposite behaviour. The contributions from internal scalars have to be taken in account and the diagrams that contain interactions between generalised gluons and scalars are dropped because of the (-2ϵ) -SRs. This subtlety was discussed in Sec. 5.3.1 for the non-vanishing contribution of the four-gluon amplitudes (5.40e).

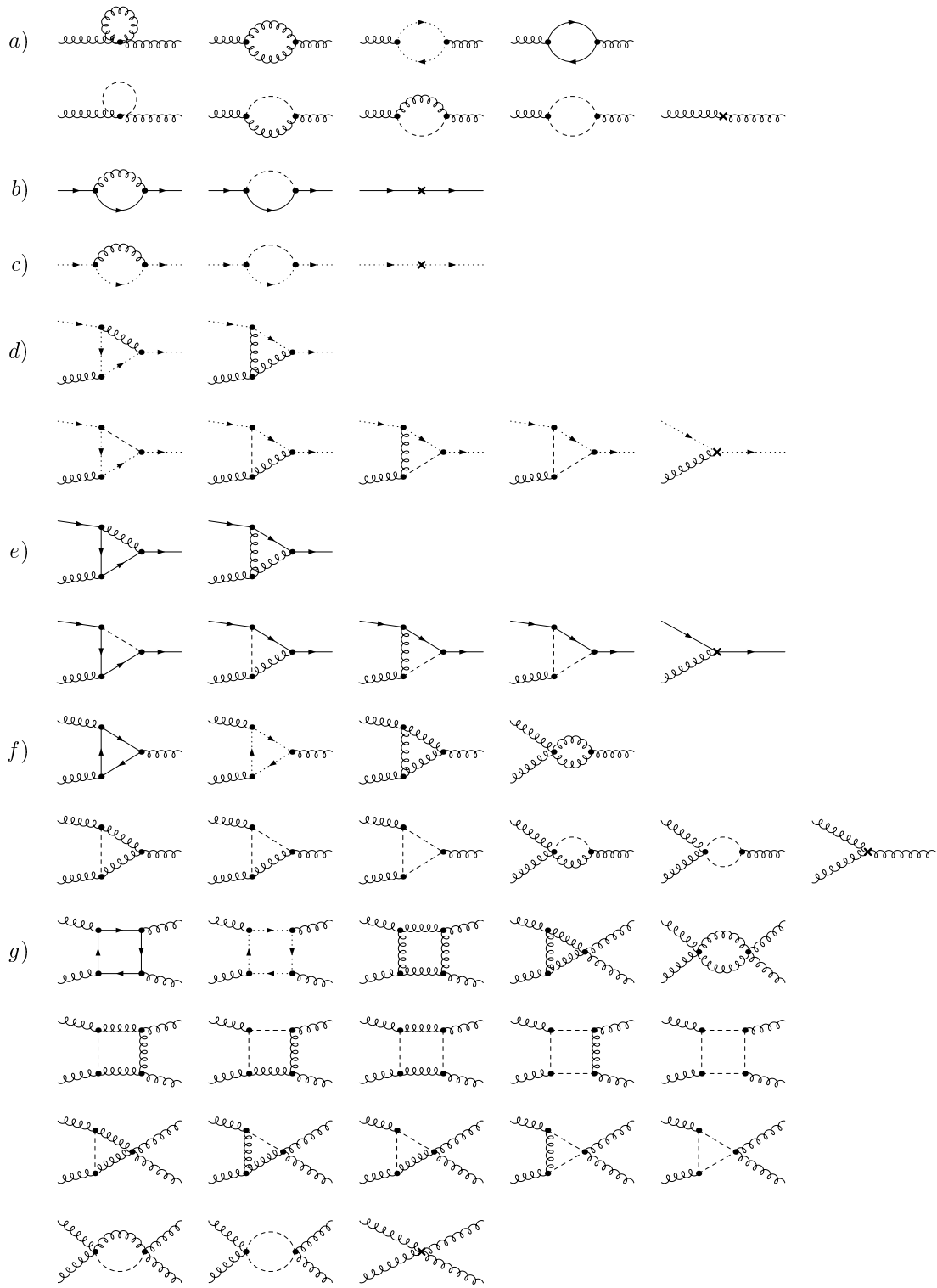


Figure 5.4: Diagrams contributing to a) gluon self energy, b) quark self energy, c) ghost self energy, d) ghost-gluon vertex, e) quark-gluon vertex, f) three-gluon vertex and g) four-gluon vertex at one-loop in CDR. The cross denotes the insertion of a coupling counter-term.

5.5 Discussion

Within the Four dimensional formulation (FDF), particles that propagate inside the loop are represented by massive particles regularising the divergences. Their interactions are described by generalised four-dimensional Feynman rules. They include selection rules accounting for the regularisation of the amplitudes. In particular, massless spin-1 particles in d -dimensions were represented in four-dimensions by a combination of massive spin-one particle and a scalar particle. Fermions in d -dimensions were represented by four-dimensional fermions obeying the Dirac equation for tachyonic particles. The integrands of one-loop amplitudes in the FDF and in the FDH scheme differ by spurious terms which vanish upon integration over the loop momentum. Therefore, the two schemes are equivalent.

FDF, in the context of generalised unitarity, may be seen as a massive implementation of d -dimensional regularisation. However, FDF is different from the most commonly used massive regularisation prescriptions, i.e. the one introducing a massive scalar particle [274] and the six-dimensional helicity method [69]. The original amplitude is computed in two steps. The cut constructible part is obtained by using four-dimensional unitarity while the rational one by using the amplitude involving a d -dimensional scalar, which is traded with a massive four-dimensional one. FDF does not rely on the existence of the supersymmetric decomposition and computes the full amplitude without splitting it. The six-dimensional helicity method casts d -dimensional on-shell momenta into a six-dimensional massless spinor and, on the cuts, uses six-dimensional helicity spinors to compute efficiently the relevant tree-level amplitudes. However, since dimensional regularisation cannot be achieved in finite dimensions, the six-dimensional helicity method delivers a result that has to be corrected by hand with the help of topologies involving six-dimensional scalars along the lines of Ref. [65]. FDF, instead, splits the d -dimensional objects into their four-dimensional and $(d - 4)$ -dimensional parts and finds a four-dimensional representation for both of them. Moreover, it introduces the (-2ϵ) -SRs to account for the orthogonality of the subspaces and for the effects of the $(d_s - 4) \rightarrow 0$ limit. No further corrections are needed since FDF properly takes care of the peculiar features of d -dimensional regularisation. Therefore, in the context of on-shell and unitarity-based methods, they are a simple alternative to approaches introducing explicit higher-dimensional extension of either the Dirac [65, 66] or the spinor [68, 69] algebra.

Within FDF, we have also seen how renormalisation can be done. At the beginning of the chapter, we saw that the difference between FDH and FDF lies at integrand level, since spurious terms vanish after integration. Nevertheless, the computation of the counter-terms within FDF produces the very same results as the ones from the FDH.

The approach of FDF is suitable for analytic as well as numerical implementation. Its main asset is the use of purely four-dimensional ingredients for the complete reconstruction of dimensionally-regulated one-loop amplitudes.

Chapter 6

Multi-gluon and Higgs scattering amplitudes

The calculation of multi-gluon scattering amplitudes at one-loop has been a very important test to develop analytic techniques in perturbative gauge theories. The complete calculation of gluon amplitudes took about 25 years, which started in the early 90's with the computation of four-gluon amplitudes [198, 277], whose methods were based on a string theory approach and, on the standard unitarity in four-dimensions. By following the same approach, the calculation of five-gluon amplitudes was done [32, 273]. Nevertheless, the computation of six-gluon scattering amplitudes for all helicity configurations was not done in a straightforward way. In fact, many techniques, based on unitarity and analyticity of the S-matrix, were invented to find the analytic structure of the amplitude [30, 33, 34, 273, 278–285].

These techniques made use of the relation that exists between QCD and supersymmetric amplitudes, where, the supersymmetric decomposition [274] allowed to decomposed any one-loop amplitude into two types of amplitudes. The first one determined by the singularities or branch cuts in the complex plane, called cut constructible and, the second one, called rational part, being just a finite contribution with no singularities.

On the other hand, the calculation of one-loop Higgs associated with gluon amplitudes, in the large m_t limit, started with the production of the Higgs associated with 1 gluon [276], then, after about a decade, the calculation of a Higgs associated with 2 gluons was done in Ref. [286, 287], in which the Higgs field is decomposed in terms of self-dual and anti-self-dual fields [288–291]. This decomposition allows to write compact building blocks, since their structure is the same structure as for the MHV case.

Despite of this, the calculation of the analytic amplitude of Higgs associated with 3 gluons is still missing, moreover, there is its numerical computation, done in Ref. [292], which was obtained with the combined use of GOSAM, SHERPA, and the MADDIPOLE/MADEVENT framework.

In this chapter, we show how FDF is suitable for the computation of higher point amplitudes in a straightforward way. Within FDF, there is no need of splitting the amplitude between cut constructible and rational parts, as discussed in Chap. 5. Indeed, the fact of having d -dimensional regulated amplitudes allows us to use knowledge of the d -dimensional unitarity.

This chapter is organised as follows. Sec. 6.1 is devoted to the calculation of one-loop gluon amplitudes, whereas Sec. 6.2 collects all results regarding the calculation of one-loop Higgs associated with gluon amplitudes.

6.1 Multi-gluon scattering amplitudes

We present the full analytic contributions of finite helicity configurations up to six gluons. However, since the expression for the remaining amplitudes could, eventually, be quite lengthy, we include a MATHEMATICA [262] notebook file for each helicity configuration¹, which notation is explained below, with the set of coefficients of MIs written in terms of momentum twistor variables. We remark that all coefficients has been checked numerically against NJET [56].

6.1.1 Five-gluon amplitudes

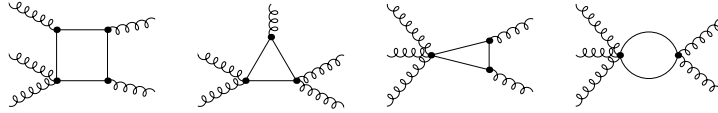


Figure 6.1: Box, triangle and bubble topologies for the five-gluon amplitude. Solid lines can refer either to generalised gluons or scalars.

As discussed in Sec. 1.5.2, we parametrise the five-point kinematics in terms of five independent variables, defined in Eq. (1.90). All the results presented in this subsection are in agreement with [273].

$$A_5^{\mathbf{1-loop}}(1^+, 2^+, 3^+, 4^+, 5^+)$$

The all plus helicity amplitude is a particularly simple example, since there are no triangle or bubble type contributions. In such a way that the full finite contribution can be obtained from the parametric form of the quadruple cut $C_{12|3|4|5}$,

$$c_{12|3|4|5;4} = \frac{2i [21] [43] [53] [54]}{\langle 12 \rangle \text{tr}_5(4, 1, 5, 3)}, \quad (6.1)$$

where the finite colour-ordered one-loop amplitude reduces to

$$A_5^{\mathbf{1-loop}}(1^+, 2^+, 3^+, 4^+, 5^+) = c_{12|3|4|5;4} I_{12|3|4|5}[\mu^4] + \text{cyclic perms.} \quad (6.2)$$

By adding all the box contributions up, and then writing the spinor product in terms of momentum twistor variables, we find

$$A_5^{\mathbf{1-loop}}(1^+, 2^+, 3^+, 4^+, 5^+) = -\frac{1}{3}i z_1^5 z_2 z_3 (z_3 z_2^2 + z_3 (z_5^2 - 2z_4) z_2 + (z_3 + 1) z_4^2) \times \Phi_5^{+++++}. \quad (6.3)$$

$$A_5^{\mathbf{1-loop}}(1^-, 2^+, 3^+, 4^+, 5^+)$$

The single minus amplitude, not as the previous amplitude, gets contribution from all topologies and can be casted in this form

$$A_5^{\mathbf{1-loop}}(1^-, 2^+, 3^+, 4^+, 5^+) = \sum_{\{i_1, i_2, i_3, i_4\}} c_4^{(i_1 i_2 i_3 i_4)} I_{i_1 i_2 i_3 i_4}[\mu^4] + \sum_{\{i_1, i_2, i_3\}} c_7^{(i_1 i_2 i_3)} I_{i_1 i_2 i_3}[\mu^2] + \sum_{\{i_1, i_2\}} c_9^{(i_1 i_2)} I_{i_1 i_2}[\mu^2], \quad (6.4)$$

¹They can be obtained from [this http URL](#).

$$= -\frac{1}{6} \sum_{\{i_1, i_2, i_3, i_4\}} c_4^{(i_1 i_2 i_3 i_4)} + \frac{1}{2} \sum_{\{i_1, i_2, i_3\}} c_7^{(i_1 i_2 i_3)} - \frac{1}{6} \sum_{\{i_1, i_2\}} c_9^{(i_1 i_2)}. \quad (6.5)$$

Plugging the coefficients of the MIs of the notebook `coe.mpppp.m` into Eq. (6.5), we get

$$A_5^{1\text{-loop}}(1^-, 2^+, 3^+, 4^+, 5^+) = -\frac{1}{3} i z_1^6 z_2^2 z_3 \left((z_2 + 1) z_4 + z_2^2 z_3 (z_3 + 1) z_5 - \frac{z_3 (z_2 - z_4)^3}{z_2 - z_4 + z_5} \right) \times \Phi_5^{-++++}. \quad (6.6)$$

All helicity configurations

Helicity	Amplitude	Notebook
1	$A_5^{1\text{-loop}}(1^+, 2^+, 3^+, 4^+, 5^+)$	<code>coe.ppppp.m</code>
2	$A_5^{1\text{-loop}}(1^-, 2^+, 3^+, 4^+, 5^+)$	<code>coe.mpppp.m</code>
3	$A_5^{1\text{-loop}}(1^-, 2^-, 3^+, 4^+, 5^+)$	<code>coe.mmppp.m</code>
4	$A_5^{1\text{-loop}}(1^-, 2^+, 3^-, 4^+, 5^+)$	<code>coe.mpmpm.m</code>

Table 6.1: Summary of the results for the one-loop five gluon amplitudes. For each helicity configuration we list its MATHEMATICA notebook.

As seen in Fig. 6.1 there are four independent topologies, where each coefficient, in the MATHEMATICA notebook, is written as follows

```
coe[helicity, cut, ordering] = {c0 -> F[{x's}], c2(4) -> G[{x's}]}
```

where `helicity` is the number shown in the Table 6.1. `cut` and `ordering` correspond to the cut under consideration and the ordering of the external particles, which always be a cyclic permutation of $\{1, 2, 3, 4, 5\}$. In the r.h.s., `c0` and `c2(4)` state for the coefficients of the MIs I_{cut} and $I_{cut}[\mu^{2(4)}]$, respectively. For instance, $C_{123|4|5}(1^-, 2^-, 3^+, 4^+, 5^+)$ we have

```
coe[3, {1, 4, 5}, {Sp[4], Sp[5], Sp[1], Sp[2], Sp[3]}] = {c0 -> 0,
  c2 -> (I*z[1]^3*z[2]^3*z[3]^2*(z[2]-z[4])^2*((1+z[3])*z[4]+
    z[2]*z[3]*(-1+z[5]))*z[5])/((z[2]*z[3]-
    (1+z[3])*z[4])^2*(z[2]-z[4]+z[5])) }
```

that means

$$c_{123|4|5:0}(1^-, 2^-, 3^+, 4^+, 5^+) = 0, \quad (6.7a)$$

$$c_{123|4|5:2}(1^-, 2^-, 3^+, 4^+, 5^+) = \frac{iz_1^3 z_2^3 z_3^2 (z_2 - z_4)^2 ((z_5 - 1) z_2 z_3 + (z_3 + 1) z_4) z_5}{(z_2 z_3 - (z_3 + 1) z_4)^2 (z_2 - z_4 + z_5)}. \quad (6.7b)$$

On the other hand, each notebook contains the physical phase $\Phi^{h_1 \dots h_5}$, that is called by simply typing

```
\[Phi][helicity]
```

and follows the notation of the sam package, e.g. for Φ^{-+++-}

```
\[Phi][4] = -(Spaa[Sp[1], Sp[3]]^5 / (Spaa[Sp[1], Sp[2]]^2
  * Spaa[Sp[1], Sp[4]]^2 * Spaa[Sp[1], Sp[5]]^2
  * Spab[Sp[3], Sp[2], Sp[1]]^3))
```

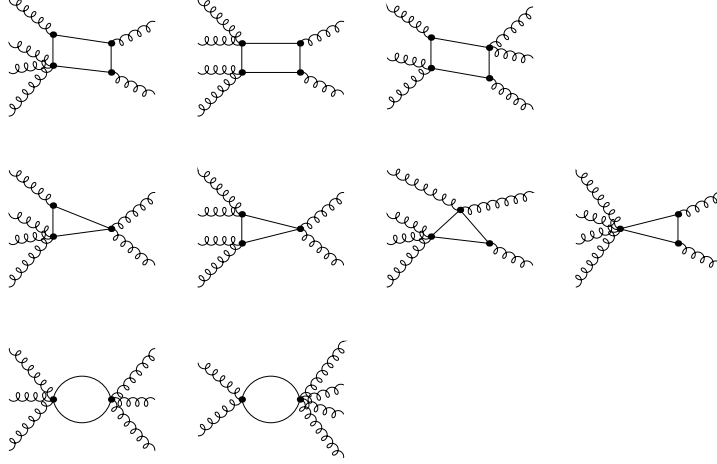


Figure 6.2: Box, triangle and bubble topologies for the six-gluon amplitude. Solid lines can refer either to generalised gluons or scalars.

6.1.2 Six-gluon amplitudes

We parametrise the six-point kinematics in terms of eight independent variables, defined in Eq. (1.93), which take the form

$$\begin{aligned}
z_1 &= s_{12}, & z_2 &= \frac{\langle 14 \rangle \langle 23 \rangle}{\langle 12 \rangle \langle 34 \rangle}, & z_3 &= \frac{\langle 15 \rangle \langle 34 \rangle}{\langle 13 \rangle \langle 45 \rangle}, & z_4 &= \frac{\langle 16 \rangle \langle 45 \rangle}{\langle 14 \rangle \langle 56 \rangle}, \\
z_5 &= \frac{s_{23}}{s_{12}}, & z_6 &= \frac{\langle 5 | 3 + 4 | 2 \rangle}{[21] \langle 51 \rangle}, & z_7 &= \frac{\langle 1 | (2 + 3) (2 + 3 + 4) | 5 \rangle}{s_{23} \langle 15 \rangle}, & z_8 &= \frac{s_{123}}{s_{12}}.
\end{aligned}$$

All the results presented in this subsection are in agreement with [30, 33, 34, 273, 278–285].

$$A_6^{\mathbf{1-loop}}(1^+, 2^+, 3^+, 4^+, 5^+, 6^+)$$

This amplitude gets contribution from boxes only, which, can be obtained from the parametric form of $C_{123|4|5|6}$, $C_{12|34|5|6}$ and $C_{12|3|45|6}$,

$$c_{123|4|5|6;4} = \frac{2i [56]}{\langle 12 \rangle \langle 23 \rangle \text{tr}_5(5, 4, 6, 1) \text{tr}_5(5, 4, 6, 3)} \left(s_{45} \langle 6 | 1 + 2 | 3 \rangle [51] [64]^2 - s_{46} \langle 5 | 1 + 2 | 3 \rangle [54]^2 [61] \right), \quad (6.8)$$

$$c_{12|34|5|6;4} = \frac{2i \langle 5 | 1 + 2 | 6 \rangle \langle 6 | 1 + 2 | 5 \rangle [12] [43] [65]^2}{\langle 12 \rangle \langle 23 \rangle \text{tr}_5(5, 2, 6, 1) \text{tr}_5(5, 4, 6, 3)}, \quad (6.9)$$

$$c_{12|3|45|6;4} = \frac{2i [12] [54] [63]^2}{\langle 12 \rangle \langle 45 \rangle \text{tr}_5(2, 3, 6, 1) \text{tr}_5(5, 3, 6, 4)} (\langle 3 | 1 + 2 | 3 \rangle \langle 6 | 1 + 2 | 6 \rangle - s_{36} s_{12}), \quad (6.10)$$

The finite colour-ordered amplitude takes the form

$$\begin{aligned}
A_6^{\mathbf{1-loop}}(1^+, 2^+, 3^+, 4^+, 5^+, 6^+) &= c_{123|4|5|6;4} I_{123|4|5|6} [\mu^4] + c_{12|34|5|6;4} I_{12|34|5|6} [\mu^4] \\
&\quad + \frac{1}{2} c_{12|3|45|6;4} I_{12|3|45|6} [\mu^4] + \text{cyclic perms.} \quad (6.11)
\end{aligned}$$

Writing the coefficient in terms of momentum twistor variables, we get

$$A_6^{\mathbf{1-loop}}(1^+, 2^+, 3^+, 4^+, 5^+, 6^+) = 2i z_1^6 z_2^2 z_3^2 z_4 \left[z_5^2 + \frac{z_2 z_3^2 z_4 ((z_7 - 1)(z_2 - z_5) z_5 + (z_2 z_6 - z_5) z_8)^2}{z_5^2} \right]$$

$$\begin{aligned}
& + z_3 \left(z_5^2 + z_2(z_5^2 + (z_5(z_7 - 2)z_7 - 2z_6)z_5 \right. \\
& \left. + z_4((z_7 - 1)z_5 + z_8)^2 + z_2(z_4(z_6 - 1)^2 + z_6^2)) \right) \Big] \times \Phi_6^{++++++}. \quad (6.12)
\end{aligned}$$

$$A_6^{1\text{-loop}}(1^-, 2^+, 3^+, 4^+, 5^+, 6^+)$$

The analytic structure of the single minus amplitude is recovered by plugging the coefficients of the MIs of the notebook `coe.mppppp.m` into Eq. (6.5),

$$\begin{aligned}
& A_6^{1\text{-loop}}(1^-, 2^+, 3^+, 4^+, 5^+, 6^+) \\
& = \frac{1}{3} z_1^7 z_2^3 z_3^2 z_4 \left\{ - (z_2 + 1) z_5 + (z_7 - 1) (z_3 + 1) z_2^2 z_3 z_5 + \frac{z_2 z_3^2 z_4 z_5 ((z_7 - 1) z_5 + z_8)^3}{z_8 ((z_7 - 1) z_5 + z_6 z_8)} \right. \\
& \quad - \frac{z_2^2 z_4 (z_4 + 1) (z_2 ((z_7 - 1) z_5 + z_6 z_8) - z_5 ((z_7 - 1) z_5 + z_8)) z_3^3}{z_5} + \frac{z_3 (z_2 z_6 - z_5)^3}{z_6 (z_2 z_6 - z_5 z_7)} \\
& \quad + \frac{1}{z_6 (z_5 (z_6 - z_7) - z_6 z_8) ((z_7 - 1) z_5 + z_6 z_8) (z_5 z_6 + z_4 (((z_7 - 1) z_2 + z_6 - 1) z_3 + z_6 - 1) z_5 + z_2 z_3 z_6 z_8))} \\
& \quad \times \left[(z_4 z_5 (z_6 - 1)^3 ((z_7 - 1) ((z_7 - 1) z_2 z_4 z_6 z_3^2 + (((z_4 + 1) z_6 - 1) (z_7 - 1) z_2 + 1) z_3 + 1) z_5^4 \right. \\
& \quad + z_6 (-2 z_2^2 z_4 (z_7 - 1)^2 z_3^2 + 2 (z_7 - 1) ((z_3 + 1) z_4 z_8 - 1) z_2 z_3 + (z_3 + 1) z_8) z_5^3 \\
& \quad + z_2 z_3 z_6 ((z_7 - 1)^2 z_3 z_4 z_2^2 - z_4 ((2 z_3 z_8 - 1) z_6 + 2 z_3 z_8 + 1) - z_6) (z_7 - 1) z_2 \\
& \quad + ((z_3 + 1) z_4 z_8 - 2 z_6) z_8 z_5^2 + ((2 (z_7 - 1) z_2 z_3 - 2 z_8 z_3 + z_6 - 1) z_4 \\
& \quad \left. + z_6) z_2^2 z_3 z_6^2 z_8 z_5 + z_2^3 z_3^2 z_4 z_6^3 z_8^2 z_3) \right] \Big\} \times \Phi_6^{-+++++}. \quad (6.13)
\end{aligned}$$

All helicity configurations

Helicity	Amplitude	Notebook
1	$A_6^{1\text{-loop}}(1^+, 2^+, 3^+, 4^+, 5^+, 6^+)$	<code>coe.pppppp.m</code>
2	$A_6^{1\text{-loop}}(1^-, 2^+, 3^+, 4^+, 5^+, 6^+)$	<code>coe.mppppp.m</code>
3	$A_6^{1\text{-loop}}(1^-, 2^-, 3^+, 4^+, 5^+, 6^+)$	<code>coe.mmpppp.m</code>
4	$A_6^{1\text{-loop}}(1^-, 2^+, 3^-, 4^+, 5^+, 6^+)$	<code>coe.mpmpmp.m</code>
5	$A_6^{1\text{-loop}}(1^-, 2^-, 3^-, 4^+, 5^+, 6^+)$	<code>coe.mmmppp.m</code>
6	$A_6^{1\text{-loop}}(1^-, 2^+, 3^-, 4^+, 5^-, 6^+)$	<code>coe.mpmpmp.m</code>

Table 6.2: Summary of the results for the one-loop six-gluon amplitudes. For each helicity configuration we list its MATHEMATICA notebook.

The coefficients of the MIs are collected in Table 6.1.

Three-mass-triangle coefficients

In Sec. 4.3 we saw that the parametrisation of the cut solution when particles are massive becomes problematic. Hence, spurious terms have to be efficiently canceled out. In the following, we show how to get rid of spurious terms, by using simple concepts of polynomial division.

Since the computation of three-mass-triangle coefficients is a bit cumbersome, we decide to write these coefficients in terms of one variable more, γ , defined in Eq. (4.31).

Let us recall the relation (4.32) satisfied by γ

$$\gamma^2 - 2\gamma K_1 \cdot K_2 + K_1^2 K_2^2 = 0. \quad (6.14)$$

Hence, when dividing our coefficients by Eq. (6.14) we just need to take the *remainder* of the division, where the dependence on γ has dropped. This division can be easily performed in MATHEMATICA with the function `PolynomialRemainder`. This operation would look like

```
(* Expr states for the three-mass-triangle coefficient *)
rel = \[Gamma]^2 - 2 \[Gamma] MP[K1, K2] + MP2[K1] MP2[K2];
PolynomialRemainder[Expr, rel, \[Gamma]]
```

We remark that this operation can be done either for the analytic or numerical expression. Moreover, efficiency of evaluation is achieved for the numerical one by considering different phase-space-points.

6.2 Higgs plus gluon amplitudes

We present the full analytic contributions of Higgs plus four gluons for all helicity configurations. Due to the symmetry of the all plus amplitude we show its structure. As in the previous section, the remaining helicity amplitudes are recovered from the set of coefficients collected in the MATHEMATICA notebook files².

On the other hand, we show preliminary results of analytic contributions of Higgs plus five gluons amplitude.³

6.2.1 Higgs plus four gluon amplitudes

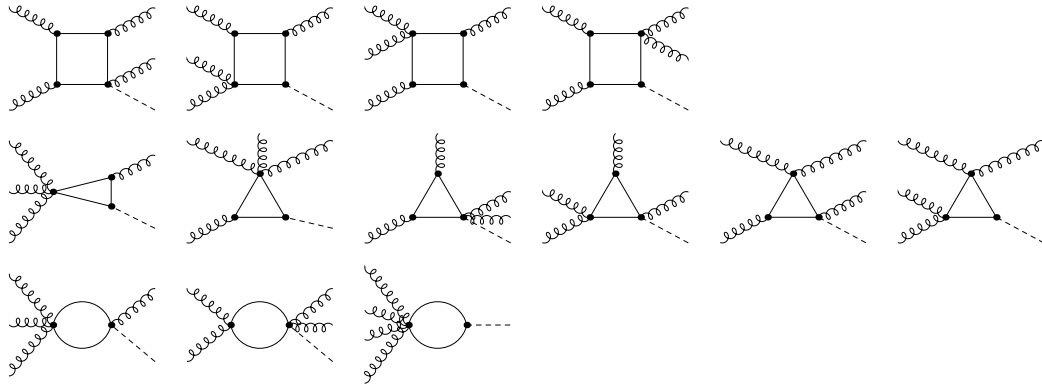


Figure 6.3: Box, triangle and bubble topologies for the Higgs plus four gluon amplitude. Solid lines can refer either to generalised gluons or scalars.

In order to compute this amplitude, we parametrise all the Lorentz invariants in terms of six variables. Differently from the five-gluon case, we need one variable more, which is chosen to be the Higgs mass. Expressing all spinor products in terms of momentum twistor variables

$$z_1 = s_{12}, \quad z_2 = \frac{\langle 14 \rangle \langle 23 \rangle}{\langle 12 \rangle \langle 34 \rangle}, \quad z_3 = \frac{\langle 15 \rangle \langle 34 \rangle}{\langle 13 \rangle \langle 45 \rangle}, \quad z_5 = \frac{s_{23}}{s_{12}}, \quad z_8 = \frac{s_{123}}{s_{12}}, \quad m_H^2 = s_{1234}. \quad (6.15)$$

All the results presented in this subsection are in agreement with [286, 287].

²They can be obtained from [this http URL](#).

³We are grateful to Simon Badger and Francesco Bucini for providing their set of coefficients for various phase-space-points.

$$A_5^{\mathbf{1-loop}}(1^+, 2^+, 3^+, 4^+, H)$$

First we show the explicit structure of the analytic contribution of the one-loop Higgs plus four gluon amplitude, originally computed in [286]. For sake of simplicity we do not write the explicit form of the finite part of the amplitude.

The leading-order contribution of the five-point can be written as,

$$A_5^{\text{tree}}(1^+, 2^+, 3^+, 4^+, H) = \frac{-i m_H^4}{\langle 12 \rangle \langle 23 \rangle \langle 34 \rangle \langle 41 \rangle}. \quad (6.16)$$

Furthermore, the amplitude (6.16), in momentum twistor variables, takes the form

$$A_5^{\text{tree}}(1^+, 2^+, 3^+, 4^+, H) \stackrel{\text{m.t.}}{=} i m_H^4 z_1^2 z_2. \quad (6.17)$$

The all plus one-loop amplitude becomes

$$\begin{aligned} A_5^{\mathbf{1-loop}}(1^+, 2^+, 3^+, 4^+, H) = & \frac{1}{2} A_5^{\text{tree}} \left[s_{12} s_{23} I_{1|2|3|4H} + (s_{123} s_{234} - s_{23} m_H^2) I_{12|3|4|H} \right. \\ & \left. - (s_{123} - m_H^2) I_{123|4|H} - (s_{234} - m_H^2) I_{1|234|H} \right] \\ & + c_{1|2|3|4H; 4} I_{1|2|3|4H} [\mu^4] + c_{1|2|34H; 2} I_{1|2|34H} [\mu^2] \\ & + c_{12|3|4H; 2} I_{12|3|4H} [\mu^2] + c_{1|23|4H; 2} I_{1|23|4H} [\mu^2] \\ & + c_{123|4H; 2} I_{123|4H} [\mu^2] + c_{12|34H; 2} I_{12|34H} [\mu^2] \\ & + \text{cyclic perm.}(1234), \end{aligned} \quad (6.18)$$

with c non-vanishing coefficients, collected in the MATHEMATICA notebook `coe.Hpppp.m`.

All helicity configurations

Helicity	Amplitude	Notebook
1	$A_5^{\mathbf{1-loop}}(1^+, 2^+, 3^+, 4^+, H)$	<code>coe.Hpppp.m</code>
2	$A_5^{\mathbf{1-loop}}(1^-, 2^+, 3^+, 4^+, H)$	<code>coe.Hmppp.m</code>
3	$A_5^{\mathbf{1-loop}}(1^-, 2^-, 3^+, 4^+, H)$	<code>coe.Hmmpp.m</code>
4	$A_5^{\mathbf{1-loop}}(1^-, 2^+, 3^-, 4^+, H)$	<code>coe.Hmpmp.m</code>

Table 6.3: Summary of the results for the one-loop six-gluon amplitudes. For each helicity configuration we list its MATHEMATICA notebook.

6.2.2 Higgs plus five gluon amplitudes

In this section we collect the results of the one-loop Higgs plus five gluon amplitude. We parametrise the kinematics of this process in terms of nine independent variables,

$$\begin{aligned} z_1 &= s_{12}, & z_2 &= \frac{\langle 14 \rangle \langle 23 \rangle}{\langle 12 \rangle \langle 34 \rangle}, & z_3 &= \frac{\langle 15 \rangle \langle 34 \rangle}{\langle 13 \rangle \langle 45 \rangle}, \\ z_4 &= \frac{\langle 45 \rangle \langle 1|H|2 \rangle}{\langle 14 \rangle \langle 5|H|2 \rangle}, & z_6 &= \frac{s_{23}}{s_{12}}, & z_9 &= \frac{\langle 1|(2+3)(2+3+4)|5 \rangle}{s_{23} \langle 15 \rangle}, \\ z_{10} &= \frac{\langle 1|(2+3)(2+3+4+5)H|2 \rangle}{s_{23} \langle 1|H|2 \rangle}, & z_{11} &= \frac{s_{123}}{s_{12}}, & m_H^2 &= s_{12345}. \end{aligned} \quad (6.19)$$

The one-loop correction to this amplitude is obtained by considering the independent topologies depicted in fig. 6.4.

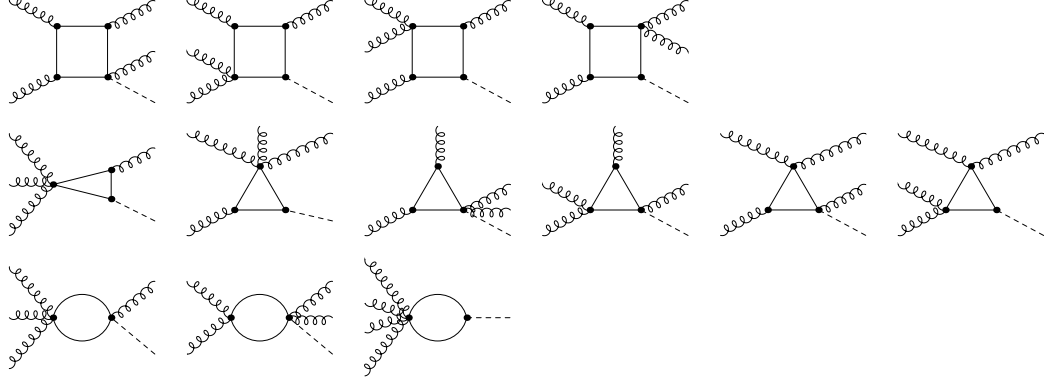


Figure 6.4: Box, triangle and bubble topologies for the Higgs plus five gluon amplitude. Solid lines can refer either to generalised gluons or scalars.

$$A_6^{\mathbf{1-loop}}(1^+, 2^+, 3^+, 4^+, 5^+, H)$$

The leading-order contribution of the six-point can be written as,

$$A_6^{\text{tree}}(1^+, 2^+, 3^+, 4^+, 5^+, H) = \frac{-i m_H^4}{\langle 12 \rangle \langle 23 \rangle \langle 34 \rangle \langle 45 \rangle \langle 51 \rangle} \stackrel{\text{m.t.}}{=} i m_H^4 z_1^3 z_2^2 z_3. \quad (6.20)$$

The all plus one-loop amplitude becomes

$$\begin{aligned} A_6^{\mathbf{1-loop}}(1^+, 2^+, 3^+, 4^+, 5^+, H) = & \frac{1}{2} A_6^{\text{tree}} \left[s_{12} s_{23} I_{1|2|3|45H} + (s_{123} s_{234} - s_{23} s_{1234}) I_{1|23|4|5H} \right. \\ & \left. + (s_{1234} s_{2345} - s_{234} m_H^2) I_{1|23|4|5H} - (s_{2345} - m_H^2) I_{1|2345|H} - (s_{1234} - m_H^2) I_{1234|5|H} \right] \\ & + c_{1|2|3|45H;4} I_{1|2|3|45H} [\mu^4] + c_{1|23|4|5H;4} I_{1|23|4|5H} [\mu^4] \\ & + c_{12|3|4|5H;4} I_{12|3|4|5H} [\mu^4] + c_{1|2|34|5H;4} I_{1|2|34|5H} [\mu^4] \\ & + c_{123|4|5H;2} I_{123|4|5H} [\mu^2] + c_{1|234|5H;2} I_{1|234|5H} [\mu^2] \\ & + c_{1|23|45H;2} I_{1|23|45H} [\mu^2] + c_{12|3|45H;2} I_{12|3|45H} [\mu^2] + c_{1|2|345H;2} I_{1|2|345H} [\mu^2] \\ & + c_{12|345H;2} I_{12|345H} [\mu^2] + c_{123|45H;2} I_{123|45H} [\mu^2] + c_{1234|5H;2} I_{1234|5H} [\mu^2] \\ & + \text{cyclic perm.}(1235), \quad (6.21) \end{aligned}$$

with c non-vanishing coefficients, collected in the MATHEMATICA notebook `coe.Hppppp.m`.

6.3 Discussion

In this chapter, we have presented how the four dimensional formulation (FDF) regularisation scheme allows for the computation of analytical expressions of one-loop amplitudes with high multiplicity. This has been tested by re-computing the gluon helicity amplitudes with up to six external legs and the production of Higgs, via gluon fusion, in association with up to two gluons. As a preliminary result of the one-loop Higgs plus five gluon amplitudes, we have shown the amplitude in which all gluons have the same helicity.

The one-loop amplitudes presented in this chapter have been reconstructed as a combination of box-, triangle- and bubble-scalar integrals. The coefficients of each master integral were obtained using the integrand reduction method through Laurent series expansion [61]. For five- and six- gluon amplitudes, we evaluated our analytic expression on several phase space points getting agreement with NJET [56]. For the Higgs plus four gluons amplitudes, we compared our

analytical results with the ones of Ref.s [286, 287]. Differently from the gluon amplitudes, a numerical check was not performed, since these codes work with the structure of full colour-dressed amplitudes. Hence, in order to extract what we need, which is the colour-ordered amplitude, a non trivial modification on the codes has to be done.

In order to show the results for gluon and Higgs amplitudes, we provide ancillary files with the set of coefficients of each MIs for all helicity configurations. These coefficients are written in terms of momentum twistor variables, whose parametrisation follows the one presented in Sec. 1.5.2. Despite of their lengthy expression, we can highlight a very important aspect regarding their numerical evaluation. In fact, writing Lorentz products in terms of a minimal set of independent variables produces a much faster evaluation.

The computation of the three-mass-triangle coefficients has been addressed in a particular way. In our analytic expressions we have added an additional variable, γ , which turns out to be spurious. We emphasise that γ does not have to be fit when evaluating our analytic expressions. In fact, its cancelation is easily achieved by performing a polynomial division.

The idea of leaving all coefficients in terms of a minimal set of independent variables allows for a much faster evaluation than existing numerical implementations. The advantage of having analytic expressions for our amplitudes grants, indeed, to recycle these results in the NNLO contribution.

Although the results presented in this chapter concentrate on applications to amplitudes with massless internal particles, the main part of the procedure applies equally to the case of massive ones.

Chapter 7

Colour-Kinematics duality in d -dimensions

In Chap. 3, we studied the C/K-duality for four-dimensional gauge theories. We showed how the off-shell Jacobi-like combination of the kinematic numerators produces an anomalous term that vanishes when the four particles are in their mass-shell. Additionally, we develop a new procedure to generate dual numerators. This procedure, based on the generalised gauge transformation, follows a pure diagrammatic approach.

This chapter extends the results of C/K-duality for four-dimensional theories to dimensional regularisation. In order to study the C/K-duality in dimensional regularisation, we apply the technology developed for the FDF scheme in Chap. 5. We anticipate that the C/K duality obeyed by the numerators of tree-level amplitudes within the FDF scheme are non-trivial relations involving the interplay of massless and massive particles. A set of BCJ identities for d -dimensionally regulated amplitudes is found, which explicitly shows the dependence on the $(d - 4)$ -components.

Furthermore, we combine BCJ identities with integrand reduction methods to establish relations between one-loop integral coefficients for dimensionally regulated QCD amplitudes. These relations can be established for the cut-constructible contributions as well as the ones responsible for rational terms. We provide explicit examples for multi-gluon scattering amplitudes at one-loop.

7.1 Tree-level identities in d -dimensions

As a starting point, we focus on four-point tree-level amplitudes, showing that C/K-duality can be established for all interactions involving particles propagating within the FDF framework. Envisaging one-loop applications of these results, we consider amplitudes with two d -dimensional external particles and two four-dimensional ones. Following the by now familiar procedure of Sec.s 3.2.1, 3.2.2 and 3.2.3, we build an off-shell Jacobi-like combination of kinematics numerators for each of the seven processes involving, according to the Feynman rules of (5.12), two external massive particles. We show that, in every case, C/K-duality holds after physical constraints are imposed.

- a) We start from the scattering of two generalised gluons producing two massless ones, $g^\bullet g^\bullet \rightarrow gg$, with on-shell conditions $p_2^2 = p_3^2 = 0$ and $p_2^2 = p_3^2 = \mu^2$. The amplitude receives contribution from the four diagrams shown in Fig. 7.1. Exactly as in the massless case discussed in Sec. 3.2.3, the four-point vertex contributes to the same colour structures as the trivalent

$$\begin{aligned}
& - (p_1^2 - p_2^2) g^{\mu_1 \mu_2} (p_3^{\mu_3} p_3^{\mu_4} - p_4^{\mu_3} p_4^{\mu_4}) + (p_4^2 - p_3^2) g^{\mu_3 \mu_4} (p_1^{\mu_1} p_1^{\mu_2} - p_2^{\mu_1} p_2^{\mu_2}) \\
& + (p_3^{\mu_1} p_3^{\mu_3} - p_1^{\mu_1} p_1^{\mu_3}) (p_2^{\mu_2} p_2^{\mu_4} - p_4^{\mu_2} p_4^{\mu_4}) + (p_2^{\mu_1} p_2^{\mu_2} - p_1^{\mu_1} p_1^{\mu_2}) (p_4^{\mu_3} p_4^{\mu_4} - p_3^{\mu_3} p_3^{\mu_4}) \}. \quad (7.6)
\end{aligned}$$

We see that C/K duality, which corresponds to $N_{g^\bullet g^\bullet gg} = 0$, is recovered because of transversality, $\varepsilon_i \cdot p_i = 0$, and on-shellness conditions.

- b) Now we consider $gg \rightarrow s^\bullet s^\bullet$ ($p_1^2 = p_4^2 = 0$, $p_2^2 = p_3^2 = \mu^2$) amplitude, whose diagrams are shown in Fig. 7.3.

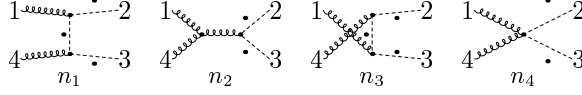


Figure 7.3: Feynman diagrams for $gg \rightarrow s^\bullet s^\bullet$.

In this case, since the four-point interaction only contributes to two colour structures,

$$c_4 n_4 = c_1 n_{1;4} + c_3 c_{3;4}, \quad (7.7)$$

we can absorb its kinematic part in the two diagrams involving a massive scalar propagator, through the substitutions,

$$\begin{aligned}
n_1 + ((p_1 + p_2)^2 - \mu^2) n_{1;4} &\rightarrow n_1, \\
n_3 + ((p_1 + p_3)^2 - \mu^2) n_{3;4} &\rightarrow n_3,
\end{aligned} \quad (7.8)$$

whereas n_2 stays the same as defined by Feynman rules. In this way, the Jacobi combination of the cubic numerators, depicted in Fig. 7.4, becomes

$$N_{ggs^\bullet s^\bullet} = J_{ggs^\bullet s^\bullet}^{\mu_1 \mu_4} \varepsilon_{\mu_1}(p_1) \varepsilon_{\mu_4}(p_4), \quad (7.9)$$

where the off-shell current is

$$J_{ggs^\bullet s^\bullet}^{\mu_1 \mu_4} = (J_{g\text{-Fey}}^{\mu_1 \mu_4} + J_{g\text{-Ax}}^{\mu_1 \mu_4}) G^{AB}. \quad (7.10)$$

We observe that, although n_1 and n_3 depend on the mass of the scalar particle, the μ -dependence cancels in their combination. Therefore, C/K-duality, *i.e.* $N_{ggs^\bullet s^\bullet} = 0$, holds in this case as well as in the massless one, according to Eqs. (3.18) and (3.19).

$$\text{b) } \begin{array}{c} \textcircled{\mathbf{J}} \\ \text{---} \end{array} \begin{array}{c} \text{---} \\ \text{---} \end{array} \begin{array}{c} \text{---} \\ \text{---} \end{array} \begin{array}{c} \text{---} \\ \text{---} \end{array} = - \begin{array}{c} \text{---} \\ \text{---} \\ n_1 \end{array} + \begin{array}{c} \text{---} \\ \text{---} \\ n_2 \end{array} + \begin{array}{c} \text{---} \\ \text{---} \\ n_3 \end{array}$$

Figure 7.4: Jacobi combination for $gg \rightarrow s^\bullet s^\bullet$.

The remaining processes, whose tree-level identities are depicted in Fig.7.5.(c)-(g) do not involve contact interactions, so that the construction of their Jacobi-combinations directly follows from the Feynman rules of (5.12). In order to avoid repetitive discussion, we simply list the results giving, for each process, the corresponding on-shell conditions and the expression of the Jacobi-combination in terms of off-shell currents.

According to the case, C/K-duality is recovered once transversality of the gluon polarisations and Dirac equation are taken into account. We recall that, for a generalised gluon g^\bullet of momentum p_i , one has $\varepsilon_i^\lambda \cdot p_i = 0$ ($\lambda = \pm, 0$), while for generalised quarks q^\bullet of momentum p_i , one has $\bar{u}(p_i)(\not{p}_i - i\mu\gamma^5) = 0$ and $(\not{p}_i + i\mu\gamma^5)v(p_i) = 0$.

$$\begin{aligned}
\text{c) } & \text{Diagram with } \mathbf{J} \text{ and four external lines } (1, 2, 3, 4) = - \text{Diagram 1} + \text{Diagram 2} + \text{Diagram 3} \\
\text{d) } & \text{Diagram with } \mathbf{J} \text{ and four external lines } (1, 2, 3, 4) = - \text{Diagram 1} + \text{Diagram 2} + \text{Diagram 3} \\
\text{e) } & \text{Diagram with } \mathbf{J} \text{ and four external lines } (1, 2, 3, 4) = - \text{Diagram 1} + \text{Diagram 2} + \text{Diagram 3} \\
\text{f) } & \text{Diagram with } \mathbf{J} \text{ and four external lines } (1, 2, 3, 4) = - \text{Diagram 1} + \text{Diagram 2} + \text{Diagram 3} \\
\text{g) } & \text{Diagram with } \mathbf{J} \text{ and four external lines } (1, 2, 3, 4) = - \text{Diagram 1} + \text{Diagram 2} + \text{Diagram 3}
\end{aligned}$$

Figure 7.5: Jacobi combinations for FDF particles.

$$\text{c) } g^\bullet g^\bullet \rightarrow \bar{q}q \quad (p_1^2 = p_4^2 = \mu^2, p_2^2 = p_3^2 = 0):$$

$$N_{g^\bullet g^\bullet \bar{q}q} = \bar{u}(p_3) J_{g^\bullet g^\bullet \bar{q}q}^{\mu_1 \mu_4} v(p_2) \varepsilon_{\mu_1}(p_1) \varepsilon_{\mu_4}(p_4), \quad (7.11)$$

with

$$-J_{g^\bullet g^\bullet \bar{q}q}^{\mu_1 \mu_4} = J_{q\text{-Fey}}^{\mu_1 \mu_4} + J_{q\text{-Ax}}^{\mu_1 \mu_4}, \quad (7.12)$$

where the terms in the r.h.s. are defined by Eq. (3.25) and (3.26).

$$\text{d) } s^\bullet s^\bullet \rightarrow \bar{q}q \quad (p_1^2 = p_4^2 = \mu^2, p_2^2 = p_3^2 = 0):$$

$$N_{s^\bullet s^\bullet \bar{q}q} = \bar{u}(p_3) J_{s^\bullet s^\bullet \bar{q}q} v(p_2), \quad (7.13)$$

with

$$-i J_{s^\bullet s^\bullet \bar{q}q} = \frac{1}{(p_2 + p_3) \cdot q} \left\{ q \cdot (p_4 - p_1) (\not{p}_2 + \not{p}_3) + (p_4^2 - p_1^2) \not{q} \right\}. \quad (7.14)$$

$$\text{e) } gg \rightarrow \bar{q}^\bullet q^\bullet \quad (p_1^2 = p_4^2 = 0, p_2^2 = p_3^2 = \mu^2):$$

$$N_{gg \bar{q}^\bullet q^\bullet} = \bar{u}(p_3) J_{gg \bar{q}^\bullet q^\bullet}^{\mu_1 \mu_4} v(p_2), \quad (7.15)$$

with

$$\begin{aligned}
-i J_{gg \bar{q}^\bullet q^\bullet}^{\mu_1 \mu_4} = & -(\not{p}_3 - i\mu\gamma^5) \gamma^{\mu_4} \gamma^{\mu_1} - \gamma^{\mu_1} \gamma^{\mu_4} (\not{p}_2 + i\mu\gamma^5) + (\not{p}_3 + \not{p}_2 + i\mu\gamma^5) g^{\mu_1 \mu_4} \\
& + p_4^{\mu_4} \gamma^{\mu_1} - p_1^{\mu_1} \gamma^{\mu_4} + J_{q\text{-Ax}}^{\mu_1 \mu_4}. \quad (7.16)
\end{aligned}$$

$$\text{f) } g^\bullet g \rightarrow \bar{q}^\bullet q \quad (p_1^2 = p_2^2 = \mu^2, p_3^2 = p_4^2 = 0):$$

$$N_{g^\bullet g \bar{q}^\bullet q} = \bar{u}(p_3) J_{g^\bullet g \bar{q}^\bullet q}^{\mu_1 \mu_4} v(p_2) \varepsilon_{\mu_1}(p_1) \varepsilon_{\mu_4}(p_4), \quad (7.17)$$

with

$$\begin{aligned}
-i J_{g^\bullet g \bar{q}^\bullet q}^{\mu_1 \mu_4} = & -\not{p}_3 \gamma^{\mu_4} \gamma^{\mu_1} - \gamma^{\mu_1} \gamma^{\mu_4} (\not{p}_2 + i\mu\gamma^5) + (\not{p}_3 + \not{p}_2 + i\mu\gamma^5) g^{\mu_1 \mu_4} + p_4^{\mu_4} \gamma^{\mu_1} - p_1^{\mu_1} \gamma^{\mu_4} \\
& + \frac{1}{\mu^2} (\not{p}_3 + \not{p}_2 + i\mu\gamma^5) (p_1^{\mu_4} p_1^{\mu_1} - p_4^{\mu_1} p_4^{\mu_4}). \quad (7.18)
\end{aligned}$$

g) $s^\bullet g \rightarrow \bar{q}^\bullet q$ ($p_1^2 = p_2^2 = \mu^2$, $p_3^2 = p_4^2 = 0$):

$$N_{s^\bullet g \bar{q}^\bullet q} = \bar{u}(p_3) J_{s^\bullet g \bar{q}^\bullet q}^{\mu_4} v(p_2) \varepsilon_{\mu_4}(p_4), \quad (7.19)$$

with

$$-i J_{s^\bullet g \bar{q}^\bullet q}^{\mu_4} = (-\not{p}_3 \gamma^{\mu_4} \gamma^5 - \gamma^5 \gamma^{\mu_4} (\not{p}_2 + i\mu \gamma^5) + p_4^{\mu_4} \gamma^5) \Gamma^A. \quad (7.20)$$

7.2 Colour-kinematics duality for $g^\bullet g^\bullet(s^\bullet s^\bullet) \rightarrow q\bar{q}g$

As a non-trivial example of C/K-duality for dimensionally regulated amplitudes, we consider again the process $gg \rightarrow q\bar{q}g$, already discussed in Section 3.3.3, but now regarding the initial state gluons as d -dimensional particles (whereas the final state remains fully four-dimensional). This amplitude would contribute to a d -dimensional unitarity cut of a loop-level amplitude where the gluons p_1 and p_2 appear as virtual states.

Within FDF, the full amplitude is obtained by combining the contributions of three different processes involving generalised four-dimensional initial particles,

$$g^\bullet g^\bullet \rightarrow q\bar{q}g, \quad s^\bullet s^\bullet \rightarrow q\bar{q}g, \quad g^\bullet s^\bullet \rightarrow q\bar{q}g. \quad (7.21)$$

However, because of the (-2ϵ) -SRs, Eq. (5.11), $g^\bullet s^\bullet \rightarrow q\bar{q}g$ vanishes and the problem decouples in the determination of the C/K-dual representation of two individually gauge invariant amplitudes, $g^\bullet g^\bullet \rightarrow q\bar{q}g$ and $s^\bullet s^\bullet \rightarrow q\bar{q}g$. The tree-level contributions to $g^\bullet g^\bullet \rightarrow q\bar{q}g$ are shown in Fig. 7.6. The Feynman diagrams for $s^\bullet s^\bullet \rightarrow q\bar{q}g$ can be easily obtained by replacing all generalised gluons g^\bullet with scalars s^\bullet .

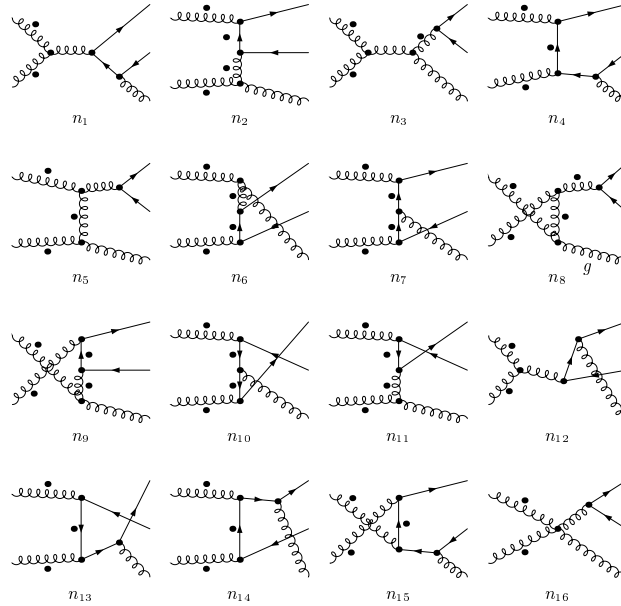


Figure 7.6: Feynman diagrams for $g^\bullet g^\bullet \rightarrow q\bar{q}g$. The contributions to $s^\bullet s^\bullet \rightarrow q\bar{q}g$ are obtained by replacing all generalised gluons g^\bullet with s^\bullet lines.

Since in both cases the number of graphs, the relations among their colour factors and, as consequence, the set of constraints to be imposed on the shifted numerators (3.40) are exactly the same as in the example of Sec. 3.3.3, we will simply discuss the relevant modifications to be taken into account in order to adapt the calculation to generalised fields.

We notice that, while for $g^\bullet g^\bullet$ the redistribution of numerator n_{16} among cubic diagrams is still given by Eq. (3.64), for the $s^\bullet s^\bullet$ case we have, as discussed in Section 7.1(b),

$$c_{16}n_{16} = c_5n_{5;16} + c_8n_{8;16}. \quad (7.22)$$

Nevertheless, for both processes the diagrammatic expansion of the amplitude can be still read from the r.h.s. of Eq. (3.68), provided the replacement

$$\begin{aligned} s_{1i} &\rightarrow (s_{1i} - \mu^2) \quad \text{for } i \neq 2, \\ s_{2i} &\rightarrow (s_{2i} - \mu^2) \quad \text{for } i \neq 1, \end{aligned} \quad (7.23)$$

which account for internal massive propagators. These modifications affect the kinematic terms of the decomposition (3.71), as well as the entries of the matrix (3.73). Finally, the anomalous terms that enter the definition of the vector (3.74) are given, for $g^\bullet g^\bullet \rightarrow q\bar{q}g$, by

$$\begin{aligned} \phi_{[1,3,12]} &= \bar{u}_3[J_q(p_1 + p_2, p_4, p_3, p_5)_{\alpha\alpha_5}]v_4\Pi_{\text{Fey}}^{\alpha\beta}V_{\beta\alpha_1\alpha_2}(-p_1 - p_2, p_1, p_2)\varepsilon_1^{\alpha_1}\varepsilon_2^{\alpha_2}\varepsilon_5^{\alpha_5} \\ &\quad + n_{3;16} = s_{12}\varphi_{[1,3,12]}, \\ \phi_{[1,4,15]} &= \bar{u}_3[J_{g^\bullet g^\bullet \bar{q}q}(p_2, p_4 + p_5, p_3, p_1)_{\alpha_2\alpha_1}(\not{p}_4 + \not{p}_5)\not{\epsilon}_5]v_4\varepsilon_1^{\alpha_1}\varepsilon_2^{\alpha_2} = s_{45}\varphi_{[1,4,15]}, \\ \phi_{[2,4,7]} &= \bar{u}_3[\not{\epsilon}_2(\not{p}_3 + \not{p}_2 + i\mu\gamma^5)J_{g^\bullet g^\bullet \bar{q}q}(p_1, p_4, p_3 + p_2, p_5)_{\alpha_1\alpha_5}]v_4\varepsilon_1^{\alpha_1}\varepsilon_5^{\alpha_5} = s_{23}\varphi_{[2,4,7]}, \\ \phi_{[2,5,11]} &= \bar{u}_3[J_{g^\bullet g^\bullet \bar{q}q}(p_1 + p_5, p_4, p_3, p_2)_{\alpha\alpha_2}]v_4\Pi_{\text{gen}}^{\alpha\beta}(p_1 + p_5, \mu^2) \\ &\quad \times V_{\beta\alpha_1\alpha_5}(-p_1 - p_5, p_1, p_5)\varepsilon_1^{\alpha_1}\varepsilon_2^{\alpha_2}\varepsilon_5^{\alpha_5} + n_{5;16} = s_{15}\varphi_{[2,5,11]}, \\ \phi_{[6,7,14]} &= \bar{u}_3[J_{g^\bullet g^\bullet \bar{q}q}(p_5, p_4 + p_1, p_3, p_2)_{\alpha_5\alpha_2}(\not{p}_4 + \not{p}_1 + i\mu\gamma^5)\not{\epsilon}_1]v_4\varepsilon_2^{\alpha_2}\varepsilon_5^{\alpha_5} = s_{14}\varphi_{[6,7,14]}, \\ \phi_{[6,8,9]} &= \bar{u}_3[J_{g^\bullet g^\bullet \bar{q}q}(p_2 + p_5, p_4, p_3, p_1)_{\alpha\alpha_1}]v_4\Pi_{\text{gen}}^{\alpha\beta}(p_2 + p_5, \mu^2) \\ &\quad \times V_{\beta\alpha_2\alpha_5}(-p_2 - p_5, p_2, p_5)\varepsilon_1^{\alpha_1}\varepsilon_2^{\alpha_2}\varepsilon_5^{\alpha_5} + n_{8;16} = s_{25}\varphi_{[6,8,9]}, \\ \phi_{[9,10,15]} &= \bar{u}_3[\not{\epsilon}_1(\not{p}_3 + \not{p}_1 + i\mu\gamma^5)J_{g^\bullet g^\bullet \bar{q}q}(p_5, p_4, p_3 + p_1, p_2)_{\alpha_5\alpha_2}]v_4\varepsilon_2^{\alpha_2}\varepsilon_5^{\alpha_5} = s_{13}\varphi_{[9,10,15]}, \\ \phi_{[11,10,13]} &= \bar{u}_3[J_{g^\bullet g^\bullet \bar{q}q}(p_1, p_4 + p_2, p_3, p_5)_{\alpha_1\alpha_5}(\not{p}_4 + \not{p}_2 + i\mu\gamma^5)\not{\epsilon}_2]v_4\varepsilon_1^{\alpha_1}\varepsilon_5^{\alpha_5} = s_{24}\varphi_{[11,10,13]}, \\ \phi_{[12,13,14]} &= \bar{u}_3[\not{\epsilon}_5(\not{p}_3 + \not{p}_5)J_{g^\bullet g^\bullet \bar{q}q}(p_2, p_4, p_3 + p_5, p_1)_{\alpha_2\alpha_1}]v_4\varepsilon_1^{\alpha_1}\varepsilon_2^{\alpha_2} = s_{35}\varphi_{[12,13,14]}, \end{aligned} \quad (7.24)$$

and, for $s^\bullet s^\bullet \rightarrow q\bar{q}g$,

$$\begin{aligned} \phi_{[1,3,12]} &= \bar{u}_3[J_q(p_1 + p_2, p_4, p_3, p_5)_{\alpha\alpha_5}]v_4\Pi_{\text{Fey}}^{\alpha\beta}(p_1 - p_2)_\beta\varepsilon_5^{\alpha_5} = s_{12}\varphi_{[1,3,12]}, \\ \phi_{[1,4,15]} &= \bar{u}_3[J_{s^\bullet s^\bullet \bar{q}q}(p_2, p_4 + p_5, p_3, p_1)(\not{p}_4 + \not{p}_5)\not{\epsilon}_5]v_4 = s_{45}\varphi_{[1,4,15]}, \\ \phi_{[2,4,7]} &= \bar{u}_3[\gamma^5(\not{p}_3 + \not{p}_2 + i\mu\gamma^5)J_{s^\bullet s^\bullet \bar{q}q}(p_1, p_4, p_3 + p_2, p_5)_{\alpha_5}]v_4\varepsilon_5^{\alpha_5} = s_{23}\varphi_{[2,4,7]}, \\ \phi_{[2,5,11]} &= \bar{u}_3[J_{s^\bullet s^\bullet \bar{q}q}(p_1 + p_5, p_4, p_3, p_2)]v_4(2p_1 + p_5) \cdot \varepsilon_5 + n_{5;16} = s_{15}\varphi_{[2,5,11]}, \\ \phi_{[6,7,14]} &= \bar{u}_3[J_{s^\bullet s^\bullet \bar{q}q}(p_5, p_4 + p_1, p_3, p_2)_{\alpha_5}(\not{p}_4 + \not{p}_1 + i\mu\gamma^5)\not{\epsilon}_1]v_4\varepsilon_5^{\alpha_5} = s_{14}\varphi_{[6,7,14]}, \\ \phi_{[6,8,9]} &= \bar{u}_3[J_{s^\bullet s^\bullet \bar{q}q}(p_2 + p_5, p_4, p_3, p_1)]v_4(2p_2 + p_5) \cdot \varepsilon_5 + n_{8;16} = s_{25}\varphi_{[6,8,9]}, \\ \phi_{[9,10,15]} &= \bar{u}_3[\gamma^5(\not{p}_3 + \not{p}_1 + i\mu\gamma^5)J_{s^\bullet s^\bullet \bar{q}q}(p_5, p_4, p_3 + p_1, p_2)_{\alpha_5}]v_4\varepsilon_5^{\alpha_5} = s_{13}\varphi_{[9,10,15]}, \\ \phi_{[11,10,13]} &= \bar{u}_3[J_{s^\bullet s^\bullet \bar{q}q}(p_1, p_4 + p_2, p_3, p_5)_{\alpha_5}(\not{p}_4 + \not{p}_2 + i\mu\gamma^5)\gamma^5]v_4\varepsilon_5^{\alpha_5} = s_{24}\varphi_{[11,10,13]}, \\ \phi_{[12,13,14]} &= \bar{u}_3[\not{\epsilon}_5(\not{p}_3 + \not{p}_5)J_{s^\bullet s^\bullet \bar{q}q}(p_2, p_4, p_3 + p_5, p_1)]v_4 = s_{35}\varphi_{[12,13,14]}. \end{aligned} \quad (7.25)$$

The systems $\mathbb{A}\Delta = \phi$ associated to both amplitudes still satisfy the condition (3.76), which ensures the existence of a C/K-dual representation, depending on four arbitrary parameters, whose expression follows the structure of (3.87).

As for the pure four-dimensional case, the analytic expressions of the dual numerators have been obtained for generic polarisations and numerical checks of the result have been performed for different helicity configurations, including longitudinal polarisations of generalised gluons.

7.3 Bern-Carrasco-Johansson relations in d -dimensions

Since the rank of the matrix \mathbb{A} turns out to be non-maximal and the consistency relation, $\text{rank}(\mathbb{A}|\mathbf{K}) = \text{rank}(\mathbb{A}) = 11$, implies the existence of four linear relations between the kinematic factors K_i 's, which can be simply found by determining a complete set of vanishing linear combinations of the rows of \mathbb{A} . In this way, we obtain the set of identities

$$\begin{aligned}
s_{45} K_1 - s_{34} K_3 - (s_{14} - \mu^2) K_6 &= 0, \\
s_{12} K_1 - (s_{23} - \mu^2) K_4 - (s_{25} - \mu^2) K_6 &= 0, \\
(s_{15} - \mu^2) K_2 - s_{45} K_4 - (s_{25} - \mu^2) K_6 &= 0, \\
(s_{23} - \mu^2) K_2 - s_{34} K_5 + (s_{23} + s_{35} - \mu^2) K_6 &= 0,
\end{aligned} \tag{7.26}$$

which reduce to two the numbers of independent K_i 's. At higher multiplicities, rather than corresponding to a single partial amplitude, each kinematic factor can be expressed as a linear combination of colour-ordered amplitudes. The relations between the K_i 's and colour-ordered amplitudes can be found either by comparing their expansions in terms of Feynman diagrams or, more conveniently, by first performing the usual colour algebra on (3.71), in order to express all c_i 's in terms of traces of generators T^{a_i} , and then by identifying the combinations of K_i 's that multiply each single trace with the corresponding colour-ordered amplitude. In this case, it can be shown that

$$\begin{aligned}
K_1 &= A_5(1, 2, 3, 4, 5) + A_5(1, 2, 4, 3, 5) + A_5(1, 3, 2, 4, 5), \\
K_2 &= -A_5(1, 4, 2, 3, 5), \\
K_3 &= A_5(1, 3, 4, 2, 5) - A_5(1, 2, 4, 3, 5), \\
K_4 &= A_5(1, 4, 2, 3, 5) - A_5(1, 3, 2, 4, 5), \\
K_5 &= -A_5(1, 3, 4, 2, 5), \\
K_6 &= A_5(1, 3, 4, 2, 5) + A_5(1, 4, 2, 3, 5) + A_5(1, 4, 3, 2, 5).
\end{aligned} \tag{7.27}$$

Therefore, by substituting (7.27) in (7.26), we can reduce from six to two the number of independent colour-ordered amplitudes and express all the others through the set of relations

$$\begin{aligned}
A_5(1, 3, 4, 2, 5) &= \frac{-P_{12}^2 P_{45}^2 A_5(1, 2, 3, 4, 5) + (P_{14}^2 - \mu^2)(P_{24}^2 + P_{25}^2 - 2\mu^2) A_5(1, 4, 3, 2, 5)}{(P_{13}^2 - \mu^2)(P_{24}^2 - \mu^2)}, \\
A_5(1, 2, 4, 3, 5) &= \frac{-(P_{14}^2 - \mu^2)(P_{25}^2 - \mu^2) A_5(1, 4, 3, 2, 5) + P_{45}^2 (P_{12}^2 + P_{24}^2 - \mu^2) A_5(1, 2, 3, 4, 5)}{P_{35}^2 (P_{24}^2 - \mu^2)}, \\
A_5(1, 4, 2, 3, 5) &= \frac{-P_{12}^2 P_{45}^2 A_5(1, 2, 3, 4, 5) + (P_{25}^2 - \mu^2)(P_{14}^2 + P_{25}^2 - 2\mu^2) A_5(1, 4, 3, 2, 5)}{P_{35}^2 (P_{24}^2 - \mu^2)}, \\
A_5(1, 3, 2, 4, 5) &= \frac{-(P_{14}^2 - \mu^2)(P_{25}^2 - \mu^2) A_5(1, 4, 3, 2, 5) + P_{12}^2 (P_{24}^2 + P_{45}^2 - \mu^2) A_5(1, 2, 3, 4, 5)}{(P_{13}^2 - \mu^2)(P_{24}^2 - \mu^2)}.
\end{aligned} \tag{7.28}$$

Identities involving other colour-ordered amplitudes can be obtained by making use of Kleiss-Kuijff identities such as

$$A_5(1, 2, 3, 4, 5) + A_5(1, 2, 3, 5, 4) + A_5(1, 2, 4, 3, 5) + A_5(1, 4, 2, 3, 5) = 0, \tag{7.29}$$

which, substituted in (7.28), gives

$$A_5(1, 2, 4, 3, 5) = \frac{(P_{14}^2 + P_{45}^2 - \mu^2) A_5(1, 2, 3, 4, 5) + (P_{14}^2 - \mu^2) A_5(1, 2, 3, 5, 4)}{(P_{24}^2 - \mu^2)}. \tag{7.30}$$

The same identities are satisfied by the colour-ordered amplitudes where the generalised gluons in the initial state are replaced by massive scalars ($s^\bullet s^\bullet \rightarrow ggg$).

Similar consideration can be made for the four-point BCJ relations, where, by following the prescription (7.23) in the system (3.56), it becomes,

$$(s_{24} - \mu^2)A(1, 2, 4, 3) = (s_{23} - \mu^2)A(1, 2, 3, 4). \quad (7.31)$$

With similar considerations we can verify that

$$(s_{24} - \mu^2)A(1, 3, 2, 4) = s_{12} A(1, 2, 3, 4), \quad (s_{23} - \mu^2)A(1, 4, 2, 3) = s_{12} A(1, 2, 4, 3). \quad (7.32)$$

The BCJ relations of Eq. (3.13), by following a pure diagrammatic approach, can be generalised to

$$\sum_{i=3}^n \left(\sum_{j=3}^i s_{2j} - \mu^2 \delta_{jn} \right) A_n^{\text{tree}}(1, 3, \dots, i, 2, i+1, \dots, n) = 0. \quad (7.33)$$

The structure of the identity (7.33) involving two generalised particles is analogous to the one of the BCJ identities for QCD amplitudes with massive quarks [148, 149].

7.4 Coefficient relations for one-loop amplitudes in d dimensions

7.4.1 Relations for pentagon coefficients

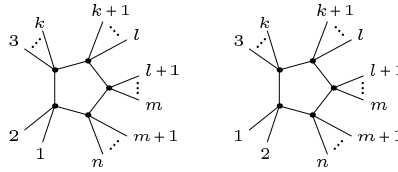


Figure 7.7: Pentagon topologies for the cuts $C_{12|3\dots k|(k+1)\dots l|(l+1)\dots m|(m+1)\dots n}$ and $C_{21|3\dots k|(k+1)\dots l|(l+1)\dots m|(m+1)\dots n}$.

We recall the extraction of the pentagon coefficient,

$$C_{i|j|k|l|m}^\pm = \frac{\mathcal{N}(l^\pm, \mu^2)}{\prod_{h \neq i_1, \dots, i_5} D_h} = c^{(ijklm)^\pm} \mu^2, \quad (7.34)$$

In order to see how the BCJ identities for tree-level amplitudes can be used to relate different pentagon coefficients, let us consider the contributions shown in Fig. 7.7, which share the same cut solutions. In addition, since these two pentagons differ in the ordering of the external particles p_1 and p_2 only, they can be obtained as the product of the same tree-level amplitudes, with the only exception of the colour-ordering of the four-point amplitude involving p_1 and p_2 . More precisely, for the ordering $\{1, 2, \dots, n\}$ we have

$$\begin{aligned} C_{12|3\dots k|(k+1)\dots l|(l+1)\dots m|(m+1)\dots n}^\pm &= A_4^{\text{tree}}(-l_1^\pm, 1, 2, l_3^\pm) A_k^{\text{tree}}(-l_3^\pm, P_{3\dots k}, l_{k+1}^\pm) A_{l-k+2}^{\text{tree}}(-l_{k+1}^\pm, P_{k+1\dots l}, l_l^\pm) \\ &\times A_{m-l+2}^{\text{tree}}(-l_{l+1}^\pm, P_{l+1\dots m}, l_m^\pm) A_{n-m+2}^{\text{tree}}(-l_{m+1}^\pm, P_{m+1\dots n}, l_1^\pm) \end{aligned} \quad (7.35)$$

and $C_{21|3\dots k|(k+1)\dots l|(l+1)\dots m|(m+1)\dots n}^\pm$ is obtained just by changing $1 \leftrightarrow 2$. The tree-level amplitudes $A_4^{\text{tree}}(-l_1^\pm, 1, 2, l_3^\pm)$ and $A_4^{\text{tree}}(-l_1^\pm, 2, 1, l_3^\pm)$ are related by the d -dimensional BCJ identity (7.32),

$$A_4^{\text{tree}}(-l_1^\pm, 2, 1, l_3^\pm) = \frac{P_{l_3^\pm 2}^2 - \mu^2}{P_{-l_1^\pm 2}^2 - \mu^2} A_4^{\text{tree}}(-l_1^\pm, 1, 2, l_3^\pm), \quad (7.36)$$

which, substituted into the expression of $C_{21|3\dots k|(k+1)\dots l|(l+1)\dots m|(m+1)\dots n}^\pm$, allow us to identify

$$C_{21|3\dots k|(k+1)\dots l|(l+1)\dots m|(m+1)\dots n}^\pm = \frac{P_{l_3^\pm 2}^2 - \mu^2}{P_{-l_1^\pm 2}^2 - \mu^2} C_{12|3\dots k|(k+1)\dots l|(l+1)\dots m|(m+1)\dots n}^\pm. \quad (7.37)$$

The ratio of the two propagators appearing in (7.37) evaluates to same constant value for both cut solutions,

$$\frac{P_{l_3^\pm 2}^2 - \mu^2}{P_{-l_1^\pm 2}^2 - \mu^2} = \alpha, \quad (7.38)$$

so that, by making use of (7.34), (7.37) becomes

$$c^{(21|\dots)^\pm} = \alpha c^{(12|\dots)^\pm}. \quad (7.39)$$

Therefore, as simple byproduct of the BCJ identities at tree-level, the knowledge of a single pentagon coefficient completely determines the other one.

7.4.2 Relations for box coefficients

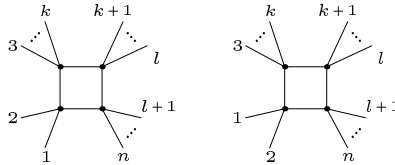


Figure 7.8: Box topologies for the cuts $C_{12|3\dots k|k+1\dots l|l+1\dots n}$ and $C_{21|3\dots k|k+1\dots l|l+1\dots n}$.

Next we consider the box contribution to the amplitude. We recall the extraction of two non-spurious coefficients $c_0^{(ijkl)}$ and $c_4^{(ijkl)}$,

$$C_{i|j|k|l}^\pm = \frac{N_\pm}{\prod_{h \neq i,j,k,l} D_{h,\pm}} \Big|_{\mu^2 \rightarrow 0} = c_0^{(ijkl)\pm}, \quad c_0^{(ijkl)} = \frac{1}{2} (c_0^{(ijkl)+} + c_0^{(ijkl)-}), \quad (7.40a)$$

$$C_{i|j|k|l}^\pm = \frac{N_\pm}{\prod_{h \neq i,j,k,l} D_{h,\pm}} \Big|_{\mu^2 \rightarrow \infty} = c_4^{(ijkl)\pm} \mu^4 + \mathcal{O}(\mu^3), \quad c_4^{(ijkl)} \equiv c_4^{(ijkl)+} = c_4^{(ijkl)-}. \quad (7.40b)$$

Analogously to the pentagon case, we consider two box topologies differing just from the ordering of the external particles p_1 and p_2 , as depicted in Fig. 7.8. When the integrand associated to the ordering $\{1, 2, \dots, n\}$ is evaluated on the on-shell solutions it factorises into

$$C_{12|3\dots k|(k+1)\dots l|(l+1)\dots n}^\pm = A_4^{\text{tree}}(-l_1^\pm, 1, 2, l_3^\pm) A_k^{\text{tree}}(-l_3^\pm, P_{3\dots k}, l_{k+1}^\pm) A_{l-k+2}^{\text{tree}}(-l_{k+1}^\pm, P_{k+1\dots l}, l_{l+1}^\pm) \\ \times A_{n-l+2}^{\text{tree}}(-l_{l+1}^\pm, P_{l+1\dots n}, l_1^\pm) \quad (7.41)$$

and the expression of $C_{21|3\dots k|(k+1)\dots l|(l+1)\dots n}^\pm$ in terms of tree-level amplitudes can be obtained by exchanging $1 \leftrightarrow 2$. Therefore, thanks to the BCJ identity between tree-level amplitudes (7.36), we can write

$$C_{21|3\dots k|(k+1)\dots l|(l+1)\dots n}^\pm = \frac{P_{l_3^\pm 2}^2 - \mu^2}{P_{-l_1^\pm 2}^2 - \mu^2} C_{12|3\dots k|(k+1)\dots l|(l+1)\dots n}^\pm. \quad (7.42)$$

It can be verified that the ratio of propagators sampled on the cut solutions converges to a constant both for $\mu^2 \rightarrow 0$ and $\mu^2 \rightarrow \infty$ limits,

$$\left. \frac{P_{l_3^\pm 2}^2 - \mu^2}{P_{-l_1^\pm 2}^2 - \mu^2} \right|_{\mu^2 \rightarrow 0} = \alpha_0^\pm, \quad (7.43)$$

$$\left. \frac{P_{l_3^\pm 2}^2 - \mu^2}{P_{-l_1^\pm 2}^2 - \mu^2} \right|_{\mu^2 \rightarrow \infty} = \alpha_4^\pm + \mathcal{O}\left(\frac{1}{\mu}\right), \quad (7.44)$$

so that, by evaluating both sides of (7.42) in the two limits, we can trivially obtain the contributions from $C_{21|3\dots k|(k+1)\dots l|(l+1)\dots n}$, once $C_{12|3\dots k|(k+1)\dots l|(l+1)\dots n}$ has been calculated,

$$c_i^{(21|\dots)^\pm} = \alpha_i^\pm c_i^{(12|\dots)^\pm}, \quad i = 0, 4. \quad (7.45)$$

7.4.3 Relations for triangle coefficients

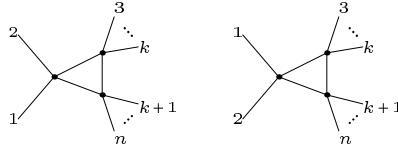


Figure 7.9: Triangle topologies for the cuts $C_{12|3\dots k|(k+1)\dots n}$ and $C_{21|3\dots k|(k+1)\dots n}$.

As discussed in Sec. 7.4.3, by considering the expansion of the integrand in the large- t limit,

$$C_{i|j|k}^\pm(t, \mu^2) = \left. \frac{N_\pm}{\prod_{h \neq i, j, k} D_{h, \pm}} \right|_{t \rightarrow \infty} = \sum_{m=0}^3 c_{m,0}^{(ijk)^\pm} t^m + \mu^2 \sum_{m=0}^1 c_{m,2}^{(ijk)^\pm} t^m. \quad (7.46)$$

The C/K-duality for tree-level amplitudes can be used to relate all coefficients of the expansions (7.46) for different triangles. As an example, we consider the two triangle contributions depicted in Fig. 7.9. When evaluated on the on-shell solutions, the triangle with external ordering $\{1, 2, \dots, n\}$ factorises into

$$C_{12|3\dots k|(k+1)\dots n}^\pm = A_4^{\text{tree}}(-l_1^\pm, 1, 2, l_3^\pm) A_k^{\text{tree}}(-l_3^\pm, P_{3\dots k}, l_{k+1}^\pm) A_{n-k+2}^{\text{tree}}(-l_{k+1}^\pm, P_{k+1\dots n}, l_1^\pm) \quad (7.47a)$$

and the analogous expression for $C_{21|3\dots k|(k+1)\dots n}^\pm$ is obtained by changing $1 \leftrightarrow 2$. As for the previous cases, we can make use of the BCJ identity (7.36) in order to establish a relation between $C_{21|3\dots k|(k+1)\dots n}^\pm$ and $C_{12|3\dots k|(k+1)\dots n}^\pm$,

$$C_{21|3\dots k|(k+1)\dots n}^\pm = \frac{P_{l_3^\pm 2}^2 - \mu^2}{P_{-l_1^\pm 2}^2 - \mu^2} C_{12|3\dots k|(k+1)\dots n}^\pm. \quad (7.48)$$

According to the expansion (7.46), both $C_{21|3\dots k|(k+1)\dots n}^\pm$ and $C_{12|3\dots k|(k+1)\dots n}^\pm$ can be parametrised as

$$\begin{aligned} C_{12|3\dots k|(k+1)\dots n}^\pm &= \sum_{m=0}^3 c_{m,0}^{(12|\dots)^\pm} t^m + \mu^2 \sum_{m=0}^1 c_{m,2}^{(12|\dots)^\pm} t^m, \\ C_{21|3\dots k|(k+1)\dots n}^\pm &= \sum_{m=0}^3 c_{m,0}^{(21|\dots)^\pm} t^m + \mu^2 \sum_{m=0}^1 c_{m,2}^{(21|\dots)^\pm} t^m. \end{aligned} \quad (7.49)$$

There, if we consider the large- t limit of the ratio of the two propagators evaluated on the cut solution, which is found in the form

$$\left. \frac{P_{l_3^\pm 2}^2 - \mu^2}{P_{-l_1^\pm 2}^2 - \mu^2} \right|_{t \rightarrow \infty} = \sum_{m=-3}^0 \alpha_{m,0}^\pm t^m + \mu^2 \sum_{m=-3}^{-2} \alpha_{m,2}^\pm t^m + \mathcal{O}\left(\frac{1}{t^4}\right), \quad (7.50)$$

we can insert the expansions (7.49) and (7.50) into (7.48) and, by matching each monomial between the two sides, obtain the set of relations

$$c_{m,0}^{(21|\dots)^\pm} = \sum_{l=0}^{3-m} \alpha_{-l,0}^\pm c_{l+m,0}^{(12|\dots)^\pm}, \quad c_{m,2}^{(21|\dots)^\pm} = \sum_{l=0}^{1-m} \left(\alpha_{-l-2,2}^\pm c_{l+m+2,0}^{(12|\dots)^\pm} + \alpha_{-l,0}^\pm c_{l+m,2}^{(12|\dots)^\pm} \right). \quad (7.51)$$

Eqs. (7.51) show that $C_{21|3\dots k|(k+1)\dots n}^\pm$ can be fully reconstructed from the knowledge of $C_{12|3\dots k|(k+1)\dots n}^\pm$.

7.4.4 Relations for bubble coefficients

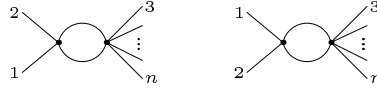


Figure 7.10: Bubble topologies for the cuts $C_{12|3\dots n}$ and $C_{21|3\dots n}$.

Finally, the bubble contribution is obtained by extracting the coefficients from the large- t expansion,

$$C_{ij}^\pm(t, y, \mu^2) = \left. \frac{N_\pm}{\prod_{h \neq i,j} D_{h,\pm}} - \sum_{k \neq i,j} \frac{\Delta_{ijk,\pm}}{D_{k,+}} \right|_{t \rightarrow \infty} = \sum_{l=0}^2 \sum_{m=0}^{2-l} c_{l,m,0}^{(ij)^\pm} t^l y^m + \mu^2 c_{0,0,2}^{(ij)^\pm}. \quad (7.52)$$

As usual, in order to show the role of the C/K-duality in the reduction of the number of coefficients to be actually computed, we consider two bubble contributions differing by the ordering of the external particles p_1 and p_2 , as illustrated in Fig. 7.10. The two coefficients are given by

$$\begin{aligned} C_{12|3\dots n}^\pm &= A_4^{\text{tree}}(-l_1^\pm, 1, 2, l_3^\pm) A_n^{\text{tree}}(-l_3^\pm, P_{3\dots n}, l_1^\pm), \\ C_{21|3\dots n}^\pm &= A_4^{\text{tree}}(-l_1^\pm, 2, 1, l_3^\pm) A_n^{\text{tree}}(-l_3^\pm, P_{3\dots n}, l_1^\pm) \end{aligned} \quad (7.53)$$

and, using (7.36) to relate $A_4^{\text{tree}}(-l_1^\pm, 1, 2, l_3^\pm)$ and $A_4^{\text{tree}}(-l_1^\pm, 2, 1, l_3^\pm)$, we obtain

$$C_{21|3\dots n}^\pm = \frac{P_{l_3^\pm 2}^2 - \mu^2}{P_{-l_1^\pm 2}^2 - \mu^2} C_{12|3\dots n}^\pm. \quad (7.54)$$

The ratio of the two propagators in the large- t limit is parametrised as

$$\left. \frac{P_{l_3^\pm 2}^2 - \mu^2}{P_{-l_1^\pm 2}^2 - \mu^2} \right|_{t \rightarrow \infty} = \sum_{l=-2}^0 \sum_{m=0}^{-l} \alpha_{l,m,0} t^l y^m + \frac{\mu^2}{t^2} \alpha_{-2,0,2} + \mathcal{O}\left(\frac{1}{t^3}\right), \quad (7.55)$$

so that, by plugging in (7.54) the expansions

$$\begin{aligned} C_{12|3\dots n}^\pm &= \sum_{l=0}^2 \sum_{m=0}^{2-l} c_{l,m,0}^{(12|\dots)^\pm} t^l y^m + \mu^2 c_{0,0,2}^{(12|\dots)^\pm}, \\ C_{21|3\dots n}^\pm &= \sum_{l=0}^2 \sum_{m=0}^{2-l} c_{l,m,0}^{(21|\dots)^\pm} t^l y^m + \mu^2 c_{0,0,2}^{(21|\dots)^\pm}, \end{aligned} \quad (7.56)$$

one can verify that the coefficients of $C_{21|3\dots n}^\pm$ are completely determined by

$$\begin{aligned} c_{l,m,0}^{(21|\dots)^\pm} &= \sum_{r=l}^2 \left(\sum_{s=\max[0,l+m-r]}^{\min[m,2-r]} \alpha_{l-r,m-s,0}^\pm c_{r,s,0}^{(12|\dots)^\pm} \right), \\ c_{0,0,2}^{(21|\dots)^\pm} &= \alpha_{-2,0,2}^\pm c_{2,0,0}^{(12|\dots)^\pm} + \alpha_{0,0,0}^\pm c_{0,0,2}^{(12|\dots)^\pm}. \end{aligned} \quad (7.57)$$

7.4.5 Examples

We hereby verify on some explicit examples the coefficient relations we have derived in the previous section. In order to obtain compact expressions and keep the discussion as simple possible, we consider scalar loop contributions to gluon amplitudes only and we present analytic results for convenient helicity configurations. Nevertheless, numerical checks of the coefficient relations have been performed for all helicity configurations and gluon loop contributions have been included as well. All results presented in this section have been numerically validated against the ones provided by the C++ library NJET [56].

In addition, we would like to mention that, besides constituting one of the FDF ingredients needed for the computation of the full amplitude, the scalar contributions presented in this section can be thought as the generators of rational terms in alternative frameworks, such as supersymmetric decomposition [255, 293].

Pentagons

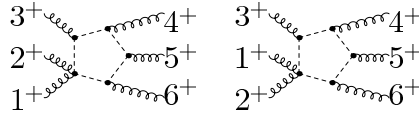


Figure 7.11: Pentagon topologies for the cuts $C_{12|3|4|5|6}$ and $C_{21|3|4|5|6}$.

To begin with, we consider the six-gluon helicity amplitude $\mathcal{A}_6^{1\text{-loop}}(1^+, 2^+, 3^+, 4^+, 5^+, 6^+)$ and we compute the quintuple cuts $C_{12|3|4|5|6}^\pm$ and $C_{21|3|4|5|6}^\pm$ of Fig. 7.11, with the use the basis $\mathcal{E}^{(45012)} = \{e_1, e_2, e_3, e_4\}$, where

$$e_1^\nu = p_4^\nu, \quad e_2^\nu = p_5^\nu, \quad e_3^\nu = \frac{1}{2} \langle 4 | \gamma^\mu | 5 \rangle, \quad e_4^\nu = \frac{1}{2} \langle 5 | \gamma^\mu | 4 \rangle, \quad (7.58)$$

The solutions of the quintuple cut are

$$l_5^{+\nu} = c e_3^\nu - \frac{\mu^2}{s_{45}c} e_4^\nu, \quad l_5^{-\nu} = c e_4^\nu - \frac{\mu^2}{s_{45}c} e_3^\nu, \quad (7.59)$$

where the parameters c and μ^2 are fixed by the on-shell conditions. From the product of tree-level amplitudes we obtain

$$\begin{aligned} C_{12|3|4|5}^\pm &= A_4^{\text{tree}}(-l_1^\pm, 1^+, 2^+, l_3^\pm) A_3^{\text{tree}}(-l_3^\pm, 3^+, l_4^\pm) A_3^{\text{tree}}(-l_4^\pm, 4^+, l_5^\pm) A_3^{\text{tree}}(-l_5^\pm, 5^+, l_6^\pm) A_3^{\text{tree}}(-l_6^\pm, 6^+, l_1^\pm) \\ &= \frac{i\mu^2 [2|1]\langle 3|l_5|4\rangle\langle 4|l_4|3\rangle\langle 5|l_1|6\rangle\langle 6|l_6|5\rangle}{\langle 1|2\rangle\langle 3|4\rangle^2\langle 5|6\rangle^2\langle 1|l_1|1\rangle} \end{aligned} \quad (7.60)$$

and

$$\begin{aligned} C_{21|3|4|5}^\pm &= A_4^{\text{tree}}(-l_1^\pm, 2^+, 1^+, l_3^\pm) A_3^{\text{tree}}(-l_3^\pm, 3^+, l_4^\pm) A_3^{\text{tree}}(-l_4^\pm, 4^+, l_5^\pm) A_3^{\text{tree}}(-l_5^\pm, 5^+, l_6^\pm) A_3^{\text{tree}}(-l_6^\pm, 6^+, l_1^\pm), \\ &= \frac{i\mu^2 [2|1]\langle 3|l_5|4\rangle\langle 4|l_4|3\rangle\langle 5|l_1|6\rangle\langle 6|l_6|5\rangle}{\langle 1|2\rangle\langle 3|4\rangle^2\langle 5|6\rangle^2\langle 2|l_1|2\rangle}. \end{aligned} \quad (7.61)$$

The two cuts are related by the BCJ identity (7.37),

$$C_{21|3|4|5}^\pm = \frac{(l_3^\pm + p_2)^2 - \mu^2}{(l_1^\pm - p_2)^2 - \mu^2} C_{\pm 12|3|4|5|6}^\pm. \quad (7.62)$$

By using momentum conservation to express l_5^\pm in terms of $l_1^\pm, l_3^\pm, l_4^\pm$,

$$l_1^\pm = l_5^\pm - p_5 - p_6, \quad l_3^\pm = l_5^\pm + p_3 + p_4, \quad l_4^\pm = l_5^\pm + p_4, \quad l_6^\pm = l_5^\pm - p_5, \quad (7.63)$$

one can verify that $C_{12|3|4|5|6}^\pm$ takes the form

$$C_{12|3|4|5|6}^\pm = \frac{i\mu^2 s_{34}^2 s_{45}^2 s_{56}^2 [2|1][4|3][6|5]\langle 3|1+2|6\rangle^2 \langle 6|1+2|3\rangle^2}{\text{tr}_5(6, 3, 5, 4)^3 \langle 1|2\rangle\langle 3|4\rangle\langle 5|6\rangle (s_{45}\text{tr}_5(1, 5, 2, 6) + s_{345}\text{tr}_5(1, 5, 4, 6) - s_{16}\text{tr}_5(3, 4, 5, 6))}, \quad (7.64)$$

where $s_{ij} = \langle ij\rangle\langle ji\rangle$ and $\text{tr}_5(1, 2, 3, 4) = \langle 1|234|1\rangle - \langle 1|432|1\rangle$.

In a similar way, according to (7.38), we find

$$\frac{(l_3^\pm + p_2)^2 - \mu^2}{(l_1^\pm - p_2)^2 - \mu^2} = \frac{s_{45}\text{tr}_5(1, 5, 2, 6) + s_{345}\text{tr}_5(1, 5, 4, 6) - s_{16}\text{tr}_5(3, 4, 5, 6)}{s_{45}\text{tr}_5(2, 5, 1, 6) + s_{345}\text{tr}_5(2, 5, 4, 6) - s_{26}\text{tr}_5(3, 4, 5, 6)}. \quad (7.65)$$

Hence, substituting (7.64) and (7.65) in (7.62), we obtain

$$C_{21|3|4|5|6}^\pm = \frac{i\mu^2 s_{34}^2 s_{45}^2 s_{56}^2 [2|1][4|3][6|5]\langle 3|1+2|6\rangle^2 \langle 6|1+2|3\rangle^2}{\text{tr}_5(6, 3, 5, 4)^3 \langle 1|2\rangle\langle 3|4\rangle\langle 5|6\rangle (s_{45}\text{tr}_5(2, 5, 1, 6) + s_{345}\text{tr}_5(2, 5, 4, 6) - s_{26}\text{tr}_5(3, 4, 5, 6))}, \quad (7.66)$$

which reproduces the same result one could obtain from similar algebraic manipulations on (7.61). The analytic expressions for the two cuts find numerical agreement with NJET.

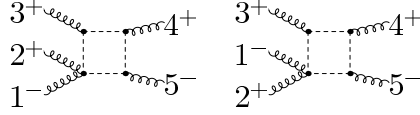


Figure 7.12: Box topologies for the cuts $C_{12|3|4|5}$ and $C_{21|3|4|5}$.

Boxes

As an example of identities between box coefficients, we consider the quadruple cuts $C_{12|3|4|5}^\pm$ and $C_{21|3|4|5}^\pm$ for the helicity amplitude $\mathcal{A}_5^{1\text{-loop}}(1^-, 2^+, 3^+, 4^+, 5^-)$, depicted in Fig. 7.12. For this configuration we use the basis $\mathcal{E}^{(40123)}$ of eq. (7.58), where the cut solutions can be parametrised as

$$l_5^{+\nu} = c_+ e_3^\nu - \frac{\mu^2}{s_{45}c_+} e_4^\nu, \quad l_5^{-\nu} = c_- e_4^\nu - \frac{\mu^2}{s_{45}c_-} e_3^\nu, \quad (7.67)$$

being c_+ and c_- coefficients determined by behaviour of the on-shell solutions for $\mu^2 \rightarrow 0$ and $\mu^2 \rightarrow \infty$. By combining tree-level amplitudes we can write

$$\begin{aligned} C_{12|3|4|5}^\pm &= A_4^{\text{tree}}(-l_1^\pm, 1^-, 2^+, l_3^\pm) A_3^{\text{tree}}(-l_3^\pm, 3^+, l_4^\pm) A_3^{\text{tree}}(-l_4^\pm, 4^+, l_5^\pm) A_3^{\text{tree}}(-l_5^\pm, 5^-, l_1^\pm) \\ &= \frac{\langle 1|l_1|2\rangle^2 \langle 3|l_5|4\rangle \langle 4|l_4|3\rangle \langle 5|l_1|1\rangle}{s_{12}[5|1]\langle 3|4\rangle^2 \langle 1|l_1|1\rangle} \end{aligned} \quad (7.68)$$

and

$$\begin{aligned} C_{21|3|4|5}^\pm &= A_4^{\text{tree}}(-l_1^\pm, 2^+, 1^-, l_3^\pm) A_3^{\text{tree}}(-l_3^\pm, 3^+, l_4^\pm) A_3^{\text{tree}}(-l_4^\pm, 4^+, l_5^\pm) A_3^{\text{tree}}(-l_5^\pm, 5^-, l_1^\pm) \\ &= \frac{\langle 1|l_1|2\rangle^2 \langle 3|l_5|4\rangle \langle 4|l_4|3\rangle \langle 5|l_1|1\rangle}{s_{12}[5|1]\langle 3|4\rangle^2 \langle 2|l_1|2\rangle} \end{aligned} \quad (7.69)$$

and then relate two cuts through (7.42),

$$C_{21|3|4|5}^\pm = \frac{(l_3^\pm + p_2)^2 - \mu^2}{(l_1^\pm - p_2)^2 - \mu^2} C_{12|3|4|5}^\pm. \quad (7.70)$$

Momentum conservation allows us to write

$$l_1^\pm = l_5^\pm - p_5, \quad l_4^\pm = l_5^\pm + p_4, \quad l_3 = l_5^\pm + p_3 + p_4 \quad (7.71)$$

and, consequently, to express $C_{12|3|4|5}^\pm$ as

$$C_{12|3|4|5}^\pm = -\frac{i\mu^4[4|3]\text{tr}_5(\eta_{1,2}, 4, 3, 5)^2}{s_{12}\text{tr}_5(3, 4, 1, 5)[5|3][5|4]\langle 3|4\rangle^2}, \quad (7.72)$$

where we have introduced the complex momenta $\eta_{i,j}^\nu = \frac{1}{2} \langle i|\gamma^\nu|j\rangle$. We have verified that, for this particular helicity configuration, the box coefficient is given by the $\sim \mu^4$ term only. Therefore, we just need to compute the ratio of the propagators in the large- μ^2 limit,

$$\left. \frac{(l_3^\pm + p_2)^2 - \mu^2}{(l_1^\pm - p_2)^2 - \mu^2} \right|_{\mu^2 \rightarrow \infty} = -1 + \mathcal{O}\left(\frac{1}{\mu}\right). \quad (7.73)$$

Thanks to this result, the expression for $C_{21|3|4|5}$ obtained from (7.72) is

$$C_{21|3|4|5}^\pm = \frac{i\mu^4[4|3]\text{tr}_5(\eta_{1,2}, 4, 3, 5)^2}{s_{12}\text{tr}_5(3, 4, 1, 5)[5|3][5|4]\langle 3|4\rangle^2}, \quad (7.74)$$

which finds again agreement with NJET.

Triangles

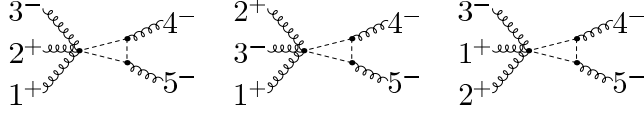


Figure 7.13: Triangle topologies for the cuts $C_{123|4|5}$, $C_{132|4|5}$ and $C_{213|4|5}$.

For triple cuts we give an example of the coefficient relations obtained through identities between five-point tree-level amplitudes, which are discussed in App. C. Let us consider $\mathcal{A}_5^{1\text{-loop}}(1^+, 2^+, 3^-, 4^-, 5^-)$ and the three cuts of Fig. 7.13, $C_{213|4|5}^\pm$, $C_{123|4|5}^\pm$ and $C_{132|4|5}^\pm$, respectively. We use the basis $\mathcal{E}^{(40123)}$ of eq. (7.58), where the cut solutions are given by

$$l_5^{+\nu} = t e_3^\nu - \frac{\mu^2}{s_{45}t} e_4^\nu, \quad l_5^{-\nu} = t e_4^\nu - \frac{\mu^2}{s_{45}t} e_3^\nu, \quad (7.75)$$

and from the product of tree-level amplitudes we obtain

$$\begin{aligned} C_{123|4|5}^\pm &= A_5^{\text{tree}}(-l_1^\pm, 1^+, 2^+, 3^-, l_4^\pm) A_3^{\text{tree}}(-l_4^\pm, 4^-, l_5^\pm) A_3^{\text{tree}}(-l_5^\pm, 5^-, l_1^\pm) \\ &= \frac{i\langle 5|l_1^\pm|4|l_5^\pm|5\rangle\langle 3|1+2|l_1^\pm|3\rangle^2}{s_{123}[5|4]^2\langle 1|2\rangle\langle 2|3\rangle\langle 1|l_1^\pm|1+2|3\rangle} - \frac{i\mu^2[2|1]\langle 3|l_4^\pm|2\rangle^2\langle 5|l_1^\pm|4|l_5|5\rangle}{[5|4]^2[3|l_4^\pm|3|2]\langle 1|l_1^\pm|1\rangle\langle 1|2+3|l_4^\pm|3\rangle}, \end{aligned} \quad (7.76)$$

$$\begin{aligned} C_{132|4|5}^\pm &= A_5^{\text{tree}}(-l_1^\pm, 1^+, 3^-, 2^+, l_4^\pm) A_3^{\text{tree}}(-l_4^\pm, 4^-, l_5^\pm) A_3^{\text{tree}}(-l_5^\pm, 5^-, l_1^\pm) \\ &= -\frac{i\langle 3|l_1^\pm|1\rangle^2\langle 3|l_4^\pm|2\rangle^2\langle 5|l_1^\pm|4|l_5^\pm|5\rangle}{[5|4]^2[2|l_4^\pm|2+3|1]\langle 1|l_1^\pm|1|3\rangle\langle 2|l_4^\pm|2|3\rangle} - \frac{i\mu^2[2|1]^4\langle 5|l_1^\pm|4|l_5^\pm|5\rangle}{s_{123}[3|1][3|2][5|4]^2[2|l_4|2+3|1]}, \end{aligned} \quad (7.77)$$

$$\begin{aligned} C_{213|4|5}^\pm &= A_5^{\text{tree}}(-l_1^\pm, 2^+, 1^+, 3^-, l_4^\pm) A_3^{\text{tree}}(-l_4^\pm, 4^-, l_5^\pm) A_3^{\text{tree}}(-l_5^\pm, 5^-, l_1^\pm) \\ &= -\frac{i\langle 5|l_1^\pm|4|l_5^\pm|5\rangle\langle 3|1+2|l_1^\pm|3\rangle^2}{s_{123}[5|4]^2\langle 1|2\rangle\langle 1|3\rangle\langle 2|l_1^\pm|1+2|3\rangle} + \frac{i\mu^2[2|1]\langle 3|l_4^\pm|1\rangle^2\langle 5|l_1^\pm|4|l_5^\pm|5\rangle}{[5|4]^2[3|l_4^\pm|3|1]\langle 2|l_1^\pm|2\rangle\langle 2|1+3|l_4^\pm|3\rangle} \end{aligned} \quad (7.78)$$

The three cuts are related by the BCJ identity (7.30),

$$C_{213|4|5}^\pm = \frac{\left(P_{l_4^\pm 2}^2 - \mu^2 + P_{23}^2\right)}{\left(P_{-l_1^\pm 2}^2 - \mu^2\right)} C_{123|4|5}^\pm + \frac{\left(P_{l_4^\pm 2}^2 - \mu^2\right)}{\left(P_{-l_1^\pm 2}^2 - \mu^2\right)} C_{132|4|5}^\pm. \quad (7.79)$$

By using momentum conservation,

$$l_1^\pm = l_5^\pm - p_5, \quad l_4^\pm = l_5^\pm + p_4, \quad (7.80)$$

and expanding $C_{123|4|5}^\pm$ and $C_{132|4|5}^\pm$ for $t \rightarrow \infty$, we obtain

$$C_{123|4|5}^+(t, \mu^2) = \frac{i\mu^2\langle 3|4\rangle^2(\langle 1|4\rangle\langle 3|5\rangle + \langle 1|3\rangle\langle 4|5\rangle)}{[5|4]\langle 1|2\rangle\langle 1|4\rangle^2\langle 2|3\rangle} - \frac{i\mu^2\langle 3|4\rangle^3}{[5|4]\langle 1|2\rangle\langle 1|4\rangle\langle 2|3\rangle}t, \quad (7.81a)$$

$$C_{123|4|5}^-(t, \mu^2) = \frac{i\mu^2\langle 3|4\rangle\langle 3|5\rangle^2}{[5|4]\langle 1|2\rangle\langle 1|5\rangle\langle 2|3\rangle} + \frac{i\mu^2\langle 3|5\rangle^3}{[5|4]\langle 1|2\rangle\langle 1|5\rangle\langle 2|3\rangle}t, \quad (7.81b)$$

$$C_{132|4|5}^+(t, \mu^2) = -\frac{i\mu^2\langle 3|4\rangle^3(\langle 1|4\rangle\langle 3|5\rangle + \langle 1|3\rangle\langle 4|5\rangle)}{[5|4]\langle 1|3\rangle\langle 1|4\rangle^2\langle 2|3\rangle\langle 2|4\rangle} + \frac{i\mu^2\langle 3|4\rangle^4}{[5|4]\langle 1|3\rangle\langle 1|4\rangle\langle 2|3\rangle\langle 2|4\rangle}t, \quad (7.81c)$$

$$C_{132|4|5}^-(t, \mu^2) = -\frac{i\mu^2(\langle 2|5\rangle\langle 3|4\rangle - \langle 2|3\rangle\langle 4|5\rangle)\langle 3|5\rangle^3}{[5|4]\langle 1|3\rangle\langle 1|5\rangle\langle 2|3\rangle\langle 2|5\rangle^2} - \frac{i\mu^2\langle 3|5\rangle^4}{[5|4]\langle 1|3\rangle\langle 1|5\rangle\langle 2|3\rangle\langle 2|5\rangle}t. \quad (7.81d)$$

In a similar way, the expansion for large- t of the ratio of propagators returns

$$\left. \frac{\left(P_{l_4^+ 2}^2 - \mu^2 + P_{23}^2\right)}{\left(P_{-l_1^+ 2}^2 - \mu^2\right)} \right|_{t \rightarrow \infty} = \frac{\mu^2 s_{12} s_{24} s_{25}}{s_{45} t^3 \langle 4|2|5 \rangle^3} + \frac{s_{12} s_{25}^2}{t^3 \langle 4|2|5 \rangle^3} + \frac{s_{12} s_{25}}{t^2 \langle 4|2|5 \rangle^2} + \frac{s_{12}}{t \langle 4|2|5 \rangle} - 1 + \mathcal{O}\left(\frac{1}{t^4}\right), \quad (7.82a)$$

$$\left. \frac{\left(P_{l_4^- 2}^2 - \mu^2 + P_{23}^2\right)}{\left(P_{-l_1^- 2}^2 - \mu^2\right)} \right|_{t \rightarrow \infty} = \frac{\mu^2 s_{12} s_{24} s_{25}}{s_{45} t^3 \langle 5|2|4 \rangle^3} + \frac{s_{12} s_{25}^2}{t^3 \langle 5|2|4 \rangle^3} + \frac{s_{12} s_{25}}{t^2 \langle 5|2|4 \rangle^2} + \frac{s_{12}}{t \langle 5|2|4 \rangle} - 1 + \mathcal{O}\left(\frac{1}{t^4}\right), \quad (7.82b)$$

$$\begin{aligned} \left. \frac{\left(P_{l_4^+ 2}^2 - \mu^2\right)}{\left(P_{-l_1^+ 2}^2 - \mu^2\right)} \right|_{t \rightarrow \infty} &= -\frac{\mu^2 s_{24} s_{25} (s_{24} + s_{25})}{s_{45} t^3 \langle 4|2|5 \rangle^3} - \frac{s_{25}^2 (s_{24} + s_{25})}{t^3 \langle 4|2|5 \rangle^3} - \frac{s_{25} (s_{24} + s_{25})}{t^2 \langle 4|2|5 \rangle^2} \\ &\quad - \frac{s_{24} + s_{25}}{t \langle 4|2|5 \rangle} - 1 + \mathcal{O}\left(\frac{1}{t^4}\right), \end{aligned} \quad (7.82c)$$

$$\begin{aligned} \left. \frac{\left(P_{l_4^- 2}^2 - \mu^2\right)}{\left(P_{-l_1^- 2}^2 - \mu^2\right)} \right|_{t \rightarrow \infty} &= -\frac{\mu^2 s_{24} s_{25} (s_{24} + s_{25})}{s_{45} t^3 \langle 5|2|4 \rangle^3} - \frac{s_{25}^2 (s_{24} + s_{25})}{t^3 \langle 5|2|4 \rangle^3} - \frac{s_{25} (s_{24} + s_{25})}{t^2 \langle 5|2|4 \rangle^2} \\ &\quad - \frac{s_{24} + s_{25}}{t \langle 5|2|4 \rangle} - 1 + \mathcal{O}\left(\frac{1}{t^4}\right). \end{aligned} \quad (7.82d)$$

Therefore, by inserting these results into (7.79) we obtain

$$C_{213|4|5}^+(t, \mu^2) = -\frac{i\mu^2 \langle 3|4 \rangle^2 (\langle 2|4 \rangle \langle 3|5 \rangle + \langle 2|3 \rangle \langle 4|5 \rangle)}{[5|4] \langle 1|2 \rangle \langle 1|3 \rangle \langle 2|4 \rangle^2} + \frac{i\mu^2 \langle 3|4 \rangle^3}{[5|4] \langle 1|2 \rangle \langle 1|3 \rangle \langle 2|4 \rangle} t, \quad (7.83)$$

$$C_{213|4|5}^-(t, \mu^2) = -\frac{i\mu^2 \langle 3|4 \rangle \langle 3|5 \rangle^2}{[5|4] \langle 1|2 \rangle \langle 1|3 \rangle \langle 2|5 \rangle} - \frac{i\mu^2 \langle 3|5 \rangle^3}{[5|4] \langle 1|2 \rangle \langle 1|3 \rangle \langle 2|5 \rangle} t, \quad (7.84)$$

which agrees with the $t \rightarrow \infty$ expansion of (7.81d). The resulting contributions of the three cuts to $\mathcal{A}_5^{1\text{-loop}}(1^+, 2^+, 3^-, 4^-, 5^-)$ have been numerically checked with NJET.

Bubbles

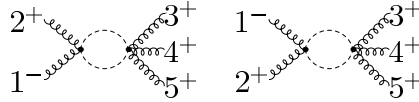


Figure 7.14: Bubble topologies for the cuts $C_{12|345}$ and $C_{21|345}$.

As a final example, we compute the double cuts $C_{12|345}$ and $C_{21|345}$ of the helicity amplitude $\mathcal{A}_5^{1\text{-loop}}(1^-, 2^+, 3^+, 4^+, 5^+)$, which are depicted in Fig. 7.14. For sake of simplicity, we will consider only pure bubble contributions but we remark that spurious terms originating from triangles, which should be subtracted in order to recover the full integral coefficient, can be related through the BCJ identities in the same way as discussed in Section 7.4.4. For this cut we use the basis $\mathcal{E}^{(02)} = \{e_1, e_2, e_3, e_4\}$, where

$$e_1^\nu = (p_1 + p_2)^\nu - \frac{s_{12}}{s_{14} + s_{24}} p_4^\nu, \quad e_2^\nu = p_4^\nu, \quad e_3^\nu = \frac{1}{2} \langle e_1 | \gamma^\nu | e_2 \rangle, \quad e_4^\nu = \frac{1}{2} \langle e_2 | \gamma^\nu | e_1 \rangle, \quad (7.85)$$

and the cut solutions are parametrised by

$$l_1^{+\nu} = y e_1^\nu + \frac{(1-y)s_{12}}{s_{14}+s_{24}} e_2^\nu + t e_3^\nu + \frac{(1-y)ys_{12}-\mu^2}{(s_{14}+s_{24})t} e_4^\nu, \quad (7.86)$$

$$l_1^{-\nu} = y e_1^\nu + \frac{(1-y)s_{12}}{s_{14}+s_{24}} e_2^\nu + t e_4^\nu + \frac{(1-y)ys_{12}-\mu^2}{(s_{14}+s_{24})t} e_3^\nu. \quad (7.87)$$

By combining the tree amplitudes in which bubble factorises, we can write the two cuts as

$$C_{12|345}^\pm = A_4^{\text{tree}}(-l_1^\pm, 1^-, 2^+, l_3^\pm) A_5^{\text{tree}}(-l_3^\pm, 3^+, 4^+, 5^+, l_1^\pm) = \frac{\mu^2[5|3+4|l_3^\pm|3]\langle 1|l_1^\pm|2\rangle^2}{s_{12}\langle 3|4\rangle\langle 4|5\rangle\langle 1|l_1^\pm|1\rangle\langle 3|l_3^\pm|3\rangle\langle 5|l_1^\pm|5\rangle}, \quad (7.88)$$

$$C_{21|345}^\pm = A_4^{\text{tree}}(-l_1^\pm, 2^+, 1^-, l_3^\pm) A_5^{\text{tree}}(-l_3^\pm, 3^+, 4^+, 5^+, l_1^\pm) = \frac{\mu^2[5|3+4|l_3|3]\langle 1|l_1^\pm|2\rangle^2}{s_{12}\langle 3|4\rangle\langle 4|5\rangle\langle 2|l_1^\pm|2\rangle\langle 3|l_3^\pm|3\rangle\langle 5|l_1^\pm|5\rangle} \quad (7.89)$$

and, according to (7.54), we can related them through

$$C_{21|345}^\pm = \frac{(l_3^\pm + p_2)^2 - \mu^2}{(l_1^\pm - p_2)^2 - \mu^2} C_{12|345}^\pm. \quad (7.90)$$

If we make use of $l_3^\pm = l_1^\pm - p_1 - p_2$ and we expand (7.88) in the large- t limit, we get

$$C_{12|345}^+ = \mu^2 \frac{i[4|2]^3\langle 1|2\rangle}{s_{34}s_{45}[4|1]\langle 3|5\rangle^2}, \quad (7.91)$$

$$C_{12|345}^- = \mu^2 \frac{i\langle 1|4\rangle^3}{\langle 1|2\rangle\langle 2|4\rangle\langle 3|4\rangle^2\langle 4|5\rangle^2}, \quad (7.92)$$

whereas the expansion of the ratios of propagators reads

$$\left. \frac{(l_3^+ + p_2)^2 - \mu^2}{(l_1^+ - p_2)^2 - \mu^2} \right|_{t \rightarrow \infty} = -\frac{(s_{14} - s_{24})[2|1]^2[4|e_1]^2 y}{(s_{14} + s_{24})[4|1]^2[4|2]^2 t^2} - \frac{[2|1]^2\langle 2|4\rangle[4|e_1]^2}{(s_{14} + s_{24})t^2[4|1]^2[4|2]t^2} \frac{1}{t^2} - \frac{[2|1][4|e_1]}{[4|1][4|2]} \frac{1}{t} - 1 + \mathcal{O}\left(\frac{1}{t^3}\right), \quad (7.93)$$

$$\left. \frac{(l_3^- + p_2)^2 - \mu^2}{(l_1^- - p_2)^2 - \mu^2} \right|_{t \rightarrow \infty} = -\frac{(s_{14} - s_{24})\langle 1|2\rangle^2\langle e_1|4\rangle^2 y}{(s_{14} + s_{24})\langle 1|4\rangle^2\langle 2|4\rangle^2 t^2} - \frac{[4|2]\langle 1|2\rangle^2\langle e_1|4\rangle^2}{(s_{14} + s_{24})\langle 1|4\rangle^2\langle 2|4\rangle t^2} \frac{1}{t^2} - \frac{\langle 1|2\rangle\langle e_1|4\rangle}{\langle 1|4\rangle\langle 2|4\rangle} \frac{1}{t} - 1 + \mathcal{O}\left(\frac{1}{t^3}\right). \quad (7.94)$$

These expansions allow us to obtain the analytic expression of $C_{21|345}^\pm$ from (7.90),

$$C_{21|345}^+ = -\mu^2 \frac{i[4|2]^3\langle 1|2\rangle}{s_{34}s_{45}[4|1]\langle 3|5\rangle^2} = -C_{12|345}^+, \quad (7.95a)$$

$$C_{21|345}^- = -\mu^2 \frac{i\langle 1|4\rangle^3}{\langle 1|2\rangle\langle 2|4\rangle\langle 3|4\rangle^2\langle 4|5\rangle^2} = -C_{12|345}^-, \quad (7.95b)$$

which agree with what we would obtain by considering the large- t expansion of (7.89).

7.5 Discussion

In this chapter we have extended the results of chapter 3 to amplitudes in gauge theories coupled with matter in d -dimensions, within the Four-Dimensional-Formulation (FDF) scheme. We have shown that the colour-kinematics (C/K) duality obeyed by the numerators of tree-level amplitudes within FDF are non-trivial relations involving the interplay of massless and massive particles.

We have derived the Bern-Carrasco-Johansson (BCJ) identities for dimensionally regulated tree-level amplitudes. These identities have been derived by working in FDF, where the effects of dimensional regularisation are carried by massive degrees of freedom.

We have also presented a set of relations between the coefficients appearing in the decomposition of one-loop QCD amplitudes in terms of master integrals, which have been derived as a byproduct of the C/K duality satisfied by tree-level amplitudes. These relations reduce the number of independent integral coefficients to be individually computed and, being valid for contributions to both cut-constructible part and rational terms, they could play an important role in the optimisation of numerical calculations. The complete decomposition of a general one-loop amplitude can be obtained via the d -dimensional integrand reduction algorithm, which can be used to express the amplitude in terms of a known basis of loop integrals, whose coefficient can be extracted through suitable Laurent expansions of the integrand evaluated on the on-shell solutions. Since the on-shell integrand factorises into a product of tree-level amplitudes, the BCJ identities at tree-level have been exploited in order to establish relations between the integral coefficients themselves.

The coefficient identities derived in this chapter have been verified on a number of contributions to multi-gluon scattering amplitudes, for which we have provided analytic expressions of the integral coefficients.

A natural extension of this work would be the study of higher-loop coefficient relations that are expected to descend from the BCJ identities at tree-level. To this end, future work will require, besides a general parametrisation of the residues of multi-loop integrands, the derivation of the BCJ identities between dimensionally regulated amplitudes involving more than two external generalised particles.

Chapter 8

Two-loop amplitudes

In the previous chapters, we studied the LO and NLO corrections to several processes. Moreover, we need more accuracy and precision, in order to compare the theoretical prediction with the experiment data. It is important to reach results at higher order in the perturbation theory, which allow us to study many observables with a low level of uncertainty. Hence, a Next-to-Next-to-Leading-Order (NNLO) is needed. All the techniques used for the NLO showed in Chap. 4, as integrand reduction, unitarity and, generalised unitarity, could be, in principle, recycled as a first attempt, to compute two-loop amplitudes in non-supersymmetric gauge theories [81–88, 193, 201, 249–251, 294–305].

However, the very same techniques could not be applied in a straightforward way. In fact, the set of MIs is not known a priori. In addition, the interplay of more loop momenta makes the classification of spurious and non-spurious terms less evident. Nevertheless, the systematic determination of the residues at higher loops is carried out by performing a polynomial division modulo Gröbner basis.

This chapter is organised as follows: in Sec. 8.1 we give a briefly review of the calculation of two-loop amplitudes by consider the polynomial division module Gröbner basis. Within integrand reduction methods, we show the calculation of the two-loop four-gluon amplitude. In Sec. 8.2 we describe the basic concepts of the new approach of Ref. [201], which treats the space-time dimensions in terms of parallel and orthogonal subspaces, allowing an immediately classification of spurious and non-spurious terms.

8.1 Basic notions

A generic l -loop Feynman integral with n external legs in a d -dimensional space can be written as

$$\mathcal{I}_{i_1 \dots i_n}^{(\ell)}[\mathcal{N}] = \int \left(\prod_{i=1}^{\ell} \frac{d^d \bar{l}_i}{\pi^{d/2}} \right) \frac{\mathcal{N}_{i_1 \dots i_n}(\bar{l}_i)}{\prod_j D_j(\bar{l}_j)}, \quad (8.1)$$

where the space-time dimensions are often split into a four-dimensional part and a (-2ϵ) -dimensional one, according to Eq. (4.28). Moreover, there is a subtlety in higher loop ($\ell \geq 2$) computations and is the definition of the (-2ϵ) -dimensional scalar products, which, now on are defined as

$$\mu_{ij} = -\tilde{l}_i \cdot \tilde{l}_j. \quad (8.2)$$

Therefore, the numerator and denominator in (8.1) become polynomials in $\ell(\ell + 9)/2$ variables, that exactly correspond to the scalar products μ_{ij} and the components of l_i with respect to a

four-dimensional basis vectors $\mathcal{E}^{(i_1 \dots i_k)}$ as discussed in Sec. 4.3. This means that we can express the integrals over the (-2ϵ) -dimensional subspace into spherical coordinates and integrate out all directions orthogonal to the relative orientations of the vectors \tilde{l}_i^α , obtaining

$$\mathcal{I}_{i_1 \dots i_n}^{(\ell)}[\mathcal{N}] = \Omega_d^{(\ell)} \int \prod_{i=1}^{\ell} d^4 l_i \int \prod_{1 \leq i < j \leq \ell} d\mu_{ij} [G(\mu_{ij})]^{\frac{d-5-\ell}{2}} \frac{\mathcal{N}_{i_1 \dots i_n}(l_i, \mu_{ij})}{\prod_j D_j(l_j, \mu_{ij})}, \quad (8.3)$$

where $G(\mu_{ij}) = \det[(\mu_i \cdot \mu_j)]$ is the Gram determinant and

$$\Omega_d^{(\ell)} = \prod_{i=1}^{\ell} \frac{\Omega_{(d-4-i)}}{2\pi^{d/2}}, \quad \Omega_n = \frac{2\pi^{\frac{n+1}{2}}}{\Gamma(\frac{n+1}{2})}. \quad (8.4)$$

8.1.1 Integrand recurrence relation

In the framework of the integrand reduction method [41, 46, 85, 86, 249, 251], the computation of dimensionally regulated ℓ -loop integrals is rephrased in terms of the reconstruction of the integrand function as a sum of integrands with residues and a subset of denominators D_{i_k} ,

$$\mathcal{I}_{i_1 \dots i_r}(q_j) \equiv \frac{\mathcal{N}_{i_1 \dots i_r}(q_j)}{D_{i_1}(q_j) \cdots D_{i_r}(q_j)} = \sum_{k=0}^r \sum_{\{i_1 \dots i_k\}} \frac{\Delta_{j_1 \dots j_k}(q_j)}{D_{j_1}(q_j) \cdots D_{j_k}(q_j)}. \quad (8.5)$$

For an integral with an arbitrary number n of external legs, the integrand decomposition formula (8.5) can be obtained by observing that both numerator and denominators are polynomials in the components of the loop momenta with respect to some basis, which we collectively label as $\mathbf{z} = \{z_1, \dots, z_{\frac{\ell(\ell+9)}{2}}\}$. Thus, we can fix a monomial ordering and build a Gröbner basis $\mathcal{G}_{i_1 \dots i_r}(\mathbf{z})$ of the ideal $\mathcal{J}_{i_1 \dots i_r}$ generated by the set of denominators,

$$\mathcal{J}_{i_1 \dots i_r} \equiv \left\{ \sum_{k=1}^r h_k(\mathbf{z}) D_{i_k}(\mathbf{z}) : h_k(\mathbf{z}) \in P[\mathbf{z}] \right\}, \quad (8.6)$$

being $P[\mathbf{z}]$ the ring of polynomials in \mathbf{z} . By performing the polynomial division of $\mathcal{N}_{i_1 \dots i_r}(\mathbf{z})$ modulo $\mathcal{G}_{i_1 \dots i_r}(\mathbf{z})$,

$$\mathcal{N}_{i_1 \dots i_r}(\mathbf{z}) = \sum_{k=1}^r \mathcal{N}_{i_1 \dots i_{k-1} i_{k+1} \dots i_r}(\mathbf{z}) D_{i_k}(\mathbf{z}) + \Delta_{i_1 \dots i_r}(\mathbf{z}) \quad (8.7)$$

we obtain the recurrence relation

$$\mathcal{I}_{i_1 \dots i_r} = \sum_{k=1}^r \mathcal{I}_{i_1 \dots i_{k-1} i_{k+1} \dots i_r} + \frac{\Delta_{i_1 \dots i_r}(\mathbf{z})}{D_{i_1}(\mathbf{z}) \cdots D_{i_r}(\mathbf{z})}, \quad (8.8)$$

whose iterative application to the integrands corresponding to subtopologies with fewer loop propagators yields to the complete decomposition (8.5).

8.1.2 All plus four-gluon amplitudes

In this section we study the two-loop corrections to the polarised all plus four-gluon amplitude. This amplitude gets contributions from the Feynman diagrams shown in Fig. 8.1 only. This amplitude has been studied in Ref.s [80, 88], whose computation is based on the product of tree- and one-loop-amplitudes. We follow a diagrammatic approach, where internal particles, because of the use of Feynman gauge, can be gluons and ghosts.

This computation is carried out in three steps:

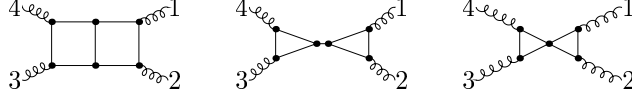


Figure 8.1: Representative topologies of the two-loop four-gluon amplitudes. Solid lines can represent either gluons or ghosts in d -dimensions.

1. Generation of the integrand: the integrand is generated by using FEYNARTS [202] and FEYNCALC [203, 204]. At this point the integrand is in d -dimensions, then, because of dimensional reduction or the prescriptions given in Eq.s (4.28,8.2) we end up with a 4-dimensional integrand written in terms of $\{l_i, \mu_{ij}\}$.
2. Fit the residue: we impose the set of on-shell conditions according to the diagram under consideration. This allows us to get a cut solution that is plugged into the numerator of the integrand. In order to do so, we use the MATHEMATICA packages S@M [205] and T@M [206]. Finally, we fit the residue by considering its generic representation at the cut, which, was automated by the MATHEMATICA package BASISDET [249].

Double box contribution

In order to compute the residue at the cut we use the constraints of the polynomial division over Gröbner basis. As mention before, this procedure has been automated by the MATHEMATICA package BASISDET. The residue $\Delta_{1234567}$ can be expressed as a combination of at most 160 coefficients multiplying various powers of the ISPs

$$(k_1 \cdot \omega), \quad (k_2 \cdot \omega), \quad (k_1 \cdot p_4), \quad (k_2 \cdot p_1), \quad \mu_{11}, \quad \mu_{22}, \quad \mu_{12}, \quad (8.9)$$

where

$$\omega^\mu = \frac{2}{s_{12}} v_\perp = \frac{\langle 2|3|1\rangle \langle 1|\gamma^\mu|2\rangle}{s_{12} \cdot 2} - \frac{\langle 1|3|2\rangle \langle 2|\gamma^\mu|1\rangle}{s_{12} \cdot 2}. \quad (8.10)$$

That is

$$\Delta_{1234567} = \sum_{i_1 \dots i_7} c_{i_1 \dots i_7} (k_1 \cdot \omega)^{i_1} (k_2 \cdot \omega)^{i_2} (k_1 \cdot p_4)^{i_3} (k_2 \cdot p_1)^{i_4} \mu_{11}^{i_5} \mu_{22}^{i_6} \mu_{12}^{i_7}. \quad (8.11)$$

With BASISDET, all the information described above can be extracted by typing the following lines in a MATHEMATICA notebook

```
L = 2;
Dim = 4 - 2 \[Epsilon];
n = 4;
ExternalMomentaBasis = {p1, p2, p4};
Kinematics = {p1^2 -> 0, p2^2 -> 0, p4^2 -> 0, p1 p2 -> s/2,
  p1 p4 -> t/2, p2 p4 -> -(s + t)/2, \[Omega]1^2 -> -t (s + t)/s};
numeric = {s -> 11, t -> 3};
Props = {11 - p1, 11, 11 - p1 - p2, p3 + p4 - 12, -12,
  p4 - 12, -11 - 12};
RenormalizationCondition = {{1, 0}, 4}, {{0, 1}, 4}, {{1, 1}, 6}};
GenerateBasis[1]
```

We now proceed to find the set of coefficients of (8.11). For this topology, we express the loop momenta as follows

$$\begin{aligned}\bar{l}_1 &= \bar{k}_1, & \bar{l}_2 &= \bar{k}_1 - p_1, & \bar{l}_3 &= \bar{k}_1 - p_1 - p_2, & \bar{l}_4 &= -\bar{k}_2 + p_3 + p_4, \\ \bar{l}_5 &= -\bar{k}_2 + p_4, & \bar{l}_6 &= -\bar{k}_2, & \bar{l}_7 &= -\bar{k}_1 - \bar{k}_2,\end{aligned}\quad (8.12)$$

where, because of the on-shell conditions, $D_i = \bar{l}_i^2 = 0$, the 4-dimensional loop momenta, k_1 and k_2 , can be parametrised as

$$k_1^\alpha = p_1^\alpha + \frac{\langle 23 \rangle \langle 1|\gamma^\alpha|2 \rangle}{\langle 13 \rangle} + \frac{[23] \langle 2|\gamma^\alpha|1 \rangle}{[13]}, \quad (8.13a)$$

$$k_2^\alpha = p_4^\alpha + \frac{\langle 41 \rangle \langle 3|\gamma^\alpha|4 \rangle}{\langle 31 \rangle} + \frac{[41] \langle 4|\gamma^\alpha|3 \rangle}{[31]}. \quad (8.13b)$$

Where the three extra-dimensional parameters μ_{ij} are determined by substituting

$$\mu_{11} = k_1^2, \quad \mu_{22} = k_2^2, \quad \mu_{12} = 2k_1 \cdot k_2. \quad (8.14)$$

Inserting Eq. (8.13) into Eq. (8.11), $\Delta_{1234567}$ at the cut becomes

$$\Delta_{1234567}|_{\text{cut}} = \sum_{i_1 \dots i_4} d_{i_1 \dots i_4} \tau_1^{i_1} \tau_2^{i_2} \tau_3^{i_3} \tau_4^{i_4}. \quad (8.15)$$

Expressions (8.11) and (8.15) are related through the relation

$$\mathbb{M} \mathbf{c} = \mathbf{d}, \quad (8.16)$$

Since we are following a diagrammatic approach, the integrand of the double box, $\mathcal{I}_{1234567}$, gets contributions from

$$\begin{aligned}\Delta_{1234567} &= \Delta \left(\text{diagram 1} \right) + \Delta \left(\text{diagram 2} \right) + \Delta \left(\text{diagram 3} \right) + \Delta \left(\text{diagram 4} \right) \\ &+ \Delta \left(\text{diagram 5} \right) + \Delta \left(\text{diagram 6} \right) + \Delta \left(\text{diagram 7} \right),\end{aligned}\quad (8.17)$$

where, because of the use of Feynman gauge, dashed lines represent d -dimensional ghosts circulating in the loop. Let us consider the first residue of the r.h.s., which at the cut takes the form

$$\Delta \left(\text{diagram 1} \right) = \frac{i\tau_1\tau_2\tau_3\tau_4 z_1^7 z_2^4}{64(z_2+1)^2} = \frac{1}{64} i\mu_{11}\mu_{22} z_1^5 z_2^2. \quad (8.18)$$

By following the same procedure with the other residues, we get

$$\Delta \left(\text{diagram 2} \right) = \Delta \left(\text{diagram 1} \right), \quad (8.19)$$

$$\Delta \left(\text{diagram 3} \right) = \Delta \left(\text{diagram 1} \right) = \frac{1}{16} i\mu_{22} (\mu_{11} + \mu_{12} + \mu_{22}) z_1^5 z_2^2, \quad (8.20)$$

$$\begin{aligned}
& + \Delta \left(\frac{1}{D_7} \text{diagram}_1 \right) + \Delta \left(\frac{1}{D_7} \text{diagram}_2 \right) + \Delta \left(\frac{1}{D_7} \text{diagram}_3 \right) \\
& + \Delta \left(\frac{1}{D_7} \text{diagram}_4 \right) + \Delta \left(\frac{1}{D_7} \text{diagram}_5 \right) + \Delta \left(\frac{1}{D_7} \text{diagram}_6 \right) \\
& + \Delta \left(\frac{1}{D_7} \text{diagram}_7 \right) - \Delta \left(\frac{1}{D_7} \Delta_{1234567} \right), \tag{8.25}
\end{aligned}$$

By performing a hexa-cut, the residue at the cut becomes,

$$\Delta_{123456}|_{\text{cut}} = i z_1^3 z_2^2 [(d_s - 2)^2 \mu_{11} \mu_{22} ((\bar{k}_1 + \bar{k}_2)^2 + z_1) + 2(d_s - 2) \mu_{12} (\mu_{11} + \mu_{22}) z_1] \times \Phi_4^{++++}. \tag{8.26}$$

From Eq.s (8.23,8.26), the two-loop all plus four-gluon amplitude takes the form

$$\begin{aligned}
A_4^{2\text{-loop}}(1^+, 2^+, 3^+, 4^+) = \int \frac{d^d \bar{k}_1}{\pi^{d/2}} \frac{d^d \bar{k}_2}{\pi^{d/2}} \left\{ \frac{\Delta_{1234567}}{D_1 D_2 D_3 D_4 D_5 D_6 D_7} + \frac{\Delta_{123456}}{D_1 D_2 D_3 D_4 D_5 D_6} \right\} \\
+ \text{cycl. perm.} \tag{8.27}
\end{aligned}$$

8.2 Adaptive Integrand Decomposition

8.2.1 Definition

In this section we describe the main ingredients of an alternative algorithm of integrand decomposition of multi-loop scattering amplitudes. This recent method proposed by Mastrolia, Primo and Peraro in Ref. [201] decomposes the space-time dimension, $d = 4 - 2\epsilon$, into parallel (or longitudinal) and orthogonal (or transverse) dimensions, as

$$d = d_{\parallel} + d_{\perp}. \tag{8.28}$$

While first studies [306–311] dealt with the structure of the integral, the recent work of Ref. [201] provides an exhaustive interpretation at integrand and integral level, purely, based on the decomposition of the space-time dimension.

Parallel and orthogonal directions show particular properties for topologies with less than five external legs. The parallel space is spanned by the n independent four-dimensional external momenta, namely $d_{\parallel} = n - 1$. Whereas, the orthogonal one is spanned by the complementary orthogonal directions. In particular, for diagrams with a number of legs $n \geq 5$, the orthogonal space embeds the -2ϵ regulating dimensions, $d_{\perp} = -2\epsilon$, while, for diagrams with $n \leq 4$, the orthogonal space is larger and it embeds also the four-dimensional complement of the parallel space, namely $d_{\perp} = (5 - n) - 2\epsilon$.

Since the decomposition of the space-time dimension, in parallel and orthogonal directions, depends on the number of external legs of individual diagrams this method is referred to as adaptive.

Recalling the structure of the Feynman integrals (8.1) at multi-loop level, we can see that numerator and denominators are written in a different set of variables. Denominators are now

in terms of $\ell(\ell + 2d_{\parallel} + 1)/2$ variables. While numerator will have a polynomial dependence on the remaining $\ell(4 - d_{\parallel})$. Thus, loop momenta in $d = d_{\parallel} + d_{\perp}$ read

$$\bar{l}_i^{\alpha} = l_{\parallel i}^{\alpha} + \lambda_i^{\alpha}, \quad (8.29)$$

with

$$\bar{l}_{\parallel i}^{\alpha} = \sum_{j=1}^{d_{\parallel}} x_{ji} e_j^{\alpha}, \quad \lambda_i^{\alpha} = \sum_{j=d_{\parallel}+1}^4 x_{ji} e_j^{\alpha} + \mu_i^{\alpha}, \quad \lambda_{ij} = \sum_{l=d_{\parallel}+1}^4 x_{li} x_{lj} + \mu_{ij}. \quad (8.30)$$

The basis $\mathcal{E}^{(i_1 \dots i_k)}$ can be chosen to lie into a subspace orthogonal to the external kinematics, i.e. $e_i \cdot p_j = 0$ ($i > d_{\parallel}, \forall j$), and $e_i \cdot e_j = \delta_{ij}$ ($i, j > d_{\parallel}$). In Eq. (8.29) $l_{\parallel i}$ is a vector of the d_{\parallel} -dimensional space spanned by the external momenta, and λ_i belongs the d_{\perp} -dimensional orthogonal subspace. In this parametrisation, all denominators become independent of the transverse components of the loop momenta,

$$D_i = l_{\parallel i}^2 + \sum_{j,l} \alpha_{ij} \alpha_{il} \lambda_{jl} + m_i^2, \quad l_{\parallel i}^{\alpha} = \sum_j \alpha_{ij} q_{\parallel i}^{\alpha} + \sum_j \beta_{ij} p_j^{\alpha}, \quad \lambda_{ij} = \sum_{l=d_{\parallel}+1}^4 x_{li} x_{lj} + \mu_{ij}, \quad (8.31)$$

with $\alpha, \beta \in \{0, \pm 1\}$.

It is worth to mention that the decomposition (8.29) allows to express a subset of components of $q_{\parallel i}^{\alpha}$ and λ_{ij} as combinations of loop denominators by solving linear relations. Therefore, we can always build differences of denominators which are linear in the loop momenta and independent of λ_{ij} , while the relation between λ_{ij} and the denominators is always linear by definition, as it can be seen from Eq. (8.31).

On the other side, the integral (8.1) with the decomposition (8.29) can be rewritten as

$$I_n^{d(\ell)}[\mathcal{N}] = \Omega_d^{(\ell)} \int \prod_{i=1}^{\ell} d^{n-1} q_{\parallel i} \int d^{\frac{\ell(\ell+1)}{2}} \mathbf{\Lambda} \int d^{(4-d_{\parallel})\ell} \mathbf{\Theta}_{\perp} \frac{\mathcal{N}(q_{\parallel}, \mathbf{\Lambda}, \mathbf{\Theta}_{\perp})}{\prod_j D_j(q_{\parallel}, \mathbf{\Lambda})}, \quad (8.32)$$

where

$$\int d^{\frac{\ell(\ell+1)}{2}} \mathbf{\Lambda} = \int \prod_{1 \leq i \leq j} d\lambda_{ij} [G(\lambda_{ij})]^{\frac{d_{\perp}-1-\ell}{2}} \quad (8.33)$$

defines integral over the norm of the transverse vectors λ_i^{α} and their relative orientations and $\mathbf{\Theta}_{\perp}$ parametrises the integral over the components of λ_i^{α} lying in the four-dimensional space.

From Eq. (8.32) we see that denominators do not depend on $\mathbf{\Theta}_{\perp}$ -components, therefore, their integration can be easily performed. In fact, we have to deal with integrals of the form

$$\int_{-1}^1 d\cos \theta_{ij} (\sin \theta_{ij})^{\alpha} (\cos \theta_{ij})^{\beta}. \quad (8.34)$$

The values of α and β depend on the specific expression of the numerator. The structure of these integrals allows to compute once and for all up to the desired rank and re-use them in every calculation. Additionally, these integrals can be evaluated by performing the Passarino-Veltman tensor reduction in the orthogonal space. Alternatively, they can be evaluated by exploiting the properties of *Gegenbauer polynomials* $C_n^{(\alpha)}(\cos \theta)$, a particular class of orthogonal polynomials over the interval $[-1, 1]$, which obey the orthogonality relation

$$\int_{-1}^1 d\cos \theta (\sin \theta)^{2\alpha-1} C_n^{(\alpha)}(\cos \theta) C_m^{(\alpha)}(\cos \theta) = \delta_{mn} \frac{2^{1-2\alpha} \pi \Gamma(n+2\alpha)}{n!(n+\alpha)\Gamma^2(\alpha)}. \quad (8.35)$$

8.2.2 Algorithm

In the previous subsection we saw how numerators and denominators are written in terms of different variables. In fact, when considering integrals with $n \leq 4$ external legs, the decomposition of $d = d_{\parallel} + d_{\perp}$ starts making sense and allows a lot of simplifications. For instance, the dependence of the denominators on the transverse components of the loop momenta is dropped.

Let us indicate with \mathbf{z} the full set of $\ell(\ell + 9)/2$ variables

$$\mathbf{z} = \{\mathbf{x}_{\parallel i}, \mathbf{x}_{\perp i}, \lambda_{ij}\}, \quad i, j = 1, \dots, \ell, \quad (8.36)$$

where $\mathbf{x}_{\parallel i}$ ($\mathbf{x}_{\perp i}$) are the components of the loop momenta parallel (orthogonal) to the external kinematics, the denominators are reduced to polynomials in the subset of variables

$$\boldsymbol{\tau} = \{\mathbf{x}_{\parallel}, \lambda_{ij}\}, \quad \boldsymbol{\tau} \subset \mathbf{z}, \quad (8.37)$$

so that the general r -point integrand has the form

$$\mathcal{I}_{i_1 \dots i_r}(\boldsymbol{\tau}, \mathbf{x}_{\perp}) \equiv \frac{\mathcal{N}_{i_1 \dots i_r}(\boldsymbol{\tau}, \mathbf{x}_{\perp})}{D_{i_1}(\boldsymbol{\tau}) \cdots D_{i_r}(\boldsymbol{\tau})}. \quad (8.38)$$

The new representation of numerators and denominators in terms of the variables $\boldsymbol{\tau}$ and the expansion of \mathbf{x}_{\perp} in terms of Gegenbauer polynomials allows for a straightforwardly identification of the spurious terms.

Therefore, the algorithm, with this adaptive integrand decomposition (AID) method, is organised in three steps:

1. **Divide:** we divide the numerator $\mathcal{N}_{i_1 \dots i_r}(\boldsymbol{\tau}, \mathbf{x}_{\perp})$ modulo the Gröbner basis $\mathcal{G}_{i_1 \dots i_r}(\boldsymbol{\tau})$ of the ideal $\mathcal{J}_{i_1 \dots i_r}(\boldsymbol{\tau})$ generated by the denominators. The polynomial division is performed by adopting the lexicographic ordering $\lambda_{ij} \ll \mathbf{x}_{\parallel}$,

$$\mathcal{N}_{i_1 \dots i_r}(\boldsymbol{\tau}, \mathbf{x}_{\perp}) = \sum_{k=1}^r \mathcal{N}_{i_1 \dots i_{k-1} i_{k+1} \dots i_r}(\boldsymbol{\tau}, \mathbf{x}_{\perp}) D_{i_k}(\boldsymbol{\tau}) + \Delta_{i_1 \dots i_r}(\mathbf{x}_{\parallel}, \mathbf{x}_{\perp}). \quad (8.39)$$

Because of the polynomial division, the dependence on the transverse variables, \mathbf{x}_{\perp} , in the residue $\Delta_{i_1 \dots i_r}$, is left untouched as well as on \mathbf{x}_{\parallel} but not on λ_{ij} that are expressed in terms of denominators and irreducible physical scalar products.

As anticipated at the end of Sec. 8.1.1, the Gröbner basis does not need to be explicitly computed, since, with the choice of variables and the ordering described here, the division is equivalent to applying the set of linear relations described above.

2. **Integrate:** Since denominators do not depend on transverse variables, \mathbf{x}_{\perp} , we can integrate the residue $\Delta_{i_1 \dots i_r}$ over transverse directions. This integration is carried out by expressing $\Delta_{i_1 \dots i_r}$ in terms of Gegenbauer polynomials, i.e.,

$$\Delta_{i_1 \dots i_r}^{\text{int}}(\boldsymbol{\tau}) = \int d^{(4-d_{\parallel})\ell} \Theta_{\perp} \Delta_{i_1 \dots i_r}(\boldsymbol{\tau}, \Theta_{\perp}). \quad (8.40)$$

Where $\Delta_{i_1 \dots i_r}^{\text{int}}$ is a polynomial in $\boldsymbol{\tau}$ whose coefficients depend on the space-time dimension d . Likewise, this polynomial is free of spurious terms.

3. **Divide:** the structure of the integrated residue suggests a second division. This can be seen from the dependence $\Delta_{i_1 \dots i_r}^{\text{int}}$ has on the variables $\boldsymbol{\tau}$. In fact, after applying the division, similarly as in the first step of this algorithm, we get

$$\Delta_{i_1 \dots i_r}^{\text{int}}(\boldsymbol{\tau}) = \sum_{k=1}^r \mathcal{N}_{i_1 \dots i_{k-1} i_{k+1} \dots i_r}^{\text{int}}(\boldsymbol{\tau}) D_{i_k}(\boldsymbol{\tau}) + \Delta'_{i_1 \dots i_r}(\mathbf{x}_{\parallel}), \quad (8.41)$$

where the new residue $\Delta'_{i_1 \dots i_r}(\mathbf{x}_{\parallel})$ can only depend on \mathbf{x}_{\parallel} . Therefore, this additional polynomial division allows us to obtain an integrand decomposition formula (8.5), where all irreducible numerators are function of the components of the loop momenta parallel to the external kinematics.

In the next subsection we apply this algorithm to the computation of the two-loop five-gluon amplitude. We describe, in all details, how the AID method is carried out. Nonetheless, we focus on two of three steps of this algorithm, leaving the second division as future work.

8.2.3 All plus five-gluon amplitudes

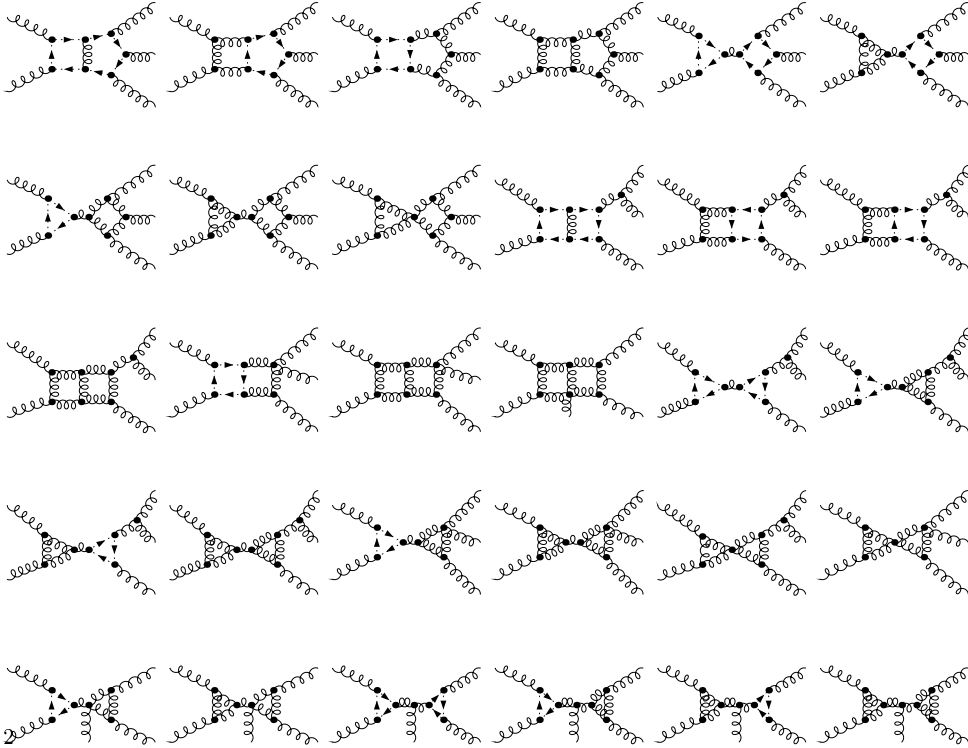


Figure 8.2: Selection of Feynman diagrams contributing to the five-gluons amplitude. Curly lines represent gluons and dashed ones indicate ghosts.

As an application of the AID we consider the leading colour contribution to the two-loop all plus five gluon amplitude [8]. This amplitude admits a decomposition of the form [88, 305, 312–314]

$$\begin{aligned}
 A_5^{2\text{-loop}}(1^+, 2^+, 3^+, 4^+, 5^+) = & \int \frac{d^d \bar{k}_1}{\pi^{d/2}} \frac{d^d \bar{k}_2}{\pi^{d/2}} \left\{ \frac{\Delta_{12345678}}{D_1 D_2 D_3 D_4 D_5 D_6 D_7 D_8} + \frac{\Delta_{1234567}}{D_1 D_2 D_3 D_4 D_5 D_6 D_7} \right. \\
 & + \frac{\Delta_{1235678}}{D_1 D_2 D_3 D_5 D_6 D_7 D_8} + \frac{\Delta_{1345678}}{D_1 D_3 D_4 D_5 D_6 D_7 D_8} + \frac{\Delta_{1245678}}{D_1 D_2 D_4 D_5 D_6 D_7 D_8} \\
 & \left. \frac{\Delta_{123567}}{D_1 D_2 D_3 D_5 D_6 D_7} + \frac{\Delta_{123567}}{D_1 D_3 D_4 D_5 D_6 D_7} + \frac{\Delta_{124567}}{D_1 D_2 D_4 D_5 D_6 D_7} \right\} \\
 & + \text{cycl. perm.} \quad (8.42)
 \end{aligned}$$

The residues of Eq. (8.42) are computed by following an analogous approach of Sec. 8.1.2 and checked numerically with [88]. The representatives topologies of this process are shown in Fig. 8.2.

In the following, we recall how the polynomial division is performed. As mentioned earlier, there is no need to pass by the Gröbner basis. In fact, AID decomposition allows us to perform the polynomial division in a straightforward way.

The loop momenta circulating in Fig. 8.2 can be parametrised as follows,

$$\begin{aligned}\bar{l}_1 &= \bar{k}_1, & \bar{l}_2 &= \bar{k}_1 - p_1, & \bar{l}_3 &= \bar{k}_1 - p_1 - p_2, & \bar{l}_4 &= \bar{k}_1 - p_1 - p_2 - p_3, \\ \bar{l}_5 &= \bar{k}_2 + p_4 + p_5, & \bar{l}_6 &= \bar{k}_2 + p_5, & \bar{l}_7 &= \bar{k}_2, & \bar{l}_8 &= -\bar{k}_1 - \bar{k}_2.\end{aligned}\quad (8.43)$$

The loop momenta, \bar{k}_1 and \bar{k}_2 , are parametrised according to the topology under consideration:

- In order to compute the residues $\Delta_{12345678}$ and $\Delta_{1235678}$, we parametrise the four-dimensional momenta as

$$\begin{aligned}\bar{k}_1^\alpha &= x_1 p_1^\alpha + x_2 p_2^\alpha + x_3 p_3^\alpha + x_4 p_4^\alpha + \lambda_1^\alpha, \\ \bar{k}_2^\alpha &= y_1 p_1^\alpha + y_2 p_2^\alpha + y_3 p_3^\alpha + y_4 p_4^\alpha + \lambda_2^\alpha,\end{aligned}\quad (8.44)$$

with $\lambda_i^\alpha = \mu_i^\alpha$. This parametrisation allows us to express some components of the loop, x_i 's and y_i 's, and λ_{ij} in terms of loop denominators. In particular, for $\Delta_{12345678}$, all variables x_i, y_i and λ_{ij} are written in terms of x_4, y_3 and y_4 and the loop denominators.

- For topologies with less than five external legs and factorised ones, the loop momenta are parametrised according to the one-loop subtopologies they are made of.

The factorised topology $\Delta_{1234567}$ is made of one box and one triangle. Therefore, as in the one-loop case, the loop momenta admit the following decomposition

$$\begin{aligned}\bar{k}_1^\alpha &= x_1 p_1^\alpha + x_2 p_2^\alpha + x_3 p_3^\alpha + \lambda_1^\alpha, & \lambda_1^\alpha &= x_4 \omega_{123}^\alpha + \mu_1^\alpha, \\ \bar{k}_2^\alpha &= y_1 p_1^\alpha + y_2 p_2^\alpha + \lambda_2^\alpha, & \lambda_2^\alpha &= y_3 \omega_+^\alpha + y_4 \omega_-^\alpha + \mu_2^\alpha,\end{aligned}\quad (8.45)$$

where, ω_{123} is an orthogonal momenta to p_1, p_2 and p_3 . While ω_+ and ω_- are orthogonal to p_4 and p_5 and satisfy the constraint $\omega_+ \cdot \omega_- = 0$. As in the previous case, the variables x_i, y_i and λ_{ii} are obtained from the difference of denominators. These variables are, again, expressed in terms of x_4, y_3 and y_4 and the loop denominators. We remark that, for factorised topologies, the value of λ_{12} has non-meaning, since this term is spurious, in the sense that it vanishes upon integration.

The residue Δ_{124567} is made of two subtopologies, which turn to be boxes. Hence, the loop momenta are parametrised as follows

$$\begin{aligned}\bar{k}_1^\alpha &= x_1 p_1^\alpha + x_2 p_4^\alpha + x_3 p_5^\alpha + \lambda_1^\alpha, & \lambda_1^\alpha &= x_4 \omega_{145}^\alpha + \mu_1^\alpha, \\ \bar{k}_2^\alpha &= y_1 p_1^\alpha + y_2 p_4^\alpha + y_3 p_5^\alpha + \lambda_2^\alpha, & \lambda_2^\alpha &= y_4 \omega_{145}^\alpha + \mu_2^\alpha,\end{aligned}\quad (8.46)$$

with ω_{145} an orthogonal momenta to p_1, p_4 and p_5 . From this decomposition, all the components of the loop are expressed in terms of x_3, x_4, y_3 and y_4 and the loop denominators.

The main outcome of the AID is the role of the new components of the loop. In fact, numerators and denominators in the integrand are written in terms of a different set variables. This difference, originated from the splitting of the space-time dimension in terms of parallel and orthogonal dimensions, allows for new roles of these variables. The traditional integrand reduction methods are slightly modified. The polynomial division is simplified, no need of passing by the Gröbner basis.

$\mathcal{I}_{i_1 \dots i_r}$	$\Delta_{i_1 \dots i_r}$	$\Delta_{i_1 \dots i_r}^{+++++}$	$\Delta_{i_1 \dots i_r}^{\text{int}}$	$\Delta_{i_1 \dots i_r}^{\text{int } +++++}$
	76 $\{1, x_4, y_3, y_4\}$	48	–	–
	160 $\{1, x_3, x_4, y_3, y_4\}$	64	–	–
	100 $\{1, x_3, x_4, y_3, y_4\}$	36	4 $\{1, \lambda_{11}, \lambda_{22}\}$	1
	50 $\{1, x_4, y_3, y_4\}$	30	6 $\{1, \lambda_{11}, \lambda_{22}\}$	3
	160 $\{1, x_3, x_4, y_3, y_4\}$	38	93 $\{1, x_3, y_3, \lambda_{11}, \lambda_{22}, \lambda_{12}\}$	39
	100 $\{1, x_3, x_4, y_3, y_4\}$	36	4 $\{1, \lambda_{11}, \lambda_{22}\}$	1

Table 8.1: Residue parametrisation within AID for the non-vanishing two loop topologies of the all plus five gluon-amplitude. In the second column, we list the number of monomials of a generic residue and the set of variables appearing in it. In the third column, we list the number of monomials that contribute to our process. Columns fourth and fifth correspond to the number of monomials for a generic residue and the one we are fitting according to our kinematics, respectively.

In order to compute the two loop contribution to the five gluon amplitude, we plug the loop momenta, according to AID algorithm. The results of this calculation are summarised in Tab. 8.1. This table shows a comparison between what is expected to obtain for any topology, generic structure of the residue, and the number of terms that contributes to this amplitude.

Since we are not providing analytical results for this computation, we attach a MATHEMATICA notebook, 5g.2L.m¹., that sketches the structure of the residues after fitting. This notebook, firstly, contains the list of monomial we refer to in Tab. 8.1. For instance, the residue $\Delta_{1234567}^{+++++}$ is written in terms of the following monomials

$$\begin{aligned}
\Delta_{1234567}^{+++++} = & c_0 y_4^2 + c_1 y_4^3 + c_2 y_3 y_4^2 + c_3 y_3^2 + c_4 y_3^2 y_4 + c_5 y_3^3 + c_6 x_4 y_4^2 + c_7 x_4 y_4^3 + c_8 x_4 y_3 y_4^2 \\
& + c_9 x_4 y_3^2 + c_{10} x_4 y_3^2 y_4 + c_{11} x_4 y_3^3 + c_{12} x_4^2 y_4^2 + c_{13} x_4^2 y_4^3 + c_{14} x_4^2 y_3 y_4^2 + c_{15} x_4^2 y_3^2 \\
& + c_{16} x_4^2 y_3^2 y_4 + c_{17} x_4^2 y_3^3 + c_{18} x_4^3 y_4^2 + c_{19} x_4^3 y_4^3 + c_{20} x_4^3 y_3 y_4^2 + c_{21} x_4^3 y_3^2 + c_{22} x_4^3 y_3^2 y_4 \\
& + c_{23} x_4^3 y_3^3 + c_{24} x_4^4 y_4^2 + c_{25} x_4^4 y_4^3 + c_{26} x_4^4 y_3 y_4^2 + c_{27} x_4^4 y_3^2 + c_{28} x_4^4 y_3^2 y_4 + c_{29} x_4^4 y_3^3.
\end{aligned} \tag{8.47}$$

Similarly, for topologies with less than five external legs or factorised ones, we can integrate the residues of Eq. (8.42) over the transverse directions. This procedure, for each residue, is presented in the second part of the MATHEMATICA notebook. It clearly shows, as anticipated

¹This notebook together with auxiliary files can be downloaded from [this http URL](#).

in the discussion, the dependence of the coefficients on the dimension. In order to make this statement clear, we integrate the residue $\Delta_{1234567}^{+++++}$, getting

$$\Delta_{1234567}^{\text{int } +++++} = \frac{(c_0 + c_3)\lambda_{22}}{d-2} + \frac{(c_{12} + c_{15})\lambda_{11}\lambda_{22}}{(d-3)(d-2)} + \frac{3(c_{24} + c_{27})\lambda_{11}^2\lambda_{22}}{(d-3)(d-2)(d-1)}. \quad (8.48)$$

Additionally, the integrated residues may lead to a new representation of the amplitude, whose discussion is, nevertheless, beyond the scope of this chapter.

8.3 Discussion

We have briefly described the extension of the unitarity based methods at multi-loop level. In particular, we have stressed on the two-loop case, reviewing the available techniques for their computation. Firstly, we described the calculation of multi-loop amplitudes by considering the polynomial division module Gröbner basis. This algorithm, based on algebraic geometry, has allowed to understand main ingredients of the integrand reduction methods. At one-loop, for instance, the structure of the residues proposed by the OPP method were elucidated. In the same manner, an automation at multi-loop level was provided by the MATHEMATICA code BASISDET [249]. The role of irreducible scalar products and spurious terms were made clear by cleverly using algebraic geometry.

This algorithm has been employed on the calculation of the well known two-loop four gluon amplitudes. The difference with previous approaches [80, 88] lies on the way the integrand is produced. We generated the two-loop integrand by following a diagrammatic study, whose set of Feynman rules is written in Feynman gauge. The reduction relies on two steps: generation of the integrand and fit the residues according to the parametric structure of the residue given by BASISDET.

As an alternative procedure, we have also reviewed the recent algorithm, adaptive integrand decomposition (AID) [201]. This algorithm decomposes the space-time dimension, $d = d_{\parallel} + d_{\perp}$, in parallel and perpendicular subspaces, allowing us to extract new properties for the calculation of multi-loop amplitudes. The polynomial division is straightforwardly computed by just applying a list of substitutions, no need of passing by the Gröbner basis. Because of the way how the cut solutions are parametrised, the spurious terms are easily identified. This identification allows us to perform a simple integration, which just takes into account the properties of the Gegenbauer polynomials.

As an application of this new method, we provided the computation of the two-loop all plus five gluon amplitude. Similar to the four-gluon amplitude, we generated, by following a diagrammatic approach, the integrands needed for the computation of the amplitude. The comparison of our results is done against the ones of Ref. [88]. Since this check was performed numerically, we provided parametric structure for non-zero residues. Consequently, we apply the second step of the algorithm, by means of the integration of the residues over the transverse variables.

Conclusion

In this thesis, we presented developments in calculating perturbative scattering amplitudes in QCD theory. In particular, we discussed computational techniques for gauge boson and fermion scattering amplitudes at tree and multi-loop level. The main focus of the thesis was the study of the on-shell methods, that exploit analyticity and unitarity properties of the S-matrix.

We introduced a four dimensional formulation (FDF) of d -dimensional regularisation of one-loop scattering amplitudes. Particles in d -dimensions propagating inside the loop are represented by massive ones. Their interactions are described by generalised four-dimensional Feynman rules. Gauge bosons in d -dimensions were represented in four-dimensions by a combination of massive gauge boson and a scalar particle. Fermions in d -dimensions were represented by four-dimensional fermions obeying the Dirac equation for tachyonic particles. Within FDF, we used the four-dimensional representation of the spinor-helicity formalism to express the polarisation and helicity states of the particles inside the loop. This representation allowed for a complete, four-dimensional, unitarity-based construction of d -dimensional amplitudes.

Within FDF, we calculated, through four-dimensional generalised unitarity and integrand reduction methods, relevant processes for the physics of the LHC. We presented a set of very non-trivial examples, showing that FDF scheme is suitable for computing important $2 \rightarrow 2, 3, 4$ partonic amplitudes at one-loop level. We first considered two gluons production by quark anti-quark annihilation. Then, the (up to four) gluon production, $gg \rightarrow ng$ with $n = 2, 3, 4$. And finally, the Higgs and (up to three) gluons production via gluon fusion, $gg \rightarrow ngH$ with $n = 1, 2, 3$, in the heavy top mass limit.

On the colour-kinematics (C/K)-duality side, we investigated, from a diagrammatic point of view, its off-shellness. We considered gauge theories couple with matter in four- as well as in d -dimensions. For the former we studied the scattering processes $gg \rightarrow ss, q\bar{q}, gg$, while for the latter we took into account all the interactions of the d -dimensional particles described by FDF. It turned out that the C/K-duality is non-trivially satisfied within higher multiplicity tree or multi-loop level graphs, originating anomalous terms. We provided an alternative procedure for the construction of dual numerators. This procedure, based on the generalised gauge transformation, accounts for the structure of the anomalous terms. We presented the explicit calculation for the tree-level contribution to $gg \rightarrow q\bar{q}g$ for the four- and d -dimensional case.

As byproduct of our procedure we found a set of relations between primitive amplitudes, which corresponded to the BCJ identities for four- and d -dimensionally regulated amplitudes. Additionally, we combined the integrand reduction method via Laurent expansion and the set of BCJ identities for d -dimensionally regulated amplitudes, finding relations between one-loop integral coefficients. Because of FDF, these relations can be established for the cut constructible contributions as well for the ones responsible for rational terms.

We showed that low-energy behaviour of radiative tree-level amplitudes in QCD is governed by the non-radiative process and depends on the quantum data of the emitter. The non-radiative

process is perturbed by universal operators. We showed that these operators can be derived from gauge invariance and from the on-shell construction. Indeed, within the spinor-helicity formalism, we showed that the subleading soft operator of single gluon emission from quark-gluon amplitudes appears as a differential operator. The form of this operator does not depend on the spin of the emitter. Our study is complement to the results derived for Yang-Mills and gravity theories.

In the multi-loop level case, we showed examples of the application of both the fit-on-the-cut and the adaptive integrand decomposition. We showed how these techniques accompanied by the OPP decomposition allowed the computation of any amplitude at multi-loop level. We believed that the technology used to compute these amplitudes will be, in the future, very useful for phenomenological studies in particle physics.

Appendix A

One-loop 2-point integrals

In this appendix we show how the 2-point tensor integrals presented in the one-loop decomposition (4.43) can be reduced to scalar integrals. While in this appendix we focus on 2-point functions, an exhaustive study of the algebraic reduction of the one-loop tensor integrals to scalar integrals was done in [315].

Let us consider the following master integrals (MIs)

$$B_0; B_\mu; B_{\mu\nu}(p^2; m_1; m_2) = \int \frac{d^n q}{i\pi^2} \frac{1; q_\mu; q_\mu q_\nu}{q^2 (q+p)^2}. \quad (\text{A.1})$$

By covariant decomposition

$$B_\mu = p_\mu B_1, \quad (\text{A.2})$$

$$B_{\mu\nu} = p_\mu p_\nu B_{21} + \bar{g}_{\mu\nu} B_{22}, \quad (\text{A.3})$$

with

$$B_1(p^2, 0, 0) = -\frac{1}{2} B_0(p^2, 0, 0), \quad (\text{A.4})$$

$$B_{21}(p^2, 0, 0) = \frac{1}{3} B_0(p^2, 0, 0) + \frac{1}{18}, \quad (\text{A.5})$$

Let us write down the explicit MIs we need

$$I_{ij}[1] = B_0, \quad (\text{A.6})$$

$$I_{ij}[(q \cdot e_2)] = e_2 \cdot B = (e_2 \cdot p) B_1 = -\frac{1}{2} (e_2 \cdot p) B_0, \quad (\text{A.7})$$

$$I_{ij}[(q \cdot e_2)^2] = e_2^\mu e_2^\nu B_{\mu\nu} = (e_2 \cdot p)^2 B_{21} = \frac{1}{3} (e_2 \cdot p)^2 B_0 + \frac{1}{18} (e_2 \cdot p)^2, \quad (\text{A.8})$$

$$I_{ij}[\mu^2] = -\frac{1}{6} p^2. \quad (\text{A.9})$$

We remark the bubble contributions from Eq. (4.43)

$$\sum_{i < j}^{n-1} \left\{ c_{2,0}^{(ij)} I_{ij}[1] + c_{2,1}^{(ij)} I_{ij}[(q \cdot e_2)] + c_{2,2}^{(ij)} I_{ij}[(q \cdot e_2)^2] + c_{2,9}^{(ij)} I_{ij}[\mu^2] \right\}. \quad (\text{A.10})$$

The cut-constructible part takes the form

$$\sum_{i < j}^{n-1} \left\{ c_{2,0}^{(ij)} - \frac{1}{2} (e_2 \cdot p) c_{2,1}^{(ij)} + \frac{1}{3} (e_2 \cdot p)^2 c_{2,2}^{(ij)} \right\} B_0, \quad (\text{A.11})$$

whereas the rational part

$$\sum_{i < j}^{n-1} \left\{ \frac{1}{18} (e_2 \cdot p)^2 c_{2,2}^{(ij)} + c_{2,9}^{(ij)} I_{ij} [\mu^2] \right\}, \quad (\text{A.12})$$

where the coefficient of $c_{2,2}^{(ij)}$ can be written in terms of $I_{ij} [\mu^2]$ as

$$\frac{1}{18} (e_2 \cdot p)^2 = -\frac{1}{3p^2} (e_2 \cdot p)^2 I_{ij} [\mu^2]. \quad (\text{A.13})$$

This relation allows us to write the rational part as

$$\sum_{i < j}^{n-1} \left\{ -\frac{1}{3p^2} (e_2 \cdot p)^2 c_{2,2}^{(ij)} + c_{2,9}^{(ij)} \right\} I_{ij} [\mu^2]. \quad (\text{A.14})$$

In the computation presented in this thesis, we always consider gauge independent quantities. Therefore, the final results must be gauge independent as well. It turns out that the coefficients $c_{2,i}$ are gauge dependent. Moreover, as soon as we reduce tensor integrals into scalar integrals everything becomes gauge independent, by meaning of the linear combination of $c_{2,i}$.

Appendix B

Further features of the Four-dimensional-formulation

B.1 One-loop equivalence

In this Appendix we show that, at one loop, the FDH scheme defined by Eqs. (5.2) – (5.5b) is equivalent to the one defined by Eqs. (5.2) – (5.5a) and (5.9).

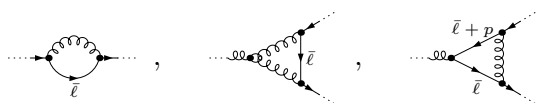
In the two approaches the only differences may arise from the manipulations of the -2ϵ components of the Dirac matrices contracted among each others. Therefore potential differences in their predictions can only be rational contributions of divergent diagrams involving at least an open fermion line. The loop-dependent part of the integrand of a one-loop diagram is a sum of integrands of the type

$$\mathcal{I}_{r,a,k} \equiv \frac{\ell^{\mu_1} \dots \ell^{\mu_r} (\mu^2)^a}{D_{i_1} \dots D_{i_k}}, \quad D_j \equiv (\ell + p_j)^2 - m_j - \mu^2. \quad (\text{B.1})$$

An integrand $\mathcal{I}_{r,a,k}$ leads to a divergent integral if it satisfies the conditions

$$4 + r + 2a - 2k \geq 0. \quad (\text{B.2})$$

At one loop in QCD the diagrams involving at least an open fermion line and integrands fulfilling the conditions (B.2) are



For these diagrams, the numerators obtained by using the two schemes differ by terms of the type

$$\begin{aligned} & \dots \tilde{\gamma}^\alpha (\ell + \tilde{\ell} + m) \tilde{\gamma}_\alpha \dots, \\ & \dots \tilde{\gamma}^\alpha (\ell + \tilde{\ell} + m) \gamma^\mu (\ell + p + \tilde{\ell} + m) \tilde{\gamma}_\alpha \dots, \end{aligned} \quad (\text{B.3})$$

where “...” represent four dimensional spinorial objects. In the FDH scheme it is easy to show that the terms (B.3) vanish in the $d_s \rightarrow 4$ limit, while in the other scheme they vanish as a consequence of Eq. (5.9). Therefore the two sets of prescriptions lead to the same integrand.

The FDF fulfills the prescriptions (5.2) – (5.5a) and (5.9), thus, at one loop, it leads to the same amplitudes of the FDH scheme.

B.2 Proof of the completeness relations

In this Appendix we show that the generalised spinors (5.17) fulfil the completeness relation (5.16). For later convenience we define the chirality projectors

$$\omega_{\pm} = \frac{\mathbb{I} \pm \gamma^5}{2}, \quad (\text{B.4})$$

and we show that:

$$\begin{aligned} \frac{|q_\ell][\ell^b| - |\ell^b][q_\ell]}{[\ell^b q_\ell]} &= \frac{|q_\ell\rangle\langle q_\ell \ell^b|[\ell^b| + |\ell^b\rangle\langle \ell^b q_\ell|q_\ell]}{2\ell^b \cdot q_\ell} = \frac{(|q_\ell\rangle\langle q_\ell|)(|\ell^b\rangle[\ell^b|) + (|\ell^b\rangle\langle \ell^b|)(|q_\ell\rangle[q_\ell])}{2\ell^b \cdot q_\ell} \\ &= \frac{\omega_- \not{q}_\ell \omega_+ \not{\ell}^b + \omega_- \not{\ell}^b \omega_+ \not{q}_\ell}{2\ell^b \cdot q_\ell} = \frac{\omega_-^2 \{\not{q}_\ell \not{\ell}^b\}}{2\ell^b \cdot q_\ell} = \omega_-, \end{aligned} \quad (\text{B.5a})$$

and similarly

$$\frac{|\ell^b\rangle\langle q_\ell| - |q_\ell\rangle\langle \ell^b|}{\langle q_\ell \ell^b \rangle} = \omega_+. \quad (\text{B.5b})$$

Using Eqs. (B.5) we get

$$\begin{aligned} \sum_{\lambda=\pm} u_\lambda(\ell) \bar{u}_\lambda(\ell) &= \left(|\ell^b\rangle + \frac{(m - i\mu)}{[\ell^b q_\ell]} |q_\ell] \right) \left([\ell^b| + \frac{(m + i\mu)}{\langle q_\ell \ell^b \rangle} \langle q_\ell| \right) \\ &\quad + \left(|\ell^b\rangle + \frac{(m + i\mu)}{\langle \ell^b q_\ell \rangle} |q_\ell] \right) \left(\langle \ell^b| + \frac{(m - i\mu)}{[q_\ell \ell^b]} \langle q_\ell| \right) \\ &= \not{\ell}^b + \frac{m^2 + \mu^2}{2\ell^b \cdot q_\ell} \not{q}_\ell + (m - i\mu) \frac{|q_\ell][\ell^b| - |\ell^b][q_\ell]}{[\ell^b q_\ell]} + (m + i\mu) \frac{|\ell^b\rangle\langle q_\ell| - |q_\ell\rangle\langle \ell^b|}{\langle q_\ell \ell^b \rangle} \\ \stackrel{\text{Eq. (B.5)}}{=} &\not{\ell}^b + \frac{m^2 + \mu^2}{2\ell^b \cdot q_\ell} \not{q}_\ell + (m - i\mu)\omega_- + (m + i\mu)\omega_+ \\ \stackrel{\text{Eq. (5.14)}}{=} &\not{\ell} + i\mu\gamma^5 + m. \end{aligned} \quad (\text{B.6})$$

B.3 Colour-ordered Feynman rules

In the FDF, the d -dimensional colour-ordered Feynman rules collected in Ref. [217] become:

$$\begin{array}{c} \bullet \\ \alpha \end{array} \begin{array}{c} \text{-----} \\ k \\ \text{-----} \\ \beta \end{array} \bullet = -i \frac{1}{k^2 - \mu^2 + i0} \left[g^{\alpha\beta} - \frac{k^\alpha k^\beta}{\mu^2} \right], \quad (\text{gluon}), \quad (\text{B.7a})$$

$$\begin{array}{c} \bullet \\ A \end{array} \begin{array}{c} \text{-----} \\ k \\ \text{-----} \\ B \end{array} \bullet = -i \frac{1}{k^2 - \mu^2 + i0} [G^{AB} - Q^A Q^B], \quad (\text{scalar}), \quad (\text{B.7b})$$

$$\begin{array}{c} \bullet \\ \text{-----} \\ k \\ \text{-----} \\ \bullet \end{array} = i \frac{\not{k} + i\mu\gamma^5 + m}{k^2 - m^2 - \mu^2 + i0}, \quad (\text{fermion}), \quad (\text{B.7c})$$

$$\begin{array}{c} \text{-----} \\ 1, \alpha \end{array} \begin{array}{c} \text{-----} \\ 2, \beta \\ \text{-----} \\ 3, \gamma \end{array} \begin{array}{c} \text{-----} \\ k_1 \\ \text{-----} \\ k_2 \\ \text{-----} \\ k_3 \end{array} = \frac{i}{\sqrt{2}} [g_{\alpha\beta}(k_1 - k_2)_\gamma + g_{\beta\gamma}(k_2 - k_3)_\alpha + g_{\gamma\alpha}(k_3 - k_1)_\beta], \quad (\text{B.7d})$$

Appendix C

Coefficient relations from 5-point BCJ identities

In this Appendix we collect the set of identities, obtained through the use of the d -dimensional BCJ relations for five-point amplitudes of the type (7.30), that can be used to relate integral coefficients associated to multiple cuts which, besides sharing the same on-shell solutions, differ from the ordering of three external particles.

C.1 Relations for pentagon coefficients

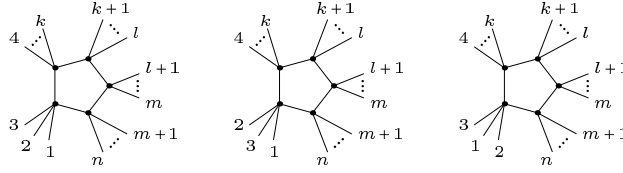


Figure C.1: Pentagon topologies for the cuts $C_{123|4\dots k|(k+1)\dots l|(l+1)\dots m|(m+1)\dots n}$, $C_{132|4\dots k|(k+1)\dots l|(l+1)\dots m|(m+1)\dots n}$ and $C_{231|4\dots k|(k+1)\dots l|(l+1)\dots m|(m+1)\dots n}$.

We consider the three quintuple-cuts shown in Fig C.1, which differ from the ordering of the particles p_1, p_2, p_3 . The contribution from the ordering $\{1, 2, 3\}$ is given by

$$C_{123|4\dots r|(r+1)\dots s|(s+1)\dots t|(t+1)\dots n}^{\pm} = A_5^{\text{tree}}(-l_1^{\pm}, 1, 2, 3, l_4^{\pm}) A_{r-1}^{\text{tree}}(-l_4^{\pm}, P_{4\dots r}, l_{r+1}^{\pm}) A_{s-r+2}^{\text{tree}}(-l_{r+1}^{\pm}, P_{r+1\dots s}, l_{s+1}^{\pm}) \\ \times A_{s-t+2}^{\text{tree}}(-l_{s+1}^{\pm}, P_{s+1\dots t}, l_{t+1}^{\pm}) A_{n-t+2}^{\text{tree}}(-l_{t+1}^{\pm}, P_{t+1\dots n}, l_1^{\pm}) \quad (\text{C.1})$$

and the other two cuts are obtained from the corresponding permutations of $\{1, 2, 3\}$. Eq. (7.30) can be used in order to relate the amplitudes $A_5^{\text{tree}}(-l_1^{\pm}, 1, 2, 3, l_4^{\pm})$, $A_5^{\text{tree}}(-l_1^{\pm}, 1, 3, 2, l_4^{\pm})$ and $A_5^{\text{tree}}(-l_1^{\pm}, 2, 1, 3, l_4^{\pm})$ and, thus, to identify

$$C_{213|4\dots r|(r+1)\dots s|(s+1)\dots t|(t+1)\dots n}^{\pm} \\ = \frac{(P_{l_4^{\pm}2}^2 + P_{23}^2 - \mu^2) C_{123|4\dots r|(r+1)\dots s|(s+1)\dots t|(t+1)\dots n}^{\pm} + (P_{l_4^{\pm}2}^2 - \mu^2) C_{132|4\dots r|(r+1)\dots s|(s+1)\dots t|(t+1)\dots n}^{\pm}}{(P_{-l_1^{\pm}2}^2 - \mu^2)}. \quad (\text{C.2})$$

Analogously to the case discussed in Section 7.4.1, the constant ratios of propagators

$$\frac{P_{l_4^\pm 2}^2 - \mu^2}{P_{-l_1^\pm 2}^2 - \mu^2} = \alpha^\pm, \quad \frac{P_{l_4^\pm 2}^2 + P_{23}^2 - \mu^2}{P_{-l_1^\pm 2}^2 - \mu^2} = \beta^\pm, \quad (\text{C.3})$$

allow us to translate (C.2) into a simple identity between the coefficients of the expansion (7.34) for the three cuts,

$$c^{(213|\dots)^\pm} = \beta^\pm c^{(123|\dots)^\pm} + \alpha^\pm c^{(132|\dots)^\pm}. \quad (\text{C.4})$$

C.2 Relations for box coefficients

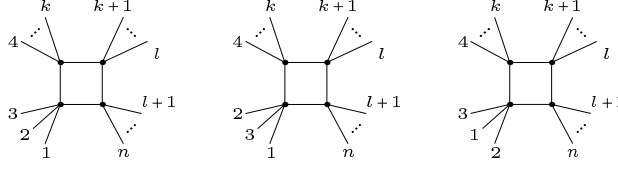


Figure C.2: Box topologies for the cuts $C_{123|4\dots k|k+1\dots l|l+1\dots n}$, $C_{132|4\dots k|k+1\dots l|l+1\dots n}$ and $C_{231|4\dots k|k+1\dots l|l+1\dots n}$.

Similarly to the previous case, we can use the BCJ identities to relate the quadruple cuts depicted in Fig. C.2, given by

$$\begin{aligned} C_{123|4\dots r|(r+1)\dots s|(s+1)\dots n}^\pm &= A_5^{\text{tree}}(-l_1^\pm, 1, 2, 3, l_4^\pm) A_{r-1}^{\text{tree}}(-l_4^\pm, P_{4\dots r}, l_{r+1}^\pm) \\ &\quad \times A_{s-r+2}^{\text{tree}}(-l_{r+1}^\pm, P_{r+1\dots s}, l_{s+1}^\pm) A_{n-s+2}^{\text{tree}}(-l_{s+1}^\pm, P_{s+1\dots n}, l_1^\pm) \end{aligned} \quad (\text{C.5})$$

and suitable permutations of $\{1, 2, 3\}$ for $C_{132|4\dots r|(r+1)\dots s|(s+1)\dots n}^\pm$ and $C_{231|4\dots r|(r+1)\dots s|(s+1)\dots n}^\pm$. If we make use of (7.30) on the amplitudes involving the particles p_1 , p_2 and p_3 , we obtain

$$\begin{aligned} C_{213|4\dots r|(r+1)\dots s|(s+1)\dots n}^\pm &= \frac{\left(P_{l_4^\pm 2}^2 + P_{23}^2 - \mu^2 \right) C_{123|4\dots r|(r+1)\dots s|(s+1)\dots n}^\pm + \left(P_{l_4^\pm 2}^2 - \mu^2 \right) C_{132|4\dots r|(r+1)\dots s|(s+1)\dots n}^\pm}{\left(P_{-l_1^\pm 2}^2 - \mu^2 \right)}. \end{aligned} \quad (\text{C.6})$$

As shown in Section 7.4.2, the two box coefficients contributing to the amplitude can be extracted by taking the $\mu^2 \rightarrow 0$ and $\mu^2 \rightarrow \infty$ limits, where the ratios of propagators behave like

$$\begin{aligned} \left. \frac{P_{l_4^\pm 2}^2 - \mu^2}{P_{-l_1^\pm 2}^2 - \mu^2} \right|_{\mu^2 \rightarrow 0} &= \alpha_0^\pm, & \left. \frac{P_{l_4^\pm 2}^2 - \mu^2}{P_{-l_1^\pm 2}^2 - \mu^2} \right|_{\mu^2 \rightarrow \infty} &= \alpha_4^\pm + \mathcal{O}\left(\frac{1}{\mu}\right), \\ \left. \frac{P_{l_4^\pm 2}^2 + P_{23}^2 - \mu^2}{P_{-l_1^\pm 2}^2 - \mu^2} \right|_{\mu^2 \rightarrow 0} &= \beta_0^\pm, & \left. \frac{P_{l_4^\pm 2}^2 + P_{23}^2 - \mu^2}{P_{-l_1^\pm 2}^2 - \mu^2} \right|_{\mu^2 \rightarrow \infty} &= \beta_4^\pm + \mathcal{O}\left(\frac{1}{\mu}\right). \end{aligned} \quad (\text{C.7})$$

Thus, starting from (C.6) we can relate the coefficients of the expansions (7.40a)-(7.40b) of the three quadruple cuts through the identities

$$c_i^{(213|\dots)^\pm} = \beta_i^\pm c_i^{(123|\dots)^\pm} + \alpha_i^\pm c_i^{(132|\dots)^\pm}, \quad i = 0, 4. \quad (\text{C.8})$$

C.3 Relations for triangle coefficients

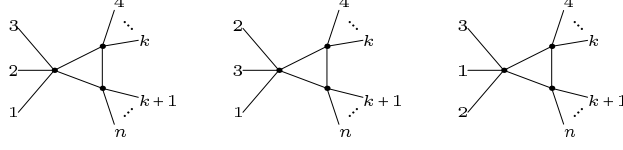


Figure C.3: Triangle topologies for the cuts $C_{123|4\dots k|(k+1)\dots n}$, $C_{132|4\dots k|(k+1)\dots n}$ and $C_{213|4\dots k|(k+1)\dots n}$.

Now we turn our attention to the triangle topologies shown in Fig. C.3. The expression of the cut with external ordering $\{1, 2, 3, \dots, n\}$ in terms of tree-level amplitudes is given by

$$C_{123|4\dots k|(k+1)\dots n}^{\pm} = A_5^{\text{tree}}(-l_1^{\pm}, 1, 2, 3, l_4^{\pm}) A_{k-1}^{\text{tree}}(-l_4^{\pm}, P_{4\dots k}, l_{k+1}^{\pm}) A_{n-k+2}^{\text{tree}}(-l_{k+1}^{\pm}, P_{k+1\dots n}, l_1^{\pm}) \quad (\text{C.9})$$

and, as usual, $C_{132|4\dots k|(k+1)\dots n}^{\pm}$ and $C_{213|4\dots k|(k+1)\dots n}^{\pm}$ are obtained from the corresponding permutations of $\{1, 2, 3\}$. Eq. (7.30) allow us to identify

$$C_{213|4\dots k|(k+1)\dots n}^{\pm} = \frac{(P_{l_4^{\pm}2}^2 + P_{23}^2 - \mu^2) C_{123|4\dots k|(k+1)\dots n}^{\pm} + (P_{l_4^{\pm}2}^2 - \mu^2) C_{132|4\dots k|(k+1)\dots n}^{\pm}}{(P_{-l_1^{\pm}2}^2 - \mu^2)} \quad (\text{C.10})$$

and, following the procedure of Section 7.4.3, we can take the large- t limit of the two ratios of propagators,

$$\begin{aligned} \left. \frac{P_{l_4^{\pm}2}^2 - \mu^2}{P_{-l_1^{\pm}2}^2 - \mu^2} \right|_{t \rightarrow \infty} &= \sum_{m=-3}^0 \alpha_{m,0}^{\pm} t^m + \mu^2 \sum_{m=-3}^{-2} \alpha_{m,2}^{\pm} t^m + \mathcal{O}\left(\frac{1}{t^4}\right), \\ \left. \frac{P_{l_4^{\pm}2}^2 + P_{23}^2 - \mu^2}{P_{-l_1^{\pm}2}^2 - \mu^2} \right|_{t \rightarrow \infty} &= \sum_{m=-3}^0 \beta_{m,0}^{\pm} t^m + \mu^2 \sum_{m=-3}^{-2} \beta_{m,2}^{\pm} t^m + \mathcal{O}\left(\frac{1}{t^4}\right), \end{aligned} \quad (\text{C.11})$$

and use it in (C.10) in order to express the coefficients of the expansion (7.46) of $C_{213|4\dots k|(k+1)\dots n}^{\pm}$ in terms of the ones of $C_{123|4\dots k|(k+1)\dots n}$ and $C_{132|4\dots k|(k+1)\dots n}$,

$$c_{m,0}^{(213|\dots)^{\pm}} = \sum_{l=0}^{3-m} \left[\beta_{-l,0}^{\pm} c_{l+m,0}^{(123|\dots)^{\pm}} + \alpha_{-l,0}^{\pm} c_{l+m,0}^{(132|\dots)^{\pm}} \right], \quad (\text{C.12})$$

$$c_{m,2}^{(213|\dots)^{\pm}} = \sum_{l=0}^{1-m} \left[\beta_{-l-2,2}^{\pm} c_{l+m+2,0}^{(123|\dots)^{\pm}} + \beta_{-l,0}^{\pm} c_{l+m,2}^{(123|\dots)^{\pm}} + \alpha_{-l-2,2}^{\pm} c_{l+m+2,0}^{(132|\dots)^{\pm}} + \alpha_{-l,0}^{\pm} c_{l+m,2}^{(132|\dots)^{\pm}} \right]. \quad (\text{C.13})$$

C.4 Relations for bubble coefficients

Finally, we use the BCJ identities in order to determine relations between the coefficients of the bubble contributions shown in Fig. C.4. The double cut with external ordering $\{1, 2, 3, \dots, n\}$ is given by

$$C_{123|4\dots n}^{\pm} = A_5^{\text{tree}}(-l_1^{\pm}, 1, 2, 3, l_4^{\pm}) A_{n-1}^{\text{tree}}(-l_4^{\pm}, P_{4\dots n}, l_1^{\pm}), \quad (\text{C.14})$$

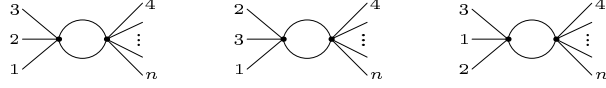


Figure C.4: Bubble topologies for the cuts $C_{123|4\dots n}$, $C_{132|4\dots n}$ and $C_{213|4\dots n}$.

whereas $C_{132|4\dots n}^\pm$ and $C_{213|4\dots n}^\pm$ are obtained from the corresponding permutations of $\{1, 2, 3\}$. Hence, thanks to (7.30), we can identify

$$C_{213|4\dots n}^\pm = \frac{\left(P_{l_4^\pm 2}^2 + P_{23}^2 - \mu^2\right) C_{123|4\dots n}^\pm + \left(P_{l_4^\pm 2}^2 - \mu^2\right) C_{132|4\dots n}^\pm}{\left(P_{-l_1^\pm 2}^2 - \mu^2\right)}. \quad (\text{C.15})$$

As we did in Section 7.4.4, after taking the $t \rightarrow \infty$ limit of the two ratios of propagators,

$$\begin{aligned} \left. \frac{P_{l_4^\pm 2}^2 - \mu^2}{P_{-l_1^\pm 2}^2 - \mu^2} \right|_{t \rightarrow \infty} &= \sum_{l=-2}^0 \sum_{m=0}^{-l} \alpha_{l,m,0}^\pm t^l y^m + \frac{\mu^2}{t^2} \alpha_{-2,0,2}^\pm + \mathcal{O}\left(\frac{1}{t^3}\right), \\ \left. \frac{P_{l_4^\pm 2}^2 + P_{23}^2 - \mu^2}{P_{-l_1^\pm 2}^2 - \mu^2} \right|_{t \rightarrow \infty} &= \sum_{l=-2}^0 \sum_{m=0}^{-l} \beta_{l,m,0}^\pm t^l y^m + \frac{\mu^2}{t^2} \beta_{-2,0,2}^\pm + \mathcal{O}\left(\frac{1}{t^3}\right), \end{aligned} \quad (\text{C.16})$$

we can substitute the expansion (7.52) for the three cuts in (C.15) and determine the coefficients of $C_{213|4\dots n}^\pm$ from the knowledge of the ones of $C_{123|4\dots n}^\pm$ and $C_{132|4\dots n}^\pm$,

$$c_{l,m,0}^{(213|\dots)^\pm} = \sum_{r=l}^2 \left(\sum_{s=\max[0,l+m-r]}^{\min[m,2-r]} \left(\alpha_{l-r,m-s,0}^\pm c_{r,s,0}^{(132|\dots)^\pm} + \beta_{l-r,m-s,0}^\pm c_{r,s,0}^{(123|\dots)^\pm} \right) \right), \quad (\text{C.17a})$$

$$c_{0,0,2}^{(213|\dots)^\pm} = \alpha_{-2,0,2}^\pm c_{2,0,0}^{(132|\dots)^\pm} + \alpha_{0,0,0}^\pm c_{0,0,2}^{(132|\dots)^\pm} + \beta_{-2,0,2}^\pm c_{2,0,0}^{(123|\dots)^\pm} + \beta_{0,0,0}^\pm c_{0,0,2}^{(123|\dots)^\pm}. \quad (\text{C.17b})$$

Bibliography

- [1] R. A. Fazio, P. Mastrolia, E. Mirabella and W. J. Torres Bobadilla, *On the Four-Dimensional Formulation of Dimensionally Regulated Amplitudes*, *Eur. Phys. J.* **C74** (2014) 3197, [[1404.4783](#)].
- [2] H. Luo, P. Mastrolia and W. J. Torres Bobadilla, *Subleading soft behavior of QCD amplitudes*, *Phys. Rev.* **D91** (2015) 065018, [[1411.1669](#)].
- [3] P. Mastrolia, A. Primo, U. Schubert and W. J. Torres Bobadilla, *Off-shell currents and color-kinematics duality*, *Phys. Lett.* **B753** (2016) 242–262, [[1507.07532](#)].
- [4] A. Primo and W. J. Torres Bobadilla, *BCJ Identities and d-Dimensional Generalized Unitarity*, *JHEP* **04** (2016) 125, [[1602.03161](#)].
- [5] P. Mastrolia, A. Primo and W. J. Torres Bobadilla, *Multi-gluon Scattering Amplitudes at One-Loop and Color-Kinematics Duality*, *In preparation* (2016) .
- [6] W. J. Torres Bobadilla, A. R. Fazio, P. Mastrolia and E. Mirabella, *Generalised Unitarity for Dimensionally Regulated Amplitudes*, *Nucl. Part. Phys. Proc.* **267-269** (2015) 150–157, [[1505.05890](#)].
- [7] W. J. Torres Bobadilla, *Generalised unitarity for dimensionally regulated amplitudes within FDF*, in *Proceedings, 12th International Symposium on Radiative Corrections (Radcor 2015) and LoopFest XIV (Radiative Corrections for the LHC and Future Colliders): Los Angeles, CA, USA, June 15-19, 2015*, 2016. [1601.05742](#).
- [8] P. Mastrolia, T. Peraro, A. Primo and W. J. Torres Bobadilla, *Adaptive Integrand Decomposition*, *PoS* **LL2016** (2016) 007, [[1607.05156](#)].
- [9] S. L. Glashow, *Partial Symmetries of Weak Interactions*, *Nucl. Phys.* **22** (1961) 579–588.
- [10] M. Gell-Mann, *A Schematic Model of Baryons and Mesons*, *Phys. Lett.* **8** (1964) 214–215.
- [11] G. Zweig, *An $SU(3)$ model for strong interaction symmetry and its breaking. Version 2*, in *DEVELOPMENTS IN THE QUARK THEORY OF HADRONS. VOL. 1. 1964 - 1978* (D. Lichtenberg and S. P. Rosen, eds.), pp. 22–101. 1964.
- [12] S. Weinberg, *A Model of Leptons*, *Phys. Rev. Lett.* **19** (1967) 1264–1266.
- [13] A. Salam, *Weak and Electromagnetic Interactions*, *Conf. Proc.* **C680519** (1968) 367–377.
- [14] ATLAS collaboration, G. Aad et al., *Observation of a new particle in the search for the Standard Model Higgs boson with the ATLAS detector at the LHC*, *Phys. Lett.* **B716** (2012) 1–29, [[1207.7214](#)].
- [15] CMS collaboration, S. Chatrchyan et al., *Observation of a new boson at a mass of 125 GeV with the CMS experiment at the LHC*, *Phys. Lett.* **B716** (2012) 30–61, [[1207.7235](#)].

- [16] SUPER-KAMIOKANDE collaboration, Y. Fukuda et al., *Evidence for oscillation of atmospheric neutrinos*, *Phys. Rev. Lett.* **81** (1998) 1562–1567, [[hep-ex/9807003](#)].
- [17] SNO collaboration, Q. R. Ahmad et al., *Measurement of the rate of $\nu_e + d \rightarrow p + p + e^-$ interactions produced by 8B solar neutrinos at the Sudbury Neutrino Observatory*, *Phys. Rev. Lett.* **87** (2001) 071301, [[nucl-ex/0106015](#)].
- [18] SNO collaboration, Q. R. Ahmad et al., *Direct evidence for neutrino flavor transformation from neutral current interactions in the Sudbury Neutrino Observatory*, *Phys. Rev. Lett.* **89** (2002) 011301, [[nucl-ex/0204008](#)].
- [19] F. A. Berends, R. Kleiss, P. De Causmaecker, R. Gastmans and T. T. Wu, *Single Bremsstrahlung Processes in Gauge Theories*, *Phys. Lett.* **B103** (1981) 124–128.
- [20] P. De Causmaecker, R. Gastmans, W. Troost and T. T. Wu, *Helicity Amplitudes for Massless QED*, *Phys. Lett.* **B105** (1981) 215.
- [21] R. Kleiss and W. J. Stirling, *Spinor Techniques for Calculating p anti- $p \rightarrow W^{+-} / Z^0 +$ Jets*, *Nucl. Phys.* **B262** (1985) 235–262.
- [22] Z. Xu, D.-H. Zhang and L. Chang, *Helicity Amplitudes for Multiple Bremsstrahlung in Massless Nonabelian Gauge Theories*, *Nucl. Phys.* **B291** (1987) 392.
- [23] S. J. Parke and T. R. Taylor, *An Amplitude for n Gluon Scattering*, *Phys. Rev. Lett.* **56** (1986) 2459.
- [24] F. A. Berends and W. T. Giele, *Recursive Calculations for Processes with n Gluons*, *Nucl. Phys.* **B306** (1988) 759–808.
- [25] R. Britto, F. Cachazo and B. Feng, *New recursion relations for tree amplitudes of gluons*, *Nucl. Phys.* **B715** (2005) 499–522, [[hep-th/0412308](#)].
- [26] R. Britto, F. Cachazo, B. Feng and E. Witten, *Direct proof of tree-level recursion relation in Yang-Mills theory*, *Phys. Rev. Lett.* **94** (2005) 181602, [[hep-th/0501052](#)].
- [27] S. Badger, E. N. Glover, V. Khoze and P. Svrcek, *Recursion relations for gauge theory amplitudes with massive particles*, *JHEP* **0507** (2005) 025, [[hep-th/0504159](#)].
- [28] S. D. Badger, E. W. N. Glover and V. V. Khoze, *Recursion relations for gauge theory amplitudes with massive vector bosons and fermions*, *JHEP* **01** (2006) 066, [[hep-th/0507161](#)].
- [29] D. Forde and D. A. Kosower, *All-multiplicity amplitudes with massive scalars*, *Phys. Rev.* **D73** (2006) 065007, [[hep-th/0507292](#)].
- [30] Z. Bern, L. J. Dixon, D. C. Dunbar and D. A. Kosower, *One loop n point gauge theory amplitudes, unitarity and collinear limits*, *Nucl. Phys.* **B425** (1994) 217–260, [[hep-ph/9403226](#)].
- [31] R. Britto, F. Cachazo and B. Feng, *Generalized unitarity and one-loop amplitudes in $N=4$ super-Yang-Mills*, *Nucl. Phys.* **B725** (2005) 275–305, [[hep-th/0412103](#)].
- [32] Z. Bern and A. G. Morgan, *Massive loop amplitudes from unitarity*, *Nucl. Phys.* **B467** (1996) 479–509, [[hep-ph/9511336](#)].
- [33] R. Britto, E. Buchbinder, F. Cachazo and B. Feng, *One-loop amplitudes of gluons in SQCD*, *Phys. Rev.* **D72** (2005) 065012, [[hep-ph/0503132](#)].

- [34] R. Britto, B. Feng and P. Mastrolia, *The Cut-constructible part of QCD amplitudes*, *Phys. Rev.* **D73** (2006) 105004, [[hep-ph/0602178](#)].
- [35] R. Britto, B. Feng and P. Mastrolia, *Closed-Form Decomposition of One-Loop Massive Amplitudes*, *Phys. Rev.* **D78** (2008) 025031, [[0803.1989](#)].
- [36] P. Mastrolia, *Double-Cut of Scattering Amplitudes and Stokes' Theorem*, *Phys. Lett.* **B678** (2009) 246–249, [[0905.2909](#)].
- [37] N. E. J. Bjerrum-Bohr, D. C. Dunbar and W. B. Perkins, *Analytic structure of three-mass triangle coefficients*, *JHEP* **04** (2008) 038, [[0709.2086](#)].
- [38] P. Mastrolia, *On Triple-cut of scattering amplitudes*, *Phys. Lett.* **B644** (2007) 272–283, [[hep-th/0611091](#)].
- [39] D. Forde, *Direct extraction of one-loop integral coefficients*, *Phys. Rev.* **D75** (2007) 125019, [[0704.1835](#)].
- [40] E. W. Nigel Glover and C. Williams, *One-Loop Gluonic Amplitudes from Single Unitarity Cuts*, *JHEP* **12** (2008) 067, [[0810.2964](#)].
- [41] R. K. Ellis, W. T. Giele and Z. Kunszt, *A Numerical Unitarity Formalism for Evaluating One-Loop Amplitudes*, *JHEP* **03** (2008) 003, [[0708.2398](#)].
- [42] G. Passarino and M. J. G. Veltman, *One Loop Corrections for $e^+ e^-$ Annihilation Into $\mu^+ \mu^-$ in the Weinberg Model*, *Nucl. Phys.* **B160** (1979) 151.
- [43] G. J. van Oldenborgh and J. A. M. Vermaseren, *New Algorithms for One Loop Integrals*, *Z. Phys.* **C46** (1990) 425–438.
- [44] A. Denner and S. Dittmaier, *Reduction schemes for one-loop tensor integrals*, *Nucl.Phys.* **B734** (2006) 62–115, [[hep-ph/0509141](#)].
- [45] Z. Nagy and D. E. Soper, *Numerical integration of one-loop Feynman diagrams for N-photon amplitudes*, *Phys. Rev.* **D74** (2006) 093006, [[hep-ph/0610028](#)].
- [46] G. Ossola, C. G. Papadopoulos and R. Pittau, *Reducing full one-loop amplitudes to scalar integrals at the integrand level*, *Nucl. Phys.* **B763** (2007) 147–169, [[hep-ph/0609007](#)].
- [47] P. Mastrolia, G. Ossola, T. Reiter and F. Tramontano, *Scattering AMplitudes from Unitarity-based Reduction Algorithm at the Integrand-level*, *JHEP* **08** (2010) 080, [[1006.0710](#)].
- [48] G. Heinrich, G. Ossola, T. Reiter and F. Tramontano, *Tensorial Reconstruction at the Integrand Level*, *JHEP* **1010** (2010) 105, [[1008.2441](#)].
- [49] T. Hahn and M. Perez-Victoria, *Automatized one loop calculations in four-dimensions and D-dimensions*, *Comput.Phys.Commun.* **118** (1999) 153–165, [[hep-ph/9807565](#)].
- [50] A. van Hameren, C. Papadopoulos and R. Pittau, *Automated one-loop calculations: A Proof of concept*, *JHEP* **0909** (2009) 106, [[0903.4665](#)].
- [51] G. Bevilacqua, M. Czakon, M. Garzelli, A. van Hameren, A. Kardos et al., *HELAC-NLO*, [1110.1499](#).

- [52] C. Berger, Z. Bern, L. Dixon, F. Febres Cordero, D. Forde et al., *An Automated Implementation of On-Shell Methods for One-Loop Amplitudes*, *Phys.Rev.* **D78** (2008) 036003, [[0803.4180](#)].
- [53] V. Hirschi, R. Frederix, S. Frixione, M. V. Garzelli, F. Maltoni et al., *Automation of one-loop QCD corrections*, *JHEP* **1105** (2011) 044, [[1103.0621](#)].
- [54] F. Cascioli, P. Maierhofer and S. Pozzorini, *Scattering Amplitudes with Open Loops*, *Phys. Rev. Lett.* **108** (2012) 111601, [[1111.5206](#)].
- [55] S. Badger, B. Biedermann and P. Uwer, *NGLuon: A Package to Calculate One-loop Multi-gluon Amplitudes*, *Comput.Phys.Commun.* **182** (2011) 1674–1692, [[1011.2900](#)].
- [56] S. Badger, B. Biedermann, P. Uwer and V. Yundin, *Numerical evaluation of virtual corrections to multi-jet production in massless QCD*, *Comput. Phys. Commun.* **184** (2013) 1981–1998, [[1209.0100](#)].
- [57] T. Peraro, *Ninja: Automated Integrand Reduction via Laurent Expansion for One-Loop Amplitudes*, *Comput. Phys. Commun.* **185** (2014) 2771–2797, [[1403.1229](#)].
- [58] G. Cullen, N. Greiner, G. Heinrich, G. Luisoni, P. Mastrolia et al., *Automated One-Loop Calculations with GoSam*, *Eur.Phys.J.* **C72** (2012) 1889, [[1111.2034](#)].
- [59] G. Cullen et al., *GOSAM-2.0: a tool for automated one-loop calculations within the Standard Model and beyond*, *Eur. Phys. J.* **C74** (2014) 3001, [[1404.7096](#)].
- [60] H. van Deurzen, G. Luisoni, P. Mastrolia, E. Mirabella, G. Ossola and T. Peraro, *Multi-leg One-loop Massive Amplitudes from Integrand Reduction via Laurent Expansion*, *JHEP* **03** (2014) 115, [[1312.6678](#)].
- [61] P. Mastrolia, E. Mirabella and T. Peraro, *Integrand reduction of one-loop scattering amplitudes through Laurent series expansion*, *JHEP* **06** (2012) 095, [[1203.0291](#)].
- [62] S. D. Badger, *Direct Extraction Of One Loop Rational Terms*, *JHEP* **01** (2009) 049, [[0806.4600](#)].
- [63] G. Ossola, C. G. Papadopoulos and R. Pittau, *On the Rational Terms of the one-loop amplitudes*, *JHEP* **0805** (2008) 004, [[0802.1876](#)].
- [64] M. Garzelli, I. Malamos and R. Pittau, *Feynman rules for the rational part of the Electroweak 1-loop amplitudes in the R_{ξ} gauge and in the Unitary gauge*, *JHEP* **1101** (2011) 029, [[1009.4302](#)].
- [65] W. T. Giele, Z. Kunszt and K. Melnikov, *Full one-loop amplitudes from tree amplitudes*, *JHEP* **0804** (2008) 049, [[0801.2237](#)].
- [66] R. Ellis, W. T. Giele, Z. Kunszt and K. Melnikov, *Masses, fermions and generalized D-dimensional unitarity*, *Nucl.Phys.* **B822** (2009) 270–282, [[0806.3467](#)].
- [67] K. Melnikov and M. Schulze, *NLO QCD corrections to top quark pair production in association with one hard jet at hadron colliders*, *Nucl.Phys.* **B840** (2010) 129–159, [[1004.3284](#)].
- [68] C. Cheung and D. O’Connell, *Amplitudes and Spinor-Helicity in Six Dimensions*, *JHEP* **0907** (2009) 075, [[0902.0981](#)].

- [69] S. Davies, *One-Loop QCD and Higgs to Partons Processes Using Six-Dimensional Helicity and Generalized Unitarity*, *Phys.Rev.* **D84** (2011) 094016, [[1108.0398](#)].
- [70] F. V. Tkachov, *A Theorem on Analytical Calculability of Four Loop Renormalization Group Functions*, *Phys. Lett.* **B100** (1981) 65–68.
- [71] K. G. Chetyrkin and F. V. Tkachov, *Integration by Parts: The Algorithm to Calculate beta Functions in 4 Loops*, *Nucl. Phys.* **B192** (1981) 159–204.
- [72] S. Laporta, *High precision calculation of multiloop Feynman integrals by difference equations*, *Int. J. Mod. Phys.* **A15** (2000) 5087–5159, [[hep-ph/0102033](#)].
- [73] R. N. Lee, A. V. Smirnov and V. A. Smirnov, *Dimensional recurrence relations: an easy way to evaluate higher orders of expansion in ϵ* , *Nucl. Phys. Proc. Suppl.* **205-206** (2010) 308–313, [[1005.0362](#)].
- [74] A. V. Kotikov, *Differential equation method: The Calculation of N point Feynman diagrams*, *Phys. Lett.* **B267** (1991) 123–127.
- [75] V. A. Smirnov, *Analytical result for dimensionally regularized massless on shell double box*, *Phys. Lett.* **B460** (1999) 397–404, [[hep-ph/9905323](#)].
- [76] M. Beneke and V. A. Smirnov, *Asymptotic expansion of Feynman integrals near threshold*, *Nucl. Phys.* **B522** (1998) 321–344, [[hep-ph/9711391](#)].
- [77] T. Binoth and G. Heinrich, *An automatized algorithm to compute infrared divergent multiloop integrals*, *Nucl. Phys.* **B585** (2000) 741–759, [[hep-ph/0004013](#)].
- [78] C. Anastasiou, S. Beerli and A. Daleo, *Evaluating multi-loop Feynman diagrams with infrared and threshold singularities numerically*, *JHEP* **05** (2007) 071, [[hep-ph/0703282](#)].
- [79] Z. Bern, J. S. Rozowsky and B. Yan, *Two loop four gluon amplitudes in $N=4$ superYang-Mills*, *Phys. Lett.* **B401** (1997) 273–282, [[hep-ph/9702424](#)].
- [80] Z. Bern, L. J. Dixon and D. A. Kosower, *A Two loop four gluon helicity amplitude in QCD*, *JHEP* **01** (2000) 027, [[hep-ph/0001001](#)].
- [81] D. A. Kosower and K. J. Larsen, *Maximal Unitarity at Two Loops*, *Phys.Rev.* **D85** (2012) 045017, [[1108.1180](#)].
- [82] K. J. Larsen, *Global Poles of the Two-Loop Six-Point $N=4$ SYM integrand*, *Phys.Rev.* **D86** (2012) 085032, [[1205.0297](#)].
- [83] S. Caron-Huot and K. J. Larsen, *Uniqueness of two-loop master contours*, *JHEP* **1210** (2012) 026, [[1205.0801](#)].
- [84] H. Johansson, D. A. Kosower and K. J. Larsen, *Two-Loop Maximal Unitarity with External Masses*, *Phys.Rev.* **D87** (2013) 025030, [[1208.1754](#)].
- [85] P. Mastrolia and G. Ossola, *On the Integrand-Reduction Method for Two-Loop Scattering Amplitudes*, *JHEP* **11** (2011) 014, [[1107.6041](#)].
- [86] S. Badger, H. Frellesvig and Y. Zhang, *Hepta-Cuts of Two-Loop Scattering Amplitudes*, *JHEP* **1204** (2012) 055, [[1202.2019](#)].
- [87] S. Badger, H. Frellesvig and Y. Zhang, *An Integrand Reconstruction Method for Three-Loop Amplitudes*, *JHEP* **1208** (2012) 065, [[1207.2976](#)].

- [88] S. Badger, H. Frellesvig and Y. Zhang, *A Two-Loop Five-Gluon Helicity Amplitude in QCD*, *JHEP* **12** (2013) 045, [[1310.1051](#)].
- [89] F. Low, *Bremsstrahlung of very low-energy quanta in elementary particle collisions*, *Phys.Rev.* **110** (1958) 974–977.
- [90] S. Weinberg, *Photons and Gravitons in s Matrix Theory: Derivation of Charge Conservation and Equality of Gravitational and Inertial Mass*, *Phys.Rev.* **135** (1964) B1049–B1056.
- [91] F. Cachazo and A. Strominger, *Evidence for a New Soft Graviton Theorem*, [1404.4091](#).
- [92] E. Casali, *Soft sub-leading divergences in Yang-Mills amplitudes*, *JHEP* **1408** (2014) 077, [[1404.5551](#)].
- [93] Z. Bern, S. Davies, T. Dennen, Y.-t. Huang and J. Nohle, *Color-Kinematics Duality for Pure Yang-Mills and Gravity at One and Two Loops*, *Phys. Rev.* **D92** (2015) 045041, [[1303.6605](#)].
- [94] C. White, *Diagrammatic insights into next-to-soft corrections*, *Phys.Lett.* **B737** (2014) 216–222, [[1406.7184](#)].
- [95] T. Burnett and N. M. Kroll, *Extension of the low soft photon theorem*, *Phys.Rev.Lett.* **20** (1968) 86.
- [96] V. Del Duca, *High-energy Bremsstrahlung Theorems for Soft Photons*, *Nucl.Phys.* **B345** (1990) 369–388.
- [97] B. U. W. Schwab and A. Volovich, *Subleading soft theorem in arbitrary dimension from scattering equations*, *Phys.Rev.Lett.* **113** (2014) 101601, [[1404.7749](#)].
- [98] N. Afkhami-Jeddi, *Soft Graviton Theorem in Arbitrary Dimensions*, [1405.3533](#).
- [99] M. Zlotnikov, *Sub-sub-leading soft-graviton theorem in arbitrary dimension*, *JHEP* **10** (2014) 148, [[1407.5936](#)].
- [100] C. Kalousios and F. Rojas, *Next to subleading soft-graviton theorem in arbitrary dimensions*, *JHEP* **01** (2015) 107, [[1407.5982](#)].
- [101] B. U. W. Schwab, *Subleading Soft Factor for String Disk Amplitudes*, *JHEP* **08** (2014) 062, [[1406.4172](#)].
- [102] M. Bianchi, S. He, Y.-t. Huang and C. Wen, *More on Soft Theorems: Trees, Loops and Strings*, *Phys. Rev.* **D92** (2015) 065022, [[1406.5155](#)].
- [103] B. U. W. Schwab, *A Note on Soft Factors for Closed String Scattering*, *JHEP* **03** (2015) 140, [[1411.6661](#)].
- [104] W.-M. Chen, Y.-t. Huang and C. Wen, *New Fermionic Soft Theorems for Supergravity Amplitudes*, *Phys. Rev. Lett.* **115** (2015) 021603, [[1412.1809](#)].
- [105] P. Di Vecchia, R. Marotta and M. Mojaza, *Soft theorem for the graviton, dilaton and the Kalb-Ramond field in the bosonic string*, *JHEP* **05** (2015) 137, [[1502.05258](#)].
- [106] M. Bianchi and A. L. Guerrieri, *On the soft limit of open string disk amplitudes with massive states*, *JHEP* **09** (2015) 164, [[1505.05854](#)].

- [107] L. V. Bork and A. I. Onishchenko, *On soft theorems and form factors in $\mathcal{N} = 4$ SYM theory*, *JHEP* **12** (2015) 030, [[1506.07551](#)].
- [108] S. Chin, S. Lee and Y. Yun, *ABJM Amplitudes in U-gauge and a Soft Theorem*, *JHEP* **11** (2015) 088, [[1508.07975](#)].
- [109] M. Campiglia and A. Laddha, *Asymptotic symmetries of gravity and soft theorems for massive particles*, *JHEP* **12** (2015) 094, [[1509.01406](#)].
- [110] M. Bianchi and A. L. Guerrieri, *On the soft limit of closed string amplitudes with massive states*, *Nucl. Phys.* **B905** (2016) 188–216, [[1512.00803](#)].
- [111] A. J. Larkoski, *Conformal Invariance of the Subleading Soft Theorem in Gauge Theory*, *Phys.Rev.* **D90** (2014) 087701, [[1405.2346](#)].
- [112] T. Adamo, E. Casali and D. Skinner, *Perturbative gravity at null infinity*, *Class. Quant. Grav.* **31** (2014) 225008, [[1405.5122](#)].
- [113] Y. Geyer, A. E. Lipstein and L. Mason, *Ambitwistor strings at null infinity and (subleading) soft limits*, *Class. Quant. Grav.* **32** (2015) 055003, [[1406.1462](#)].
- [114] D. Kapec, V. Lysov, S. Pasterski and A. Strominger, *Semiclassical Virasoro symmetry of the quantum gravity \mathcal{S} -matrix*, *JHEP* **08** (2014) 058, [[1406.3312](#)].
- [115] J. Broedel, M. de Leeuw, J. Plefka and M. Rosso, *Constraining subleading soft gluon and graviton theorems*, *Phys.Rev.* **D90** (2014) 065024, [[1406.6574](#)].
- [116] Z. Bern, S. Davies, P. Di Vecchia and J. Nohle, *Low-Energy Behavior of Gluons and Gravitons from Gauge Invariance*, *Phys. Rev.* **D90** (2014) 084035, [[1406.6987](#)].
- [117] T. He, P. Mitra, A. P. Porfyriadis and A. Strominger, *New Symmetries of Massless QED*, *JHEP* **1410** (2014) 112, [[1407.3789](#)].
- [118] V. Lysov, S. Pasterski and A. Strominger, *Low's Subleading Soft Theorem as a Symmetry of QED*, *Phys.Rev.Lett.* **113** (2014) 111601, [[1407.3814](#)].
- [119] M. Campiglia and A. Laddha, *Asymptotic symmetries and subleading soft graviton theorem*, *Phys. Rev.* **D90** (2014) 124028, [[1408.2228](#)].
- [120] Z.-W. Liu, *Soft theorems in maximally supersymmetric theories*, *Eur. Phys. J.* **C75** (2015) 105, [[1410.1616](#)].
- [121] J. Rao, *Soft theorem of $\mathcal{N} = 4$ SYM in Grassmannian formulation*, *JHEP* **02** (2015) 087, [[1410.5047](#)].
- [122] D. Kapec, V. Lysov and A. Strominger, *Asymptotic Symmetries of Massless QED in Even Dimensions*, [[1412.2763](#)].
- [123] A. Sabio Vera and M. A. Vazquez-Mozo, *The Double Copy Structure of Soft Gravitons*, *JHEP* **03** (2015) 070, [[1412.3699](#)].
- [124] A. Mohd, *A note on asymptotic symmetries and soft-photon theorem*, *JHEP* **02** (2015) 060, [[1412.5365](#)].
- [125] M. Campiglia and A. Laddha, *New symmetries for the Gravitational S-matrix*, *JHEP* **04** (2015) 076, [[1502.02318](#)].

- [126] S. Pasterski, A. Strominger and A. Zhiboedov, *New Gravitational Memories*, [1502.06120](#).
- [127] A. E. Lipstein, *Soft Theorems from Conformal Field Theory*, *JHEP* **06** (2015) 166, [[1504.01364](#)].
- [128] D. Kapec, M. Pate and A. Strominger, *New Symmetries of QED*, [1506.02906](#).
- [129] S. G. Avery and B. U. W. Schwab, *Burg-Metzner-Sachs symmetry, string theory, and soft theorems*, *Phys. Rev.* **D93** (2016) 026003, [[1506.05789](#)].
- [130] T. T. Dumitrescu, T. He, P. Mitra and A. Strominger, *Infinite-Dimensional Fermionic Symmetry in Supersymmetric Gauge Theories*, [1511.07429](#).
- [131] W.-M. Chen, Y.-t. Huang and C. Wen, *From $U(1)$ to E_8 : soft theorems in supergravity amplitudes*, *JHEP* **03** (2015) 150, [[1412.1811](#)].
- [132] F. Cachazo, S. He and E. Y. Yuan, *New Double Soft Emission Theorems*, *Phys. Rev.* **D92** (2015) 065030, [[1503.04816](#)].
- [133] A. Volovich, C. Wen and M. Zlotnikov, *Double Soft Theorems in Gauge and String Theories*, *JHEP* **07** (2015) 095, [[1504.05559](#)].
- [134] G. Georgiou, *Multi-soft theorems in Gauge Theory from MHV Diagrams*, *JHEP* **08** (2015) 128, [[1505.08130](#)].
- [135] P. Di Vecchia, R. Marotta and M. Mojaza, *Double-soft behavior for scalars and gluons from string theory*, *JHEP* **12** (2015) 150, [[1507.00938](#)].
- [136] I. Low, *Double Soft Theorems and Shift Symmetry in Nonlinear Sigma Models*, *Phys. Rev.* **D93** (2016) 045032, [[1512.01232](#)].
- [137] S. He, Y.-t. Huang and C. Wen, *Loop Corrections to Soft Theorems in Gauge Theories and Gravity*, *JHEP* **1412** (2014) 115, [[1405.1410](#)].
- [138] Z. Bern, S. Davies and J. Nohle, *On Loop Corrections to Subleading Soft Behavior of Gluons and Gravitons*, *Phys.Rev.* **D90** (2014) 085015, [[1405.1015](#)].
- [139] F. Cachazo and E. Y. Yuan, *Are Soft Theorems Renormalized?*, [1405.3413](#).
- [140] A. Brandhuber, E. Hughes, B. Spence and G. Travaglini, *One-Loop Soft Theorems via Dual Superconformal Symmetry*, *JHEP* **03** (2016) 084, [[1511.06716](#)].
- [141] D. Bonocore, E. Laenen, L. Magnea, L. Vernazza and C. D. White, *The method of regions and next-to-soft corrections in Drell–Yan production*, *Phys. Lett.* **B742** (2015) 375–382, [[1410.6406](#)].
- [142] D. Bonocore, E. Laenen, L. Magnea, S. Melville, L. Vernazza and C. D. White, *A factorization approach to next-to-leading-power threshold logarithms*, *JHEP* **06** (2015) 008, [[1503.05156](#)].
- [143] Z. Bern, J. Carrasco and H. Johansson, *New Relations for Gauge-Theory Amplitudes*, *Phys.Rev.* **D78** (2008) 085011, [[0805.3993](#)].
- [144] Z. Bern, J. J. M. Carrasco and H. Johansson, *Perturbative Quantum Gravity as a Double Copy of Gauge Theory*, *Phys.Rev.Lett.* **105** (2010) 061602, [[1004.0476](#)].

- [145] H. Johansson and A. Ochirov, *Pure Gravities via Color-Kinematics Duality for Fundamental Matter*, *JHEP* **11** (2015) 046, [[1407.4772](#)].
- [146] S. G. Naculich, *Scattering equations and BCJ relations for gauge and gravitational amplitudes with massive scalar particles*, *JHEP* **09** (2014) 029, [[1407.7836](#)].
- [147] S. Weinzierl, *Fermions and the scattering equations*, *JHEP* **03** (2015) 141, [[1412.5993](#)].
- [148] H. Johansson and A. Ochirov, *Color-Kinematics Duality for QCD Amplitudes*, *JHEP* **01** (2016) 170, [[1507.00332](#)].
- [149] L. de la Cruz, A. Kniss and S. Weinzierl, *Proof of the fundamental BCJ relations for QCD amplitudes*, *JHEP* **09** (2015) 197, [[1508.01432](#)].
- [150] L. de la Cruz, A. Kniss and S. Weinzierl, *The CHY representation of tree-level primitive QCD amplitudes*, *JHEP* **11** (2015) 217, [[1508.06557](#)].
- [151] M. Chiodaroli, M. Gunaydin, H. Johansson and R. Roiban, *Spontaneously Broken Yang-Mills-Einstein Supergravities as Double Copies*, [1511.01740](#).
- [152] S. He and Y. Zhang, *Connected formulas for amplitudes in standard model*, [1607.02843](#).
- [153] R. Kleiss and H. Kuijf, *Multi - Gluon Cross-sections and Five Jet Production at Hadron Colliders*, *Nucl. Phys.* **B312** (1989) 616.
- [154] Z. Bern and T. Dennen, *A Color Dual Form for Gauge-Theory Amplitudes*, *Phys.Rev.Lett.* **107** (2011) 081601, [[1103.0312](#)].
- [155] Z. Bern, T. Dennen, Y.-t. Huang and M. Kiermaier, *Gravity as the Square of Gauge Theory*, *Phys.Rev.* **D82** (2010) 065003, [[1004.0693](#)].
- [156] N. Bjerrum-Bohr, P. H. Damgaard and P. Vanhove, *Minimal Basis for Gauge Theory Amplitudes*, *Phys.Rev.Lett.* **103** (2009) 161602, [[0907.1425](#)].
- [157] N. Bjerrum-Bohr, P. H. Damgaard, T. Sondergaard and P. Vanhove, *Monodromy and Jacobi-like Relations for Color-Ordered Amplitudes*, *JHEP* **1006** (2010) 003, [[1003.2403](#)].
- [158] N. Bjerrum-Bohr, P. H. Damgaard, B. Feng and T. Sondergaard, *Proof of Gravity and Yang-Mills Amplitude Relations*, *JHEP* **1009** (2010) 067, [[1007.3111](#)].
- [159] N. Bjerrum-Bohr, P. H. Damgaard, T. Sondergaard and P. Vanhove, *The Momentum Kernel of Gauge and Gravity Theories*, *JHEP* **1101** (2011) 001, [[1010.3933](#)].
- [160] N. Bjerrum-Bohr, P. H. Damgaard, R. Monteiro and D. O'Connell, *Algebras for Amplitudes*, *JHEP* **1206** (2012) 061, [[1203.0944](#)].
- [161] S. Stieberger, *Open & Closed vs. Pure Open String Disk Amplitudes*, [0907.2211](#).
- [162] C. R. Mafra, O. Schlotterer, S. Stieberger and D. Tsimpis, *A recursive method for SYM n-point tree amplitudes*, *Phys.Rev.* **D83** (2011) 126012, [[1012.3981](#)].
- [163] C. R. Mafra, O. Schlotterer and S. Stieberger, *Explicit BCJ Numerators from Pure Spinors*, *JHEP* **1107** (2011) 092, [[1104.5224](#)].
- [164] C. R. Mafra, O. Schlotterer and S. Stieberger, *Complete N-Point Superstring Disk Amplitude I. Pure Spinor Computation*, *Nucl.Phys.* **B873** (2013) 419–460, [[1106.2645](#)].

- [165] P. A. Grassi, A. Mezzalana and L. Sommovigo, *BCJ and KK Relations from BRST Symmetry and Supergravity Amplitudes*, [1111.0544](#).
- [166] T. Sondergaard, *Perturbative Gravity and Gauge Theory Relations: A Review*, *Adv.High Energy Phys.* **2012** (2012) 726030, [[1106.0033](#)].
- [167] B. Feng, R. Huang and Y. Jia, *Gauge Amplitude Identities by On-shell Recursion Relation in S-matrix Program*, *Phys.Lett.* **B695** (2011) 350–353, [[1004.3417](#)].
- [168] Y. Jia, R. Huang and C.-Y. Liu, *U(1)-decoupling, KK and BCJ relations in $\mathcal{N} = 4$ SYM*, *Phys.Rev.* **D82** (2010) 065001, [[1005.1821](#)].
- [169] Y.-X. Chen, Y.-J. Du and B. Feng, *A Proof of the Explicit Minimal-basis Expansion of Tree Amplitudes in Gauge Field Theory*, *JHEP* **1102** (2011) 112, [[1101.0009](#)].
- [170] Y.-J. Du, B. Feng and C.-H. Fu, *BCJ Relation of Color Scalar Theory and KLT Relation of Gauge Theory*, *JHEP* **1108** (2011) 129, [[1105.3503](#)].
- [171] Y.-J. Du, B. Feng and C.-H. Fu, *Note on Permutation Sum of Color-ordered Gluon Amplitudes*, *Phys.Lett.* **B706** (2012) 490–494, [[1110.4683](#)].
- [172] C.-H. Fu, Y.-J. Du and B. Feng, *An algebraic approach to BCJ numerators*, *JHEP* **1303** (2013) 050, [[1212.6168](#)].
- [173] Y.-J. Du, B. Feng and C.-H. Fu, *The Construction of Dual-trace Factor in Yang-Mills Theory*, *JHEP* **1307** (2013) 057, [[1304.2978](#)].
- [174] D. Vaman and Y.-P. Yao, *Constraints and Generalized Gauge Transformations on Tree-Level Gluon and Graviton Amplitudes*, *JHEP* **1011** (2010) 028, [[1007.3475](#)].
- [175] R. H. Boels and R. S. Isermann, *Yang-Mills amplitude relations at loop level from non-adjacent BCFW shifts*, *JHEP* **1203** (2012) 051, [[1110.4462](#)].
- [176] R. H. Boels, B. A. Kniehl, O. V. Tarasov and G. Yang, *Color-kinematic Duality for Form Factors*, *JHEP* **1302** (2013) 063, [[1211.7028](#)].
- [177] R. H. Boels, R. S. Isermann, R. Monteiro and D. O’Connell, *Colour-Kinematics Duality for One-Loop Rational Amplitudes*, *JHEP* **1304** (2013) 107, [[1301.4165](#)].
- [178] S. Oxburgh and C. White, *BCJ duality and the double copy in the soft limit*, *JHEP* **1302** (2013) 127, [[1210.1110](#)].
- [179] R. Saotome and R. Akhoury, *Relationship Between Gravity and Gauge Scattering in the High Energy Limit*, *JHEP* **1301** (2013) 123, [[1210.8111](#)].
- [180] J. Broedel and J. J. M. Carrasco, *Virtuous Trees at Five and Six Points for Yang-Mills and Gravity*, *Phys.Rev.* **D84** (2011) 085009, [[1107.4802](#)].
- [181] J. Broedel and L. J. Dixon, *Color-kinematics duality and double-copy construction for amplitudes from higher-dimension operators*, *JHEP* **1210** (2012) 091, [[1208.0876](#)].
- [182] F. Cachazo, *Fundamental BCJ Relation in $N=4$ SYM From The Connected Formulation*, [1206.5970](#).
- [183] J. J. M. Carrasco, *Gauge and Gravity Amplitude Relations*, [1506.00974](#).

- [184] M. Tolotti and S. Weinzierl, *Construction of an effective Yang-Mills Lagrangian with manifest BCJ duality*, *JHEP* **1307** (2013) 111, [[1306.2975](#)].
- [185] Y.-J. Du and H. Luo, *On General BCJ Relation at One-loop Level in Yang-Mills Theory*, *JHEP* **1301** (2013) 129, [[1207.4549](#)].
- [186] J. Nohle, *Color-Kinematics Duality in One-Loop Four-Gluon Amplitudes with Matter*, *Phys.Rev.* **D90** (2014) 025020, [[1309.7416](#)].
- [187] Z. Bern, J. Carrasco, L. Dixon, H. Johansson and R. Roiban, *Simplifying Multiloop Integrands and Ultraviolet Divergences of Gauge Theory and Gravity Amplitudes*, *Phys.Rev.* **D85** (2012) 105014, [[1201.5366](#)].
- [188] J. J. Carrasco and H. Johansson, *Five-Point Amplitudes in $N=4$ Super-Yang-Mills Theory and $N=8$ Supergravity*, *Phys.Rev.* **D85** (2012) 025006, [[1106.4711](#)].
- [189] N. E. J. Bjerrum-Bohr, T. Dennen, R. Monteiro and D. O’Connell, *Integrand Oxidation and One-Loop Colour-Dual Numerators in $N=4$ Gauge Theory*, *JHEP* **1307** (2013) 092, [[1303.2913](#)].
- [190] J. J. M. Carrasco, M. Chiodaroli, M. Günaydin and R. Roiban, *One-loop four-point amplitudes in pure and matter-coupled $N \leq 4$ supergravity*, *JHEP* **1303** (2013) 056, [[1212.1146](#)].
- [191] Z. Bern, C. Boucher-Veronneau and H. Johansson, *$N \geq 4$ Supergravity Amplitudes from Gauge Theory at One Loop*, *Phys.Rev.* **D84** (2011) 105035, [[1107.1935](#)].
- [192] C. Boucher-Veronneau and L. Dixon, *$N > 4$ Supergravity Amplitudes from Gauge Theory at Two Loops*, *JHEP* **1112** (2011) 046, [[1110.1132](#)].
- [193] P. Mastrolia, E. Mirabella, G. Ossola and T. Peraro, *Integrand-Reduction for Two-Loop Scattering Amplitudes through Multivariate Polynomial Division*, *Phys. Rev.* **D87** (2013) 085026, [[1209.4319](#)].
- [194] D. Chester, *Bern-Carrasco-Johansson relations for one-loop QCD integral coefficients*, *Phys. Rev.* **D93** (2016) 065047, [[1601.00235](#)].
- [195] R. H. Boels and R. S. Isermann, *New relations for scattering amplitudes in Yang-Mills theory at loop level*, *Phys. Rev.* **D85** (2012) 021701, [[1109.5888](#)].
- [196] N. E. J. Bjerrum-Bohr, P. H. Damgaard, H. Johansson and T. Sondergaard, *Monodromy-like Relations for Finite Loop Amplitudes*, *JHEP* **05** (2011) 039, [[1103.6190](#)].
- [197] S. Badger, G. Mogull, A. Ochirov and D. O’Connell, *A Complete Two-Loop, Five-Gluon Helicity Amplitude in Yang-Mills Theory*, *JHEP* **10** (2015) 064, [[1507.08797](#)].
- [198] Z. Bern and D. A. Kosower, *The Computation of loop amplitudes in gauge theories*, *Nucl. Phys.* **B379** (1992) 451–561.
- [199] Z. Bern, A. De Freitas, L. J. Dixon and H. L. Wong, *Supersymmetric regularization, two loop QCD amplitudes and coupling shifts*, *Phys. Rev.* **D66** (2002) 085002, [[hep-ph/0202271](#)].
- [200] W. Giele and E. N. Glover, *Higher order corrections to jet cross-sections in e^+e^- annihilation*, *Phys.Rev.* **D46** (1992) 1980–2010.

- [201] P. Mastrolia, T. Peraro and A. Primo, *Adaptive Integrand Decomposition in parallel and orthogonal space*, *JHEP* **08** (2016) 164, [[1605.03157](#)].
- [202] T. Hahn, *Generating Feynman diagrams and amplitudes with FeynArts 3*, *Comput. Phys. Commun.* **140** (2001) 418–431, [[hep-ph/0012260](#)].
- [203] R. Mertig, M. Bohm and A. Denner, *FEYN CALC: Computer algebraic calculation of Feynman amplitudes*, *Comput. Phys. Commun.* **64** (1991) 345–359.
- [204] V. Shtabovenko, R. Mertig and F. Orellana, *New Developments in FeynCalc 9.0*, [1601.01167](#).
- [205] D. Maitre and P. Mastrolia, *S@M, a Mathematica Implementation of the Spinor-Helicity Formalism*, *Comput. Phys. Commun.* **179** (2008) 501–574, [[0710.5559](#)].
- [206] W. J. Torres Bobadilla, *T@M, a Mathematica Implementation of the Momentum-twistor Formalism*, *Unpublished* (2016) .
- [207] P. Cvitanovic, P. G. Lauwers and P. N. Scharbach, *Gauge Invariance Structure of Quantum Chromodynamics*, *Nucl. Phys.* **B186** (1981) 165–186.
- [208] F. A. Berends and W. Giele, *The Six Gluon Process as an Example of Weyl-Van Der Waerden Spinor Calculus*, *Nucl. Phys.* **B294** (1987) 700–732.
- [209] M. L. Mangano, S. J. Parke and Z. Xu, *Duality and Multi - Gluon Scattering*, *Nucl.Phys.* **B298** (1988) 653.
- [210] D. Kosower, B.-H. Lee and V. P. Nair, *MULTI GLUON SCATTERING: A STRING BASED CALCULATION*, *Phys. Lett.* **B201** (1988) 85–89.
- [211] Z. Bern and D. A. Kosower, *Color decomposition of one loop amplitudes in gauge theories*, *Nucl. Phys.* **B362** (1991) 389–448.
- [212] V. Del Duca, A. Frizzo and F. Maltoni, *Factorization of tree QCD amplitudes in the high-energy limit and in the collinear limit*, *Nucl. Phys.* **B568** (2000) 211–262, [[hep-ph/9909464](#)].
- [213] V. Del Duca, L. J. Dixon and F. Maltoni, *New color decompositions for gauge amplitudes at tree and loop level*, *Nucl. Phys.* **B571** (2000) 51–70, [[hep-ph/9910563](#)].
- [214] F. Maltoni, K. Paul, T. Stelzer and S. Willenbrock, *Color flow decomposition of QCD amplitudes*, *Phys. Rev.* **D67** (2003) 014026, [[hep-ph/0209271](#)].
- [215] H. Elvang and Y.-t. Huang, *Scattering Amplitudes*, [1308.1697](#).
- [216] S. Weinzierl, *Tales of 1001 Gluons*, 2016. [1610.05318](#).
- [217] L. J. Dixon, *Calculating scattering amplitudes efficiently*, in *QCD and beyond. Proceedings, Theoretical Advanced Study Institute in Elementary Particle Physics, TASI-95, Boulder, USA, June 4-30, 1995*, pp. 539–584, 1996. [hep-ph/9601359](#).
- [218] M. E. Peskin, *Simplifying Multi-Jet QCD Computation*, in *Proceedings, 13th Mexican School of Particles and Fields (MSPF 2008): San Carlos, Sonora, Mexico, October 2-11, 2008*, 2011. [1101.2414](#).
- [219] S. Weinberg, *The Quantum theory of fields. Vol. 1: Foundations*. Cambridge University Press, 2005.

- [220] R. Blumenhagen and E. Plauschinn, *Introduction to conformal field theory*, *Lect. Notes Phys.* **779** (2009) 1–256.
- [221] J. M. Drummond, J. Henn, V. A. Smirnov and E. Sokatchev, *Magic identities for conformal four-point integrals*, *JHEP* **01** (2007) 064, [[hep-th/0607160](#)].
- [222] A. Hodges, *Eliminating spurious poles from gauge-theoretic amplitudes*, *JHEP* **05** (2013) 135, [[0905.1473](#)].
- [223] N. Arkani-Hamed, J. L. Bourjaily, F. Cachazo, S. Caron-Huot and J. Trnka, *The All-Loop Integrand For Scattering Amplitudes in Planar $N=4$ SYM*, *JHEP* **01** (2011) 041, [[1008.2958](#)].
- [224] J. L. Bourjaily, *Efficient Tree-Amplitudes in $N=4$: Automatic BCFW Recursion in Mathematica*, [1011.2447](#).
- [225] N. Arkani-Hamed, J. L. Bourjaily, F. Cachazo and J. Trnka, *Local Integrals for Planar Scattering Amplitudes*, *JHEP* **06** (2012) 125, [[1012.6032](#)].
- [226] J. L. Bourjaily, S. Caron-Huot and J. Trnka, *Dual-Conformal Regularization of Infrared Loop Divergences and the Chiral Box Expansion*, *JHEP* **01** (2015) 001, [[1303.4734](#)].
- [227] S. Badger, H. Frellesvig and Y. Zhang, *Multi-loop integrand reduction techniques*, *PoS LL2014* (2014) 010, [[1407.3133](#)].
- [228] H. A. Frellesvig, *Generalized Unitarity Cuts and Integrand Reduction at Higher Loop Orders*. PhD thesis, Faculty of Science - University of Copenhagen, 2014.
- [229] S. Badger, *Automating QCD amplitudes with on-shell methods*, *J. Phys. Conf. Ser.* **762** (2016) 012057, [[1605.02172](#)].
- [230] S. Badger, *Unitarity and On-shell Methods*, in *School of Analytic Computing in Theoretical High-Energy Physics*, (Atrani, Italy), October, 2015.
- [231] S. Badger, *Non-planar integrands for two-loop QCD amplitudes*, in *Amplitudes 2015*, (Zurich, Switzerland), July, 2015.
- [232] M.-x. Luo and C.-k. Wen, *Recursion relations for tree amplitudes in super gauge theories*, *JHEP* **0503** (2005) 004, [[hep-th/0501121](#)].
- [233] J. Rao and B. Feng, *Note on Identities Inspired by New Soft Theorems*, *JHEP* **04** (2016) 173, [[1604.00650](#)].
- [234] R. W. Brown and S. G. Naculich, *BCJ relations from a new symmetry of gauge-theory amplitudes*, *JHEP* **10** (2016) 130, [[1608.04387](#)].
- [235] A. Luna, S. Melville, S. G. Naculich and C. D. White, *Next-to-soft corrections to high energy scattering in QCD and gravity*, *JHEP* **01** (2017) 052, [[1611.02172](#)].
- [236] D.-p. Zhu, *Zeros in Scattering Amplitudes and the Structure of Nonabelian Gauge Theories*, *Phys.Rev.* **D22** (1980) 2266.
- [237] S. Henry Tye and Y. Zhang, *Dual Identities inside the Gluon and the Graviton Scattering Amplitudes*, *JHEP* **1006** (2010) 071, [[1003.1732](#)].
- [238] R. H. Boels and R. S. Isermann, *On powercounting in perturbative quantum gravity theories through color-kinematic duality*, *JHEP* **06** (2013) 017, [[1212.3473](#)].

- [239] R. Eden, P. Landshoff, D. Olive and J. Polkinghorne, *The Analytic S–Matrix*. Cambridge University Press, 1966.
- [240] L. F. Alday and R. Roiban, *Scattering Amplitudes, Wilson Loops and the String/Gauge Theory Correspondence*, *Phys.Rept.* **468** (2008) 153–211, [[0807.1889](#)].
- [241] R. Britto, *Loop Amplitudes in Gauge Theories: Modern Analytic Approaches*, *J.Phys.A* **A44** (2011) 454006, [[1012.4493](#)].
- [242] J. M. Henn, *Dual conformal symmetry at loop level: massive regularization*, *J.Phys.A* **A44** (2011) 454011, [[1103.1016](#)].
- [243] Z. Bern and Y.-t. Huang, *Basics of Generalized Unitarity*, *J.Phys.A* **A44** (2011) 454003, [[1103.1869](#)].
- [244] J. J. M. Carrasco and H. Johansson, *Generic multiloop methods and application to $N=4$ super-Yang-Mills*, *J.Phys.A* **A44** (2011) 454004, [[1103.3298](#)].
- [245] L. J. Dixon, *Scattering amplitudes: the most perfect microscopic structures in the universe*, *J.Phys.A* **A44** (2011) 454001, [[1105.0771](#)].
- [246] R. K. Ellis, Z. Kunszt, K. Melnikov and G. Zanderighi, *One-loop calculations in quantum field theory: from Feynman diagrams to unitarity cuts*, *Phys. Rept.* **518** (2012) 141–250, [[1105.4319](#)].
- [247] H. Ita, *Susy Theories and QCD: Numerical Approaches*, *J.Phys.A* **A44** (2011) 454005, [[1109.6527](#)].
- [248] G. Ossola, C. G. Papadopoulos and R. Pittau, *Numerical evaluation of six-photon amplitudes*, *JHEP* **0707** (2007) 085, [[0704.1271](#)].
- [249] Y. Zhang, *Integrand-Level Reduction of Loop Amplitudes by Computational Algebraic Geometry Methods*, *JHEP* **09** (2012) 042, [[1205.5707](#)].
- [250] P. Mastrolia, E. Mirabella, G. Ossola and T. Peraro, *Scattering Amplitudes from Multivariate Polynomial Division*, *Phys. Lett.* **B718** (2012) 173–177, [[1205.7087](#)].
- [251] P. Mastrolia, E. Mirabella, G. Ossola and T. Peraro, *Multiloop Integrand Reduction for Dimensionally Regulated Amplitudes*, *Phys. Lett.* **B727** (2013) 532–535, [[1307.5832](#)].
- [252] R. K. Ellis and G. Zanderighi, *Scalar one-loop integrals for QCD*, *JHEP* **02** (2008) 002, [[0712.1851](#)].
- [253] G. 't Hooft and M. J. G. Veltman, *Scalar One Loop Integrals*, *Nucl. Phys.* **B153** (1979) 365–401.
- [254] R. E. Cutkosky, *Singularities and discontinuities of Feynman amplitudes*, *J. Math. Phys.* **1** (1960) 429–433.
- [255] Z. Bern, L. J. Dixon, D. C. Dunbar and D. A. Kosower, *Fusing gauge theory tree amplitudes into loop amplitudes*, *Nucl. Phys.* **B435** (1995) 59–101, [[hep-ph/9409265](#)].
- [256] W. B. Kilgore, *One-loop Integral Coefficients from Generalized Unitarity*, [0711.5015](#).
- [257] R. Britto and B. Feng, *Solving for tadpole coefficients in one-loop amplitudes*, *Phys. Lett.* **B681** (2009) 376–381, [[0904.2766](#)].

- [258] R. Britto and E. Mirabella, *Single Cut Integration*, *JHEP* **01** (2011) 135, [[1011.2344](#)].
- [259] T. Peraro, *Advanced methods for scattering amplitudes in gauge theories* *Advanced methods for scattering amplitudes in gauge theories* *Advanced methods for scattering amplitudes in gauge theories* *Advanced methods for scattering amplitudes in gauge theories*. PhD thesis, Technische Universität München - Max-Planck-Institut für Physik (Werner-Heisenberg-Institut), 2014.
- [260] G. Ossola, C. G. Papadopoulos and R. Pittau, *CutTools: a program implementing the OPP reduction method to compute one-loop amplitudes*, *JHEP* **03** (2008) 042, [[0711.3596](#)].
- [261] R. Pittau, *Primary Feynman rules to calculate the epsilon-dimensional integrand of any 1-loop amplitude*, *JHEP* **1202** (2012) 029, [[1111.4965](#)].
- [262] I. Wolfram Research, *Mathematica 11.0*, 2016.
- [263] J. A. M. Vermaseren, *New features of FORM*, [math-ph/0010025](#).
- [264] Y. Katayama, K. Sawada and S. Takagi, *Five dimensional approach to regularized quantum electrodynamics*, *Progress of Theoretical Physics* **5** (1950) 14–24.
- [265] G. 't Hooft, *Renormalization of Massless Yang-Mills Fields*, *Nucl.Phys.* **B33** (1971) 173–199.
- [266] D. Leiter and G. Szamosi, *Pseudoscalar mass and its relationship to conventional scalar mass in the relativistic dirac theory of the electron*, *Lettere al Nuovo Cimento* **5** (1972) 814–816.
- [267] M. Trzetrzelewski, *On the mass term of the Dirac equation*, [1101.3899](#).
- [268] U. D. Jentschura and B. J. Wundt, *From Generalized Dirac Equations to a Candidate for Dark Energy*, *ISRN High Energy Phys.* **2013** (2013) 374612, [[1205.0521](#)].
- [269] G. Mahlon and S. J. Parke, *Deconstructing angular correlations in $Z H$, $Z Z$, and $W W$ production at LEP-2*, *Phys.Rev.* **D58** (1998) 054015, [[hep-ph/9803410](#)].
- [270] F. Wilczek, *Decays of Heavy Vector Mesons Into Higgs Particles*, *Phys.Rev.Lett.* **39** (1977) 1304.
- [271] S. Dawson, *Radiative corrections to Higgs boson production*, *Nucl.Phys.* **B359** (1991) 283–300.
- [272] Z. Kunszt, A. Signer and Z. Trocsanyi, *One loop helicity amplitudes for all $2 \rightarrow 2$ processes in QCD and $N=1$ supersymmetric Yang-Mills theory*, *Nucl.Phys.* **B411** (1994) 397–442, [[hep-ph/9305239](#)].
- [273] Z. Bern, G. Chalmers, L. J. Dixon and D. A. Kosower, *One loop N gluon amplitudes with maximal helicity violation via collinear limits*, *Phys.Rev.Lett.* **72** (1994) 2134–2137, [[hep-ph/9312333](#)].
- [274] A. Brandhuber, S. McNamara, B. J. Spence and G. Travaglini, *Loop amplitudes in pure Yang-Mills from generalised unitarity*, *JHEP* **0510** (2005) 011, [[hep-th/0506068](#)].
- [275] Z. Bern, L. J. Dixon and D. A. Kosower, *One loop corrections to two quark three gluon amplitudes*, *Nucl.Phys.* **B437** (1995) 259–304, [[hep-ph/9409393](#)].

- [276] C. R. Schmidt, $H \rightarrow ggg$ ($gq\bar{q}$) at two loops in the large m_t limit, *Phys.Lett.* **B413** (1997) 391–395, [[hep-ph/9707448](#)].
- [277] Z. Bern and D. A. Kosower, Efficient calculation of one loop QCD amplitudes, *Phys. Rev. Lett.* **66** (1991) 1669–1672.
- [278] G. Mahlon, Multi - gluon helicity amplitudes involving a quark loop, *Phys.Rev.* **D49** (1994) 4438–4453, [[hep-ph/9312276](#)].
- [279] S. J. Bidder, N. Bjerrum-Bohr, L. J. Dixon and D. C. Dunbar, $N=1$ supersymmetric one-loop amplitudes and the holomorphic anomaly of unitarity cuts, *Phys.Lett.* **B606** (2005) 189–201, [[hep-th/0410296](#)].
- [280] J. Bedford, A. Brandhuber, B. J. Spence and G. Travaglini, Non-supersymmetric loop amplitudes and MHV vertices, *Nucl.Phys.* **B712** (2005) 59–85, [[hep-th/0412108](#)].
- [281] Z. Bern, L. J. Dixon and D. A. Kosower, Bootstrapping multi-parton loop amplitudes in QCD, *Phys.Rev.* **D73** (2006) 065013, [[hep-ph/0507005](#)].
- [282] Z. Bern, N. Bjerrum-Bohr, D. C. Dunbar and H. Ita, Recursive calculation of one-loop QCD integral coefficients, *JHEP* **0511** (2005) 027, [[hep-ph/0507019](#)].
- [283] C. F. Berger, Z. Bern, L. J. Dixon, D. Forde and D. A. Kosower, Bootstrapping One-Loop QCD Amplitudes with General Helicities, *Phys.Rev.* **D74** (2006) 036009, [[hep-ph/0604195](#)].
- [284] C. F. Berger, Z. Bern, L. J. Dixon, D. Forde and D. A. Kosower, All One-loop Maximally Helicity Violating Gluonic Amplitudes in QCD, *Phys.Rev.* **D75** (2007) 016006, [[hep-ph/0607014](#)].
- [285] Z. Xiao, G. Yang and C.-J. Zhu, The Rational Part of QCD Amplitude. III. The Six-Gluon, *Nucl.Phys.* **B758** (2006) 53–89, [[hep-ph/0607017](#)].
- [286] S. Badger and E. N. Glover, One-loop helicity amplitudes for $H \rightarrow$ gluons: The All-minus configuration, *Nucl.Phys.Proc.Suppl.* **160** (2006) 71–75, [[hep-ph/0607139](#)].
- [287] S. Badger, E. Nigel Glover, P. Mastrolia and C. Williams, One-loop Higgs plus four gluon amplitudes: Full analytic results, *JHEP* **1001** (2010) 036, [[0909.4475](#)].
- [288] L. J. Dixon, E. N. Glover and V. V. Khoze, MHV rules for Higgs plus multi-gluon amplitudes, *JHEP* **0412** (2004) 015, [[hep-th/0411092](#)].
- [289] C. F. Berger, V. Del Duca and L. J. Dixon, Recursive Construction of Higgs-Plus-Multiparton Loop Amplitudes: The Last of the Phi-nite Loop Amplitudes, *Phys.Rev.* **D74** (2006) 094021, [[hep-ph/0608180](#)].
- [290] E. N. Glover, P. Mastrolia and C. Williams, One-loop phi-MHV amplitudes using the unitarity bootstrap: The General helicity case, *JHEP* **0808** (2008) 017, [[0804.4149](#)].
- [291] S. Badger, E. N. Glover and K. Risager, One-loop phi-MHV amplitudes using the unitarity bootstrap, *JHEP* **0707** (2007) 066, [[0704.3914](#)].
- [292] G. Cullen, H. van Deurzen, N. Greiner, G. Luisoni, P. Mastrolia, E. Mirabella et al., Next-to-Leading-Order QCD Corrections to Higgs Boson Production Plus Three Jets in Gluon Fusion, *Phys. Rev. Lett.* **111** (2013) 131801, [[1307.4737](#)].

- [293] Z. Bern, L. J. Dixon and D. A. Kosower, *One loop corrections to five gluon amplitudes*, *Phys. Rev. Lett.* **70** (1993) 2677–2680, [[hep-ph/9302280](#)].
- [294] R. H. P. Kleiss, I. Malamos, C. G. Papadopoulos and R. Verheyen, *Counting to One: Reducibility of One- and Two-Loop Amplitudes at the Integrand Level*, *JHEP* **12** (2012) 038, [[1206.4180](#)].
- [295] B. Feng and R. Huang, *The classification of two-loop integrand basis in pure four-dimension*, *JHEP* **1302** (2013) 117, [[1209.3747](#)].
- [296] H. Johansson, D. A. Kosower and K. J. Larsen, *Maximal Unitarity for the Four-Mass Double Box*, *Phys. Rev.* **D89** (2014) 125010, [[1308.4632](#)].
- [297] H. Johansson, D. A. Kosower, K. J. Larsen and M. Søgaard, *Cross-Order Integral Relations from Maximal Cuts*, *Phys. Rev.* **D92** (2015) 025015, [[1503.06711](#)].
- [298] M. Søgaard and Y. Zhang, *Multivariate Residues and Maximal Unitarity*, *JHEP* **12** (2013) 008, [[1310.6006](#)].
- [299] M. Søgaard, *Global Residues and Two-Loop Hepta-Cuts*, *JHEP* **09** (2013) 116, [[1306.1496](#)].
- [300] M. Søgaard and Y. Zhang, *Elliptic Functions and Maximal Unitarity*, *Phys. Rev.* **D91** (2015) 081701, [[1412.5577](#)].
- [301] M. Sogaard and Y. Zhang, *Massive Nonplanar Two-Loop Maximal Unitarity*, *JHEP* **12** (2014) 006, [[1406.5044](#)].
- [302] M. Sogaard and Y. Zhang, *Unitarity Cuts of Integrals with Doubled Propagators*, *JHEP* **07** (2014) 112, [[1403.2463](#)].
- [303] H. Ita, *Two-loop Integrand Decomposition into Master Integrals and Surface Terms*, [1510.05626](#).
- [304] K. J. Larsen and Y. Zhang, *Integration-by-parts reductions from unitarity cuts and algebraic geometry*, *Phys. Rev.* **D93** (2016) 041701, [[1511.01071](#)].
- [305] S. Badger, G. Mogull and T. Peraro, *Local integrands for two-loop all-plus Yang-Mills amplitudes*, *JHEP* **08** (2016) 063, [[1606.02244](#)].
- [306] J. C. Collins, *Renormalization: an introduction to renormalization, the renormalization group, and the operator-product expansion*. Cambridge monographs on mathematical physics. Cambridge Univ. Press, Cambridge, 1984.
- [307] D. Kreimer, *One loop integrals revisited. 1. The Two point functions*, *Z. Phys.* **C54** (1992) 667–672.
- [308] D. Kreimer, *The Two loop three point functions: General massive cases*, *Phys. Lett.* **B292** (1992) 341–347.
- [309] A. Czarnecki, U. Kilian and D. Kreimer, *New representation of two loop propagator and vertex functions*, *Nucl. Phys.* **B433** (1995) 259–275, [[hep-ph/9405423](#)].
- [310] A. Frink, U. Kilian and D. Kreimer, *New representation of the two loop crossed vertex function*, *Nucl. Phys.* **B488** (1997) 426–440, [[hep-ph/9610285](#)].

- [311] D. Kreimer, *XLOOPS: An Introduction to parallel space techniques*, *Nucl. Instrum. Meth.* **A389** (1997) 323–326.
- [312] T. Gehrmann, J. M. Henn and N. A. Lo Presti, *Analytic form of the two-loop planar five-gluon all-plus-helicity amplitude in QCD*, *Phys. Rev. Lett.* **116** (2016) 062001, [[1511.05409](#)].
- [313] D. C. Dunbar and W. B. Perkins, *Two-loop five-point all plus helicity Yang-Mills amplitude*, *Phys. Rev.* **D93** (2016) 085029, [[1603.07514](#)].
- [314] D. C. Dunbar, G. R. Jehu and W. B. Perkins, *The two-loop n-point all-plus helicity amplitude*, *Phys. Rev.* **D93** (2016) 125006, [[1604.06631](#)].
- [315] R. G. Stuart, *Algebraic Reduction of One Loop Feynman Diagrams to Scalar Integrals*, *Comput. Phys. Commun.* **48** (1988) 367–389.

Acknowledgements

And here we are, about to write the acknowledgements for my Ph.D thesis and close a period in my life. I never imagine that this three-year journey would have been so productive for the academic and, as well as, for the personal side. Since I moved to Padova many experiences happened, none of them would have been possible without the people who I crossed path with. Although, I am not the best person in expressing feelings to others I really would like to thank those that have been part of my journey.

First of all, I would like to thank my supervisor Pierpaolo Mastrolia, for everything I have learnt over the last three years. I have to thank him for all the time he spent with me. His door was always open to answer my questions with knowledge, enthusiasm and great patience. I was very fortunate for having worked with such a brilliant physicist.

I would also like to thank my collaborators without whom this thesis would not be what it is. In particular, Amedeo Primo for our long discussions sorting out both ideas and technical details, and for his patience with my over-excitement as well as my concerns.

I am indebted with Raffaele Fazio, he introduced me to the world of on-shell methods. I am thankful for the countless discussions and the encouragement he gave and keeps giving me.

I wish to thank the theoretical physics group in Padova, for creating such a wonderful environment, for the activities shared in these years, and also the computing power that was needed to finish some of the projects described in this thesis. Especially, I want to thank Gianguido Dall'Agata and Andrea Vitturi for their help with all administrative issues. I would also like to thank my officemates Jagjit Singh, Raj Kumar Gupta, Dionysis Karagiannis, Denise Vicino, Niccolò Cribiori, Andrea Galliani and Mária Guzzetti for the stimulating discussions, and for all the fun we have had in the last years.

I am thankful to Simon Badger and the Higgs Center of Theoretical Physics in Edinburgh for hosting me for three months during the completion of part of the work presented in this thesis. Being in Edinburgh allowed me to have interesting discussions with Tiziano Peraro and Francesco Buciuni, whom I thank.

I am grateful to many physicists outside Padova for helpful conversations, including Zvi Bern, John Joseph Carrasco, Einan Gardi, David Kosower, Lorenzo Magnea and Edoardo Mirabella. I would like to thank Giovanni Ossola, for having shared with me very interesting projects and ideas. Of course, I thank Simon Badger and Stefan Weinzierl for accepting to review my thesis, their feedback helped me to improve its content.

During my stay in Padova there were several people outside physics I spent time with. In particular, I would like to thank my Colombian friends for not letting me forget where I come from and why the friends are needed for: Jaime, Sebastián, Ana Paola, Carolina and Ana. Likewise, many of my good friends scattered across Padova region: Christos, Hiroshi, Rossynell, Daniel, Tarek and Luigi.

Last but not the least, I would to thank my parents and sisters for helping me to grow up and evolve into who I am now.

This work was funded by Fondazione Cassa di Risparmio di Padova e Rovigo (CARIPARO).